IDENTIFICATION OF PUTATIVE TARGETING FACTORS REQUIRED FOR SPECIFIC FUSION AMONGST ORGANELLES OF THE ENDOCYTIC PATHWAY

by

BIENYAMEEN BAKER

Submitted in fulfilment of the requirement for the degree of

DOCTOR OF PHILOSOPHY

in the

FACULTY OF MEDICINE (MEDICAL BIOCHEMISTRY)

UNIVERSITY OF CAPE TOWN

15 February 2001

DECLARATION

I **BIENYAMEEN BAKER**, hereby declare that this thesis is my own unaided work, both in concept and execution, and that apart from normal guidance from my supervisor. Neither the substance nor any part of this thesis has been submitted in the past, or is being, or is to be submitted in the University or any other university.

SIGNED:___ _____

DATE: 15/02/2001

ACKNOWLEDGEMENTS

Dedicated to my loving and understanding mother
and in loving memory of my late father, who sacrificed so much
to afford me a tertiary education

I also sincerely wish to express my deep appreciation and thanks to the following:

Professor Lutz Thilo, for his indulgence, encouragement, constructive criticism and scientific guidance. It was a pleasurable and informative experience.

Dr. Chantal de Chastellier for her expert help with the electron microscopy.

Dr. Thomas Haylett, Roshan Ebrahim and Ray-Dean Pietersen for their friendship and thought provoking discussions.

Dr. Colin Hughes for kindly providing anti-galectin-3 antibodies.

Messrs Riedwaan Majiet, Robert Samuels and Steven Fortuin for technical assistance when needed.

Mr. Harry Hall for his skilful and dedicated workmanship in producing the necessary equipment required for this study.

Mrs. Sia Samuels for her substitutive role as a caring mother figure in the work place.

ABSRACT

IDENTIFICATION OF TARGETING FACTORS REQUIRED FOR SPECIFIC FUSION AMONGST ORGANELLES OF THE ENDOCYTIC PATHWAY

Endocytic processing involves specific fusion between distinct populations of organelles along the endocytic pathway. Homotypic fusion occurs amongst early endosomes, late endosomes and lysosomes. Heterotypic fusion occurs between late endosomes and lysosomes. The targeting molecules that convey specificity to these fusion events have not been fully defined. Therefore, a binding assay was developed to find putative targeting molecules. Luminally cross-linked endosomes and lysosomes, which were fusion inactive and detergent insoluble, were used as *'acceptors'* to bind potential targeting molecules by incubating them with metabolically labelled *'donor'*, either cytosol or detergent-solubilised membrane. The binding assay was also done in the absence of detergent, allowing for intact membrane in both acceptor and membrane donor preparation. For this purpose, acceptors were prepared as phagosomes that contained paramagnetic latex beads. Membrane donor was prepared by sonicating metabolically labelled membrane in the presence of an excess of phospholipid in order to separate donor proteins into individual vesicles. Bound material was isolated and analysed by two-dimensional electrophoresis and subsequent radioactive scanning. The proteins of interest were then analysed by mass spectrometry and compared with existing information in protein data banks. The identity of a specific protein was confirmed by Edman microsequencing.

The most interesting find was that cross-linked lysosomes especially bound galectin-3 (a β-galactoside binding lectin) and lysozyme C from the fully soluble metabolically labelled membrane donor, preferentially under ATP-depleting conditions in the binding assay. Both types of cross-linked acceptors bound voltage-dependent anion-selective channel (PM-Porin) and β_2 microglobulin. Compatible results were obtained for the binding assay with intact membranes.

To determine the origin of bound material as being either endosomes or lysosomes, the membrane composition of paramagnetic latex bead-containing phagosomes was analysed by two-dimensional electrophoresis. Electron microscopy confirmed that beads with a hydrophobic surface remained in endosomes whereas beads with a hydrophilic surface were processed normally towards lysosomes. It was found that phago-endosomes were enriched for galectin-3, thioredoxin peroxidase II and cofilin, while phago-lysosomes were enriched for annexin IV, superoxide dismutase and vacuolar ATP synthase E subunit.

Galectin-3 was found compositionally enriched in phago-endosomes and was especially bound by lysosome acceptors in binding assays. This was suggestive of a possible specific role for galectin-3 in the interaction of endosomes with lysosomes. The N-terminal domain of galectin-3 is highly homologous to proline-rich domains present in annexins VII and XI. Annexins in general have been implicated to play a role in intracellular membrane traffic.

To test whether galectin-3 played a role in fusion, a novel biochemical assay was set up to investigate the fusion of purified paramagnetic latex bead-containing phago-lysosomes with a mixed endosome/lysosome population of organelles. The assay was based on monitoring the transfer of HRP from endocytic organelles to phagosomes as a measure of fusion. As expected, ATPγS completely inhibited fusion. The presence of thiodigalactoside, a specific ligand for galectin-3, inhibited fusion by 40%. Mac-2, a monoclonal antibody directed towards the N-terminus of galectin-3, inhibited fusion by 80%. CRD, a polyclonal antibody directed towards the carbohydrate-recognition domain of galectin-3, inhibited fusion by 50%. These results supported the unexpected notion that galectin-3 might play a role in targeting or fusion between endosomes and lysosomes.

ABBREVIATIONS

Ab	= antibody
AMP, ADP, ATP	= 5' mono-, di- and triphosphates of adenosine
ATPase	= adenosine triphosphatase
ATPγS	= adenosine 5'-O-(3-thiotriphosphate)
ARF	= ADP- ribosylation factor
BoTx	= botulinum toxin
BSA	= bovine serum albumin
°C	= degrees Celsius
cAMP	= adenosine 3': 5'-cyclic monophosphate
CGN	= cis-Golgi network
Ci	= curie (3.7×10^{10} disintegrations per second)
COP	= coat protein
CRD	= carbohydrate-recognition domain
Da	= Dalton
DAB	= 3,3'-diaminobenzidine
dpm	= disintegrations per minute
DMEM	= Dulbecco's minimum essential medium
DTT	= dithiothreitol
ECVs	= endosomal carrier vesicles
EDTA	= ethylenediamine tetraacetic acid
EGTA	= ethylene glycol-bis(β-aminoethyl ether) tetraacetic acid
En	= endosome
ER	= endoplasmic reticulum
FCS	= fetal calf serum
GAP	= GTPase-activating protein
GDI	= GDP dissociation inhibitor
GDP	= guanosine 5'-diphosphate
GEF	= guanine nucleotide exchange factor
GlcNAc	= N-acetylglucosamine
Gαβγ	= GTPase α, β and γ subunits
Giα	= inhibitory GTPase α subunit
Gsα	= stimulatory GTPase α subunit
GTP	= guanosine 5'-triphosphate
GTPase	= guanosine triphosphatase
HA	= haemagglutinin
H_2O_2	= hydrogen peroxide
HRP	= horse-radish peroxidase
IEF	= isoelectric focussing
IgG	= immunoglobulin G
kVh	= kilo-volt hours
karyogamy	= nuclear envelope fusion process
kDa	= kiloDalton
KKXX or KXKXX	= K - lysine, X - any amino acid
LDL	= low-density lipoprotein
Lf	= low-density fraction
l	= litre
Lys	= lysosome

Maldi-MS	= matrix assisted laser desorption/ionization – mass spectrometry
Maldi-TOF	= matrix assisted laser desorption/ionization – time of flight
M	= molar concentration
min	= minute
mg	= milligram
ml	= millilitre
mm	= millimetre
mM	= millimolar concentration
Mts	= microtubules
Mw	= molecular weight
Myo LC/HC	= myosin light chain / heavy chain
NEM	= N-ethylmaleimide
NSF	= NEM sensitive factor
NSF-myc	= NSF epitope-tagged with Myc peptide
ng	= nanogram
pg	= picogram
PAGE	= polyacrylamide gel electrophoresis
pH	= nagative logarithm of the hydrogen ion concentration
phago-En	= phago-endosomes
phago-Ly	= phago-lysosomes
pI	= isoelectric pH
PM	= plasma membrane
PMSF	= phenylmethyl sulphonyl fluoride
PNS	= postnuclear supernatant
RME	= receptor-mediated endocytosis
rpm	= revolutions per minute
RPMI	= RPMI-1640 medium
S	= Svedberg constant
SDS	= sodium dodecyl sulphate
SNAPs	= soluble NSF attachment proteins (α-, β- and γ-SNAP)
SNAP-25	= synaptosome associated protein of 25 kDa
SNARE	= SNAP receptor
t-SNARE	= target membrane SNARE
v-SNARE	= vesicle membrane SNARE
SV	= secretory vesicle
TDG	= thiodigalactoside
TeTx	= tetanus toxin
Tf	= transferrin
Tf-R	= transferrin receptor
TGN	= trans Golgi network
Tris	= tris (hydroxymethyl) aminomethane
TX-100	= Triton X-100
UDP	= uridine diphosphate
µg	= microgram
VAMP	= vesicle associated membrane protein
VSV	= vesicular stomatitis virus
v/v	= volume per volume
w/v	= weight per volume
X-En	= cross linked endosomes
X-Ly	= cross linked lysosomes

TABLE OF CONTENTS

LIST OF FIGURES

Page No.

CHAPTER 1

INTRODUCTION

A major aspect of modern cell biological research is aimed at understanding the 3-D organisation of cells in terms of its underlying biochemistry. Eukaryotic cells are divided into membrane-bound compartments which allow specialised and segregated functions to occur in a series of distinct environments. Transport of macromolecules out of cells by secretion and into cells by endocytosis, intracellular transport required for biogenesis of the intracellular membrane-bound organelles and the generation of the distinct apical and basal plasma-membrane surfaces required in polarised cells, represents the core of the functions of this organellar network. In general, transfer of material between compartments occurs by means of small membrane-bound vesicles (i.e. vesicular traffic). This transfer must be highly specific to ensure that the characteristics of individual compartments are maintained. The present study was aimed at the identification of molecules that are involved in conveying specificity. As a background to this work, the mechanistic and molecular events governing membrane transport will be broadly overviewed, leading up to a focussed molecular dissection of the protein machinery that initiates targeting and fusion.

1.1 THE SECRETORY PATHWAY

The **secretory pathway** [Figure 1.1] has been extensively studied and has provided much insight about the organisation and dynamics of the intracellular compartments involved [1,2,18b]. Three functionally distinct secretory compartments exist, namely the Endoplasmic Reticulum (ER), the Pre-Golgi Intermediates (PGIs) and the Golgi complex.

1.1.1 Formation of the Nuclear Membrane and Endoplasmic Reticulum

In eukaryotic cells, the nuclear membrane functions to separate the genome from the cytoplasm, thereby permitting types of regulation not found in prokaryotes. The nuclear

membrane consists of two concentric lipid bilayers, with the outer bilayer continuous with the ER [3]. The nuclear envelope disassembles at the onset of mitosis and is reassembled at the end of mitosis. Assembly involves the attachment of vesicles to the chromatin. Association of membranes with chromatin is regulated by phosphorylation [4], and is followed by their fusion to produce the double membrane system. Different fractionation protocols brought about the identification of two classes of precursor vesicle populations involved in nuclear membrane assembly [5,6]. One class appears to be involved in targeting the membranes to the surface of chromatin and formation of nuclear pore complexes, while the second class contributes most of the nuclear membrane lipid [7]. The binding/targeting of vesicles to chromatin does not require adenosine triphosphate (ATP), but ATP and GTP are essential for fusion of chromatin-bound vesicles [7]. The nuclear envelope is assembled from a subset of ER-derived vesicles [5,6].

1.1.2 Transport from the ER to the PGIs

Nascent proteins, synthesised on ribosomes in the cytoplasm, are targeted to the ER-membrane by signal sequences and translocated to the lumen of the ER [8a]. Translocation is driven by a heat-shock protein known as BiP (Hsp70 family member) together with folding factors that catalyse disulfide-bond exchange and oligosaccharide transfer. Unfolded or misfolded proteins are tagged with glucose residues at the termini of N-linked sugar chains, forcing their association with lectins (calnexin, calreticulin) thereby restricting their export from the ER [8b].

Folded proteins leave the ER via COPII (coat protein complex II)-coated vesicles [see Section 1.3], which fuse to form Pre-Golgi intermediates (PGIs) [9] losing their COPII coats. The salvage of ER residents by retrograde transport is mediated by the formation of COPI-coated vesicles on PGIs. COPI-coats bind [10] to KKXX cytoplasmic signals common to ER membrane proteins [11]. Luminal ER proteins (like BiP) with the C-terminal sequence as KDEL are retrieved by the KDEL receptor [12]. Retrieval starts at

the PGI and continues throughout the Golgi compartments [13,14a]. The matured PGIs move along microtubules towards the Golgi complex [15].

1.1.3 Transport across the Golgi

The Golgi is organised into three functionally distinct regions, the cis-Golgi network (CGN), the Golgi stack (cis, medial and trans cisternae) and the trans-Golgi network (TGN). The immature proteins destined for secretion, are moved off to the Golgi stack for post-translational modifications (such as glycosylation, phosphorylation, sulfation, proteolytic cleavages etc.).

In contrast to the ER, no cytoplasmic sorting signals have been detected in the Golgi stack proteins, but possess a single transmembrane (TM) domain that is sufficient to mediate their retention in the Golgi stack [16]. The TM domain length of Golgi enzymes/proteins (~ 17 residues) as compared to PM proteins (~ 21 residues), instead of specific amino acid sequence, seems to be the overriding feature which mediates Golgi stack retention [17].

Transport across the Golgi stack may occur by vesicular traffic [18a] or maturation [18b]. The vesicular traffic model visualises the cisternae as permanent structures from which COPI-coated vesicles bud and fuse with the next cisternae in anterograde transport or the previous cisternae in retrograde transport. The maturation model predicts that the cis-cisterna is formed de-novo by the fusion of PGI-derived vesicles, which then mature into medial- and then trans- cisterna, due to the selective removal of non-cargo components via COPI-coated vesicles in retrograde transport.

The passage of the proteins destined for secretion then continue towards the trans-Golgi network (TGN), in which final processing takes place [19]. Proteins destined to the plasma membrane, to secretory storage vesicles or to the endocytic pathway [discussed in Section 1.2], are separated upon exit from the TGN [19].

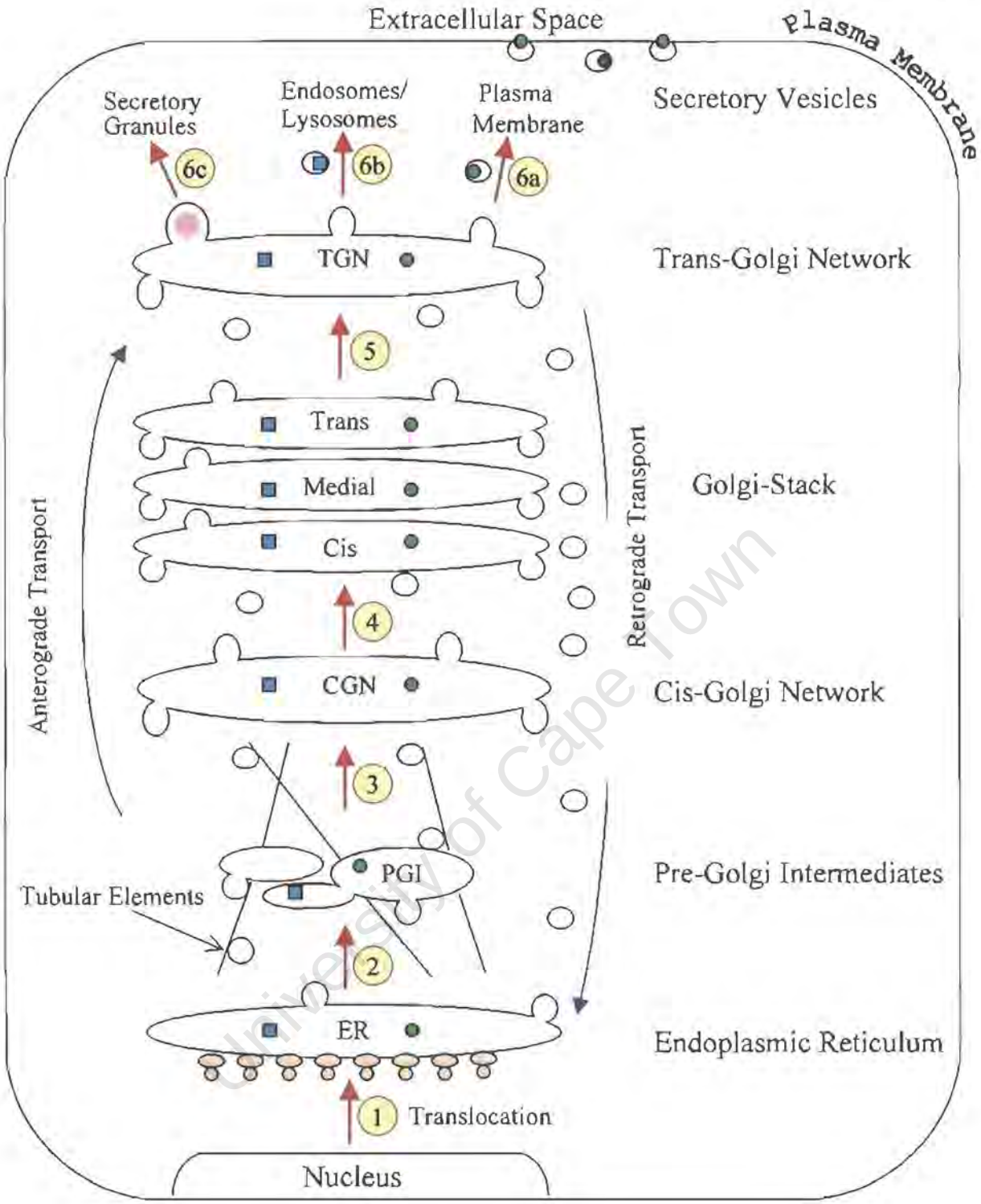

Figure 1.1 : Secretory Pathway. Newly synthesised proteins are translocated into the ER catalysed by BiP {step 1}. Cargo proteins are folded before exit from the ER via vesicles that fuse to form the PGI {step 2}. The PGI sort and concentrate cargo proteins before transport to the CGN along microtubules {step 3}. Cargo is then transported to the Golgi-stack {step 4}. The cargo proteins undergo posttranslational modifications during their sequential passage across the Golgi-stack to the TGN {step 5}. Upon delivery to the TGN, proteins are sorted and packaged into vesicles intended for the Plasma Membrane {step 6a} or Endosomes/Lysosomes {step 6b} or as Secretory granules in specialised secretory cells {step 6c}. Recycling of transport machinery factors and salvage of resident ER proteins occurs via retrograde transport .

1.2 THE ENDOCYTIC PATHWAY

Endocytosis [Figure 1.2] is the process by which cells internalise extracellular material by enclosing them within inward foldings of the plasma membrane that seal to form intracellular vesicles [20]. The endocytic organelles (tubulovesicular early endosomes, endosomal carrier vesicles, late endosomes and lysosomes) which make up the endocytic pathway have been characterised based on their morphology and biochemical composition [21].

Two modes of endocytosis exist, viz. clathrin-dependent receptor-mediated endocytosis (RME, selective uptake of macromolecules such as nutrients, hormones, viruses etc.) and clathrin-independent phagocytosis (ingestion of large particulate matter such as cell debris, bacteria etc.). Receptor-mediated endocytosis and phagocytosis follow the same general pathway for delivery of materials to lysosomes.

1.2.1 Receptor-mediated endocytosis (RME)

In RME, ligands bind to specific cell-surface receptors, clustered in clathrin-coated pits [22], before internalisation [23,24] via coated vesicles. Transport proteins [25], growth factors [26], asialoglycoproteins [40] and other nutrients enter cells by RME. Fluid-phase endocytosis (a non-selective uptake of solutes) is also mediated by coated vesicles [27,28].

The coated pit invaginates and pinches off to form a coated vesicle (0,1 - 0,2 μm diameter). Dynamin, a 100 kDa member of the GTPase superfamily [29], is the mammalian homologue of the *Drosophila shibire* gene product [30,31] and may direct membrane fission, since mutations in dynamin lead to accumulation of coated pits and deep invaginations at the plasma membrane, that look like constricted vesicles [32-34]. Dynamin self-assembly into helical structures [35], enable it to wrap around the necks of invaginated coated pits.

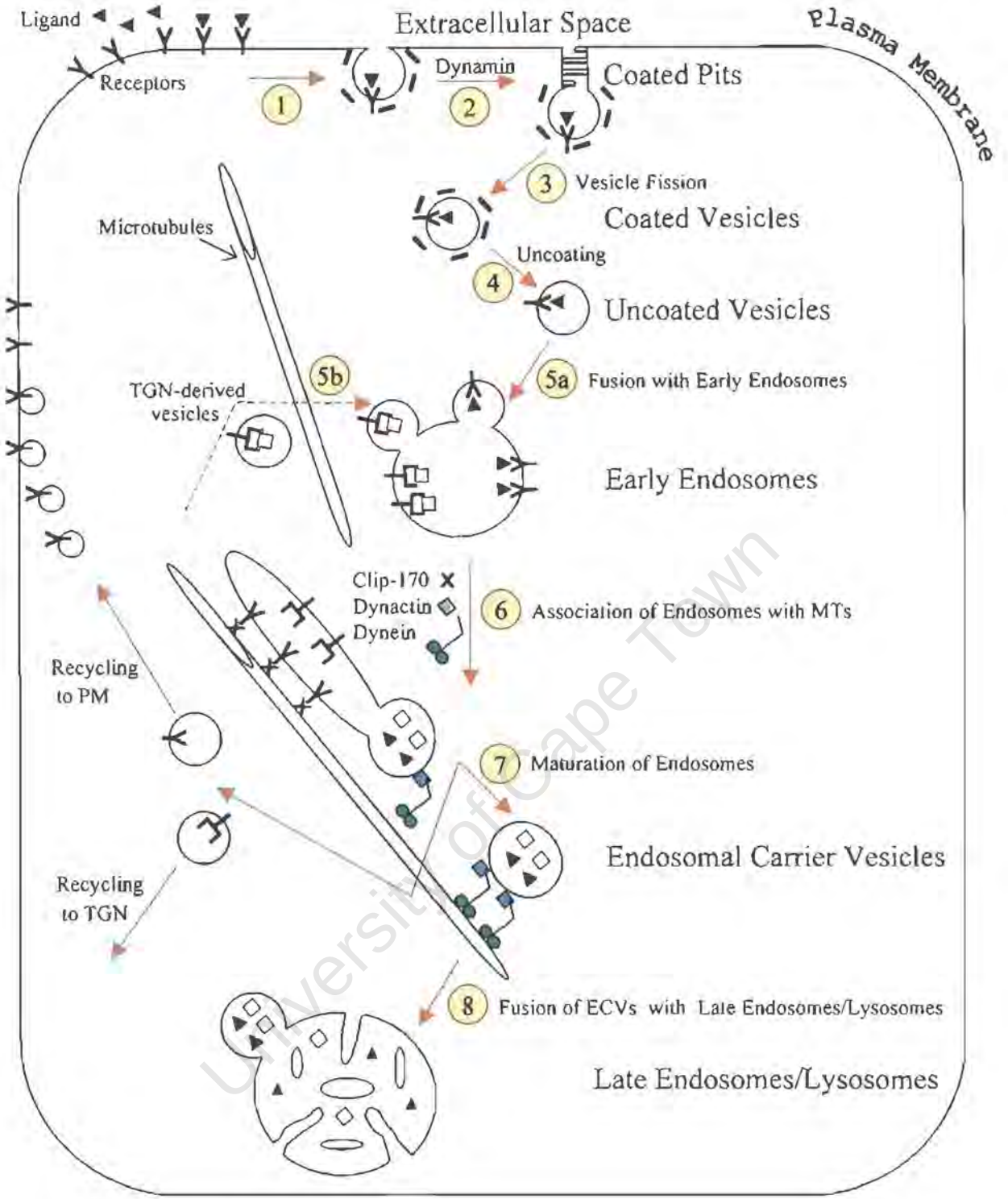

Figure 1.2 : Endocytic Pathway. Ligand (▲) binds to its receptor (Y) at the cell surface, and the receptor-ligand complexes localise to clathrin coated pits {step 1}. The binding of dynamin {step 2}, leads to vesicle fission {step 3}. After fission the clathrin coat disassembles {step 4} and uncoated PM-derived or TGN-derived vesicles (containing hydrolases ◇ bound to MPR Y) fuse with early endosomes {steps 5a & 5b}. Endosomes then associate with microtubules while receptor and ligand dissociate due to low pH. The receptors accumulate in the tubular parts while ligand and hydrolases are concentrated in the vesicular part of the maturing endosome {step 6}. Upon fission, the receptors are recycled back to the PM or TGN, with concomitant formation of ECVs {step 7} which are transported along microtubules (via dynein/dynactin) and then fuse with late endosomes/lysosomes {step 8}. [Adapted from Ref. 91]

The presence of dynamin-coated tubules not capped by a clathrin coated end, suggest that dynamin and possibly other associated proteins, may be sufficient to generate a tubular invagination and therefore support endocytosis in a clathrin-independent mechanism [36]. Subsequently, however, it has been indicated that dynamin may function as a regulator of RME, as opposed to a force-generating GTPase [37].

1.2.2 Delivery of receptor-ligand complexes to Early Endosomes and Sorting

After budding, the clathrin coat is removed in an ATP-dependent fashion [38]. Uncoated vesicles containing the internalised ligand-receptor complex then fuse with tubulovesicular early endosomes [39-41]. Early endosomes exhibit a high tendency to undergo fusion in vitro, in reconstituted fusion assays making use of both fluid phase markers and probes internalised by RME [42-45].

Rapid acidification of early endosomes (pH 6) [46,47] results in dissociation of ligands from receptors which typically occurs below neutral pH [40,41]. The fate of internalised ligands and receptors appears to result from the interplay of three factors: acidification of the endosomal lumen [39], inherent structural features of the receptor [48], and ligand-receptor dissociation rate relative to the rate of vesicle movement [49]. Receptors appear to accumulate in tubular regions of the early endosome after the release of ligand [50,51], before subsequent recycling in recycling vesicles (0,05 - 0,1 μm in diameter) [52] via vesicular traffic to the cell surface [41,51,55-60].

Material destined for degradation, appear subsequently in late endosomes and lysosomes in the perinuclear region of the cell [41,57,60,53]. Some ligands internalised by RME have different fates. For example, transferrin (Tf) is recycled to the cell surface complexed to its receptor [26], some ligands are transported to the lysosome where they are either stored or degraded [25]; in other cases the ligand-receptor complex as a unit is degraded in the lysosome [54].

1.2.3 Transport from Early Endosomes to Late Endosomes

1.2.3.1 The Mechanism of membrane transport

Early and late endosomes are morphologically and functionally distinct [40,41,50,53,57,61-63], as well as differing in lumenal pH and protein composition [60,64,65]. The mechanism of membrane transport between early and late endosomes is still unclear. Maturation, vesicular traffic or combination models have been proposed.

The *maturation* model proposes that early endosomes are formed de novo by the coalescence of newly formed plasma membrane-derived vesicles and gradually turn into late endosomes/lysosomes by sequential addition and subtraction of material [66-68].

The *vesicular traffic* model proposes the permanent existence of early endosomes, late endosomes and lysosomes, as discrete compartments, through which incoming ligand is sequentially transported by vesicular traffic [69,70].

A *combination* model of 1 and 2 proposes that early endosomes are not permanent stations but form by de novo fusion of PM-derived uncoated vesicles, which then mature into endosomal carrier vesicles (ECVs) which then transport their contents via vesicular traffic to lysosomes [71,72]. This model is substantiated by a host of data, and is thus described in more detail below [Section 1.2.3.3].

1.2.3.2 The role of Microtubules and the Actin Cytoskeleton

Although the mechanisms of transport remain to be established, it is clear that endocytosed materials are translocated from the peripheral to the perinuclear region of the cell, as they progress from early to late endosomes [73-76]. This process requires the microbutule network as revealed by morphological and biochemical observations [77,78] and an intact actin cytoskeleton [79]. Microtubules (Mts) have also been shown to be involved in the clustering of late endosomes and lysosomes in the perinuclear region of the cell [80-82]. Additionally, a lysosomal membrane protein has been identified which mediates nucleotide-dependent binding of lysosomes to Mts [83]. It has been shown that movement of organelles along Mts in vitro requires other cytosolic proteins in addition to dynein [85] and kinesin [84]. When cells are treated with cytoskeletal inhibitors (such as nocodazole or colchicine), segregation [86] and degradation of ligand is inhibited [59,87-89].

In the presence of ATP, ligand-containing endocytic vesicles are released from microtubules, while those containing receptor are not. In addition, several proteins including cytoplasmic dynein, associated with microtubules, are released in the presence of ATP [90]. Subsequently it has been shown that binding of ligand-containing vesicles correlates well with binding of dynein to microtubules, but not kinesin, while binding of receptor-containing vesicles is independent of both dynein and kinesin binding [91]. Moreover, it could be demonstrated by immunoprecipitation that dynein is tightly associated with ligand-containing vesicles. The dynactin complex [92,93], which copurifies with cytoplasmic dynein, may serve as a "bridge" between dynein and vesicles [Figure 2].

Microtubule-based proteins such as CLIPs [94a] and actin-based motor proteins such as myosins [94b], have also been implicated in the movement of vesicles in membrane traffic.

1.2.3.3 Endosomal Carrier Vesicles (ECVs)

After segregation of ligand and receptors, endocytosed markers appear in spherical, multivesicular bodies before they are observed in late endosomes [53]. When microtubules are depolymerised by nocodazole, the endocytosed markers reach these multivesicular bodies, but do not appear in late endosomes. Due to these observations, Gruenberg et al. it is proposed that these vesicles mediate microtubule-dependent transport from peripheral early endosomes to perinuclear late endosomes, and thus termed them endosomal carrier vesicles (ECVs, ~ 0,5 μm in diameter) [53].

ECVs have also been observed along both the apical and basolateral endocytic pathways as intermediates between early and late endosomes, in Madin Darby canine kidney (MDCK) cells [74]. In primary hippocampal neurons, similar vesicles are observed along both axonal and dendritic endocytic pathways [95].

Fusion between ECVs and late endosomes has been demonstrated in vitro, and is dependent on microtubules and microtubule-associated proteins including cytoplasmic dynein, but not kinesin [64,96]. ECVs, however, do not exhibit homotypic fusion nor fusion with early endosomes. Microtubules may play a role in increasing the encounter frequency between ECVs and late endosomes for fusion, although it cannot be ruled out that ECVs mature into late endosomes.

1.2.4 Transport from Late Endosomes to Lysosomes

It has been shown that late endosomes, like early endosomes, exhibit a high capacity to undergo homotypic fusion [64,74]. The efficiency of homotypic late endosome fusion in cell-free assays range from 7% [74] to 25% [64].

It has been suggested that late endosomes mature into lysosomes [97], from the observation that 3T3 cell endosomes appear at a density characteristic of lysosomes, when examined on Percoll gradients after incubation with ATP. On the other hand, rat postmitochondrial supernatants containing ^{125}I-labelled asialofentuin (ASF) loaded late endosomes, show that radiolabel appears at lysosomal density on Nycodenz gradients only if lysosomes are present [98].

Fusion between dense endosomes and lysosomes has been demonstrated [99], by an in vitro content mixing assay, using asialofentuin-avidin loaded dense endosomes and biotinylated ^{125}I-labelled polymeric IgA loaded lysosomes. Homotypic fusion of lysosomes has also been observed in vivo [100a] and in vitro [100b].

1.2.5 **Phagocytosis (clathrin-independent)** [Figure 1.3]

Phagocytic uptake of extracellular large particulate matter is stimulated by RME [for review, see ref. 101]. After internalisation, the newly formed phagosomes interact with early endosomes by fusion/fission events, resulting in intermingling of membrane and contents [102-108]. As observed for maturing early endosomes [68,72], phagosomes mature to a state where they are unable to fuse with early endosomes, but acquire the ability to fuse with lysosomes [105]. The same molecular machinery applies to the processing of phagosomes as outlined here and as reviewed before [456].

It has been shown that the maturation of phagosomes is affected by the nature of the particulate matter [108-109]. Phagosomes containing degradable bacteria or hydrophilic latex beads 1μm in size mature and are able to fuse with lysosomes, whereas phagosomes containing pathogenic mycobacteria or hydrophobic latex beads 1μm in size remain fusogenic towards early endosomes and are unable to fuse with lysosomes [108-109]. Analysis of the association between the membrane and the beads or mycobacteria has led to the proposal, that a close apposition of membrane to the particle surface is important to impede phagosome maturation, thus preventing fusion with lysosomes [Figure 1.3].

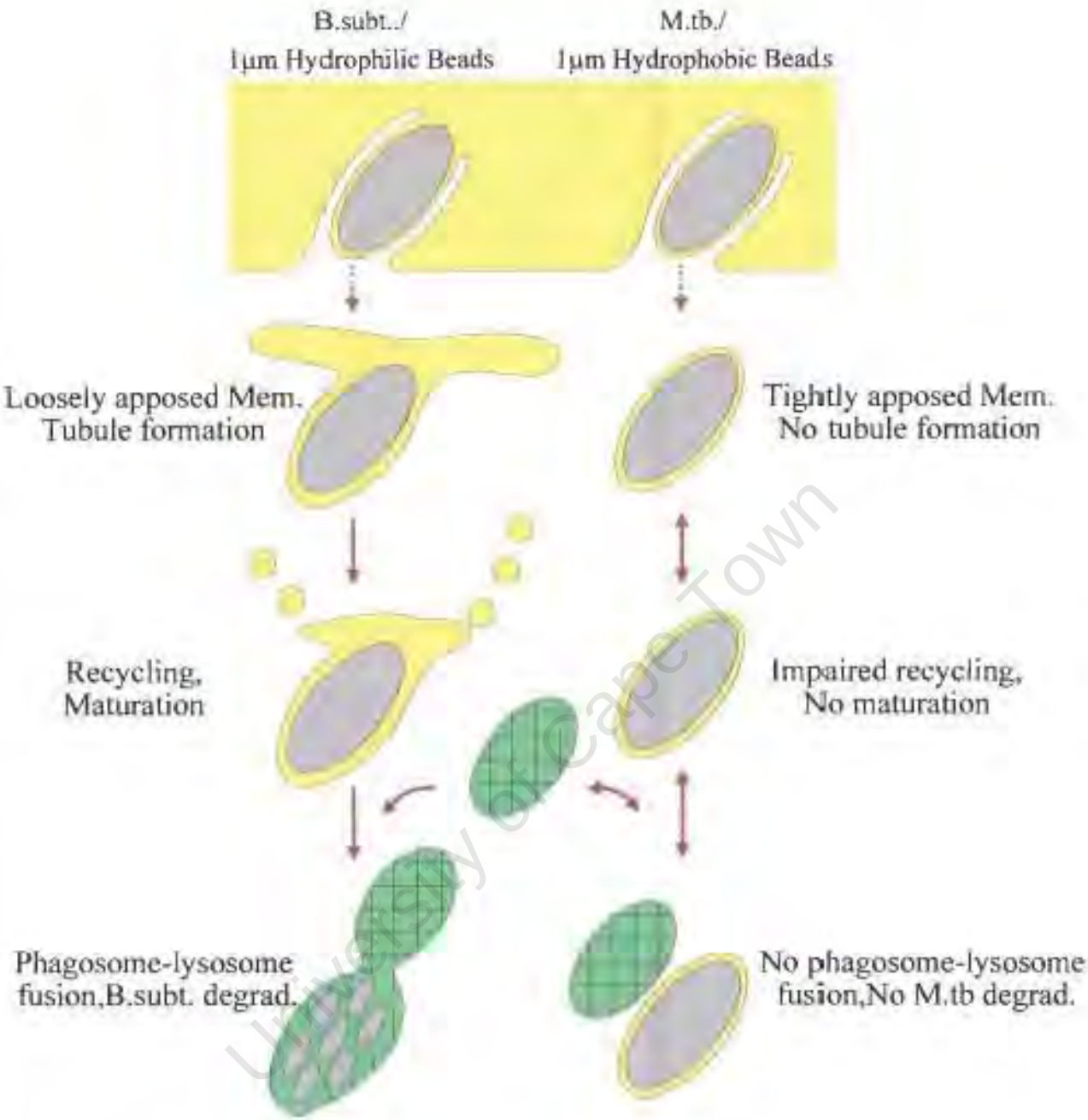

Figure 1.3 : Proposed mechanism for prevention of phagosome-lysosome fusion by Mycobacteria. (A: for non-pathogenic bacteria like B.subt and 1μm hydrophilic beads) Phagosomes interact with early endosomes by fusion/fission events, resulting in intermingling of membrane and contents. As observed for maturing early endosomes, the phagosomes would mature (due to recycling of fusion mediating factors) to a state where they are unable to fuse with early endosomes, but aquire the ability to fuse with lysosomes. (B: for pathogenic bacteria like M.tb. and 1μm hydrophobic beads) When tubule formation is prevented due to a close apposition of membrane to the particle surface, recycling of fusion mediating factors is reduced. Maturation is impeded, thus preventing fusion with lysosomes.

1.3 Vesicle Budding, Targeting and Fusion [Figure 1.4]

Transport between the membrane-bound compartments in the cytoplasm of eukaryotic cells is generally mediated by vesicular traffic which involves transport vesicles that bud from the membrane of a donor compartment and fuse selectively with the membrane of an acceptor compartment [1]. In vitro systems, reconstituting every discernible step along the secretory and endocytic pathways [110] and secretion mutants in yeast [111], have been crucial for studying the molecular mechanisms of vesicular transport. The cloning and sequencing of affected genes of temperature-sensitive and other secretion (sec) mutants, and phenotypic observations by electron microscopy, has led to the identification of a repertoire of protein transport machinery [112] and delineation of its regulation [113].

The discoveries are based on the use of a cell-free system, which reconstitutes intercisternal transport within the Golgi stack [114,115,119,120]. This cell-free system measures the movement of vesicular stomatitis virus glycoprotein (VSV-G) from the cis compartment of a donor Golgi population to the medial compartment of an acceptor Golgi population. Since transport between successive Golgi compartments is unidirectional [116,117] and the glycoslyated VSV-G protein is confined to the acceptor stack that remains distinct from the donor stack [118]; movement must be mediated by diffusible vesicles. These vesicles (0,07 μm in diameter) [119] fully formed or still in the process of budding, exhibit a distinct coat [120] that resembles the clathrin coat of endocytic vesicles [121]. Transport is blocked by GTPγS [122], and by low concentrations of the cysteine-alkylating agent N-ethylmaleimide (NEM). GTPγS leads to the accumulation of coated vesicles in the cytoplasm [122], whereas NEM leads to the accumulation of uncoated vesicles [Figure 1.4, step 9 blocked, therefore no reactant for step5 [123]. GTPγS and NEM together produce only coated vesicles [124], indicating that the GTPγS block precedes the NEM block and that uncoating takes place after budding. The identification of the proteins affected by GTPγS and NEM has led researchers to the molecular core of budding and fusion mechanisms.

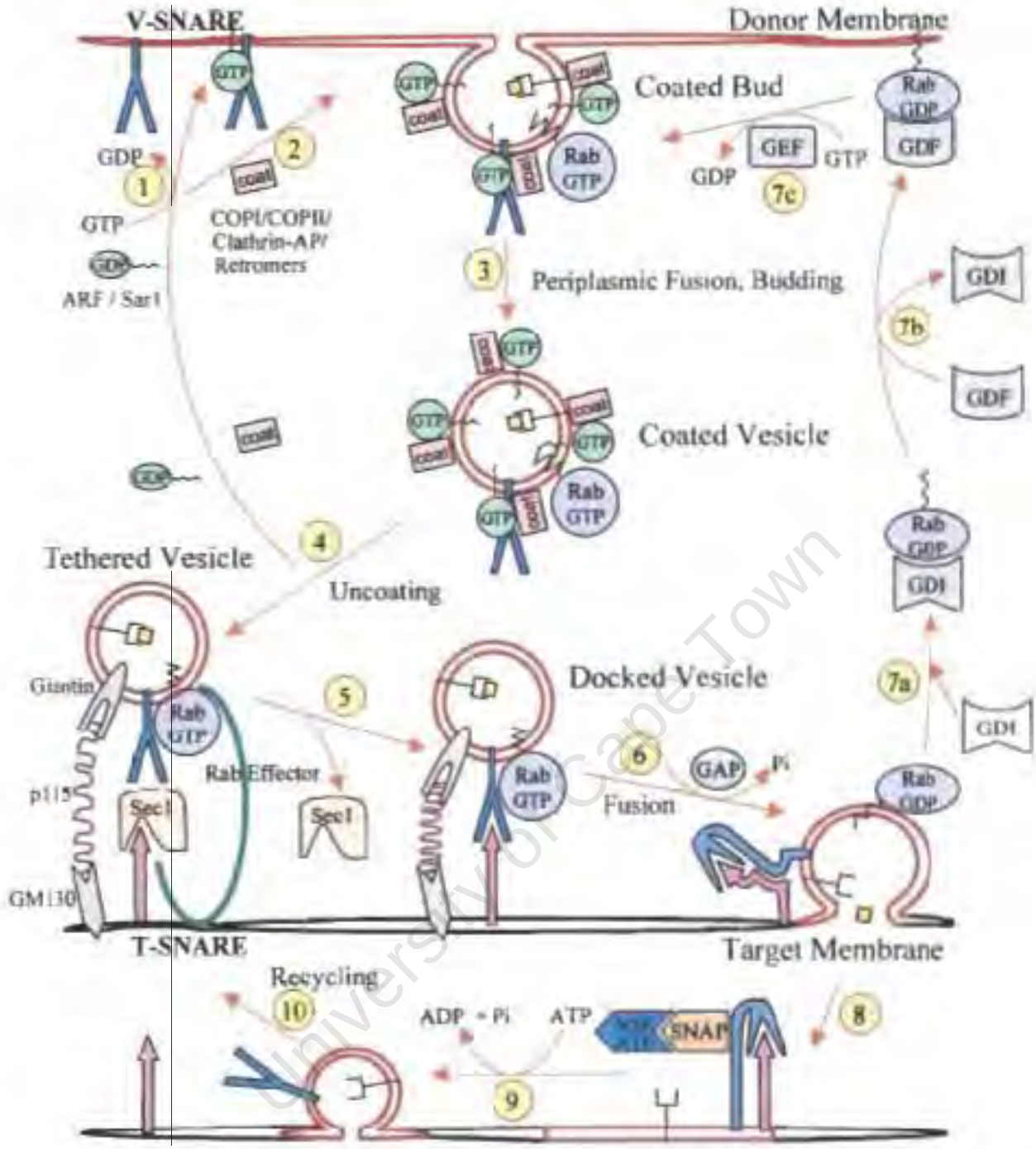

Figure 1.4 : Vesicle Budding and Targeting. Coat assembly is initiated by the binding of a GTP-binding protein to the donor membrane (in this case via direct interaction with the v-SNARE) [ARF(COPI) /Sar1(COP II) /Dynamin (Clathrin-AP)] (step1) that recruits coat proteins [COPI(CGN→Golgi→ER) /COPII(ER→CGN) /Clathrin-AP(PM→EN;TGN→EN) /Retromers(EN→TGN)] involved in cargo selection, followed by the binding of Rab, thus forming a coated bud (step 2). Periplasmic fusion leads to budding(step 3). The Coat disassembles due to GTP hydrolysis by ARF/Sar1 and is recycled, followed by tethering of the vesicle to the target membrane via the action of p115 (step 4). Once tethered Rab effectors may displace SNARE regulators (Sec1) freeing SNAREs to associate for docking (step 5). Fusion of membrane and possibly with concurrent GAP initiated GTP hydrolysis inactivating Rab (step 6) which is recycled (step 7). After fusion SNAP and NSF bind to SNARE complexes (step 8). ATP hydrolysis by NSF disassembles the SNARE complex (step 9). The donor compartments' v-SNAREs and Receptors are recycled (step 10). [Adapted from Refs. 14 a,b]

1.3.1 **Vesicle Budding and Uncoating** [Figure 1.4, steps 3 & 4]

The selection and concentration of cargo during vesicle formation, is mediated by interactions between the cytoplasmic coat and sorting signals on the cargo or its' receptor [11,125]. Coat protein also recruits components (termed SNAREs, discussed later in Section 1.3.2.1) required for targeting and fusion of the transport vesicle with the target membrane [126,127]. A variety of coat complexes have been identified. Vesicle budding [Figure 1.4, step 3] is directed by COP-II (coat protein complex II) on the ER [147,148]; COP-I (coat protein complex I) on PGI [131], Golgi [132] and endocytic compartments [133a,b]; clathrin and its adapters (AP) on the TGN [144] and PM [121]; and retromers on the endosome [128] for retrograde transport to the Golgi. Coat assembly [Figure 1.4, step 2] is initiated by the binding of a GTPase to the donor membrane [Figure 1.4, step 1], which includes ARF (ADP-ribosylation factor) [145] that directs COPI function, Sar1p (yeast ARF homologue) [149] that directs COPII function and dynamin [discussed earlier in Section 1.2.1] influencing clathrin-AP function.

COPI-coated vesicles form from Golgi stacks incubated with cytosol and ATP [114,124]. The purification of COPI-coated vesicles [129-131], revealed that their coats consist of ARF (21 kDa) and a complex of seven distinct proteins termed coatomer [132] consisting of α-COP (170 kDa), ß-COP (110 kDa), ß'-COP (100 kDa), γ-COP (98 kDa), δ-COP (61 kDa), ε-COP (34 kDa) and η-COP (20 kDa). Coatomer and ARF exist separately in the cytosol, but coassemble to form coats. This assembly is initiated when GTP-ARF (N-myristoylated) binds to an `ARF-Receptor' [136] following a brefeldin A (BFA)-sensitive nucleotide exchange step [134,135]. The binding of ARF affords a binding site for coatomer [137,140], which stimulates budding [138,139]. In addition Golgi membranes also require fatty acyl-CoA for coated vesicle formation [142].

The generality of the budding mechanism established in the Golgi becomes evident when other transport steps are analysed in vitro. ARF is required for budding of secretory

vesicles and constitutive transport vesicles from the TGN [144]. Indications are however, that clathrin and COP-coated vesicles bud in related fashion. The mechanism of budding of clathrin-coated endocytic vesicles [146] has been influenced by the discovery of dynamin [discussed earlier in Section 1.2.1]. The structure of the clathrin coat is well characterised. An outer lattice is composed of clathrin heavy chain (180 kDa) and two distinct but related light chains (30-40 kDa, depending on tissue source. The clathrin cage is linked to the enclosed membrane by adaptor particles consisting of four subunits: two related 100-115 kDa, one 47-50 kDa and one 16-19 kDa adaptor chains [121]. The TGN and PM possess their own distinct set of clathrin adaptors [150]. The sequence of the 100-115 kDa adaptin family is homologous to ß-COP [151].

The coat may essentially act as a mechanical device to initiate a local membrane structure that enables "periplasmic fusion" (a fusion event initiated from the lumenal side of the bud) to occur [141]. Periplasmic fusion may occur via either a molecularly precise or a stochastic mechanism [141]. A molecularly precise mechanism would require the precise coupling of fusion with completion of coat assembly, resulting in a fully coated vesicle without a scar [141]. A stochastic (random) mechanism on the other hand, fusion would be triggered merely by the close proximity of the lumenal membrane surfaces at the base of the bud, thereby generating uncoated scars of variable size [141]. Evidence for stochastic periplasmic fusion has been suggested by the observation of uncoated scars on some coated vesicles [142].

The coat disassembles and is recycled for another round of transport [Figure 1.4, step 4) when ARF is triggered to hydrolyse its bound GTP [143]. Uncoating precedes fusion, as coated vesicle buds cannot fuse with acceptor Golgi [142]. Uncoating is driven by Sec23p, a GTPase-activating protein (GAP) for Sar1p [147,148].

1.3.2 Vesicle Targeting/Docking Specificity and the SNARE Hypothesis

1.3.2.1 General Fusion Machinery

NSF

As described above, mild NEM treatment leads to the accumulation of uncoated vesicles on the acceptor Golgi cisternae [123,124], and this observation has led to the identification and purification of the NEM-sensitive fusion protein NSF [152,153]. NSF is a soluble tetramer of identical 76 kDa subunits, which can be released from membranes by incubation with ATP and Mg^{2+} [152]. An NSF subunit has 2 homologous ATP-binding domains [154], and mutation of both sites eliminates its intrinsic ATPase activity, thereby blocking fusion [155] of transport vesicles with their target membrane at multiple points along the secretory and endocytic pathways [129,158-160].

The NSF homologue in yeast is encoded by the SEC18 gene [156] originally implicated in transport from the ER to the Golgi [113]. Sec18p can substitute for NSF in an in vitro mammalian Golgi transport system [156]; moreover, even plant cytosol can replace animal [157] cytosol. Not all intracellular fusion events require NSF [166], however, so possibly other (related perhaps) proteins exist to drive fusion (see Section 1.5 on homotypic fusion, the p97/cdc48 paradigm).

SNAPs

NSF requires additional cytoplasmic factors to attach to Golgi membranes [166,167]. Three species of soluble NSF attachment proteins (SNAPS) have been identified: α-SNAP (35 kDa), ß-SNAP (36 kDa), and γ-SNAP (39 kDa) [161]. ß-SNAP is confined to brain, and closely resembles α-SNAP. γ-SNAP is weakly related to α- and ß-SNAP [163].

α- and ß-SNAP compete for the same site on alkali-treated membranes. γ-SNAP binds to a non-competitive site in the same complex [168], and increases the complex's affinity for NSF [174]. SNAPs do not interact with NSF in solution.

Sec17p is the yeast homologue of α-SNAP, since α-SNAP (but not ß- or γ-SNAP) can restore animal cell Golgi-transport activity to cytosol prepared from sec17 mutant yeast [162]. Sec17p and α-SNAP are functionally equivalent, in that Sec17p can mediate Sec18p binding to Golgi membranes [165]. Fusion is inhibited in the absence of functional Sec17p or Sec18p, resulting in the accumulation of transport vesicles in yeast [164]. SNAPs bind to distinct sites in membranes, creating a binding site for NSF [168].

In vitro, NSF and SNAPs are also essential for homotypic early-endosome fusion [158] and ER to Golgi transport [159]. Fusion between ECVs and late endosomes also requires NSF, and by inference probably SNAPs as well [discussed in Ref. 70]. NEM has also been shown to inhibit fusion between late endosomes and lysosomes [99].

A squid complementary DNA encoding a full-length SNAP (33 kDa) has been isolated [169]. This squid SNAP (S-SNAP) is 67%, 65%, 17%, 33% identical to α-SNAP, ß-SNAP, γ-SNAP and Sec17p (yeast), respectively [169]. The homology between α/ß-SNAPs across evolutionary divisions, suggests a conserved function for SNAPs in neurons [169]. Injection of peptides that mimic the sites at which SNAP interacts with its binding partners inhibits transmitter release, downstream of synaptic vesicle docking [169].

SNAREs

The sites to which the SNAPs bind, are termed SNAP-receptors (SNAREs) [179] which are integral membrane proteins. The multisubunit complex of α/γ-SNAP-SNARE-NSF disassembles when NSF hydrolyses ATP [174], but is trapped as a complex by the presence of either ATPγS or ATP without magnesium (Mg^{2+}) [174]. This multisubunit

particle is proposed to form the core of a generalised fusion apparatus [123,162,174].

Neurons are highly specialised for synaptic vesicle fusion with the pre-synaptic axonal PM, for neurotransmitter release at synapses. To purify the SNAREs specific for bovine brain synaptic-vesicle exocytosis, the specificity inherent in the assembly and disassembly of 20S fusion particles has been used as a basis for a two-step affinity purification technique [179]. 20S particles have been assembled from a Triton X-100 extract of bovine brain membranes, by the addition of pure recombinant α-SNAP, γ-SNAP and NSF-myc (NSF epitope-tagged with a Myc peptide) [12] at 0°C [163], in the presence of ATPγS and EDTA (Mg chelator) [179]. Three SNAREs have been found [179], namely VAMP (vesicle-associated membrane protein, or alternatively synaptobrevin) [171,190], syntaxin [187,188] and SNAP-25 (synaptosome-associated protein of 25 kDa) [170].

The fact that the same SNAP-NSF complex can bind both VAMP (localised to the transport vesicle), and syntaxin and SNAP-25 (localised to the target membrane), and that all three SNAREs are cleaved by a particular form of botulinum or tetanus neurotoxins known to block neurotransmitter release from synapses [184-186], demonstrates the involvement of these SNAREs in docking and fusion.

1.3.2.2 The SNARE Hypothesis

For the maintenance of the organised pattern of individual membrane-bound compartments within the cell, targeting specificity is crucial in all vesicular transport fusion events, from the ubiquitous steps in the constitutive secretory and endocytic pathways to the specialised and regulated forms of exocytosis (such as the Ca^{2+} triggered fusion of a synaptic vesicle containing neurotransmitter with the pre-synaptic PM).

The SNARE hypothesis [179] is based on the finding that VAMP, syntaxin and SNAP-25 are localised to synapses and certain specialised secretory cells [191], while a general NSF-SNAP system acts within and among different cell types [14]. The SNARE hypothesis postulates that each kind of transport vesicle bears a unique vesicle SNARE (v-SNARE, generally VAMP homologues, obtained from its parental membrane during budding) which forms a unique match with its cognate target SNARE (t-SNARE, generally syntaxin and/or SNAP-25 homologues) present on the target membrane, thereby achieving targeting/docking specificity. This hypothesis has been tested and confirmed by an accumulation of evidence from genetic studies in yeast [197-215] and mammals [170,194,195,196,216-237] that has identified a host of v- and t-SNAREs, which are compartment specific in terms of location.

1.3.3 Fusion

The SNARE hypothesis is directly supported by the demonstration that SNAREs alone, can direct in-vitro fusion of liposomes [180]. VAMP, syntaxin and SNAP-25 contain one or more α-helical coiled-coil domains [181,182,183]. Analysis of SNARE complexes has revealed that SNAREs form helical coiled-coil assemblies, which may facilitate bilayer fusion [172,173,192], reminiscent of fusion by viral envelope fusion proteins [176,177]. NSF and SNAPs, instead of driving fusion, serve to dissociate v-/t-SNARE complexes [Figure 1.4, step 9] after fusion [178].

However, it has been shown that multiple v-SNAREs are often present on a single class of transport vesicle [397,398] and that a single v-SNARE can direct both retrograde and anterograde transport [399]. Moreover it has been demonstrated that a variety of v-SNAREs and t-SNAREs pair indiscriminately [193] in vitro. Thus SNAREs alone cannot account for specific membrane trafficking. Consequently, it is thought that Rab proteins [Section 1.4.2] and their effectors [Section 1.4.3] provide the fidelity and additional specificity required for SNARE-mediated docking and subsequent fusion.

1.4 Molecular Dissection of Transport Machinery

1.4.1 SNARE Homologues (from yeast to mammals) [Table 1 (a & b)]

VAMP/Synaptobrevin family

Synaptobrevin (18 kDa) is an integral membrane protein anchored to synaptic vesicles by its carboxy-terminal trans-membrane domain [171,190]. Synaptobrevin is cleaved by tetanus (TeTx) and botulinum (BoTx) B/D/F neurotoxins [184,189], implicating it in exocytosis. An homologue of neuronal synaptobrevin, termed cellubrevin (VAMP 3) is ubiquitously expressed in virtually all cells [194]. Cellubrevin co-localises with transferrin receptor and is highly enriched in clathrin-coated vesicles, suggesting that it localises to organelles involved in constitutive membrane traffic between the TGN and the PM (i.e. exocytotic transport vesicles, clathrin-coated vesicles, and early endosomes) [194]. The homology between cellubrevin and synaptobrevins is high (≈ 59% identity), particularly in the central conserved region on the cytoplasmic side in which the TeTx cleavage site resides [194]. Cellubrevin, however, is not involved in early endosome fusion, as its complete proteolysis by TeTx light chain does not affect in vitro early endosome fusion [196a], but does impair exocytosis [196b]. Approximately thirteen syntaxin-related proteins [See Table 1(b)] have been identified in mammals [194,196,216-221], all of which display a broad tissue distribution and are localised to different membrane compartments.

In yeast, 8 Synaptobrevin-related (Bos1p,Bet1p,Sec22p,Snc1p,Snc2p,Ykt6p,Nyv1p,Vti1p) proteins have been identified [See Table 1]. Snc1p is closely related to synaptobrevin homologue (40% identity) [204]. Snc2p is 32% identical to synaptobrevin, and is 79% identical to Snc1p [199]. Both Snc1p and Snc2p are located in post-Golgi transport vesicles [199]. Yeast strains lacking Snc1p or Snc2p, have no apparent phenotype [199,204], however, if both are lacking, defects in post-Golgi secretion result [199], expounding their role in exocytosis. BOS1 gene has been identified as being able to suppress the secretory mutants bet1 and sec22 [205], and shown to be required for

vesicular transport in yeast [198]. Bet1p and Sec22p have similar tertiary structure, and like Bos1p, Sec22p [197] are concentrated in ER-derived transport vesicles, required for docking/fusion with Golgi in vitro and in vivo [201,205]. Bos1p is either degraded or recycled after fusion of ER-derived vesicles with the Golgi, because it has not been detected in the Golgi apparatus [206]. Ykt6p is required for ER-Golgi transport [207]. Nyv1p is required for homotypic Vacuole fusion [208]. Vti1p mediates transport from TGN-PVC [209a] and from PVC-Vacuole [209b].

Syntaxin family

Syntaxin (A & B, ≈ 35 kDa) is an integral membrane protein (like synaptobrevin), but is localised to the pre-synaptic PM, also by a membrane-spanning domain [185,188]. Each member of the syntaxin family also contains several α-helical coiled-coil domains [181]. Cleavage of syntaxin by BoTx C1 inhibits neurotransmitter release, implicating it directly in exocytotic membrane fusion [185], corroborated by the observation that micro-injection of syntaxin fragments or anti-syntaxin Ab's (antibodies) reduces exocytosis in PC12 cells [195]. About seventeen syntaxin-related proteins [Table 1(b)] have been identified in mammals [195,222-230] displaying a broad tissue distribution and are localised to different membrane compartments.

Seven syntaxin homologues (Sso1p,Sso2p,Sed5p,Pep12p,Tlg2p,Ufe1p,Vam3p] have been identified [Table 1] in yeast, and implicated to function at different stages along the yeast secretory pathway [200,213,214,210,211,215a,215b]. Sso1p and Sso2p are closely related to the syntaxins, and are 72% identical to each other. Disruption of both Sso1p and Sso2p expression blocks post-Golgi transport [200]. Sed5p is required for ER→Golgi transport, and is localised to the membrane of the target cis-Golgi [212,213]. Pep12p is required for Golgi→Vacuole transport, and localises to the target vacuole membrane [214]. Tlg2p is implicated in Early Endosome biogenisis [210]. Ufe1p mediates homotypic ER→ER fusion [211]. Vam3p is implicated in PVC→Vacuole [215a,215b] and homotypic Vacuole→Vacuole fusion [208].

SNAP-25 family

SNAP-25 (25 kDa) is anchored to pre-synaptic membranes via covalently attached fatty-acyl chains [183], and is also predicted to have extensive coiled coil domains. SNAP-25 is sensitive to cleavage by BoTx A/E near the C-terminus [186,189]. Two mammalian SNAP-25 homologues, named SNAP-23 [227,231] and SNAP-29 [225] have been identified. Only two yeast SNAP-25 homologues (Sec9p,Vam7p) have been identified [202,203]. Sec9p was implicated in yeast post-Golgi→PM transport [202]. Vam7p is involved in homotypic Vacuole fusion [203].

VAMP-associated proteins (VAPs)

A new class of mammalian SNARE proteins termed VAMP-associated proteins (VAPs), have been discovered. The first VAP was identified in Aplysia, named aVAP-33 [235]. Subsequently human homologues of aVAP-33 termed VAP-A and VAP-B, have been identified [236,237]. VAPs also possess a coiled-coil domain and a carboxyl-terminal transmembrane domain. It has been shown that VAPs associate with each other via their transmembrane domains to form complexes, which might be important for mammalian vesicular traffic [237].

Table 1(a) : Functional distribution of known yeast SNAREs.

Stage of transport	v-SNAREs	t-SNAREs	References
ER-ER	?	Ufe1p	211
ER-Golgi	Bos1p,Bet1p,Sec22p,Ykt6p	Sed5p	205-207,212
TGN-PM	Snc1, Snc2	Sso1, Sso2, Sec9p	199,200,202
TGN-PVC	Vti1p	Pep12p	209a,214
Early EN biogenisis	?	Tlg2p	210
PVC-Vacuole	Vti1p	Vam3p, Vam7p	209b,215,203
Vacuole-Vacuole	Nyv1p	Vam3p, Vam7p	208,203

Table 1(b) : Localisation of known mammalian SNAREs.

SNAREs	Localisation	References
VAMP 1	PM/SG	216
2	PM/SG	217
3	EE/RE	194, 196a, 196b
4	TGN	218
5	PM/EE	219
7	LE	218, 220
8	EE	221
hYkt6	ER/Golgi	232
rSec22	ER	233
rBet1	PGI/Golgi	233
GOS-28	Golgi	233
Membrin	Golgi	234
Syntaxin 1-4	PM	195
5	PGI/Golgi	195
6	EE/TGN	222
7	EE/LE	223, 224
8	EN	225
10	TGN	226
11	LE/TGN	227, 218
12	EE/LE	228
13	EE/RE	218, 229
16	Golgi	230
17	ER	225
SNAP-23	PM/SG/TGN/LE	231, 227
25	PM	170
29	Golgi/TGN/E/PM	225
VAP-33	?	235
A	?	236,237
B	?	237

1.4.2 Rab family

A role for GTP-binding proteins in the regulation of vesicular membrane traffic has first been indicated by the finding that micro-injection of GTPγS into mast cells leads to degranulation, even in the absence of Ca^{2+} [241]. Sec4p has been the first GTP-binding protein to be implicated in this role, as mutations in the SEC4 gene of yeast blocked Golgi→PM transport and lead to the accumulation of secretory vesicles [246]. Sequence analysis of Sec4p show that it is a homologue of the mammalian GTPase, Ras. The yeast Ras homologue Ypt1p is required for transport from the ER to and through the Golgi apparatus [166,242]. A large family of Ras-related GTP-binding proteins (termed 'Rabs') has been identified in yeast and mammalian cells, required at various steps along the secretory, endocytic and recycling pathways [242].

Rab proteins are intrinsically hydrophilic, but are attached to membranes via their C-terminal attached isoprenyl lipid (geranyl-geranyl). These proteins are specifically localised to the cytoplasmic surface of intracellular compartments owing to their functional distribution [Table 2]. No Rab proteins have been localised to lysosomes as yet. Because of the functional distribution of rab proteins, it was proposed that they direct vesicle transport targeting [242]. However, this functional attribution seems untenable due to the findings that a chimera of Ypt1p and Sec4p can provide Rab function to the entire secretory pathway from the ER to the PM without misorting [238a,b], and that overexpression of v-SNAREs [197] can overcome the requirement of Ypt1p. Although it has been shown that Rab proteins facilitate the assembly of SNAREs [Figure 1.4, step 5], they do not, however, form part of the isolated docking complexes [175,207].

Rab Accessory proteins

The conversion between the GTP-bound and GDP-bound states of Rabs are regulated by

accessory proteins which include GAP (GTPase-activating protein), GEF (Guanine nucleotide exchange factor) and GDI (GDP dissociation inhibitor).

A GAP that acts on Ypt6p has been cloned from yeast [256]. GEFs that act on Sec4p [255] and Rab3A [254] have been identified. A GDI that acts on a broad range of Rab proteins, termed Rab-GDI, has been purified from bovine brain [257]. The role of Rab accessory proteins during Rab action in SNARE assembly has been proposed [Figure 1.4, steps 7a,b,c].

Table 2: Functional distribution of Rab family members in intracellular vesicular transport

Protein	Function	References
Mammalian		
Rab 1	ER → Golgi; intra-Golgi	247,240
2	ER → Golgi	247
3	Regulated exocytosis	244
4	early Endosomes → PM	248
5	PM → early Endosomes	239
6	? (Medial-Golgi location)	250
7	Early → late Endosomes	251a,b
8	TGN → basolateral PM	243
9	Late endosome → TGN	245
11	En → PM (Recycling)	253
Budding Yeast		
Ypt1p	ER → Golgi; intra-Golgi	242
Sec4p	Golgi → PM	246
Vps21p	Golgi → Endosome	252
Ypt7p	Endocytosis	249

1.4.3 Rab Effectors

A variety of downstream effector proteins of Rab activity (viz. Rabphillin 3A, Rabaptin-5, EEA1, Rab-kinesin-6, Noc2, Rim, Hrs-2, TIP47, p40, exocyst, Vac1p) have been identified [258-268]. Each effector protein contains a Rab-binding domain (RBD) followed by a linker region, and a second domain that can interact with a variety of molecules. The second domain can either interact with another Rab (e.g. Rabaptin-5 binds Rab4 and Rab5) or with the cytoskeleton (eg. Rab-kinesin-6 binds kinesin, Noc2 binds zyxin, Rabphillin-3A binds α-actinin), or bind to a target membrane (e.g. the exocyst binds the PM), or with a second messenger (e.g. Rabphillin-3A binds Ca^{2+}, EEA1 binds PIP), or possibly with SNAREs (eg. Hrs-2 binds SNAP-25), or with cargo proteins (e.g. TIP-47 binds MPR). Thus, a wide variety of functions can be attributed to the action of Rab/effector complexes. A list of Rab effectors is shown by Table 3.

Table 3 : A list of known Rab Effectors

Rabs	Rab Effectors	References
Mammalian		
Rab 3	Rim	258
3A	Rabphilin-3A, Noc2	259,260
4	Rabaptin-5	261
5	Rabaptin-5, EEA1	261,262
6	Rab-kinesin-6	263
9	p40	264
?	Hrs-2	265
?	TIP-47	266
Budding Yeast		
Sec4p	Exocyst	267
Vps21p	Vac1p	268

1.4.4 The Sec-1 Family

SNARE assembly in addition to the role of Rabs, is also regulated by members of a Sec1p family [269,192]. Their discovery is rooted by the finding that a sec1 yeast mutant, defective in post-Golgi transport [115], is restored to normality by overexpression of putative PM t-SNAREs Sso1p and Sso2p [200]. Yeast homologues of Sec1p, termed Sly1p [197] and Slp1p [270], have been implicated in ER→Golgi and Golgi→Vacuole transport, respectively.

Since a deletion of the YPT1 gene (encoding ER→Golgi Rab protein) can be overcome by a mutated Sly1p (i.e. the ER→Golgi Sec1p homologue), or by overexpression of Sec2p (i.e. the putative ER v-SNARE) [197], and N-sec1p (a neuronal homologue of Sec1p) binds tightly to syntaxin and prevents VAMP from binding [271,272], it is thought that Sec1p family members oppose the function of Rabs by preventing SNARE assembly [Figure 1.4, step 5]. Like Rab proteins, Sec1p members display a functional distribution [Table 4]. Thus Rab and Sec1p families provide an additional layer of specificity to control SNARE assembly. However, like Rabs, the Sec1p family members do not form part of the core-docking complex [271,272].

Table 4(a) : Functional distribution of known yeast Sec1p homologues.

Stage of transport	Sec1p family	Rab counterpart	References
Yeast			
ER→Golgi	Sly1p	Ypt1p	197
Golgi→Vacuole	Vps45p	Vps21p	252
Golgi→Vacuole	Slp1p	?	270
Golgi→PM	Sec1p	Sec4p ?	192,269
Mammals			
Exocytosis	N-sec1p	Rab-3	271,272

1.4.5 Velcro Factors

Tethering (an event which precedes docking mediated by SNAREs) of a transport vesicle with its target membrane [Figure 1.4, before step 5], was found to be mediated by a group of proteins termed as 'velcro' factors. The velcro factor known as p115 was found to be required for intra-Golgi transport [273] and Golgi→PM transport [274]. Uso1p, the yeast homologue of p115 is required for ER→Golgi transport [275,276]. The velcro p115 forms a bridge [277] between a receptor on the ER-derived vesicles known as giantin [278] and a receptor on the target Golgi membrane known as GM130 [279a,b]. As for SNAREs and Rabs, other p115 homologues may also be discovered, being required to tether vesicles to target membranes at other transport steps.

1.4.6 Annexins

Considerable evidence has been accumulated which suggests a role for annexins in membrane traffic [280]. Annexin VII (synexin) has been the first member of this family to be implicated in membrane interactions [284]. Subsequently, annexin VII [287] and annexin I (lipocortin) [283,286] have been shown to promote liposome fusion. Furthermore, annexin VII, annexin IV (endonexin I) and annexin VI (p67) can mediate chromaffin granule aggregation in vitro [268]. In addition, annexin VI has also been implicated in clathrin-coated vesicle budding at the PM [285], even though other findings suggest otherwise [457]. Annexin II is involved in aggregation and fusion of chromaffin granules with phospholipid vesicles [283] and seemingly with the PM [282], and has recently also been suggested to play a role in homotypic early endosome fusion [281]. In an in vitro assay that follows the proteins transferred from a labelled donor to an immobilised acceptor upon fusion of early endosomes, annexin II is efficiently transferred and immunogold labelling of cryosections confirm its presence on early endosomes in vivo [281]. Further studies are required to understand the precise function of annexins in membrane traffic.

1.4.7 The role of Heterotrimeric G-Proteins in membrane traffic

Heterotrimeric G-proteins are known to mediate signal transduction by linking PM receptors to downstream effectors [291]. Two classes of heterotrimeric G-proteins, namely G_S (stimulatory) and G_i (inhibitory) exist. G-proteins are a complex of α, ß and γ subunits. The α subunit cycles between an inactive GDP-bound state (which exists as a Gαßγ trimeric complex) and an active GTP-bound state. When an extracellular signal in the form of a ligand binds to a receptor (or when light interacts with rhodopsin), it induces a conformational change in the cytoplasmic domain of the receptor. Then, receptor-G protein interaction causes GDP release and binding of GTP, which in turn causes the G-protein to dissociate into α and ßγ subunits. The free GTP-bound α subunit and ßγ subunit can now activate downstream effectors [291,290].

It is well known that there are intracellular pools of heterotrimeric G-proteins, either bound to internal membranes [292] or free in the cytoplasm [293,294], but their functional significance has not been clear. Evidence has accumulated that implicates a role for these intracellular trimeric G-proteins in vesicular transport [299]. Indirect evidence comes from the finding that Aluminium fluoride (AlF_3; acts as a complex that mimics the γ-phosphate of GTP) which acts on trimeric G-proteins [295], but not on small GTP-binding proteins (i.e. ARF, Rab, Rap and Ras) [296], inhibits various steps along the secretory [126] and endocytic [297] pathways. Mastoparon (an amphipathic peptide that activates Gα subunits) potently inhibits ER to Golgi transport [301]. More direct evidence comes from the finding that overexpression of G_{i-3}, which is partially localised to the cytoplasmic membrane surface of the Golgi [298], slows proteoglycan transport through the Golgi [299]. It has also been shown that in vitro budding of constitutive and regulated secretory vesicles from the TGN is inhibited by AlF_3, but stimulated by addition of purified ß subunits [300]. Furthermore, G_S and G_i have been implicated in vesicular transport in polarised cells [302]. Recently it has been shown that G_S, present in early endosomes in CHO cells [303], regulates endosome fusion [304].

1.5 Dissection of Homotypic fusion

Not all intracellular fusion events are governed by a NSF-based SNARE system. Initial indications come from the observation in MDCK cells, that fusion of Golgi-derived transport vesicles with the apical PM involves a mechanism independent of NSF, SNAPs and Rabs [305]. Karyogamy (i.e. nuclear envelope fusion), which follows mating in yeast, can be reconstituted in vitro by using an ER fusion assay (as the ER is continuous with the nuclear envelope), and has been shown to be independent of NSF (Sec18p) and SNAP (Sec17p) [306]. The cell division cycle gene product, Cdc48, has been implicated in this process. A temperature-sensitive cdc48 mutant is arrested late in mitosis and accumulates elongated nuclei with no apparent fission and is conditionally defective in ER fusion in vitro [307]. The defect can be complemented by addition of wild-type Cdc48p or inhibited by anti-Cdc48p antibodies.

The Cdc48p seems to be conserved throughout evolution. A homohexamer has been found in Xenopus, with its monomer p97 (97 kDa) sharing 76% sequence identity with Cdc48p (112 kDa) [291]. Cdc48p and p97 exhibits significant sequence homology to yeast and mammalian NSF [308,311]. Another homologue of Cdc48, VCP (i.e. Vasolin Containing Protein, but incorrectly named as it is not the precursor to vasolin), has been identified in different species [309,310,313]. A 92 kDa VCP that is 70% identical to Cdc48p has been characterised in Pig [310]. A 100 kDa VCP has been shown in vitro to interact with clathrin heavy chain in bovine brain extracts [312]. This association with clathrin hinted at the involvement of VCP in membrane transport interactions. In yeast, a 117 kDa hydrophilic protein, Pas1p, which is also a member of the novel family of putative ATPases, has been implicated in peroxisome biogenesis [314]. Another member of this family, Afg2p, also in yeast, serves an essential role in mitosis, though its exact function is unknown [315].

During mitosis, endocytic and secretory pathways are arrested, accompanied by disintegration of complex organelles (like the ER and Golgi) thought to assist in their positioning between the two daughter cells [316]. In particular, Golgi fragments are generated during metaphase, becoming dispersed within the cytoplasm [317]. After telophase, the Golgi apparatus rapidly reassembles [317], so do other complex organelles [141]. This reassembly process has been reconstituted in vitro using Golgi complex membranes dissociated by exposure to mitotic cytosol or the drug ilimiquinone, at 37°C [319,321]. A role for p97 has been illustrated by the finding that complete Golgi regrowth from mitotic fragments (mixture of cisternal elements and vesicular structures) requires the addition of either p97 or NSF/SNAPs/p115 (vesicle docking protein) [274] to NEM or salt treated membranes [319], while assembly of Golgi stacks from VGMs (vesiculated Golgi membranes) requires the sequential action of NSF/SNAPs followed by p97 [321]. This point of difference (i.e. the independent versus sequential action of NSF/SNAPs and p97) may be reconciled by noting that the membranes in the two different assays are derived by different procedures. Nonetheless, a p97-mediated Golgi fusion event, independent of NSF/SNAPs, is demonstrated.

Vesicular protein traffic (involving heterotypic fusion events) between membrane compartments of both the endocytic [297] and exocytic [242] pathways is inhibited by GTPγS. Similarly GDI (guanine nucleotide dissociation inhibitor) has been shown to inhibit vesicular transport from ER to Golgi [324], between Golgi cisternae [323] and from endosomes to TGN [322]. In contrast to these NSF-dependent fusion events, p97-dependent fusion events are not affected by GTPγS nor Rab-GDI [321]. Despite the structural homology, ATPase features and NEM sensitivities of NSF and p97, it is quite clear that p97 is by no means a simple isoform of NSF. A functional distinction between NSF and p97 may be premature considering that fusion events are defined somewhat arbitrarily as homotypic or heterotypic. For example, early endosome fusion in vitro has been defined as a homotypic fusion event, even though fusogenecity depends on Rabs [325] and NSF [158,326].

1.6 Thesis Approach

Endocytic processing involves specific fusion events between distinct populations of organelles along the endocytic pathway [Figure 1.5]. Homotypic fusion occurs amongst early endosomes and amongst late endosomes and lysosomes. Heterotypic fusion occurs between late endosomes and lysosomes. The targeting molecules that confer specificity to these fusion events have only been partially defined. Furthermore, existing in vitro assays for organellar fusion do not distinguish between targeting and the subsequent fusion event.

The SNARE hypothesis [Section 1.3.2.2] postulates that each kind of transport vesicle bears a unique vesicle SNARE (v-SNARE) that forms a unique match with its cognate target SNARE (t-SNARE) present on the target membrane, thereby achieving targeting/docking specificity. However, it has been shown that multiple v-SNAREs are often present on a single class of transport vesicle [397,398] and that a single v-SNARE can direct both retrograde and anterograde transport between two compartments [399]. Thus specific compartmental localisation of SNAREs is not absolute. Moreover, it has been demonstrated that a variety of v-SNAREs and t-SNAREs pair indiscriminately [193] in vitro. Thus SNAREs alone cannot account for specificity of membrane trafficking.

Due to the functional distribution of Rab proteins, it is proposed that they direct targeting of transport vesicles [242]. However, this functional attribution also seems untenable due to the observation that a chimera of yeast Rab homologues Ypt1p (ER to Golgi) [242] and Sec4p (Golgi to PM) [246] can provide Rab function to the entire secretory pathway from the ER to the PM without misorting [238a,b], and that overexpression of v-SNAREs [197] can overcome the requirement of Ypt1p. Rab proteins facilitate the assembly of SNAREs, but do not form part of the docking complex [175,207].

Though SNAREs or Rabs alone are insufficient to ensure selective targeting for specific fusion they may cooperate to specify the target membrane. However, it has been shown

that SNARE-Rab interactions are non-selective since the nucleotide-free forms of six Rabs bind with comparable low affinity to three SNAREs (Ssop, Pep12p, and Sncp) [400]. Thus SNAREs and Rabs also do not seem to cooperate to specify the target membrane for fusion.

Recently, it has been proposed that unique stage-specific factors such as TRAPP (ER to Golgi)[276a,b], the exocyst (Golgi to PM) [267a,b] and EEA1 (homotypic endosome fusion)[262] may direct fusion fidelity. Additionally, factors that mediate vesicle interactions with the cytoskeleton may also play pivotal roles in vescle targeting.

Considering the above, it remained likely that other factors (yet to be discovered) might play crucial roles in mediating high fidelity docking, before SNARE interactions. To search for such additional or novel targeting molecules, two methods (named the crosslink approach and phagosome approach) were employed in this study. The crosslink approach [Figure 1.6] involved the use of luminal cross-linking to render endosomes and lysosomes to render these organelles fusion-inactive and detergent-insoluble. Purified cross-linked endosomes or lysosomes were used as *'acceptors'* to bind potential targeting molecules by incubating them with metabolically labelled *'donor'*, either cytosol or detergent-solubilised membrane. In the phagosome approach [Figure 1.7], the binding assay was done in the absence of detergent, allowing for intact membrane in both acceptor and membrane donor preparation. For this purpose, paramagnetic latex beads [see Section 1.2.5] were used to purify phago-endosomes and phago-lysosomes as acceptors. Membrane donor was prepared by sonicating metabolically labelled membrane in the presence of an excess of phospholipid in order to separate donor proteins into individual vesicles. Bound material was isolated and analysed by two-dimensional electrophoresis and subsequent radioactive scanning. To determine the origin of bound material as being from endosomes or lysosomes, the membrane composition of paramagnetic latex bead-containing phagosomes was analysed by two-dimensional electrophoresis. The proteins of interest were then analysed by mass spectrometry or Edman microsequencing.

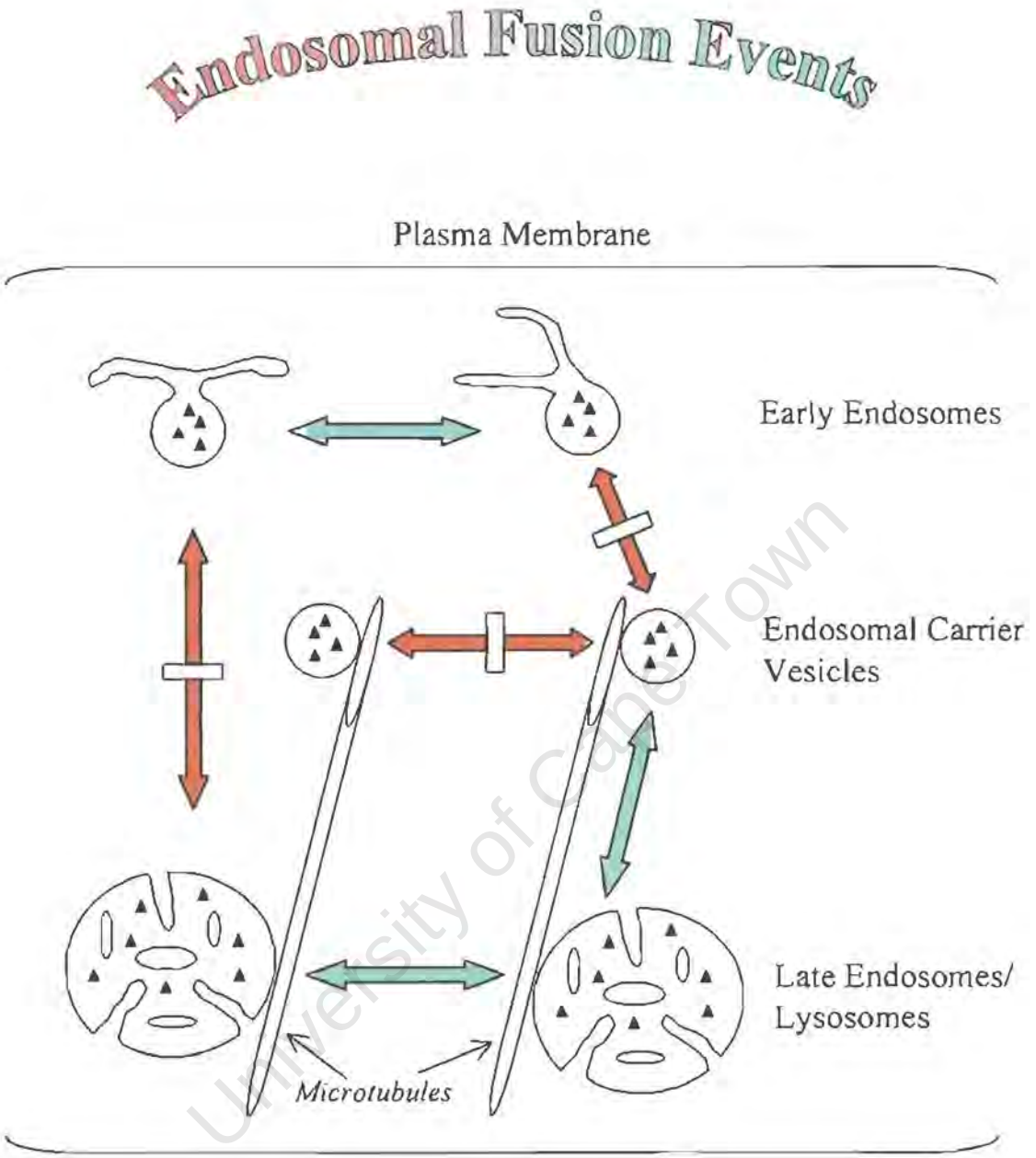

Figure 1.5 : Endosomal Fusion Events in vitro. Reconstituted fusion events include homotypic fusion between Early Endosomes or between Late Endosomes and the heterotypic fusion of ECVs with Late Endosomes {⟺}. Fusion events which cannot be reconstituted include heterotypic interactions of Early Endosomes with ECVs or Late Endosomes and homotypic interactions between ECVs {⟸⊣⟹}. [Redrawn according to Ref. 69]

Figure 1.6 : **CROSSLINK APPROACH**

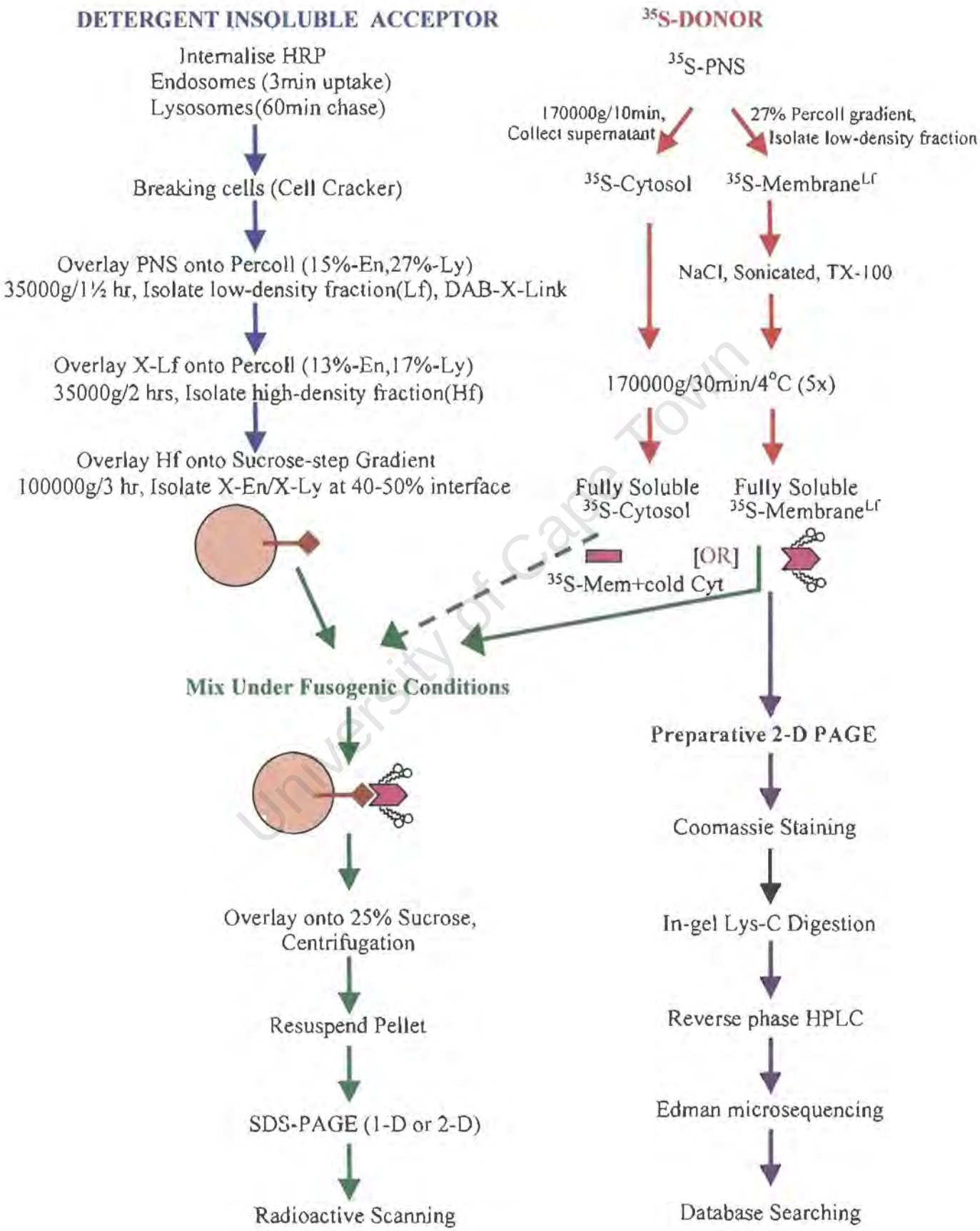

Figure 1.7 : **PHAGOSOMAL APPROACH**

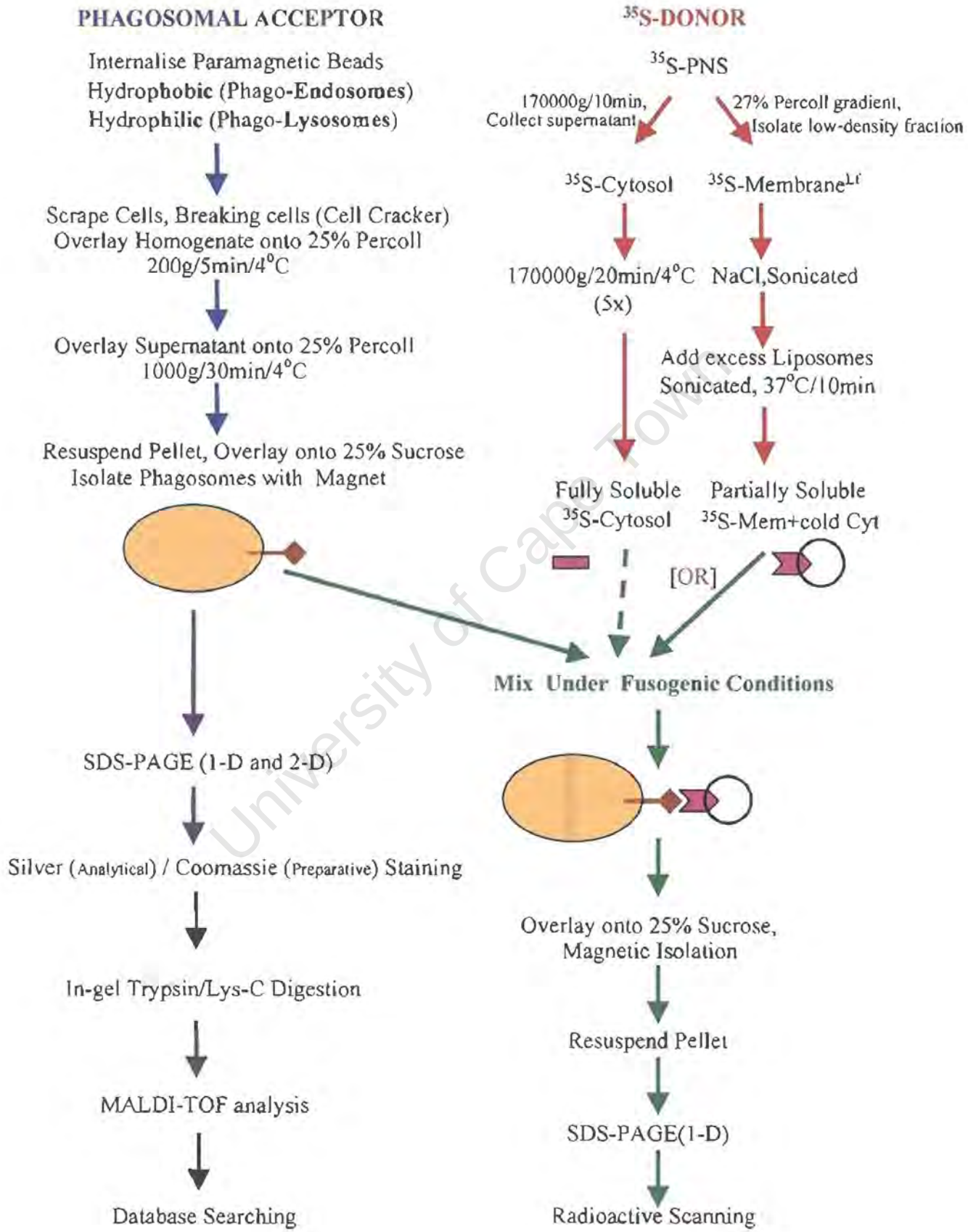

CHAPTER 2

PURIFICATION AND CHARACTERISATION OF DETERGENT INSOLUBLE ACCEPTORS

2.1 BACKGROUND

Endocytic processing involves specific fusion events between distinct populations of organelles along the endocytic pathway. Homotypic fusion occurs amongst early endosomes and amongst late endosomes and lysosomes. The targeting molecules that confer specificity onto these fusion events have not been unambiguously defined.

The main reason for this delay is due to the difficulty in isolating pure (homogenous) endocytic organelles. Ficoll, percoll and sucrose gradients have been used to achieve some degree of purification, but these techniques have not brought about sufficient information to delineate the whole of the machinery involved in the docking and/or fusion process.

In an attempt to purify organelles along the endocytic pathway and define their constituents, the horseradish peroxidase (HRP)-3,3'-diaminobenzidine (DAB) density-shift procedure was developed [340,341]. The technique involves loading endocytic structures with HRP that is able to catalyse (in the presence of H_2O_2) the polymerisation of DAB (a membrane permeable molecule) and thereby increasing the buoyant density of these vesicles, and allowing their separation from other organelles on density (sucrose or percoll) gradients. Unfortunately, subsequent analysis showed that the cross-linking reaction also oxidises the luminal contents of the vesicles, rendering them detergent insoluble [342]. Thus, it was not possible to extract the protein from these organelles to analyse their composition. Since the membrane components (particularly the cytoplasmic domains) could be expected to remain unaffected by the luminal DAB cross-linking, the detergent insoluble vesicles could be used as acceptors to pull out cytosolic and membrane machinery (from a fully soluble donor) that bind to them, including possible molecules

involved in the docking process.

In this study, the DAB density-shift procedure was modified to purify cross-linked endosomal or lysosomal structures to render these organelles fusion-inactive and detergent-insoluble. P388D_1 mouse macrophages were pulsed with HRP for 3 min to load early endosomes (since early endosomes mature within 3-5 min into a state where they no longer fuse with subsequently formed early endosomes [63,67]), or additionally chased for 60 min to load lysosomes. The integrity of the cross-linked organelles was first assessed, before a binding assay was designed to employ them as macro acceptors [Chapter 3].

2.2 MATERIALS AND METHODS

2.2.1 Cell culture and harvesting

Mouse macrophage cells of the line $P388D_1$ were cultivated in RPMI 1640 medium (Highveld Biological, SA) supplemented with 10% bovine foetal calf serum (Highveld Biological, SA), penicillin and streptomycin at 100 U/ml and 100 µg/ml respectively. The cells were kept at 37°C in a 5% CO_2 environment incubator (Queue). The macrophages were propagated into suspension from monolayer cultures in 175 cm^2 tissue culture flasks (Nunc A/S, Roskilde, Denmark) with 30 ml of medium per flask replaced every 24 hours.

Cells in suspension from 12 flasks (360 ml) were harvested into sterile 50 ml specimen tubes (Evergreen, Los Angeles, CA, USA) and centrifuged at 200g for 5 minutes at 4°C (Beckman TJ-6 centrifuge, Beckman Instruments, Palo Alto, CA, USA) [334]. The cell pellets were combined and washed twice in a 20 ml volume of appropriate medium or buffer depending on the purpose for which the cells were to be used.

2.2.3 Determination of cell number and viability

A 50 µl aliquot of the cell suspension was taken into 20 ml of isotonic saline solution (Isoton, Coulter Electronics, SA) and cell number determined by means of a Coulter counter (Coulter Electronics, Florion, USA). Cell viability was determined by the extent of trypan blue dye exclusion from viable cells. 50 µl of cell suspension was combined with 50 µl buffer Trypan blue solution (0.5% trypan blue, 140 mM NaCl, 4.7 mM KCl, 1.2 mM KH_2PO_4, 0.6 mM $MgSO_4$, 10 mM Hepes, pH 7.2). An aliquot was placed in a haemocytometer, viewed under a microscope and the percentage trypan blue free cells determined. Cells were deemed unfit for experimental work if viability was less than 90%.

2.2.4 Cell homogenisation

After experimental manipulations, cells were resuspended at 4 x 10^7 cells/ml in cold homogenisation buffer (250 mM sucrose, 0.5 mM EGTA, 20 mM Hepes-KOH, pH 7.0, 1 mM dithiothreitol, 1 mM PMSF, 0.1 mM Leupeptin, 1 μM Pepstatin) [104,327]. The cells were then disrupted using a stainless steel ball homogeniser, pre-chilled on ice. Typically, 12 strokes through the homogeniser yielded 80-90% breakage as determined by trypan blue exclusion [Section 2.2.3]. The homogenate was centrifuged at 1000g for 20 minutes (Beckman TJ-6 centrifuge, Beckman Instruments, Palo Alto, CA, USA) and the resulting post-nuclear supernatant (PNS), collected and processed further or snap frozen and stored in 300 μl aliquots at -80°C.

2.2.5 Purification of Acceptors [Figure 1.6, blue arrows, page 36]

2.2.5.1 Preparation of age-specific Acceptors

Cells were washed twice in cold RPMI-Hepes-BSA (RPMI 1640 medium, 10 mM Hepes, pH 7.4, 0.1% BSA) before resuspension at 5 x 10^6 cells/ml in this buffer in a 100 ml Erlenmeyer flask. The cell suspension was then warmed to 37°C for 15 minutes in an orbital shaking water bath. At time zero horse radish peroxidase (HRP) was added at 1 mg/ml and the cells allowed to internalise the marker for 3 minutes. This filled early endosomes with the marker [329,60]. After the incubation period the cell suspension was made to 50 ml with cold Hepes-Saline-BSA and the cells pelleted by centrifugation at 200g for 5 minutes at 4°C. The supernatant was aspirated off, the cell pellet resuspended in 10 ml Hepes-Saline-BSA and transferred to a new tube to eliminate the effects of HRP adhered to the tube walls. The cells were washed three times with cold Hepes-Saline-BSA. To label lysosomes with the HRP marker [90,329], the washed cells were resuspended in warm RPMI-Hepes-BSA and incubated for 60 minutes at 37°C. Cells were then washed

twice with cold Hepes-Saline-BSA and once with homogenisation buffer prior to homogenisation [Section 2.2.4]. The PNS was collected and then placed on a Percoll solution (15% Percoll solution for endosomes, 27% Percoll solution for lysosomes) and centrifuged at 35000g for 1½ hours at 4°C in an swing-out type rotor (SW-40) in a Beckman ultracentrifuge (Beckman Instruments, Palo Alto, CA, USA). The gradient was fractionated and the low-density fraction was collected for subsequent cross-linking [Section 2.2.2.5]. The gradient distribution of different compartments was followed by performing marker assays [Section 2.2.6].

2.2.5.2 DAB (3,3' diaminobenzidine) cross-linking of HRP containing organelles

DAB (3,3' diaminobenzidine) cross-linking of HRP-containing organelles, was performed as described previously [340]. DAB (Sigma Chemical Company, St. Louis MO, USA) was made at 3 mg/ml in Hepes-Saline buffer and the resultant suspension placed in an ultrasonic bath for 5 minutes to aid dissolution of the DAB. The solution was filtered through a 0,22 µm Millex filter (Millipore, France) to remove undissolved DAB. This solution was prepared fresh prior to it being required. 180 µl of the DAB solution was added per ml material (low-density fraction) and incubated on ice for 10 minutes in the dark. 20 µl of a 0.3% H_2O_2 solution was then added per ml material and the solution was then incubated at room temperature for 20 minutes in a the dark after which an equal volume of cold Hepes-Saline-BSA buffer was added in order to quench excess peroxide present.

2.2.5.3 Isolation of cross-linked material

The crosslinked material was placed on a Percoll solution (13% Percoll for cross-linked endosomes, 17% Percoll solution for cross-linked lysosomes), and centrifuged at 35000g for 2 hours in an swing-out type rotor (SW-40) in an Beckman ultracentrifuge (Beckman Instruments, Palo Alto, CA, USA). The high-density fraction was collected and overlaid

onto a sucrose-step gradient (prepared with 2 ml of each of the following sucrose concentrations: 85%, 60%, 50%, 40% and 20%), and then centrifuged at 100000g for 3 hours at 4°C in a swing-out type rotor (SW-40) in a Beckman ultracentrifuge. The fraction at the 40-50% sucrose interface was collected as the enriched cross-linked acceptor fraction, and stored in aliquots at -80°C.

2.2.6 Marker Assays

2.2.6.1 Golgi

Galactosyltransferase, (UDP galactose: 2-acetamido-2-deoxy-D-glucosylglycopeptide-galactosyltransferase) was utilised as a marker for Golgi [331]. The enzyme activity was measured by a modification of the method previously described [330,332]. UDP-^{14}C-galactose was used as the substrate and N-acetylglucosamine was employed as the acceptor molecule. Specific galactosyltransferase activity was defined as the total hydrolysis and transfer (assays in the presence of N-acetylglucosamine) minus the non-specific substrate hydrolysis (assays in the absence of N-acetylglucosamine). Assay mixtures (in a final volume of 200 µl) contained the following reagents (final concentrations): 40 mM cacodylic acid, pH 6.6, 1 mM DTT, 0.4% (w/v) Triton X-100, 40 mM $MnCl_2$, 20 mM N-acetylglucosamine or H_2O, 1.05 mM UDP-^{14}C-galactose (≈ 25,000 cpm/assay), and 1 mM ATP added to protect against non-specific substrate hydrolysis [333]. The reactions were carried out at 37°C for 60 min and terminated with the addition of 100 µl of 0.25 M EDTA (pH 7.4) and immediate chilling in an ice bath. N-acetyllactosamine, the product of the transferase reaction, was separated from unreacted UDP-galactose, galactose-1-phosphate, and free galactose by chromatography on AG 1-X8 (200-400 mesh, Cl form) anion exchange columns. Washed resin was poured to a bed height of 5 cm in pasteur pipette columns (I.D. = 8 mm). Columns were washed with 5 ml of 5% (w/v) sodium borate and 3 ml of water before applying the 300 µl sample. Assay tubes were washed with 500 µl of water, which was also applied to the columns before eluting with 5 ml of water. The entire

effluent (5.8 ml) was collected in scintillation vials, mixed with 6 ml of scintillation fluid, and counted in a Packard TriCarb 19a CA liquid scintillation analyser. The columns were reused 8-10 times by using the following regeneration procedure. UDP-galactose, galactose-1-phosphate and galactose were removed by elution with 5 ml 1M NaCl and the protein was removed by washing with 3 ml 1M NaOH, 3 ml H_2O, 3 ml 1M HCl, and 3 ml H_2O. The columns were converted to the borate form [333] by washing with 5 ml of 5% (w/v) sodium borate and washed to neutrality with water.

2.2.6.2 Endocytic Organelles

Horseradish peroxidase was determined in a similar manner as previously described [334]. Equal aliquots of 10-50 µl, sufficient to give an adequate absorbance overall, were taken from each gradient fraction and substrate solution (0.55 mg/ml 2,2-azino-di-3-ethylbenzthiazoline sulfonate, 0.003% H_2O_2, 150 mM NaCl, 0.1% Triton X-100, 20 mM phosphate citrate buffer, pH 4.3) was added to make up a volume of 500 µl. After incubation for 30 min at room temperature, the reaction was stopped by the addition of 500 µl stop solution (100 mM citric acid, 0.01% NaN_3). The absorbance was measured at 420 nm. A background curve, prepared from a gradient overlaid with postnuclear supernatant obtained from horseradish peroxidase-free cells, was subtracted.

2.2.6.3 Lysosomes

N-Acetylglucosaminidase (GlcNAc-ase) was measured as described previously [335]. Equal aliquots of 10-50 µl, sufficient to give an adequate absorbance overall, were taken from each gradient fraction and the volume made up to 100 µl with 150 mM NaCl. Then, 100 µl substrate solution (2 mM p-nitro-phenyl-N-acetyl-ß-D-glucosamine, 150 mM NaCl, 0.2% Triton X-100, 25 mM citrate buffer, pH 5.0) was added. After incubating for 60 min at 37°C, the reaction was stopped with 800 µl 50 mM NaOH. The absorbance was measured at 400nm.

2.2.6.4 Plasma Membrane

The Plasma Membrane (PM) was labelled with radioactive galactose, to monitor its' distribution upon fractionation [Section 2.2.7.1 & 2.2.7.2]. Cell membranes were labelled using a technique whereby ^{3}H or ^{14}C labelled galactose is enzymatically linked to terminal N-acetyl glucosamine residues on cell-surface glycoconjugates by the enzyme galactosyl-transferase [337]. The entire procedure was carried out on ice in order to arrest membrane internalisation.

2.2.7 PM labelling to measure cross-linking efficiency

2.2.7.1 Removal of terminal 1,4 ß-galactose moieties prior cell surface labelling

Cells were resuspended in one volume of Hepes-Saline-BSA buffer containing 0.2 U/ml ß-galactosidase (a glycosidase from *Streptococcus pneumoniae*) and incubated at 0°C for 5 minutes with frequent gentle agitation to prevent sedimentation of the cells and ensure efficient mixing of the reagents. Pre-treatment of the cells increased the efficiency of the subsequent surface labelling procedure (≈ 10-fold) [337] increasing the number of sites available for glycosylation. After incubation the reaction was terminated by 10-fold dilution of the suspension in cold Hepes-Saline-BSA buffer. The cells were then pelleted and kept on ice.

2.2.7.2 Cell surface membrane labelling

The labelling mixture containing 50 µl 50 mM $MnCl_2$, 50µl galactosyl transferase (0,25 units, Sigma Chemical Co., St. Louis, MO.), 20 µl UDP[6-^{3}H]-galactose (ammonium salt, 20 Ci/mmol, Amersham, UK) and 5 µl cold UDP-galactose was adjusted to 0.5 ml with Hepes-Saline-BSA buffer. This mixture was then added at 0°C to the cell pellet (≈ 0.5 ml) and the cells resuspended. The final concentrations were as follows: 5 mM $MnCl_2$, 0.5

U/ml galactosyltransferase, 2 μM UDP[6-^{3}H]-galactose. The cell suspension was incubated at 0°C for 30 minutes with frequent gentle agitation. The reaction was stopped by 10-fold dilution of the cell suspension with cold Hepes-Saline-BSA buffer.

2.2.7.3 Internalisation of labelled membrane glycoconjugates

Cells surface-labelled with UDP[6-^{3}H]-galactose were washed once with cold RPMI-Hepes-BSA, before resuspension in the same buffer at a concentration of 5 x 10^6 cells/ml. The cell suspensions were warmed to 37°C in an orbital shaking waterbath (Labline Instruments, ILL, USA) and the respective labels internalised for 45 minutes. Internalisation was halted, by diluting the cells 10-fold in cold Hepes-Saline-BSA buffer. The cells were then washed once with cold Hepes-Saline-BSA.

2.2.7.4 Removal of remaining cell surface label

To each cell pellet an equal volume of 0.5 U/ml ß-galactosidase in Hepes-Saline-BSA was added and incubated for 30 minutes at 0°C with frequent agitation. The reaction was stopped by ten-fold dilution in cold Hepes-Saline-BSA buffer. Cells were then washed three times with Hepes-Saline-BSA buffer and finally with homogenisation buffer prior to homogenisation [Section 2.2.4].

2.2.8 Scanning Electron Microscopy of X-linked Acceptors

Triton X-100 treated non-crosslinked PNS and purified X-acceptors were spread onto separate 0.02 μm filters, then fixed sequentially (10 min each at 25°C) with 2.5% gluteraldehyde, 1% osmium tetroxide and 1% uranyl acetate. Dried samples were mounted onto aluminium stubs and then subjected to scanning electron microscopy.

2.3 RESULTS AND DISCUSSION

2.3.1 20-70% Sucrose Gradient Method

$P388D_1$ mouse macrophages were allowed to internalise HRP for 15min at 37°C. After washing, cells were disrupted using a cell cracker, and a postnuclear supernatant (PNS) was produced. Half of the PNS was subjected to DAB crosslinking [Section 2.2.5.2]. In an attempt to purify X-linked acceptors, samples were overlaid onto a continuous 20%-70% sucrose gradient, and spun at 130000g for 4 hours in a SW-40 rotor. The gradients were then subjected to fractionation using a fraction collector (1ml portions) and the HRP content was measured in each fraction [Section 2.2.5.2]. Even though crosslinking inactivated the bulk of the HRP, a measurable amount was still present. Upon analysis it was observed that a density shift between the brown X-linked material (peaking at fraction 9) and the white non X-linked material (peaking at fraction 10), had occurred [Figure 2.1A].

The material in fractions 8, 9, and 10 were pooled and loaded onto a sucrose-step gradient [Section 2.2.5.3] and then centrifuged at 270000g for 3 hours. After centrifugation the following was observed. A white/creamish band was seen above the 20% sucrose layer, a faint brown band was evident at the 20%-40% sucrose interface, whereas a dark brown band was visible at the 40%-50% sucrose interface [Figure 2.1B]. Thus the majority of X-linked material exhibited a density range of approximately 1.19 to 1.22 mg/ml, comparable to what was observed previously [340,341]

Although the 20%-70% sucrose gradient produced a shift in the X-linked material, the shift was not appreciable enough to allow for satisfactory subsequent purification. Thus an alternative technique was sought to produce a greater separation between X-linked and non X-linked material. Therefore, it was tried to purify acceptors by Percoll gradients, prior to centrifugation on a sucrose step gradient [Section 2.3.2].

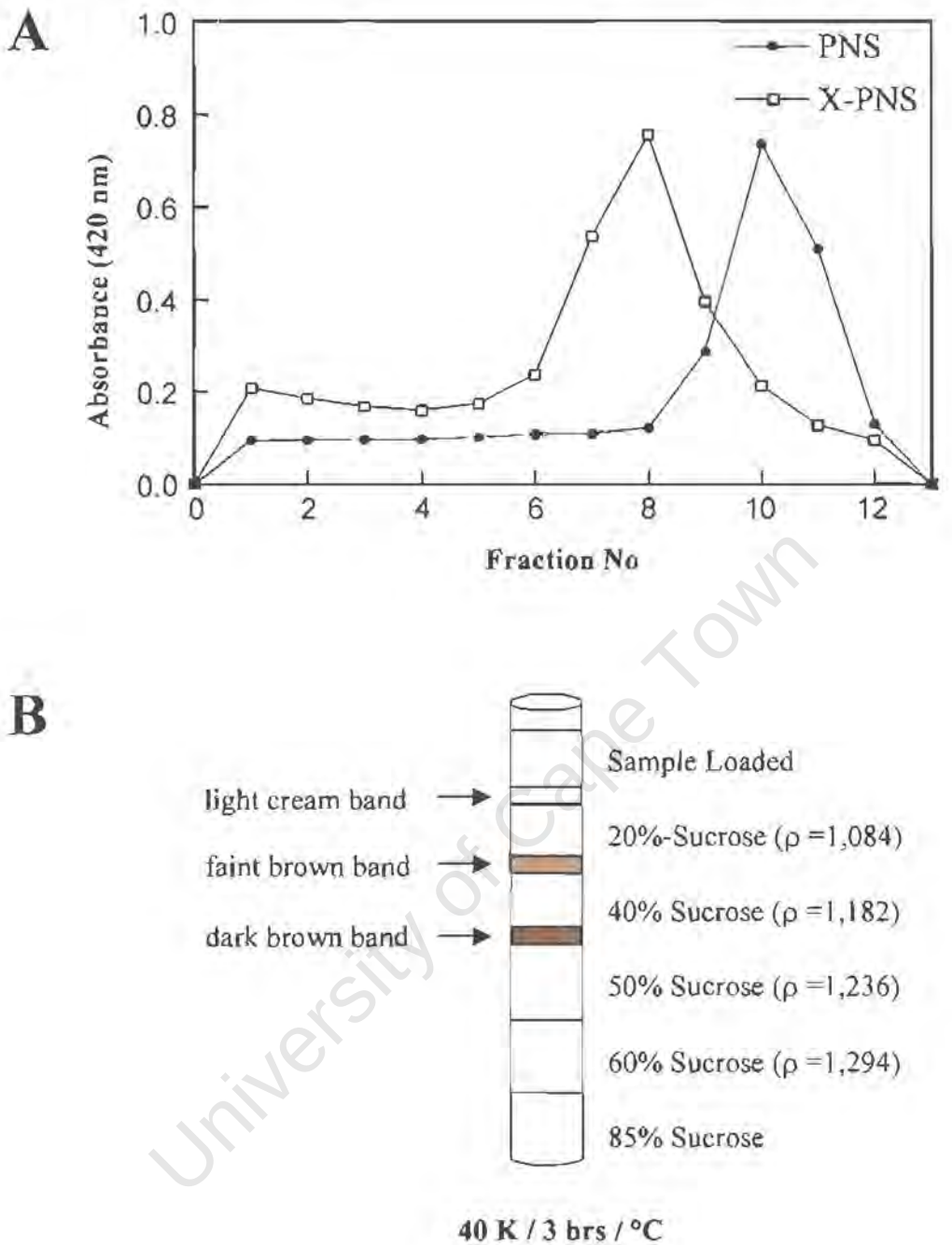

Figure 2.1 : Shift of DAB X-Linked material on a continuous 20-70% Sucrose (A) Gradient and a Step Gradient (B). **A)** P388D$_1$ mouse macrophages were allowed to internalise HRP for 15min at 37°C. Half of the postnuclear supernatant (PNS) was DAB crosslinked (X-PNS). Samples were overlaid onto a continuous 20%-70% sucrose gradient, and spun at 130000g for 4 hours in a SW-40 rotor. The gradients were then fractionated and the HRP content was measured. **B)** The material of fractions 8, 9, and 10 were pooled and loaded onto a sucrose-step gradient [Section 2.2.5.3] and centrifuged at 270000g for 3 hours. [Representative of four separate experiments]

2.3.2 Percoll and Sucrose-step gradient Purification of Acceptors

Purification of acceptors (i.e. X-endosomes and X-lysosomes) was performed by employing Percoll and sucrose-step gradients. A purification procedure was adapted from previously described purification methods [340-342]. To assess the effectiveness of Percoll gradients in the purification of acceptors the gradient distribution of various compartments were monitored by measuring the distribution of marker enzymes (their activities of HRP was decreased by X-linking) or radioactive label. The marker-enzyme assays [Section 2.2.6] for Lysosomes [N-Acetylglucosaminidase], Golgi [Galactosyltransferase] and HRP-containing endocytic structures were adapted from procedures as described previously [331,335,336]. The localisation of PM-label was followed as described [Section 2.2.6.4].

2.3.2.1 X-Endosome Acceptors

After loading P388D$_1$ macrophages for 3 min with HRP (1 mg/ml), the cells were subjected to cell cracking and PNS was prepared. The PNS was loaded onto a 15%-Percoll solution and centrifuged. The gradients were tapped from the bottom, and fractions were analysed for the marker enzymes and [^{3}H]-PM. The results were as indicated in Table 2.1(a) and Figure 2.2(A).

The low-density fractions (fractions 16,17,18), which represent ≈ 37% of the HRP-containing organelles, were pooled and then subjected to DAB-X-linking [Section 2.2.5.2]. The X-linked fraction was then overlaid onto a 13%-Percoll solution and centrifuged. This lower Percoll concentration improved yields. The resultant high-density fractions (fractions 1,2,3) as shown in Table 2.1(b), which contained 20.6% endosomes, 5.5% lysosomes, 7.2% Golgi and 12% PM of the original PNS, were pooled and overlaid onto a sucrose-step gradient [Section 2.2.5.3] and centrifuged. The fraction at the 40-50% sucrose interface was collected as the enriched X-endosome acceptor fraction [Figure 2.1(B)].

Table 2.1(a) : Fraction analysis for label and marker enzymes (PNS on 15%-Percoll).

Fraction No.	PM 15%W	HRP 15%W	NAG 15%W	GAL 15%W
1	3.442	0.991	10.825	2.000
2	13.247	7.112	11.471	2.000
3	2.096	3.034	7.187	2.000
4	0.738	1.286	3.083	0.670
5	0.463	1.665	2.133	0.670
6	0.507	1.226	1.972	0.670
7	0.395	1.135	1.846	0.670
8	0.342	1.211	1.721	0.670
9	0.528	0.832	1.568	0.670
10	0.595	1.021	1.389	0.670
11	0.241	0.961	1.371	0.670
12	0.287	0.870	1.586	0.670
13	0.507	0.696	1.479	0.670
14	0.397	1.021	1.550	0.670
15	0.771	1.695	1.819	0.670
16	***4.548***	***9.533***	***6.174***	***20.000***
17	***20.846***	***14.247***	***9.392***	***20.000***
18	***33.573***	***13.649***	***6.855***	***20.000***
19	10.324	8.777	4.051	3.700
20	1.404	4.880	4.552	3.700
21	0.855	5.130	3.925	3.700
22	1.054	4.547	3.486	3.700
23	0.837	4.445	3.450	3.700
24	0.981	4.729	3.441	3.700
25	1.019	5.304	3.674	3.700

Fractions 16,17 ,18 were pooled and overlaid onto a 13% percoll gradient.

[Values represent the mean of four separate experiments]

Table 2.1(b) : Fraction analysis for label and marker enzymes (X-En on 13%-Percoll)

Fraction No.	PM X,13%	HRP X,13%	NAG X,13%	GAL X,13%
1	*1.075*	*20.460*	*2.473*	*4.000*
2	*7.527*	*22.758*	*10.220*	*4.000*
3	*11.828*	*11.548*	*12.034*	*4.000*
4	4.301	3.239	4.142	3.700
5	4.301	2.288	2.638	3.700
6	2.151	1.813	2.390	3.700
7	2.151	1.773	2.267	3.700
8	1.075	1.694	2.638	3.700
9	2.151	1.892	2.411	3.700
10	2.151	1.773	2.514	3.700
11	4.301	1.892	2.782	3.700
12	5.376	1.971	3.008	3.700
13	7.527	2.566	3.977	3.700
14	17.204	4.309	7.171	3.700
15	5.376	10.014	11.333	11.000
16	4.301	4.468	5.522	11.000
17	2.151	0.902	2.741	11.000
18	2.151	0.268	2.328	2.000
19	2.151	0.228	2.576	2.000
20	1.075	0.664	2.576	2.000
21	1.075	0.704	2.576	2.000
22	2.151	0.664	2.390	2.000
23	1.075	0.664	2.514	2.000
24	2.151	0.823	2.514	2.000
25	3.226	0.624	2.267	2.000

Fractions 1,2 ,3 were pooled and overlaid onto a sucrose-step gradient.

[Values represent the mean of four separate experiments]

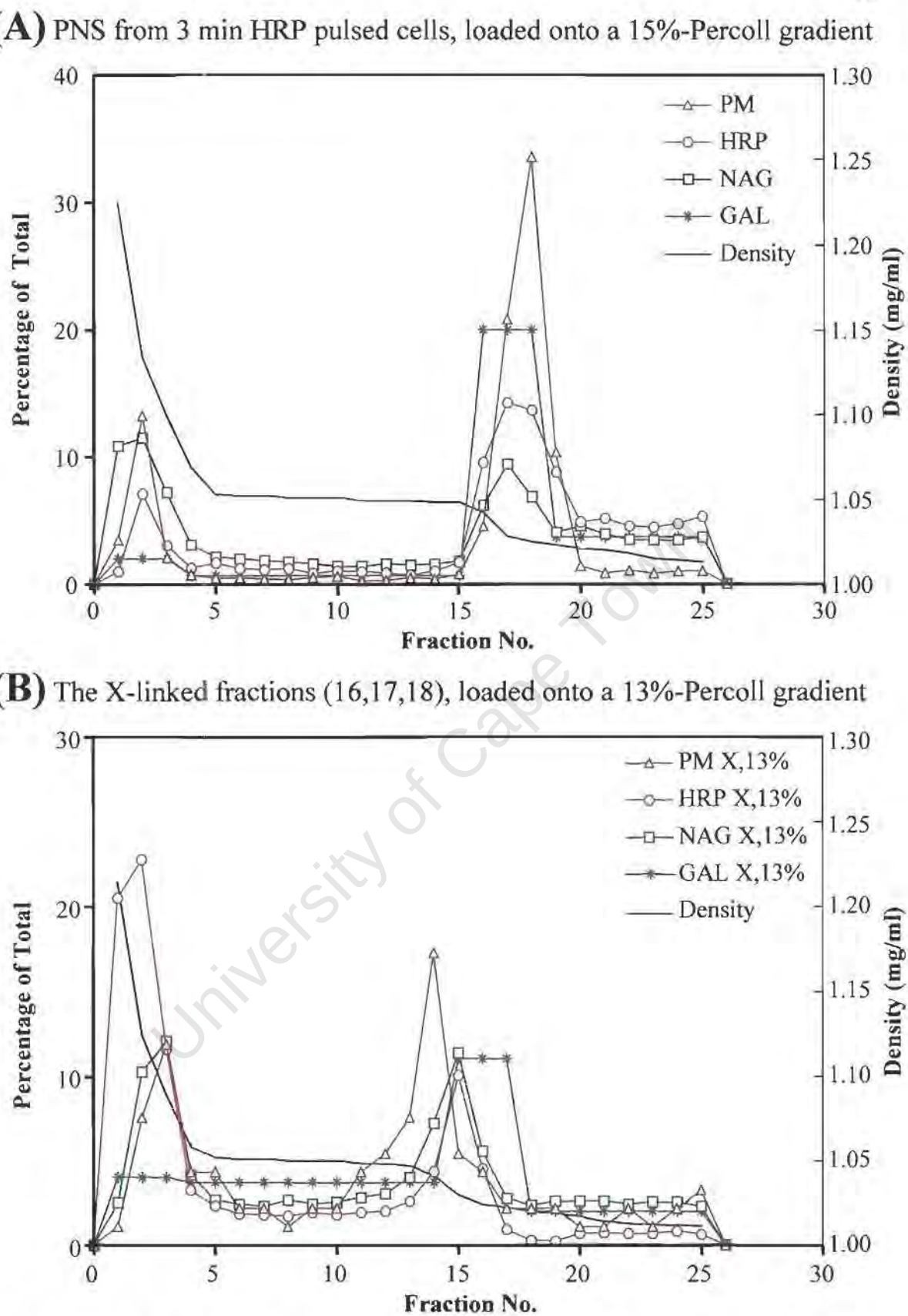

Figure 2.2 : Purification of X-Endosomes (A) After loading cells for 3 min with HRP, a PNS (mixed with [^{3}H]-PM PNS) was loaded onto a 15%-Percoll gradient and centrifuged. The gradients were tapped from the bottom, and fractions were analysed for marker enzymes and [^{3}H]-PM. The resultant low-density fractions (fractions 16,17,18), which represented ~ 37% of the HRP-containing organelles, were pooled and then subjected to DAB-X-linking. **(B)** The X-linked material was overlaid onto a 13%-Percoll gradient and centrifuged. The fractions collected were analysed for marker-enzymes and [^{3}H]-PM. [Representative of the mean of four separate experiments]

2.3.2.2 X-Lysosome Acceptors

$P388D_1$ macrophages were loaded with HRP (1 mg/ml) for 5 min at 37°C, washed, and then chased for 60 min at 37°C, to allow accumulation of HRP in lysosomes. The cells were then subjected to cell cracking and a postnuclear supernatant (PNS) produced. The PNS was loaded onto a 27%-percoll solution and centrifuged at 35000g for 1½ hours in a SW-40 rotor. The gradients were tapped from the bottom as 0.5 ml fractions. The fractions were analysed for marker-enzymes and [^{3}H] PM label. The results were as indicated in Table 2.2(a) and Figure 2.3(A).

The low-density fractions (i.e. fractions 19,20,21), which represent ≈ 40% of the HRP-containing organelles, were pooled and then subjected to DAB X-linking [Section 2.2.5.2]. The X-linked fraction was then overlaid onto a 17%-Percoll solution and centrifuged. This lower percoll concentration was used to improve yields, without sacrificing purity. The resultant high-density fractions (i.e. fractions 1,2,3) as shown in Table 2.2(b) and Figure 2.3(B), which contained 23.1% HRP containing organelles corresponding to the 21.7% lysosomes, 7.64% Golgi and 5.4% PM from the original PNS, were pooled and overlaid onto a sucrose-step gradient [Section 2.2.5.3] and centrifuged. The fraction at the 40-50% sucrose interface was collected as the enriched X-lysosome acceptor fraction [Figure 2.1(B)].

Table 2.2(a): Fraction analysis for label and marker enzymes (PNS on 27%-Percoll)

Fraction No.	PM 27%W	HRP 27%W	NAG 27%W	GAL 27%W
1	0.079	1.961	4.261	0.330
2	0.253	15.033	12.809	0.330
3	0.311	4.654	6.463	0.330
4	0.218	1.786	2.359	0.100
5	0.216	1.255	1.733	0.100
6	0.197	1.011	1.499	0.100
7	0.204	0.924	1.251	0.100
8	0.225	1.011	1.173	0.100
9	0.196	0.793	1.277	0.100
10	0.212	0.802	1.212	0.100
11	0.195	0.863	1.173	0.100
12	0.221	0.924	1.173	0.100
13	0.217	0.915	1.225	0.100
14	0.232	0.915	1.186	0.100
15	0.228	0.959	1.199	0.100
16	0.216	0.993	1.368	0.100
17	0.259	1.264	1.564	0.100
18	0.503	2.092	2.359	0.100
19	***7.426***	***10.109***	***10.008***	***24.000***
20	***45.981***	***16.279***	***15.116***	***24.000***
21	***29.561***	***13.386***	***11.702***	***24.000***
22	6.227	7.277	6.281	5.120
23	3.102	5.473	4.274	5.120
24	1.913	4.784	3.740	5.120
25	1.611	4.540	3.597	5.120

Fractions 19,20 ,21 were pooled and overlaid onto a 17% percoll gradient.

[Values represent the mean of four separate experiments]

Table 2.2(b) : Fraction analysis for label and marker enzymes (X-Ly on 17%-Percoll)

Fraction No.	PM X,17%	HRP X,17%	NAG X,17%	GAL X,17%
1	*1.015*	*26.917*	*25.565*	*3.500*
2	*4.010*	*24.320*	*26.161*	*3.500*
3	*1.405*	*6.718*	*7.100*	*3.500*
4	1.140	1.788	1.716	0.670
5	1.256	1.597	1.252	0.670
6	1.138	1.406	0.775	0.670
7	1.296	1.264	0.656	0.670
8	1.355	1.144	0.550	0.670
9	1.253	1.025	0.457	0.670
10	1.257	0.882	0.391	0.670
11	1.408	0.930	0.338	0.670
12	1.238	0.954	0.298	0.670
13	1.521	1.025	0.391	0.670
14	1.955	1.049	0.722	0.670
15	3.482	1.526	1.451	0.670
16	10.532	3.289	4.179	19.500
17	30.371	8.650	8.683	19.500
18	19.577	6.958	5.822	19.500
19	4.373	1.669	2.404	3.500
20	2.200	1.454	2.073	3.500
21	1.902	1.192	2.100	3.500
22	1.646	1.454	2.047	3.500
23	1.604	1.168	1.795	3.500
24	1.347	0.787	1.477	3.500
25	1.720	0.835	1.596	3.500

Fractions 1,2,3 were pooled and overlaid onto a sucrose-step gradient.

[Values represent the mean of four separate experiments]

(A) PNS from 60 min HRP chased cells, loaded onto a 27%-Percoll gradient

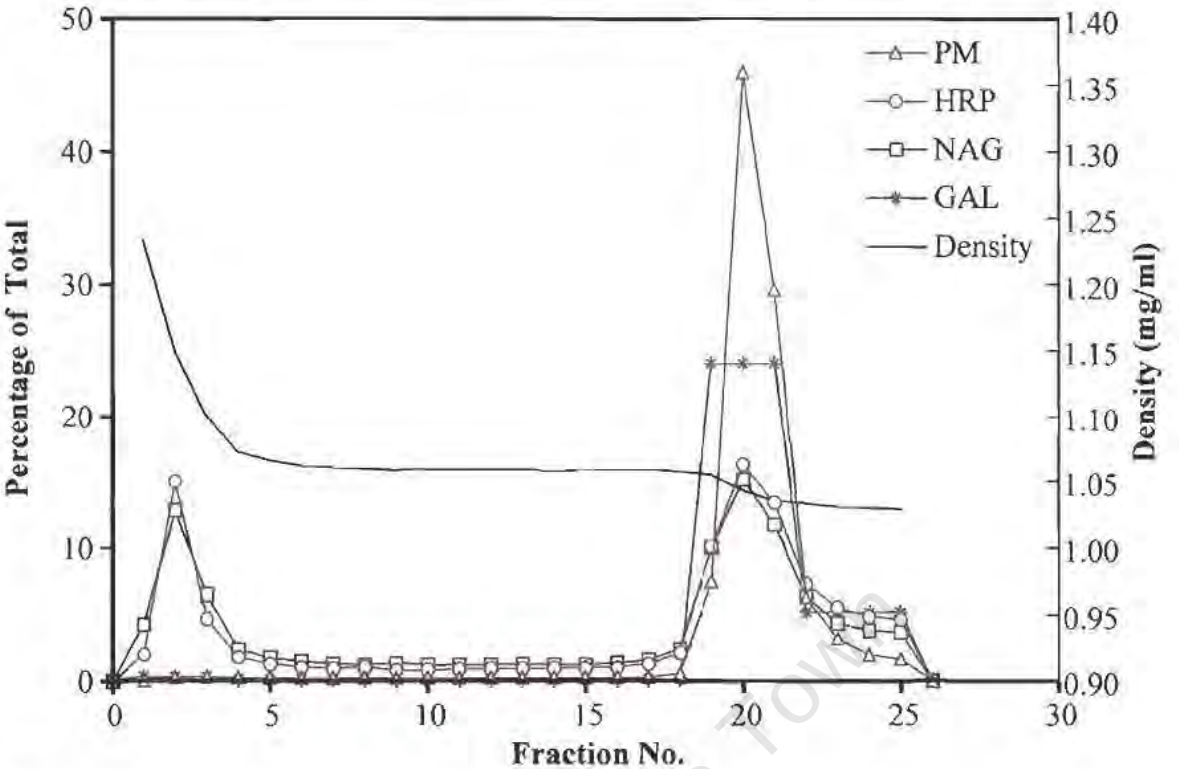

(B) The X-linked fractions (19,20,21), loaded onto a 17%-Percoll gradient

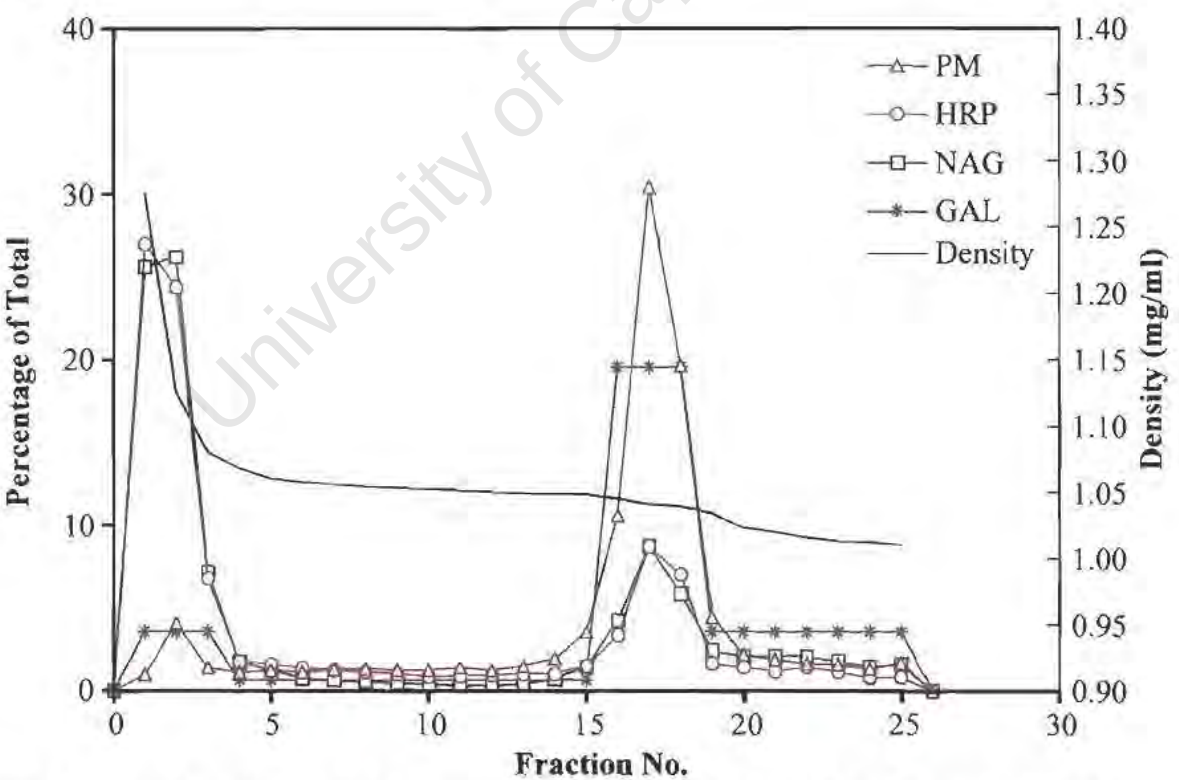

Figure 2.3 : Purification of X-Lysosomes **(A)** After loading cells for 3 min with HRP and chasing for 60 min, a PNS (mixed with [^{3}H]-PM PNS) was loaded onto a 27%-percoll gradient and centrifuged. The gradients were tapped from the bottom, and fractions were analysed for marker enzymes and [^{3}H]-PM. The resultant low-density fractions (fractions 19,20,21), which represented ~ 40% of the HRP-containing organelles, were pooled and then subjected to DAB-X-linking. **(B)** The X-linked material was overlaid onto a 17%-percoll gradient and centrifuged. The fractions collected were analysed for marker enzymes and [^{3}H]-PM. [Representative of the mean of four separate experiments]

2.3.2.3 Acceptor Purification-The Triton X-100 Dilemma

Though the acceptors could be purified to some degree [Sections 2.3.2.1 and 2.3.2.2], the need for Triton X-100 as a final purification step still existed to obtain ultra pure acceptors. Triton X-100 would solubilise the remaining contaminant of non DAB-X-linked organelles within the acceptor preparation, not removed by the Percoll and sucrose-step gradient purification steps.

However, Triton X-100 posed a problem in that it might remove integral membrane proteins which possessed a small (or no) luminal domain not big enough to be trapped by DAB-X-linking. In addition the lipid bilayer might prevent the free movement of proteins, thereby contributing to the trapping phenomenon. If the lipid bilayer is removed by Triton X-100 it may lead to free movement, allowing non-covalently entangled proteins to disentangle themselves from the X-linked organellar matrix. Important membrane factor/s involved in targeting and/or fusion might be lost due to Triton X-100 solubilisation. Furthermore, removal of the lipid bilayer by Triton X-100 might expose non-physiological non-specific binding sites.

In the case of cytosolic donor to be co-incubated with X-acceptor, the use of Triton X-100 solubilisation could be avoided. However, in the case of membrane donor the use of Triton X-100 is unavoidable. Considering that the search for membrane factors was the main aim of this study, it was decided to use Triton X-100 as a final purification step of X-acceptors as a norm. The resistance of X-acceptor membrane proteins to Triton X-100 solubilisation was thus analysed [Section 2.3.3.1].

2.3.3 Integrity of X-Linked Acceptors

The integrity of the X-acceptors was analysed with regard to its intrinsic ability to trap membrane factors upon Triton X-100 solubilisation [Figure 2.4(A)], SDS treatment or sonication [Figure 2.5(A)]. To do this type of analysis, the PM was radioactively labelled with [^{3}H]-galactose [Section 2.2.6.4] before a 15 min uptake pulse of HRP. The cells were then treated with β-Galactosidase (to remove label not internalised). A PNS was placed onto a 27%-Percoll gradient and the low-density fraction isolated. The sample was split into two parts, and one of them DAB X-linked. Both samples were then Triton X-100 solubilised, followed by centrifugation. The amount of radioactivity pelleted was then measured.

2.3.3.1 The Resistance of X-linked Acceptors to Triton X-100 Solubilisation

The amount of Triton X-100 releasable label, was measured before and after DAB-X-linking. Subtracting the Triton X-100 resistant value of non-crosslinked material (i.e. 5%) from the value obtained for X-linked material (i.e. 35%), a value indicative of trapping (i.e. 30%) by DAB X-linking [see Figure 2.4(A)] was derived. This measured trapping value is within the region of the expected trapping value (i.e. 34%) as derived from the calculation below.

About 65% of the radioactive label was removed by Triton X-100 treatment. The reason for this fairly large solubilisation activity can be explained by the activity exhibited by the ß-Galactosidase, which was in the region of 90% [Figure 2.4(B)], the internalisation rate [70] and recycling process. This can be depicted by the following diagram:

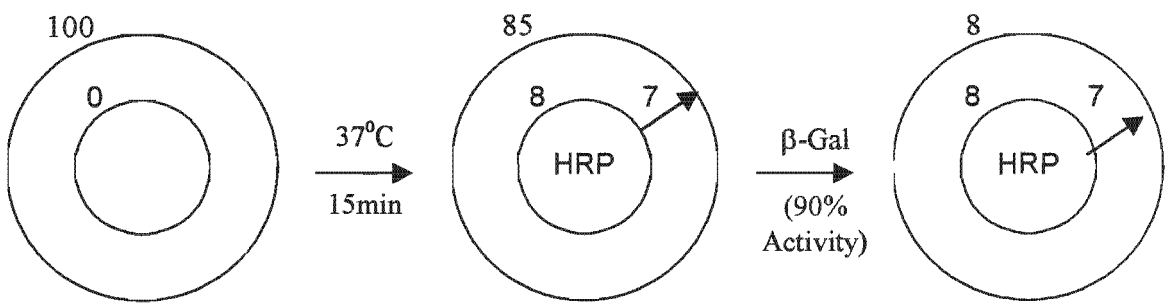

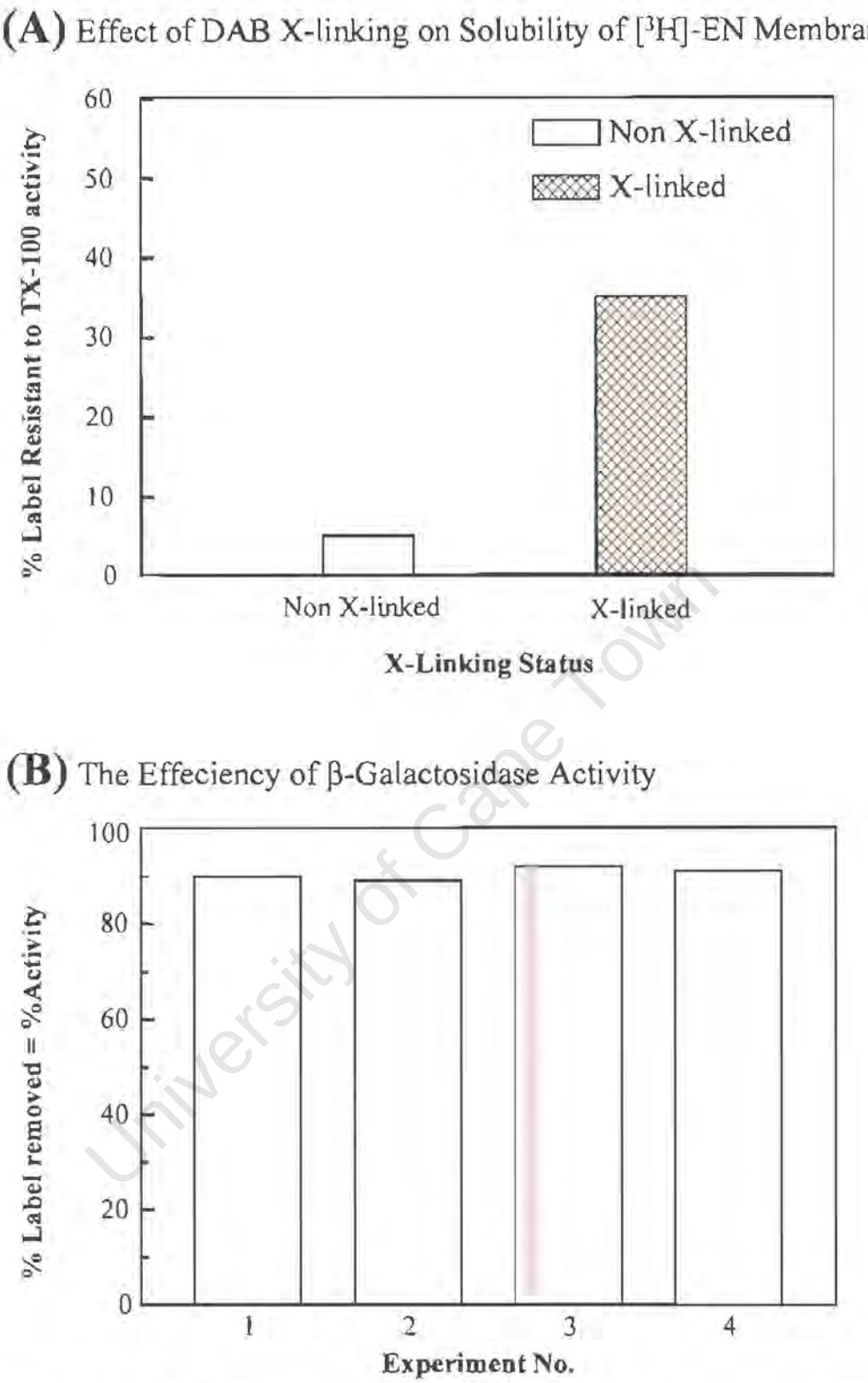

Figure 2.4 : (A) The cell surface of cells were labelled with [^{3}H]-Galactose and then internalised in the presence of HRP for 15 min. The cells were then treated with β-Galactosidase (to remove label not internalised). A PNS was placed onto a 27%-Percoll gradient, centrifuged, and the low-density fraction isolated. The sample was split into two parts and one of them DAB X-linked. Both samples were then Triton X-100 solubilised followed by centrifugation. The amount of radioactivity pelleted was measured. **(B)** After labelling the cell surface with [^{3}H]-Galactose the cells were washed extensively before treatment with β-Galactosidase. The cells were centrifuged and the activity of β-Galactosidase was analysed by measuring the amount of label remaining in the supernatant. [**A** represents the mean of 3 separate experiments]

With 100% label on the PM after labelling in the cold, subsequent membrane internalisation (endocytosis at 37°C) leads to ≈18% of label on internalised membrane after 15 min for $P388D_1$ macrophages [72,343,344]. At steady state, about 60% of the internalised label is on the recycling pathway (recycling of HRP is prevented by the presence of mannan to block any mannose receptors to inhibit receptor mediated uptake), based on its inaccessibility to crosslinking by HRP [72]. This leaves only 7.2% of the label associated with HRP filled endocytic organelles. Bearing in mind that ß-Galactosidase removes about 90% of the cell-surface label [Figure 2.4(B)], leaving 8.2% on the cell surface, it becomes clear that from a total of 26.2% (8.2+7.2+10.8) remaining cell associated label, approximately 27% remains accessible for trapping by HRP induced DAB-X-linking. The calculated value corresponds well with the measured trapping of about 30% of the [^{3}H]-labelled membrane [Figure 2.4(A)]. These results in essence suggest that the HRP DAB-X-linking procedure may prove to be a viable method for trapping at least PM-derived membrane components in early endocytic organelles.

Figure 2.4(A) shows that about 5% of non-crosslinked membrane was resistant to Triton X-100. It is known that lipid-anchored (glyco) proteins, in contrast to many transmembrane proteins, are relatively insoluble in non-ionic detergents such as Triton X-100 [347,349,350]. It has been suggested that detergent-resistant domains represent caveolae (i.e. non-clathrin coated invaginations of the PM) in some cell types, including epithelial cells, smooth muscle cells and fibroblasts [346-348]. However, in neuronal cells caveolin is not essential for the existence of detergent-resistant complexes [345].

2.3.3.2 Effect of Sonication and SDS on X-linked Acceptors

The stability of Triton X-100 treated X-acceptors was further analysed by sonication and SDS treatment. Sonication (3 minutes in a bath sonicator) disrupts the acceptor, causing a loss of approximately 30% of label into the soluble state and therefore membrane constituents. As implicit from the observation in Figure 2.5(A), SDS-treatment allowed the extraction of proteins from cross-linked acceptors. Therefore, it could be concluded that the procedure of DAB X-linking did not destroy the structure of proteins, in contrast to a report that protein function cannot be retrieved after DAB cross-linking [458]. SDS denatures proteins by altering their conformation, which may allow them to escape the DAB-X-linked network, causing the disintegration of the X-linked acceptors.

2.3.3.3 Recovery of X-linked Acceptors after centrifugation through sucrose

To be able to use the X-linked acceptors to bind soluble factors in binding assays, it is critical to separate the X-linked acceptor from the rest of the medium. Centrifugation using a sucrose underlay was tested for this purpose. As shown by Figure 2.5(B), a 25% sucrose underlay results in a 15% loss of acceptor to the supernatant. This concentration of sucrose underlay (i.e. 25%), however, proved optimal, since a minimal background was pelleted from incubation of cytosol alone in the binding assay. Above this percentage of sucrose underlay, however, the loss in acceptor was too high (in the region of 40-90%) to consider for use in the centrifugation step of the binding assay.

2.3.3.4 Scanning Electron Microscopy of X-linked Acceptors

Triton X-100 treated non-crosslinked PNS and purified X-acceptors were spread onto separate 0.02 μm filters and then fixed sequentially with glutaraldehyde, osmium tetroxide and uranyl acetate. The dried samples were then subjected to scanning electron microscopy. No vesicular structures were visible for non-crosslinked PNS [Figure 2.6(A)], but vesicular structures were seen for X-acceptors [Figure 2.6(B,C)], providing evidence that the X-acceptors were resistant to Triton X-100 solubilisation. A low magnification was shown [Figure 2.6(A)] to indicate that the entire filter was clear of vesicular structures.

(A) Effect of Sonication and SDS on TX-100 treated [^{3}H]-Acceptor.

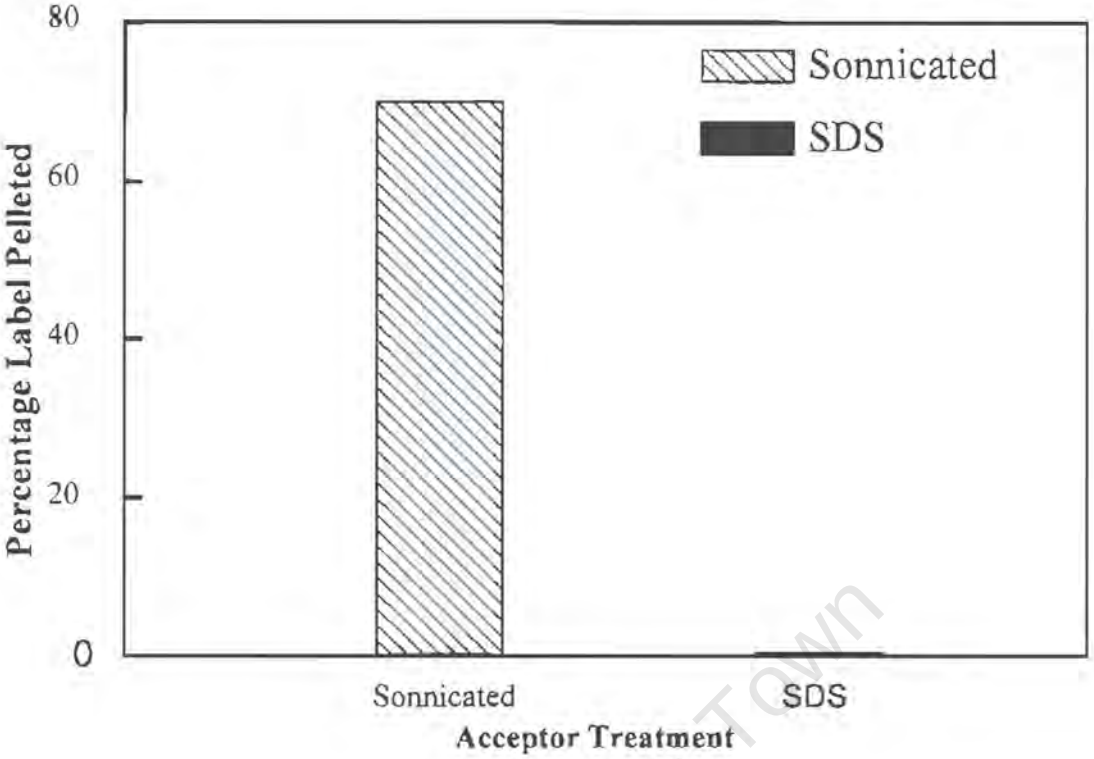

(B) Retrieval of [^{3}H]-Acceptor$^{TX\text{-}100}$ after centrifugation through Sucrose

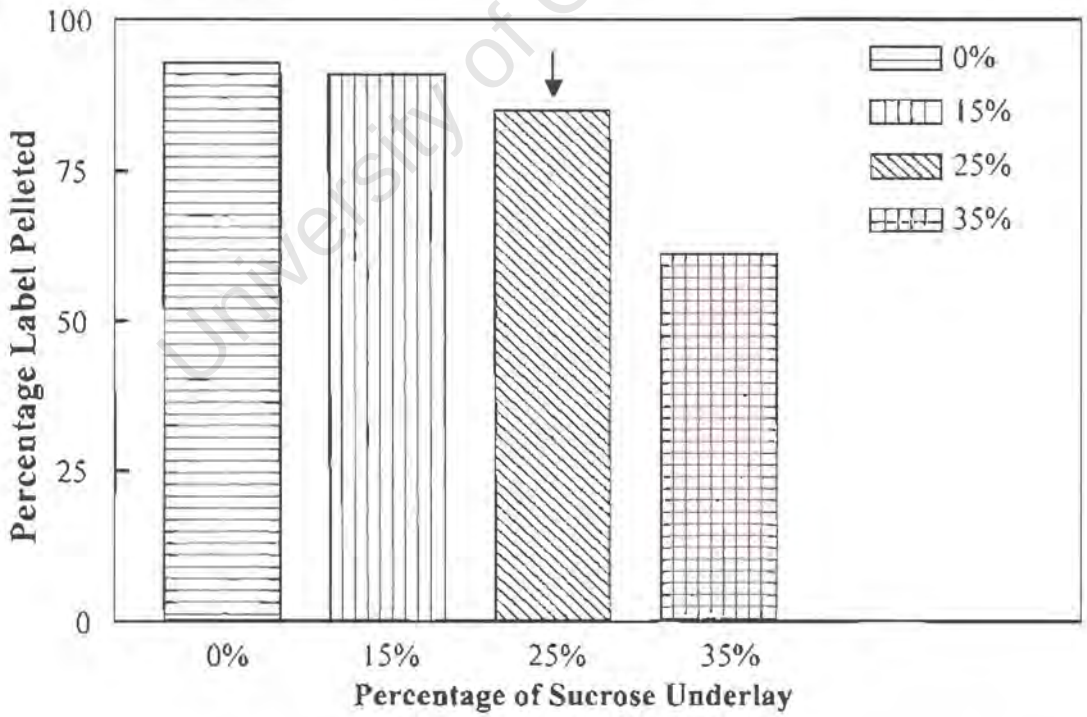

Figure 2.5 : **(A)** Triton X-100 treated [^{3}H]-Acceptors were subjected either to sonication (3 min) or SDS (1%). The material was then centrifuged and the amount of label in the pellet was measured. **(B)** Triton X-100 treated [^{3}H]-Acceptors were loaded onto different sucrose concentrations and then centrifuged. The amount of label in the pellet was measured. [Representative of the mean of three separate experiments]

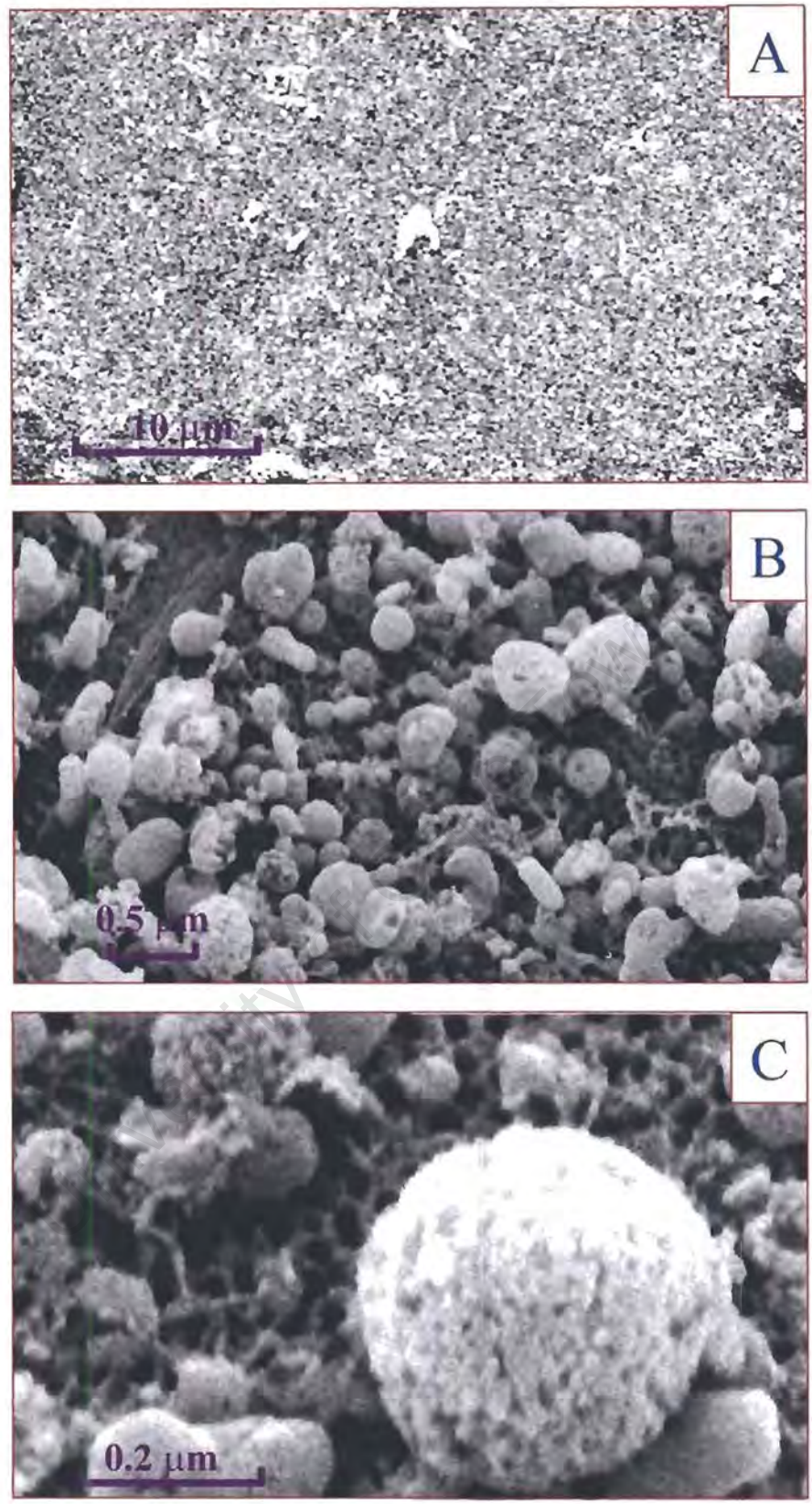

Figure 2.6 : Scanning electron micrographs of X-linked acceptors. Triton X-100 treated non-crosslinked PNS and purified X-acceptors were spread onto separate 0.02 µm filters, then fixed sequentially with glutaraldehyde, osmium tetroxide and uranyl acetate. Dried samples were mounted onto aluminium stubs and then scanned. (**A**) Triton X-100 treated non-crosslinked PNS. (**B**) Triton X-100 treated X-acceptors. (**C**) Higher magnification of a sub area of image B.

CHAPTER 3

BINDING ASSAYS USING CROSS-LINKED ACCEPTORS

3.1 BACKGROUND

Several methods have been employed to identify the cytosolic and membrane machinery involved in the docking and/or fusion process. Thus far the elucidation of these factors has been more forthcoming for the secretory pathway, than for the endocytic pathway.

In a photo cross-linking approach [351], used to pull out factors associated with Rab5 under varying nucleotide conditions, it is found that under ATP-depletion polymerised actin and intermediate filaments can be recovered in a pellet after sucrose gradient centrifugation together with Rab5. Due to these membrane or organellar independent protein-protein interactions taking place under specific nucleotide conditions, all isolation techniques needed to be developed which distinguish between the detection of membrane or organellar dependent binding and not de-novo cytosolic interactions.

Free flow electrophoresis (FFE) has been used to produce endosomal fractions devoid of ER and Golgi membrane and with minimal lysosomal contamination (<10% by protein) [133a]. The binding capabilities of an endosome enriched fraction and an ER/Golgi enriched fraction was analysed. The main finding is that endosomes recruit members from the COPI and ARF families under GTPγS incubation conditions. However only coat assembly proteins were detected, with no docking and/or fusion factors obvious.

In vitro fusion assays have also been applied to identity factors involved in endocytic processing. One approach has studied the transfer of early endosomal proteins from a metabolically labelled early-endosome population to an unlabelled acceptor early-endosome population immobilised onto beads [281]. This approach is unable to distinguish between fusion and docking factors. In the present study, this distinction was

possible because the cross-linked organelles were obviously fusion inactive whereas the factors that mediate docking could still be bound from a fully soluble donor. This technique depends on the assumption that these factors are trapped by the DAB crosslinking reaction [discussed in Section 2.3.2.3].

Immunoprecipitation/immunoadsorption techniques have also been applied to isolate factors that are capable of interacting with a specific protein immobilised by antibodies. Synaptic SNAREs (Syntaxin, VAMP and SNAP-25) have been discovered by using NSF-myc, immobilised by anti-myc antibodies attached to beads [179]. Since then homologues of syntaxin and VAMP have been immuno-localised to different organelles along the secretory pathway. VAMP [218,220,221] and syntaxin [222-225] homologues have also been localised to endocytic structures.

Other approaches involve screening of DNA libraries for sequences related to a specific probe sequence of a known targeting or fusion factor. This approach has been successfully applied for SNAREs (syntaxins and VAMPs).

It appears that depending on the methodological approach different and sometimes irreconcilable, observations have been made. The SNARE hypothesis has become into disrepute since multiple v-SNAREs are often present on a single class of transport vesicle [397,398], a single v-SNARE can direct both retrograde and anterograde transport between two compartments [399], a variety of v-SNAREs and t-SNAREs pair indiscriminately [193] in vitro. Thus SNAREs alone cannot account for specific membrane trafficking.

The targeting function attributed to Rabs also seems untenable due to the findings that a chimera of yeast Rab homologues Ypt1p (ER to Golgi) [242] and Sec4p (Golgi to PM) [246] can provide Rab function to the entire secretory pathway from the ER to the PM without misorting [238a,b], and that overexpression of v-SNAREs [197] can overcome the

requirement of Ypt1p. Although it has been shown that Rab proteins facilitate the assembly of SNAREs, they do not form part of docking complex [175,207].

Additionally it has also been shown that SNARE-Rab interactions are non-selective since the nucleotide-free forms of six Rabs bind with comparable low affinity to three SNAREs [400]. Thus SNAREs and Rabs also do not seem to cooperate to specify the target membrane for fusion.

Recently, it has been proposed that unique stage-specific factors such as TRAPP (ER to Golgi)[276a,b], the exocyst (Golgi to PM) [267a,b] and EEA1 (homotypic endosome fusion)[262] may direct fusion fidelity. Additionally, factors that mediate vesicle interactions with the cytoskeleton may play pivotal roles in vescle targeting.

Considering the former, it may be that other factors (yet to be discovered) may play crucial roles in mediating high fidelity docking, before SNARE interactions. Thus the door for discovery of novel factors has not been shut completely, and requires a macro approach to fish out novel factors. In the present study, cross-linked endosomes or lysosomes were used as acceptors to bind potential targeting/fusion molecules by incubating them with metabolically labelled cytosol or detergent-solubilised membrane. Bound material was collected by centrifugation and analysed by SDS-PAGE and radioactive scanning.

3.2 MATERIALS AND METHODS

3.2.1 Preparation of cold cytosol and membrane fractions [44,104,327]

3.2.1.1 Cell homogenisation

Cells were harvested and resuspended at 4 x 10^7 cells/ml in cold homogenisation buffer (250 mM sucrose, 0.5 mM EGTA, 20 mM Hepes-KOH, pH 7.0, 1 mM dithiothreitol, 1 mM PMSF, 0.1 mM Leupeptin, 1 μM Pepstatin) [44,104,327,328]. The cells were then disrupted using a stainless steel ball homogeniser, pre-chilled on ice. Typically, 12 strokes through the homogeniser yielded 80-90% breakage as determined by trypan blue exclusion. The homogenate was centrifuged at 1000g for 20 minutes (Beckman TJ-6 centrifuge, Beckman Istruments, Palo Alto, CA, USA) and the resulting post-nuclear supernatant (PNS) collected.

3.2.1.2 Separation of cytosol and membrane

The resultant PNS was centrifuged at 170000g for 30 minutes at 4°C in an airfuge (Beckman Instruments, A-100 30° Rotor, Palo Alto, CA, USA). The resulting high-speed supernatant (cytosol) was collected and the membrane pellet resuspended in a volume of homogenisation buffer equalling the volume of the collected cytosol. Both fractions were aliquoted and stored at -80°C.

3.2.2 Preparation of radioactive donor [Figure 1.6, red arrows, page 36]

3.2.2.1 Metabolic labelling

Cells were metabolically labelled with Tran^{35}S-label (ICN Biomedicals, California, USA) (containing 70% ^{35}S L-Methionine, 15% ^{35}S L-Cysteine) in the following way. Cells were

washed twice in 20ml cold EMEM medium without methionine (ICN Biomedicals, California, USA). Cells were then resuspended at 10 x 10^6 cells/ml in cold EMEM (w/o methionine) in a 50 ml Erlenmeyer flask and 100 µCi Tran^{35}S-label (ICN Biomedicals, California, USA) added per ml cell suspension. The Erlenmeyer flask was placed on an orbital shaker in a 5% CO_2 environment incubator (Queue) at 37°C. The cell suspension was incubated for 2 hours while gently agitating. The suspension was then transferred into a volume of cold Hepes-Saline-BSA (10 mM Hepes, 150 mM NaCl, pH 7.4, 0.1% BSA) to make the volume of the suspension to 50 ml. The cells were pelleted by centrifugation at 200g for 5 minutes at 4°C. The supernatant was aspirated off and the cells transferred to a new tube and washed five times by repeated resuspension and centrifugation in 10 ml of Hepes-Saline-BSA. The cells were given a final wash in homogenisation buffer [327] before homogenisation [Section 3.2.1.1].

3.2.2.2 Separation of labelled cytosol and membrane

The PNS obtained from a homogenate of ^{35}S-methionine metabolically labelled cells was split into 2 fractions. One fraction was centrifuged [as outlined in Section 3.2.1.2] and the supernatant collected as the ^{35}S-cytosol donor. The second fraction was overlaid onto a 27% percoll gradient and centrifuged at 35000g for $1^1/_2$ hours at 4°C and the low-density fraction collected as the ^{35}S-membrane^{Lf} (Lf, abbreviation for *low-density fraction*) donor.

3.2.2.3 Pre-clearing of labelled cytosol and membrane

Triton X-100 was added to each fraction to a final concentration of 1%. The detergent solubilised fractions were incubated at 37°C for 30 minutes and then spun at 1.5 x 10^5g for 30 minutes at 4°C in an airfuge (Beckman Instruments, A-100 30° Rotor, Palo Alto, CA, USA) and the resultant supernatants collected. This was repeated 5 times. The final supernatants represented the donor ^{35}S-Cytosol and ^{35}S-Membrane^{Lf} used in the Binding assays. All preparations were performed on ice and in the presence of protease inhibitors.

3.2.3 *In vitro* Binding Assay [Figure 1.6, green arrows, page 36]

3.2.3.1 Acceptor titration

Increasing amounts (0 → 40 µl) of crosslinked acceptors (not salt-extracted) were added to 30 µl of Binding buffer [250 mM sucrose, 50 mM KCl, 0.5 mM EGTA, 20 mM Hepes-KOH, pH 7.4, 1 mM dithiothreitol, 1.5 mM $MgCl_2$, 1 mM PMSF, 0.1 mM Leupeptin, 1 µM Pepstatin) supplemented with either an ATP regenerating system (1 mM ATP, 5 mM Creatine phosphate, 31 U/ml Creatine phosphokinase, Boehringer Mannheim, Germany) or an ATP depleting system (5 mM Glucose, 25 U/ml Hexokinase, Boehringer Mannheim, Germany)], 30 µl pre-cleared labelled donor (cytosol or membrane). The volume of each reaction mixture adjusted to 100 µl with Binding buffer. The tubes were warmed to 37°C and incubated for 90 minutes in a water bath. The reaction was stopped by snap cooling on ice. Acceptors with bound material were then separated from the rest of the incubation mixture as below [Section 3.2.3.2].

3.2.3.2 Separation of soluble from insoluble radiolabel

The samples were overlaid onto 0.5 ml of 25% sucrose (prepared with Binding buffer supplemented with or without ATP) and centrifuged at 15000g in a benchtop centrifuge (Beckman Instruments, Palo Alto, CA, USA) for 20 min at 4°C. After centrifugation, the supernatant and sucrose were aspirated off and the pellet resuspended in 50 µl of Binding buffer. Duplicate 5 µl samples of the total sample and of the resuspended pellet were taken separately into plastic mini-scintillation vials (Packard Instrument Co., Meriden, CT, USA). 5 ml of Scintillation cocktail (Ready Solv, Beckman Instruments, Palo Alto, CA, USA) was added to each vial and radioactivity quantitated by means of liquid-scintillation counting. The radiolabel bound to the acceptor was determined by expressing the radioactivity in the pellet as a percentage of the radioactivity in the total sample.

3.2.3.3 Standard Binding Assay

30 µℓ acceptor, 30 µℓ Binding buffer (either with an ATP regenerating system or ATP depleting system as required) and 30 µℓ of ^{35}S-cytosol or ^{35}S-membrane donor fraction were mixed and incubated at 37°C in a water bath for 2 hours. The reaction was stopped, by snap cooling on ice. Acceptors with bound material were then separated from the rest of the incubation mixture as detailed above [Section 3.2.3.2].

For 1-D electrophoresis [Section 3.2.4], the pellet was resuspended in 50µℓ Binding buffer and then added to 50 µℓ 1-D 2x Sample buffer (20% glycerol, 5% SDS, 10% ß-mercaptoethanol, 0,004% bromophenol blue, 0.08 M Tris-HCl, pH 6.8) and boiled for two minutes. Samples were then applied to a 5-13% gradient SDS-polyacrylamide slab gel. The procedure for 2-D electrophoresis is described below [Section 3.2.5].

3.2.4 SDS Polyacrylamide gel electrophoresis

Protein separation was performed according to the method of Laemmli [357] using 1,5 mm thick, 250 mm long and 180 mm wide 5-13% gradient polyacrylamide slab gel employing a discontinuous buffer system (25 mM Tris, 192 mM glycine, 0.1 % SDS, pH 7.6). A mixture of high and low molecular weight markers (MW-SDS kits, Sigma Chemical Co., St Louis, Missouri, USA) was used for calibration purposes. Gels were run overnight at 15 mA using a Pharmacia power pack (Amersham Pharmacia, Sweden). Protein bands were then visualised by radioactive scanning using a Packard electronic autoradiographer (Packard Instantimager Co., Meriden, CT, USA).

3.2.5 2-Dimensional Electrophoresis

3.2.5.1 In-gel sample reswelling procedure for Isoelectric focussing

In-gel sample reswelling procedure was followed as previously described [352a,b]. Each sample (binding assay pellets) was resuspended in 350 μℓ 2-D sample buffer (8M urea, 2M Thiourea, 4% CHAPS, 2% pH 3-10 carrier ampholytes, 20mM Tris base, 30mM DTT). Solubilisation was allowed to take place for 30 minutes at room temperature with frequent agitation. The samples were then centrifuged in a Beckman bench-top centrifuge (Beckman Instruments, Palo Alto, CA, USA) at 15000g for 5 minutes to pellet undissolved material, and 320 μℓ of the supernatant applied into each groove of the sample reswelling chamber (Amersham Pharmacia, Sweden). The Immobiline pH gradient (IPG) strips (pH 3-10 nonlinear, 180mm) were then placed into the grooves with the gel side facing the sample and 3 ml of low viscosity silicon oil (350 stokes) layered on top. Reswelling was allowed for at least 12 hours or left overnight. Isoelectric focusing was performed at 17°C, and voltage was increased step-wise from 300V to 3000V in 4 hours and continued for 20 hours until equilibrium (65 kVh).

3.2.5.2 Equilibration of IEF Strips and SDS-PAGE

After isoelectric focussing, IPG strips were equilibrated for 10 minutes in fresh Equilibration solution (6 M Urea, 2 % SDS, 30 % Glycerol, 0.05 M Tris-HCl pH 6.8, a trace of bromophenol blue) containing 2 % DTT, then for 10 minutes in fresh Equilibration solution containing 2.5 % Iodoacetamide. The IPG strips were then trimmed by 1.5 cm off the acidic end. The second dimension was performed using a 5-13% gradient SDS-PAGE, followed by radioactive scanning or Coomassie blue [described in Section 5.2.3.2] staining (for preparative gels). Spots on preparative gels were cut out for subsequent mass spectrometry or Edman microsequencing analysis [Chapter 6].

3.3 RESULTS AND DISCUSSION

3.3.1 Radioactive donor preparation [Figure 1.6, red arrows, page 36]

3.3.1.1 ^{35}S-Cytosol

To investigate the interaction of acceptors (X-endosomes or X-lysosomes) with soluble cytosolic components, the postnuclear supernatant (PNS) from metabolically labelled mouse macrophages was depleted of membrane by centrifugation (170 000g for 30min). This centrifugation step also removed polymerised cytoskeletal elements [351]. These polymerised filaments were not present in the centrifugation pellet when the cytosol was incubated in the presence of an ATP-regenerating (ATP_R) system, indicating that these filaments polymerised de novo under ATP-depleting conditions. To remove the bulk of these factors from the donor, the cytosol was extensively pre-cleared by multiple consecutive incubations (37°C for 30min) and centrifugation (170 000 g for 30min) steps until the amount of radioactive material pelleted was minimal [Figure 3.1(B), blue bars]. The result was that minimal background was detected when no acceptor was added during the binding assays [Figure 3.2(B)]. Such pre-cleared cytosol was employed in all binding assays. Thus, material pelleted with acceptors present was most probably due to specific molecular interactions [Figures 3.5 and 3.6].

3.3.1.2 ^{35}S-Membrane

Labelled PNS was overlaid onto a 27% percoll gradient and the low-density fraction was collected and pelleted by centrifugation (170 000g for 1 hour). The pellet was then extensively washed with homogenisation buffer. The ^{35}S-Membrane^{Lf} was then either solubilised directly or treated with high salt and sonicated prior Triton X-100 solubilisation.

Treating the non-solubilised ^{35}S-Membrane^{Lf} with high salt (1M NaCl) resulted in the removal of ≈ 6,3% of the total radioactive material. In addition, subsequent sonication induced a loss of ≈ 9,6% of the total radioactive material present in the PNS derived ^{35}S-Membrane. This latter loss was due to release of material within the luminal region of the membrane organelles due to sonication, which otherwise would become part of the Triton X-100 solubilised membrane donor. A final wash with homogenisation buffer removed ≈ 1% of the starting material. Thus, whatever bound to acceptors in subsequent binding assays, was derived from either solubilised integral membrane proteins or tightly associated high-salt resistant factors remaining bound to these integral membrane proteins.

The washed membrane was solubilised with Triton X-100 (1%) and subjected to multiple centrifugation/resuspension steps to remove any de novo precipitable material and obtain a homogenous solubilised fraction of ^{35}S-Membrane^{Lf}. The percentage of label removed after each step was measured [Figure 3.1(B), red-slash bars]. The initial pellet was approximately 20% of the original label before separation. A large proportion of this precipitate would be the Triton X-100 resistant membrane fraction. However, this might also partially be due to trapping of radioactive material within Percoll, which pelleted upon ultra-centrifugation. From Figure 3.1(B) we could conclude that proper pre-clearing was essential to decrease the potential non-specific background. Such pre-cleared membrane was employed in all binding assays.

A potential problem though, might be that the membrane factors potentially involved in the hypothesised targeting were removed by the multiple centrifugation procedure in the precipitable material. This is possible since it is known that detergent resistant complexes (such as Caveolae, lipid-anchored (glyco) proteins, etc.) are insoluble in nonionic detergents such as Triton X-100 [346-350, discussed earlier in Section 2.3.3.1, page 60, last paragraph]

(A) Amount of label removed by consecutive Salt-washing, Sonication and Buffer-washing of ^{35}S-Membrane^{Lf} prior Triton X-100 solubilisation.

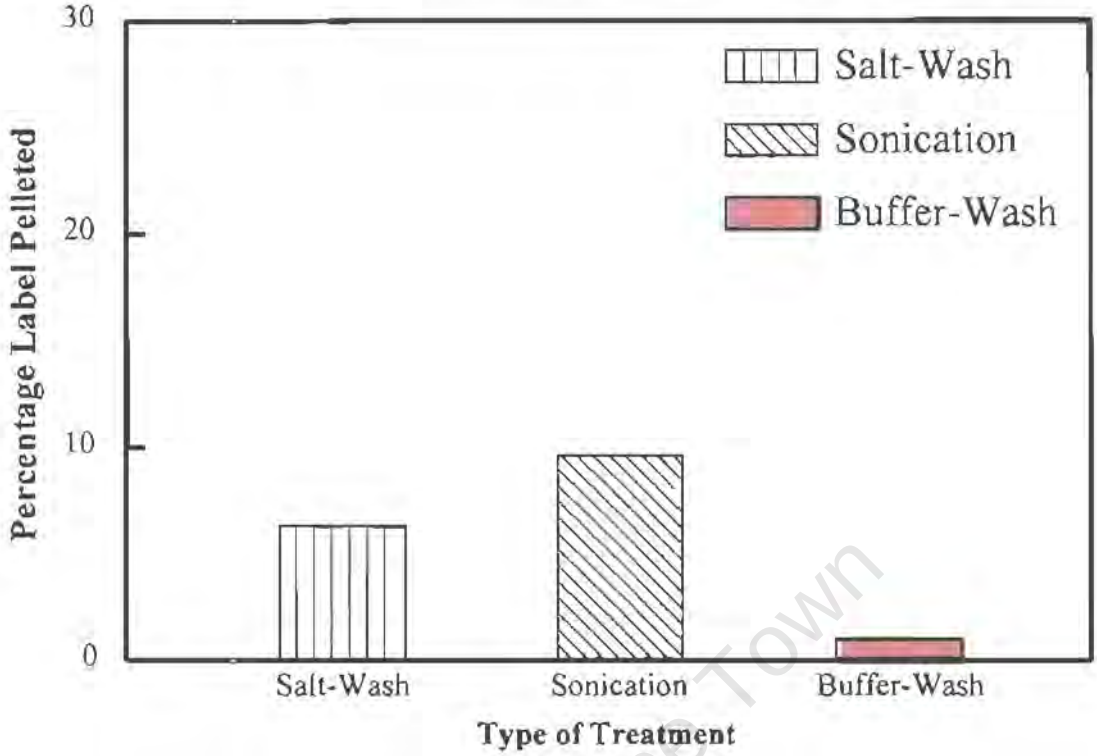

(B) Pre-Clearing of ^{35}S-Cytosol and Triton X-100 treated ^{35}S-Membrane^{Lf}

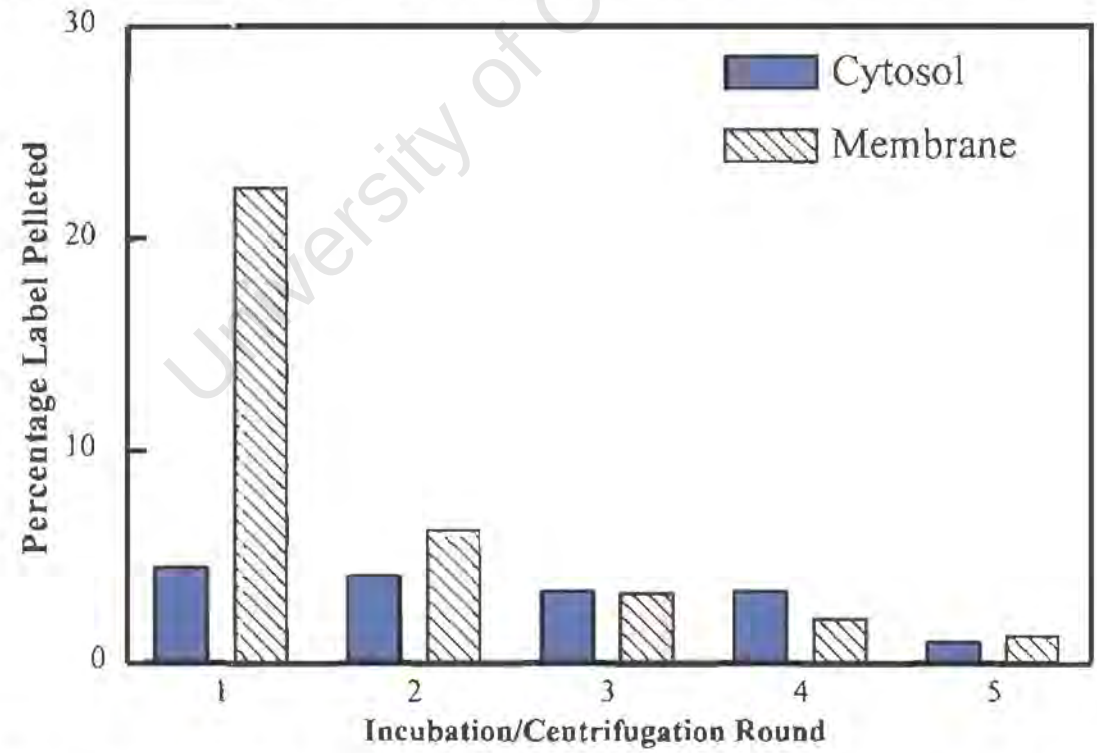

Figure 3.1 : **(A)** ^{35}S-Membrane^{Lf} (prior Triton X-100 solubilisation and pre-clearing) was subjected consecutively to salt-washing, sonication (3min) and buffer-washing. The material was centrifuged and the amount of label in the pellet was measured. **(B)** ^{35}S-Cytosol and Triton X-100 treated ^{35}S-Membrane^{Lf} was pre-cleared by multiple incubations and centrifugation steps [Section 3.2.2.3]. The amount of label in the pellet was measured. [Representative of the mean of three separate experiments]

3.3.2 Characterisation of ATP-precipitable material

3.3.2.1 Acceptor titration

To determine the amount of acceptor that was required for maximal precipitation relative to a specified arbitrary amount of ^{35}S-Cytosol (say 30 µl, from a 3mg/ml stock), binding assay incubations were performed as a function of acceptor volume at 37°C for 90 minutes, either in an ATP_R (ATP-regenerating) or ATP_D (ATP-depleting) system [explained in Section 3.2.3.1]. Figure 3.2(A) shows that ≈ 30 µl acceptor (not salt-extracted) relative to 30 µl ^{35}S-cytosol (i.e. equal volumes) was optimal to precipitate saturated amounts of radioactivity for an incubation period of 90 minutes.

3.3.2.2 Optimal binding incubation period

The incubation period for optimal binding was determined by incubating the acceptors in the binding assay, as a funtion of time either in an ATP_R or ATP_D system. It could be concluded from figure 3.2(B) that saturation point was reached after ≈ 120 minutes. Henceforth, a standard incubation time of 120 minutes was used for all binding assays.

3.3.2.3 Is the binding of Donor, ATP Reversible?

To test whether subsequent addition of ATP, could release ^{35}S-cytosol pre-bound in the absence of ATP, acceptors were incubated at 37°C for 120 minutes in an ATP_D system, donor cytosol removed, followed by a 30 min incubation in an ATP_R system. As shown by figure 3.3(A), the expected saturation at 120 min in an ATP_D system was reached (i.e. ≈ 1.2 % of the total label in pellet), then upon ATP addition this adsorbed material was rapidly released. Reversible binding in an ATP_D system was thus indicated, with ≈ 80% releasable upon ATP addition.

(A) Acceptor titration relative to a fixed amount of pre-cleared ^{35}S-Cytosol.

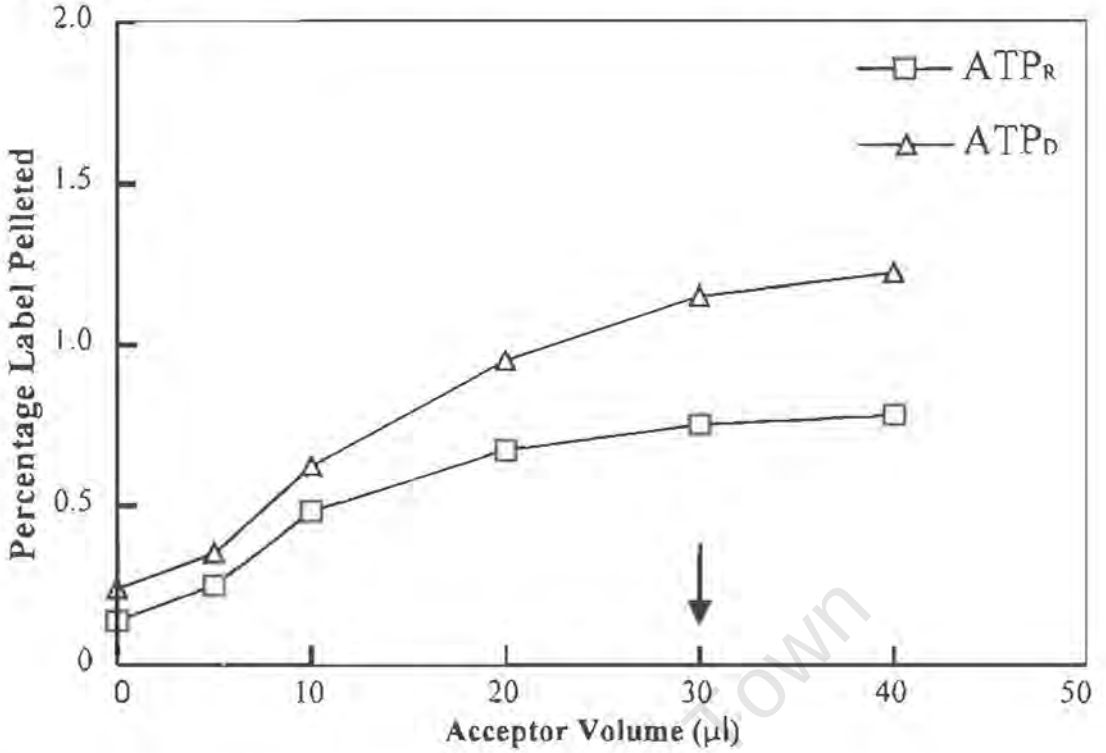

(B) Binding as F(Time) in an ATP_R /ATP_D system with/without Acceptor

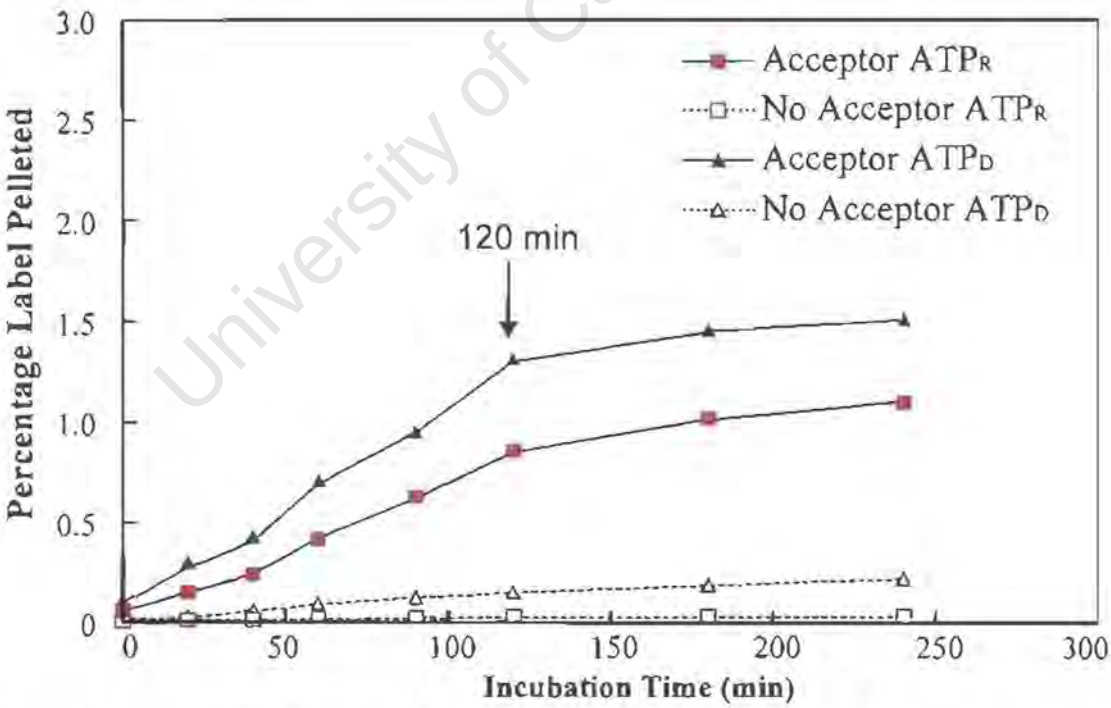

Figure 3.2 : **(A)** The amount of acceptor was varied relative to a fixed amount pre-cleared ^{35}S-Cytosol (30 µl from a 3 mg/ml stock) in a binding assay performed for 90 min, either in an ATP_R or ATP_D system. Saturated amounts of label in the pellet was reached from 30 µl of acceptor onwards. **(B)** To determine the optimum incubation time, a binding assay mix (30 µl acceptor, 30 µl ^{35}S-cytosol and 30 µl binding buffer) was incubated as a function of time either in an ATP_R or ATP_D system. After ≈ 2 hours saturation point was reached. All binding assays were thus performed routinely for 2 hours. [Values representative of the mean of 3 separate experiments, SD ≈ 7%]

3.3.2.4 Comparison of binding capacity of X-Endosomes and X-Lysosomes

The binding capacity of X-endosomes and X-lysosomes was compared by incubating them with ^{35}S-cytosol in an ATP_R-system as a function of time. The binding profiles displayed in figure 3.3(B) were almost identical, indicating that the binding assay procedure was optimised for both acceptors. Identical profiles might be expected since most of the targeting/fusion machinery may be ubiquitous (like NSF, SNAPs etc.), some homologous (like SNAREs, Rabs etc.) and a possibly a few unique stage-specific molecules (like EEA1, TRAPP etc.). Because of the former a macro analysis measurement determining the amount of radioactivity in the pellet might not be able to distinguish molecular differences in what was bound by the two different X-linked acceptors. Differences were observed employing 1-dimentional electrophoresis [Figures 3.5-3.10], but more differences were evident when 2-dimentional electrophoresis [Figures 3.12-3.15] was employed.

3.3.2.5 Blocking Agents: BSA & Milk Powder

To minimise non-specific binding to the acceptors, blocking agents (BSA & Milk Powder) were tested. Before incubation in the binding assay, the acceptors (X-endosomes and X-lysosomes) were resuspended in binding buffer with BSA or milk powder added. Incubations were performed in the presence of an ATP_D system. The amount of radioactivity pelleted with the acceptors was analysed. The mean results were displayed in Figure 3.4. It is evident that the blocking agents (BSA and Milk Powder) decreased the percentage radioactivity pelleted significantly, thereby removing a non-specific component interacting with the acceptor. Since the content of milk powder is complex, BSA was chosen as the standard blocking agent in all subsequent binding assays.

(A) ATP Reversible Binding of pre-cleared ^{35}S-Cytosol.

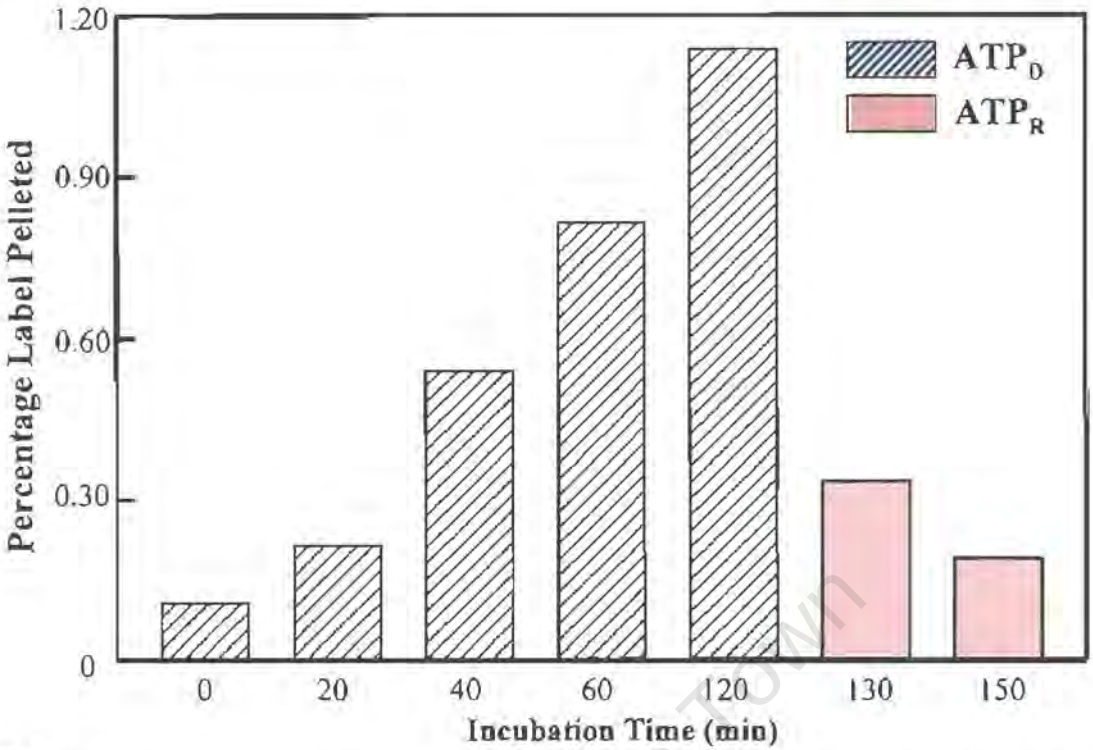

(B) X-Endosome vs X-Lysosome Binding as F(Time) in an ATP$_R$ system

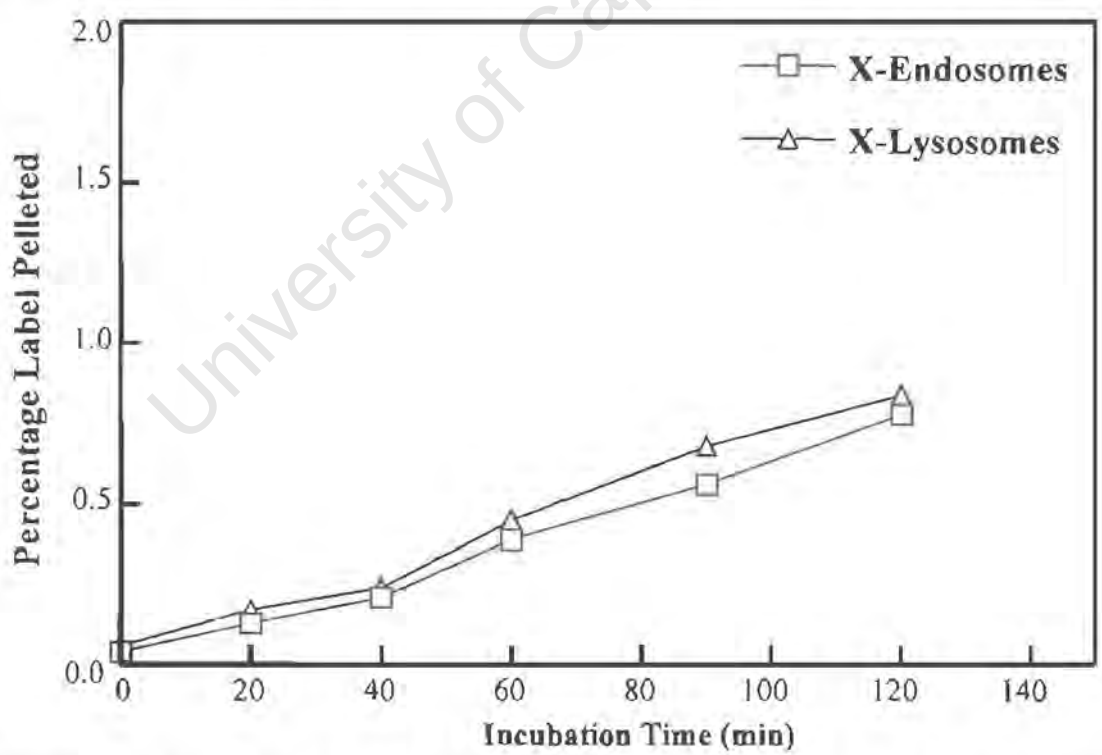

Figure 3.3 : **(A)** To establish whether binding was reversible, acceptors were incubated as a function of time first in an ATP-depleting system and then in an ATP-regenerating system at 37°C [binding assay mixture as described in Figure 3.2(B)]. **(B)** A comparison between the binding capacity of X-endosomes and X-lysosomes was performed as a function of time in an ATP-regenerating system at 37°C [binding assay mixture as described in Figure 3.2(B)]. The curves for X-endosomes and X-lysosomes were almost identical [discussed in Section 3.3.2.4]. [Values representative of the mean of three separate experiments]

The Effect of Acceptor Blocking Agents (BSA or Milk Powder) on the Binding of Donor Material

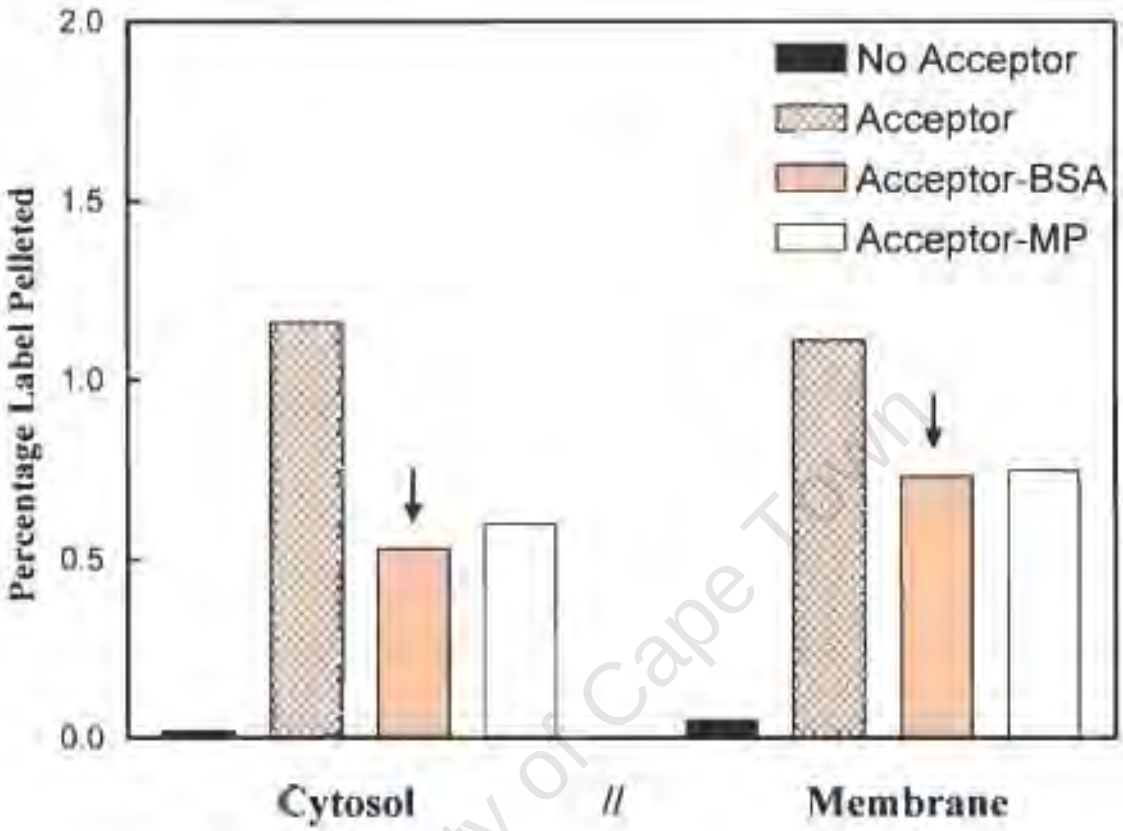

Figure 3.4 : To determine whether non-specific blocking agents could affect binding capacity, acceptors (X-endosomes or X-lysosomes) were first incubated with BSA (0.1%) or milk powder (0.1%) at 4°C for 30min. The acceptors were then washed before used in the binding assay. Incubations were performed in an ATP-depleting system at 37°C for 2 hours [binding assay mixture as described in Figure 3.2(B)]. The amount of radioactivity pelleted with the acceptors was determined. The blocking agents (BSA and Milk Powder) decreased the amount of label pelleted by approximately 50% for Cytosol and 33% for Membrane$^{TX\text{-}100}$. BSA was chosen as the standard acceptor blocking agent for all subsequent binding assays. [Values representative of the mean of three separate experiments]

3.3.3 SDS-PAGE and Autoradiography

3.3.3.1 Nucleotide Conditions

The different nucleotide conditions used in the binding assays were chosen on the basis of what is known about targeting and/or fusion. An ATP-regenerating (ATP_R) system was chosen because of the requirement for ATP by the fusion process. ATP is required for action of an NEM-sensitive ATPase like NSF [discussed in Section 1.3.2.1, see also Figure 1.4 steps 8-10], however other unknown factors may also require ATP for binding. To distinguish ATP dependent binding from other non-ATP dependent factors, an ATP-depleting (ATP_D) system was employed. However it may be that some factors bind upon association with ATP, but then rapidly dissociate upon subsequent ATP-hydrolysis. This can be counteracted by introducing a non-hydrolysable ATP analogue such as ATPγS, which would lock the ATP dependent binding factor in the active binding conformation. In addition to the requirement of ATP, it has been shown that targeting and/or fusion requires small GTPases called Rabs [discussed in Section 1.4.2, see also Figure 1.4] that require GTP for their function. To distinguish between the binding effects of ATP and GTP, they were employed individually, but to detect potential synergestic effects both nucleotides were included in the binding assay (ie. an ATP_R / GTP system).

Binding assays performed employing these different nucleotide conditions produced different banding patterns upon polyacrylamide gel electrophoresis. The complex protein-protein interactions, which govern the targeting and/or fusion process, can only be delineated if the investigation can limit the binding of only a subset of these factors under specified conditions. Of course there would be factors that will bind ubiquitously irrespective of the nucleotide conditions imposed in the binding assays.

The nucleotide conditions employed to bind cytosolic factors were also used to detect membrane factors. Results presented were performed at least thrice and were reproducible.

3.3.3.2 Cytosol binding assays

In binding assays performed using pre-cleared ^{35}S-cytosol [as described in Section 3.3.1.1] as donor, different banding patterns were observed depending on the nucleotide condition employed. In addition, under certain nucleotide conditions (ATP-regenerating or ATP-depleting) the patterns changed if the acceptors were salt-extracted prior to incubation in the binding assays. Salt-extraction (before addition of BSA) of X-acceptors was performed to remove peripheral membrane proteins or adsorbed cytosolic factors that might compete with the binding of their radioactive counterparts from the metabolically labelled donor. In this regard the results of the binding assays for each nucleotide condition was related to whether the acceptors were treated with NaCl (Acceptor^{NaCl}) prior to incubation in the binding assays. Essentially the same banding patterns were observed for both X-endosomes and X-lysosomes.

As summarised in Figure 3.5 and 3.6, the following observations were made. In an ATP_R system it was evident that X-endosomes has bound bands of 63 and 45 kDa [Figure 3.5, lane 1], whereas X-lysosomes bound an additional band of 70 kDa [Figure 3.5, lane 5). This difference implies that X-lysosomes but not X-endosomes, contained a factor/s involved in the binding of a 70 kDa band. However, this was not the case since salt-extraction created a binding site for the 70 kDa band at the expense of the 63 kDa band for both acceptors [Figure 3.5, lanes 3 & 7]. Several explanations could account for this phenomenon. Firstly, salt-extraction the acceptors might have removed a factor involved in binding the 63 kDa band which in turn could have blocked the binding of the 70 kDa band. Secondly, a receptor capable of switching its binding affinity for either the 63 or 70 kDa bands might have been allosterically promoted by a conformational change which could be altered by high salt treatment. In the native state perhaps only a 63 kDa affinity state might be present in early endosomes, but both 63 and 70 kDa affinity states existing in lysosomes. Salt-extraction might allosterically affect the receptors' conformation, thereby promoting the 70 kDa affinity state.

When the non-hydrolysable ATP analogue ATPγS was included in the binding assay, only the 45 kDa band persisted [Figure 3.6, lanes 4 & 8]. This indicated that the binding of the 70 kDa band as well as the 63 kDa band was dependent on ATP hydrolysis, either for an allosteric conformational change and/or phosphorylation events, which affected their binding capacity. The binding of the 70 kDa band is enriched relative to the 63 kDa band, since the intensity of the 70 kDa band is much less than the 63 kDa band in the cytosol [Figure 3.5, lane 9].

Under ATP_D conditions [Figure 3.5, lanes 2 and 6], bands at 190, 45, 35, 19, 18 and 16 kDa were observed. However, in the case of salt-extracted acceptors [Figure 3.5, lanes 4 & 8] bands 190, 45, 35 and 31 kDa were bound. Thus, salt-extraction interferes with the binding of bands 19, 18 and 16 kDa, but conversely promotes the binding of a 31 kDa band.

In the presence of an ATP_D system with GTP added [Figure 3.6 lanes 3 & 7], bands at 90, 50, 45, 44 and 35 kDa are evident. When the binding assay was performed in the presence of GTP alone [Figure 3.6, lanes 1 & 5], only the 90 and 35 kDa bands were detected. These results were not affected by salt-treatment of X-acceptors. Thus, binding of the 90 kDa band is dependent on the presence of GTP, binding of the 190 kDa band is dependent on the absence of both ATP and GTP, while binding of the 44 kDa band requires the presence of GTP and additionally the absence of ATP.

A multitude of bands were pelleted after incubation of acceptors in an ATP_R system plus GTP added [Figure 3.6, lanes 2 & 6]. When the banding patterns of lanes 2 & 6 were compared with the cytosol [Figure 3.5, lane 9], it was noted that bands 61 and 48 kDa were not obviously present in the cytosol. This suggested a specific enrichment of these bands or possible changes in molecular weight due to phosphorylation or de-phosphorylation of other visible bands of the cytosol lane.

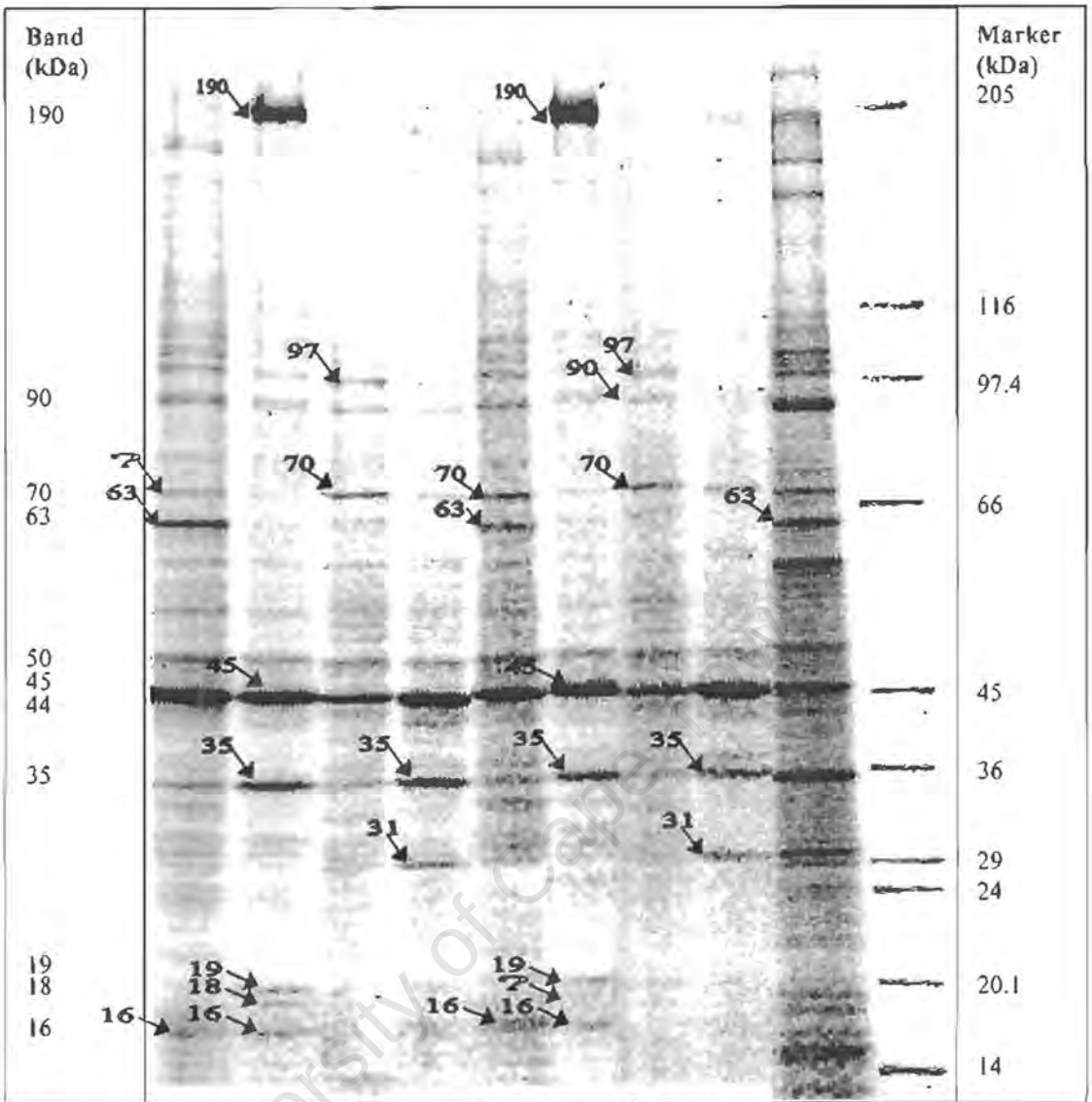

Lane Number	1	2	3	4	5	6	7	8	9	10
Acceptor Type	X-En		$X\text{-}En^{NaCl}$		X-Ly		$X\text{-}Ly^{NaCl}$		^{35}S-Cyt	Marker
Nucleotide	ATP_R	ATP_D	ATP_R	ATP_D	ATP_R	ATP_D	ATP_R	ATP_D		
^{35}S-Donor	^{35}S-Cytosol									

Figure 3.5 : Cytosol binding assay pellets (using BSA or salt-washed/BSA treated X-acceptors) run on a SDS-PAGE gradient gel followed by radioactive scanning. BSA or salt-washed/BSA treated X-endosomes and X-lysosomes were resuspended in Binding buffer. X-endosomes {BSA (lanes 1-2), salt-washed/BSA (lanes 3-4)} or X-lysosomes {BSA (lanes 5-6), salt-washed/BSA lanes 7-8)} were incubated at 37°C for 2 hours with fully soluble ^{35}S-Cytosol (lanes 1-8), either in an ATP-regenerating system (lanes 1, 3 ,5 & 7 or ATP-depleting system (lanes 2, 4, 6 & 8). Samples were overlaid onto 25% sucrose and acceptors with bound radioactive material collected by centrifugation. The pellets were resuspended and run on a 5-13% gradient SDS-PAGE gel followed by radioactive scanning. A sample of ^{35}S-Cytosol was run in lane 9. The Mw Marker was run in lane 10 and was marked with radioactive ink. Bands were labelled according to their molecular weight. [Representative of 3 separate experiments]

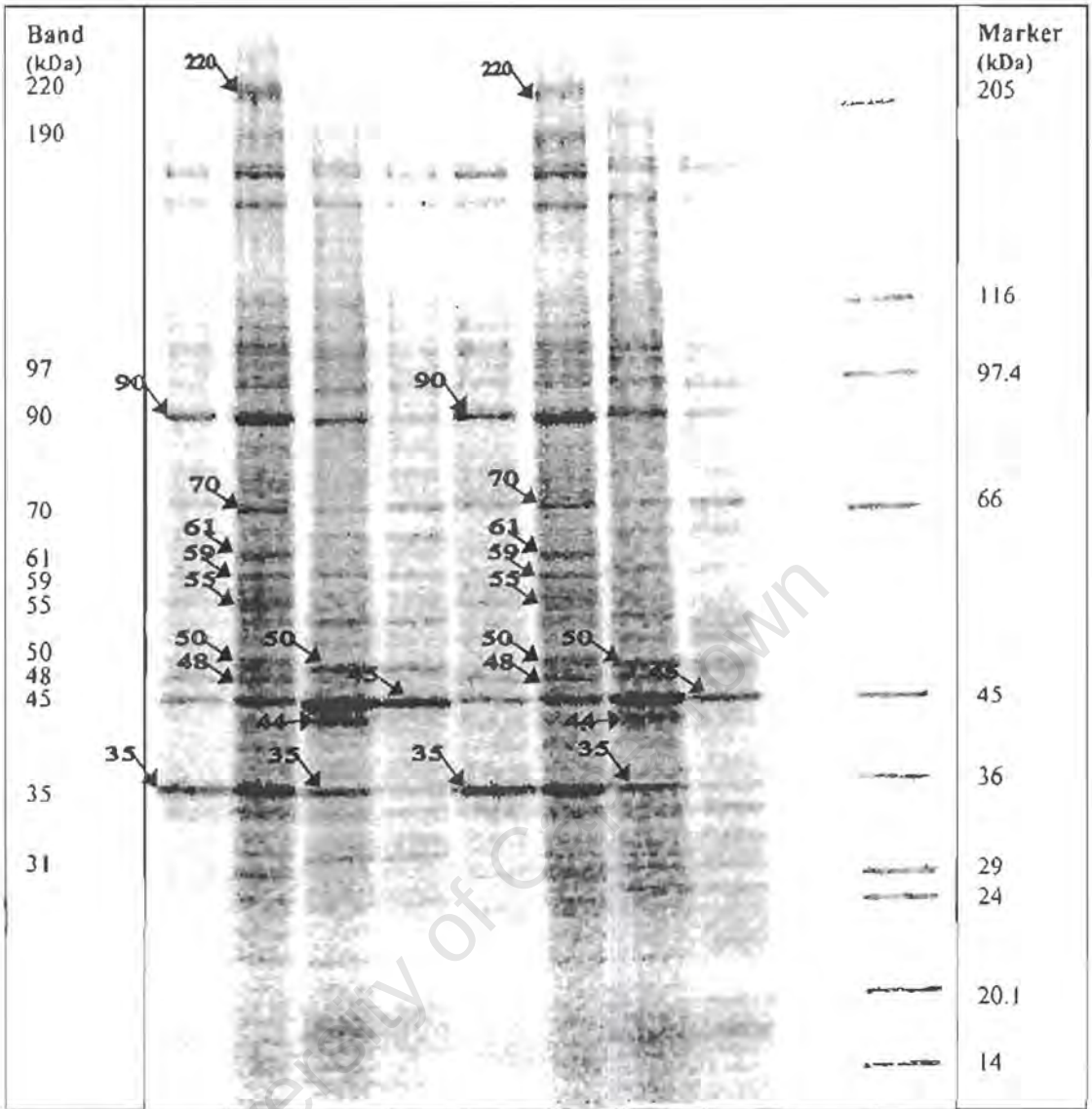

Lane Number	1	2	3	4	5	6	7	8	9	10
Acceptor Type	X-Endosomes^{NaCl}				X-Lysosomes^{NaCl}				No Acceptor	Marker
Nucleotide	GTP	ATP_R GTP	ATP_D GTP	ATPγS	GTP	ATP_R GTP	ATP_D GTP	ATPγS	ATP_R	
^{35}S-Donor	^{35}S-Cytosol									

Figure 3.6 : Cytosol binding assay pellets (using salt-washed/BSA treated X-acceptors only) run on a SDS-PAGE gradient gel followed by radioactive scanning. Salt-washed/BSA treated X-endosomes and X-lysosomes were resuspended in Binding buffer. X-endosomes (lanes 1-4) or X-lysosomes (lanes 5-8) were then incubated at 37°C for 2 hours with fully soluble ^{35}S-Cytosol, either in the presence GTP (lanes 1-3 & 5-7 with 2 & 6 additionally in the presence of an ATP-regenerating system and lanes 3 & 7 additionally in the presence of an ATP-depleting system) or ATPγS (lanes 4 & 8). Samples were processed further as described in Figure 3.5. A control incubation with ^{35}S-Cytosol in the absence of acceptors in an ATP-regenerating system was run in lane 9. The Mw Marker was run in lane 10. [Representative of three separate experiments]

The different banding patterns observed under different nucleotide conditions in the binding assays, were to some extent difficult to analyse. Bands were labelled according to their apparent or observed molecular weights, to develop a working framework. Analysis of the banding patterns considered mainly relative differentials of band intensities under different conditions rather than absolute band intensities. To explain this point, if one considered a particular band, say the 45 kDa band, this appeared most intense under ATP_D/GTP conditions, but even its lesser intensity under ATP_R conditions was still relatively more intense than the bands that bound specifically under ATP_R conditions. It was decided that the bands of weaker intensity were of greater interest in the context of the present study than the 45 kDa band that showed up with high intensity under ATP_R conditions." The results of this type of analysis have been summarised and the molecular weights of these bands have been corresponded with known proteins [Figure 3.7].

The banding pattern was essentially common for both acceptors. These proteins might form part of a ubiquitous machinery involved in the endocytic pathway. Their identity as members of the cytoskeleton should be considered, in particular, microtubules are required for transfer of organelles along the endocytic pathway [Section 1.2.3.2]. Major bands of 45 kDa and 35 kDa might be tubulin and actin, respectively. Since the cytosol was extensively pre-cleared before incubation in the binding assays, precipitation of the 45 and 35 kDa bands might either be due specific association with the X-acceptors or due to de novo complex formation of microtubules or actin filaments.

In support of this study's findings, two other studies also detect bands at 45 and 35 kDa and identified as tubulin and actin respectively [351,133a]. In the one study, a photo cross-linking approach has been used to pull out factors associated with Rab5 under varying nucleotide conditions, showing that under ATP-depletion, polymerised actin and intermediate filaments can be recovered in a pellet after sucrose gradient centrifugation together with Rab5 [351]. In the other study, using free flow electrophoresis (FFE) [133a] to produce endosomal fractions devoid of ER and Golgi membrane and with minimal

lysosomal contamination (<10% by protein), it is found that endosomes bind members from the COPI and ARF families under GTPγS incubation conditions. However only coat assembly proteins is detected, with no docking and/or fusion factors obvious.

The present observation that a 45 and 35 kDa band was collected on X-acceptors, mainly under ATP_D conditions, could be understood in terms of previous work showing the involvement of microtubules [94a] and cytoskeletal elements [94b] during endocytic processing. Endosomal carrier vesicles (ECVs) accumulate in-vivo under microtubule depolymerisation conditions (i.e. in the presence of nocodazole) [53]. ECVs that accumulate under these conditions, bind to microtubules in-vitro in a cytosol and nucleotide sensitive fashion, but independent of kinesin and cytoplasmic dynein, even though they are ascribed to be involved in movement along the microtubules. It has also been shown that a 170 kDa protein (CLIP 170) links ECVs to microtubules [354]. Research on the role of microtubules in vesicular transport is thus well established, but the role of the actin cytoskeleton is still unclear. However, evidence implicating unconventional myosins [94b] in the endocytic recycling pathway and the finding that phagosome-endosome fusion is stimulated by the actin-severing fragment of gelsolin (90 kDa) [355], has stimulated this area of research. Recently, it has been shown that phagosomes with pathogenic mycobacteria disrupt the actin filament network [356].

It may well be that the cytoskeletal associated elements possess greater functional responsibility in addition to the structural properties ascribed to them thus far inside the cell. However, since the main objective of this study was to search for membrane factors (which are more likely to be involved in targeting) the interesting phenomena observed for cytosol was not analysed further. The main reason for using cytosol as donor in the binding assay was to establish the procedure in terms of nucleotide conditions. The same conditions were thus applied for membrane binding assays.

OBSERVED BANDS (MW in kDa)							CANDIDATES
Band No.	ATP_R	ATP_O	ATP_O GTP	$ATP\gamma S$	GTP	ATP_S GTP	ACTIN-FILAMENTS, SNARE COMPLEX
CYTOSOL							
1						220m	
2		190s				190w	Myo Hc (200)
3	97						p97 (97)
4			90m		90m	90s	Gelsolin (90)
5	70						NSF (76)
6	63 (rsa)						
7-9						61,59,55	
10			50m			50m	
11						48m	
12	45m	45s	45s	45m			Tubulin (45)
13			44s				
14		35s	35m		35s	35m	Actin (42)
15		31 (dsa)					SNAPs (35-39) Tropomyosin (32)
16		19 (rsa)					Myo Lc (22)
17		18 (rsa)					Myo Lc (18)
18	16	16 (rsa)					
MEMBRANE							
1-5			170-74		SNAREs (15-35 kDa)		
6	57	57	57				
7	56		56				
8-10			52,48,46				
11	34m		34s	34m			
12	33m		33s				
13/Lys	32m	[redacted]	32s	32m			
14	26			26			
15		21					
16			15				

Figure 3.7 : Tabulated summary of the molecular weights of the observed cytosolic and membrane bands. The band molecular weights (indicated within brackets) were comparable to known and predicted factors involved in membrane transport. Relative band intensities are indicated by the letters s (strong), m (medium) and w (weak). Cytosolic bands removed (rsa) or dependent (dsa) by/on salt-washing acceptors were shown. **The only organelle specific band detected** (not removed from the donor by salt-washing and sonication) **is a 32 kDa Membrane band bound especially by X-Lysosomes.**

3.3.3.3 Membrane binding assays

Acceptors (X-endosomes and X-lysosomes) were incubated with pre-cleared ^{35}S-Membrane^{Lf} [Section 3.2.2.2] in the presence of cold cytosol (in the event that any binding between membranous factors might be mediated by cytosolic factors not adsorbed to the labelled membrane) under different nucleotide conditions in the binding assay. The results of these binding assays have been illustrated by Figures 3.8, 3.9 and 3.10.

Figure 3.8 exhibited a result obtained when the donor source was not salt-extracted or sonicated prior to solubilisation with Triton X-100. Bands at ≈ 90, 74, 56, 51, 46, 34, 33, 32 and 26 kDa are detected when ATP_R conditions was employed in the binding assays [Figure 3.8, lanes 1 & 5]. Under ATP_D conditions the banding pattern is similar for both acceptors, except for a 32 kDa band bound especially intense by X-lysosomes [Figure 3.8, compare lane 6 vs. lane 2]. The bands pelleted in binding assay incubations with ATP_D/GTP condition [Figure 3.8, lanes 3 & 7] such as ≈ 170, 106, 100, 76, 57, 56, 51, 46, 34, 33, 32 (Lys) and 15 kDa, might not simply be integral membrane proteins, but possibly peripheral membrane proteins or tightly adsorbed cytosolic proteins. Also, they might be derived from soluble factors present in the luminal region (i.e. the interior) of the membrane donor vesicles. In this regard, donor membrane was sonicated and salt-extracted prior Triton X-100 solubilisation.

Figure 3.9 exhibited a result obtained when the donor ^{35}S-Membrane^{Lf} *was* salt-extracted and sonicated prior to solubilisation with Triton X-100. Bands became less prominent under all nucleotide conditions employed, with the exception of bands 34, 33 and 32 kDa. These bands (34, 33 and 32) actually became more prominent [Figure 3.9]. The enhanced binding capacity for the 32 kDa band by X-lysosomes under all conditions, but more specifically under ATP-depleting conditions [Figure 3.9, lane 6] prompted further analysis.

Even though X-endosomes served as a concomitant experimental control to indicate that the specific binding of the 32 kDa band by X-lysosomes was not artifactual, an unrelated non-specific acceptor was sought. For this purpose, latex beads coated with HRP and then DAB cross-linked was produced. The specific binding of the 32 kDa band by X-lysosomes, could not be matched by the non-specific acceptor DAB-latex [Figure 3.9 (lane 9), Figure 3.10 (lane 1)]. This result served to confirm that the specific binding of the 32 kDa band by X-lysosomes under ATP-depleting conditions was not an artifact.

The results were summarised [Figure 3.7]. Under ATP_R/ATPγS conditions the bands 34, 33 and 32 kDa were the most prominent. According to accepted dogma specific targeting amongst endocytic organelles (and secretory structures) depends upon the existence of organellar-specific membrane proteins. Protein families like the Rabs and SNAREs have similar molecular weight and perform the same type of function, albeit with organellar-specific distribution. Thus, it is not inconceivable that the 34 and 33 kDa bands bound ubiquitously by both acceptors might be organellar specific homologues. The latter possibility and specific enhancement for the 32 kDa band by X-lysosomes under ATP-depleting conditions, prompted further analysis by 2-dimensional electrophoresis [Figures 3.12-3.15].

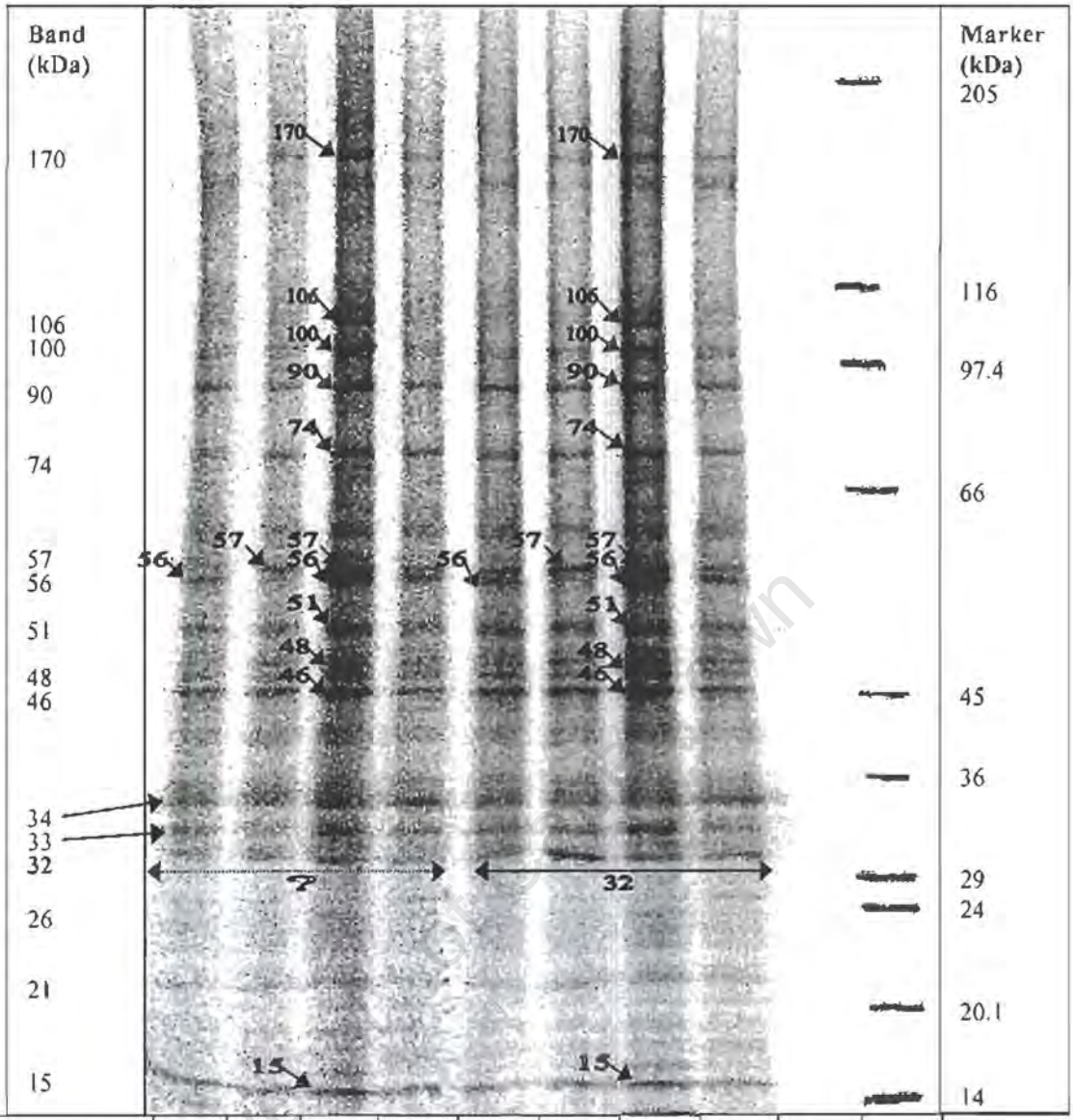

Lane Number	1	2	3	4	5	6	7	8	9	10
Acceptor Type	X-Endosomes^{NaCl}				X-Lysosomes^{NaCl}				No Acceptor	Marker
Nucleotide	ATP_R	ATP_D	ATP_D GTP	ATP_R ATPγS	ATP_R	ATP_D	ATP_D GTP	ATP_R ATPγS	ATP_D	
^{35}S-Donor	^{35}S-Membrane^{Lf} + Cold-Cytosol									

Figure 3.8 : Membrane binding assay pellets (using ^{35}S-Membrane^{Lf} as donor) run on a SDS-PAGE gradient gel followed by radioactive scanning. Salt-washed/BSA treated X-acceptors were resuspended in Binding buffer. The X-endosomes (lanes 1-4) or X-lysosomes (lanes 5-8) were then incubated at 37°C for 2 hours with fully soluble ^{35}S-Membrane^{Lf} (lanes 1-8), either in an ATP-regenerating system (lanes 1, 4 ,5 & 8 with 4 & 8 additionally in the presence of ATPγS) or ATP-depleting system (lanes 2, 3, 6 & 7 with 3 & 7 additionally in the presence of GTP). Samples were processed further as described in Figure 3.5. A control incubation with ^{35}S-Membrane^{Lf} in the absence of acceptors in an ATP-depleting system was run in lane 9. The Mw Marker was run in lane 10 and was marked with radioactive ink. Bands were labelled according to their molecular weight. [Representative of 3 separate experiments]

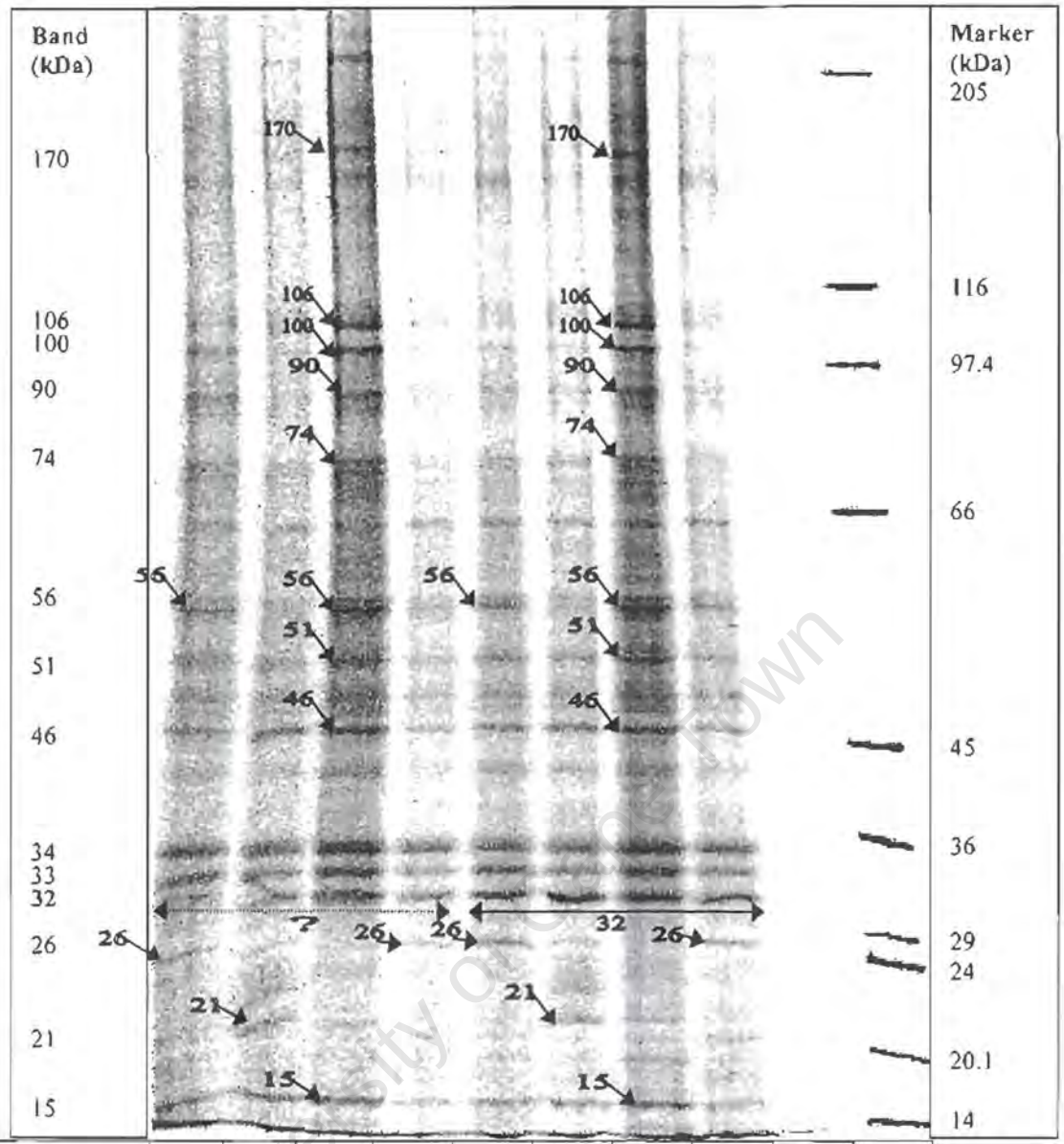

Lane Number	1	2	3	4	5	6	7	8	9	10
Acceptor Type	X-Endosomes^{NaCl}				X-Lysosomes^{NaCl}				DAB-Latex	Marker
Nucleotide	ATP_R	ATP_D	ATP_D GTP	ATP_R ATPγS	ATP_R	ATP_D	ATP_D GTP	ATP_R ATPγS	ATP_D	
^{35}S-Donor	^{35}S-Membrane^{Lf} (salt-washed and sonicated) + cold-Cytosol									

Figure 3.9 : Membrane binding assay pellets (using salt-washed/sonicated ^{35}S-Membrane^{Lf} as donor) run on a SDS-PAGE gradient gel followed by radioactive scanning. Experimental details as described in Figure 3.8, except that salt-washed and sonicated ^{35}S-Membrane^{Lf} was used as donor and that a control incubation with DAB-latex in an ATP-depleting system was run in lane 9. The big horizontal arrow (↔) shows that the 32 kDa band was enriched for X-lysosomes (as compared with X-endosomes) under all nucleotide conditions, but especially under ATP-depleting conditions. [Representative of 3 separate experiments]

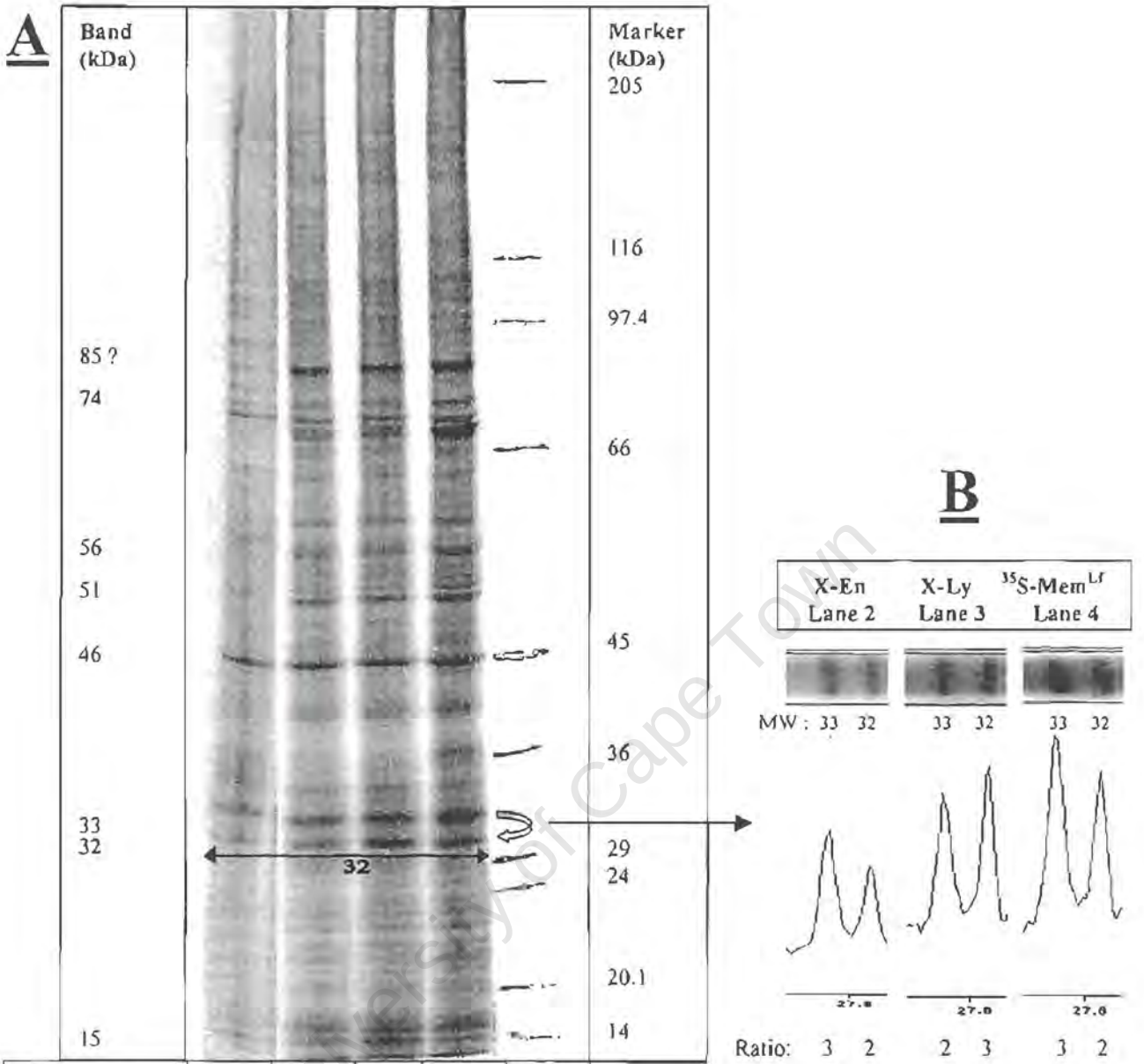

Lane Number	1	2	3	4	5
Acceptor Type	DAB-Latex	X-En	X-Ly	Mem^{Lf}	Marker
Nucleotide	ATP_D				
^{35}S-Donor	^{35}S-$Membrane^{Lf}$ (salt-washed & sonicated)				

Figure 3.10 : Comparison of binding assay pellets of X-endosomes, X-lysosomes, DAB-latex, and salt-washed/sonicated ^{35}S-$Membrane^{Lf}$ donor. A) Salt-washed/BSA treated DAB-latex, X-endosomes and X-lysosomes were resuspended in Binding buffer. The non-specific DAB-latex acceptor (lane 1), X-endosomes (lanes 2) or X-lysosomes (lane 3) were incubated at 37°C for 2 hours with fully soluble salt-washed/sonicated ^{35}S-$Membrane^{Lf}$ (lanes 1-3) in an ATP-depleting system. A sample of ^{35}S-$Membrane^{Lf}$ was run in lane 4. The Mw Marker was run in lane 5. The big horizontal arrow (↔) shows that the 32 kDa band was enriched for X-lysosomes as compared to DAB-latex and X-endosomes. B) A radioactivity plot of the 31-35 kDa region for lanes 2-4, which shows that the intensity of the 32 kDa is enriched in terms of relative quantities of the 33 and 32 kDa bands present in the ^{35}S-$Membrane^{Lf}$ donor.

3.3.4 2-D Electrophoresis

Polyacrylamide gel electrophoreis (PAGE) is a simple method used for separation of proteins in a slab gel by applying an electric field. Proteins are typically detected by coomassie blue or silver staining of the slab gel. Alternatively, proteins may be metabolically labelled with ^{35}S-methionine and then detected in the gel by autoradiography.

One-dimensional gel electrophoresis, SDS-PAGE, is used to monitor purification processes or even as a final purification step, by separating proteins according to their size. Although SDS-PAGE can separate relatively complex protein mixtures, protein components of similar size may comigrate into the same position on the gel.

Improved separation and resolution is obtained by employing 2-dimensional electrophoresis (2D-PAGE)[367a]. In the first dimension, proteins are separated according to their isoelectric point (pI), and then separated in the second dimension by SDS-PAGE. Due to the high resolution of such a system, thousands of proteins may be separated in a single experiment. 2D-PAGE is, therefore, the separation method of choice for proteome studies. The use of commercial immobilised pH gradient (IPG) strips has enabled reproducibility of analytical protein isoelectric focussing separations [367b,c]. In general, 2-D analysis of membrane proteins is limited by solubility problems attributed to their hydrophobic properties. Preparative separations of protein samples (> 1mg), especially membrane proteins, have been made possible by the use of in-gel sample loading [352a] and thiourea [352c]. In this study, an optimised combination protocol was applied [352b].

To determine the pI of unknown spots, a sample of standard isoelectric pH markers was run on an IPG strip (pH 3-10 non-linear, 180mm) [Figure 3.11A]. A plot of standard isoelectric pH versus the distance migrated was performed [Figure 3.11B]. IEF reprodubility facilitated pI determinations.

A) Isoelectric focussing standards run on an IPG-strip (pI 3-10 NL,180mm)

B) Standard Plot of Isoelectric pH versus Distance

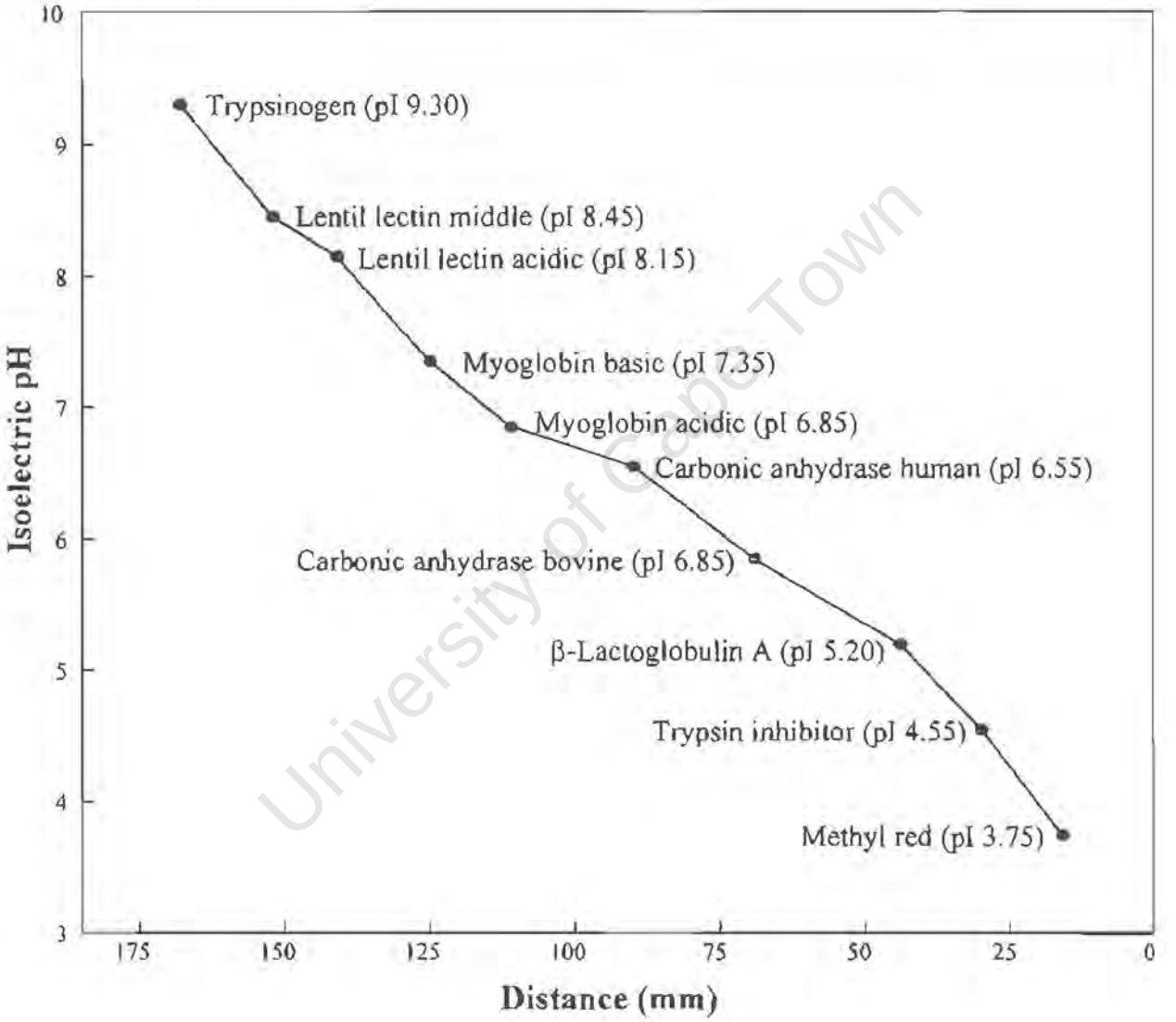

Figure 3.11 : Standard Plot of Isoelectric pH versus Distance. **A**) Pharmacia pI marker proteins (0.1mg) was loaded during reswelling of an IPG strip (pH 3-10 NL, 180mm) in sample buffer (8M urea, 2M Thiourea, 4% CHAPS, 2% pH 3-10 carrier ampholytes, 20mM Tris base, 30mM DTT). Isoelectric focusing was performed at 17°C until equilibrium (65 kVh) followed by coomassie staining. **B**) A standard plot of Isoelectric pH versus distance (mm) migrated.

2-Dimensional gels of salt-extracted and sonicated ^{35}S-Membrane bound by X-endosomes or X-lysosomes was exhibited by Figures 3.12 and 3.13, respectively. Comparison of these gels to the 2-D gel of salt-extracted and sonicated ^{35}S-Membrane^{Lf} [Figure 3.14] used as ^{35}S-donor source in the binding assays, it was evident that only a subset of spots {74Lb(5.1), 56Eb(5.2), 52b(7.7), 51b(8.0), 50b(5.1), 45b(5.4), 34b(5.7), 33b(8.6), 32Lb(8.4), 15Lb(9.4) and 14b(7.5)} from the donor was bound by the X-acceptors. Spots have been labelled according to their molecular weight and specific acceptor association (**Eb** for spots **b**ound by X-**E**ndosomes only, **Lb** for spots **b**ound by X-**L**ysosomes only and **b** for spots **b**ound by both X-acceptors). The pI of spots was indicated within brackets.

The regions (A, B, and C) boxed in Figures 3.12, 3.13 and 3.14, was expanded in Figure 3.15, to allow direct comparison between what was bound by X-endosomes [Figure 3.12] and X-lysosomes [Figure 3.13] from the donor salt-extracted and sonicated ^{35}S-Membrane^{Lf} [Figure 3.14]. It was obvious from Figure 3.15 that X-lysosomes exhibited enhanced binding of spots 32Lb (region A, circles), 15Lb (region B, circles) and 74Lb (region C, circles), while X-endosomes exhibited enhanced binding of spot 56Eb (region C, triangles). Both acceptors exhibited similar binding capacity for spots 33b (region A, squares) and 14b and (region B, squares). Spots 57 and 68 (region C, hexagons) are examples of the numerous spots not bound by both acceptors. The radioactivity plots of spots 33b, 32Lb and 15Lb that showed their relative intensity ratios within the indicated peak areas, were also displayed in Figure 3.15. These plots were obtained by applying Instant Imager Software designed for 1-D analysis. Basically, spots were aligned vertically to simulate 1-D separation and then scanned for relative intensities.

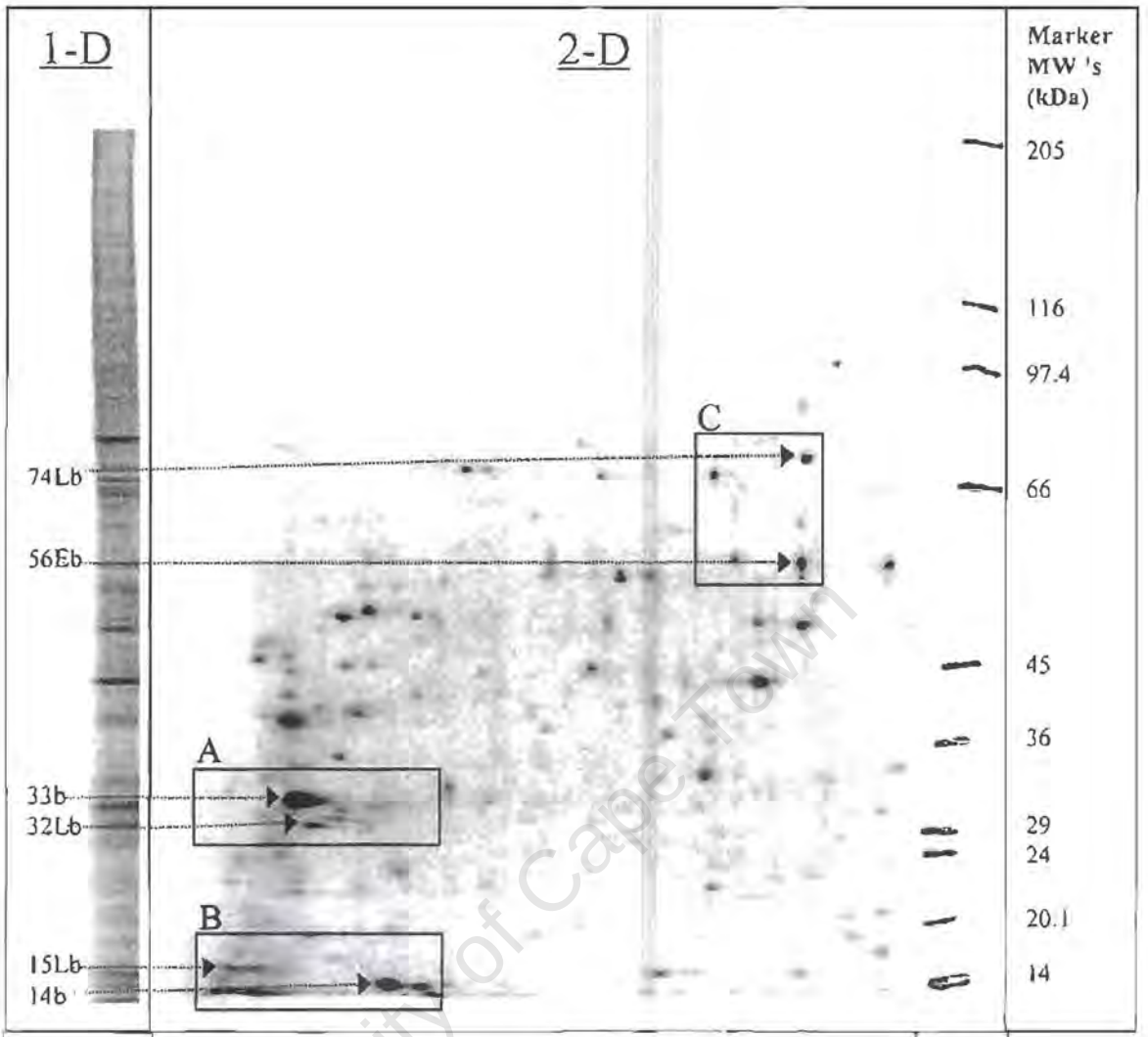

pH-Scale	9.7					4	Marker
Spot No.	74Lb	56Eb	33b	32Lb	15Lb	14b	
pI-value	5.1	5.2	8.6	8.4	9.4	7.5	

Figure 3.12 : 2-Dimensional gel of salt-washed and sonicated ^{35}S-Membrane^{Lf} bound by X-Endosomes. Salt-washed/BSA treated X-endosomes were resuspended in Binding buffer. The X-Endosomes were incubated at 37°C for 2 hours with fully soluble salt-washed/sonicated ^{35}S-Membrane^{Lf} in an ATP-depleting system. The sample was overlaid onto 25% sucrose and acceptors with bound radioactive material collected by centrifugation. The pellet was loaded during reswelling of an IPG strip (pH 3-10 NL, 180mm) in sample buffer (8M urea, 2M Thiourea, 4% CHAPS, 2% pH 3-10 carrier ampholytes, 20mM Tris base, 30mM DTT). Isoelectric focusing was performed at 17°C until equilibrium (65 kVh). The second dimension was performed using a 5-13% gradient SDS-PAGE followed by radioactive scanning. The boxed regions were enlarged in Figure 3.15.

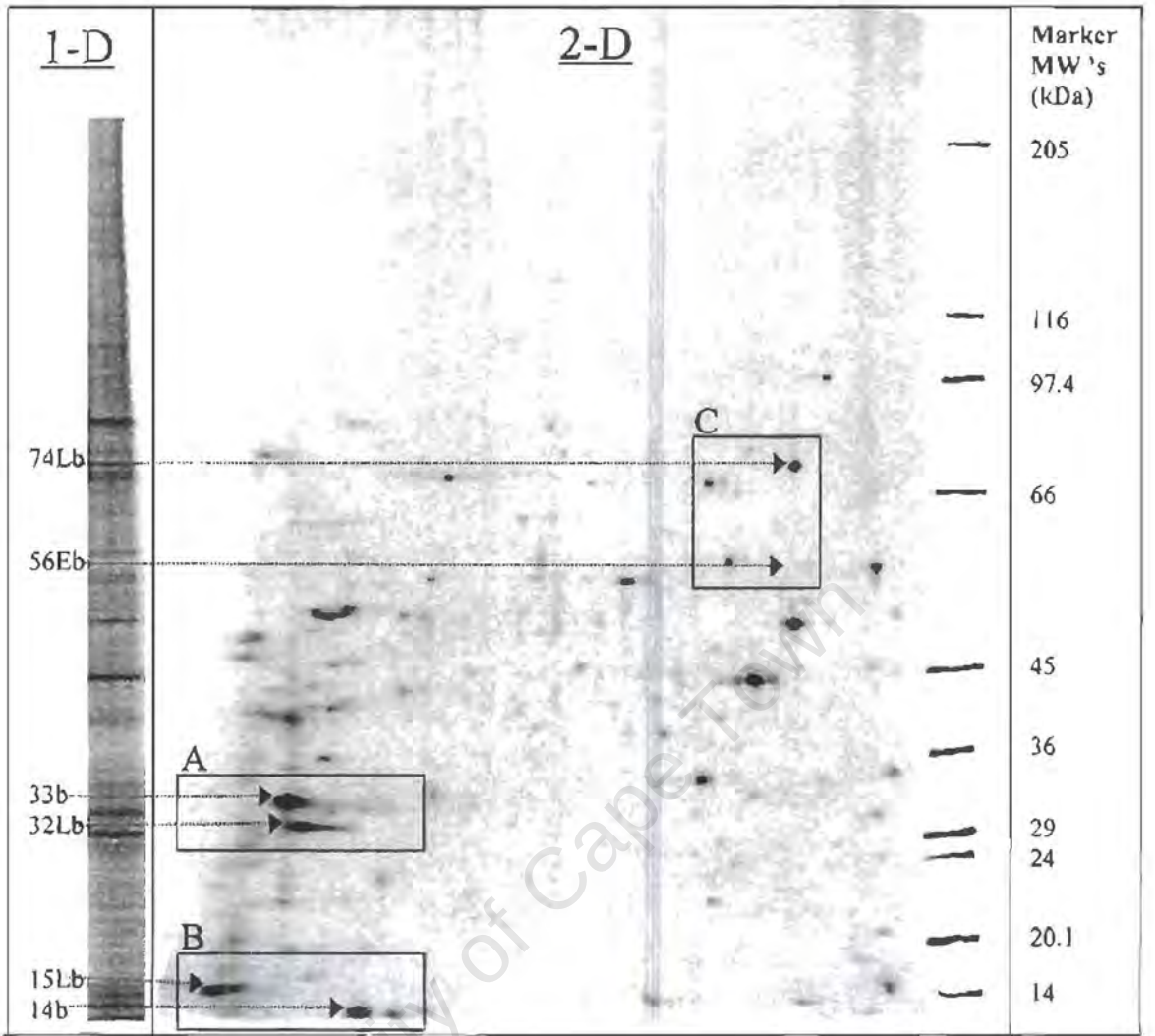

Figure 3.13 : 2-Dimensional gel of salt-washed and sonicated ^{35}S-Membrane^{Lf} bound by X-Lysosomes. Salt-washed/BSA treated X-Lysosomes were resuspended in Binding buffer. The X-Lysosomes were incubated at 37°C for 2 hours with fully soluble salt-washed/sonicated ^{35}S-Membrane^{Lf} in an ATP-depleting system. The samples were processed further as described in Figure 3.12. The boxed regions were enlarged and reproduced in Figure 3.15 to facilitate direct comparisons with what was bound by X-endosomes.

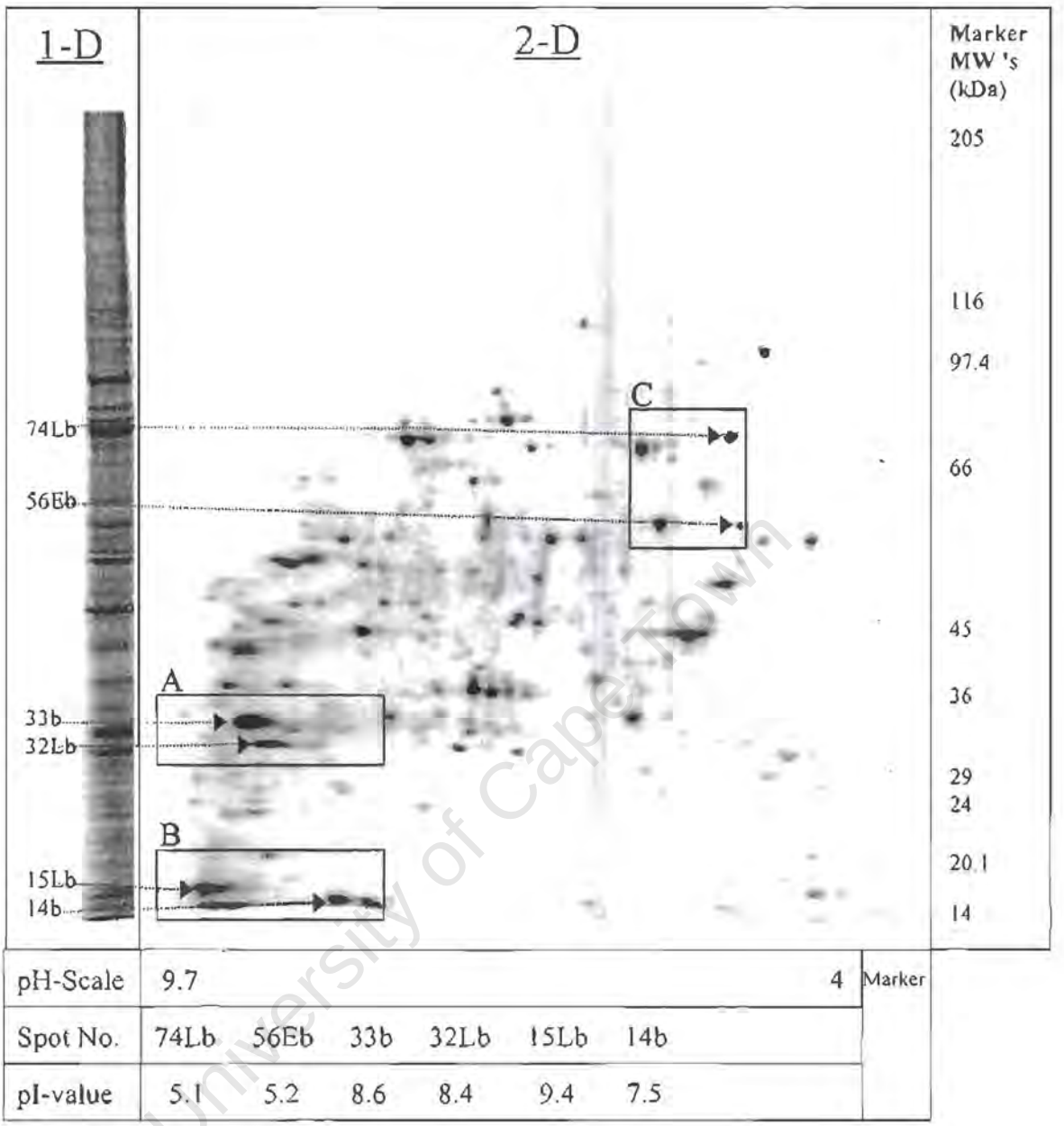

Figure 3.14 ; 2-Dimensional gel of salt-washed and sonicated ^{35}S-Membrane^{Lf} used as donor in the binding assays. A sample of the salt-washed and sonicated ^{35}S-Membrane^{Lf} was loaded during reswelling of an IPG strip (pH 3-10 NL, 180mm) in sample buffer (8M urea, 2M Thiourea, 4% CHAPS, 2% pH 3-10 carrier ampholytes, 20mM Tris base, 30mM DTT). Isoelectric focusing was performed at 17°C until equilibrium (65 kVh). The second dimension was performed using a 5-13% gradient SDS-PAGE followed by radioactive scanning. The boxed regions were enlarged and reproduced in Figure 3.15 to facilitate direct comparisons with what was bound by X-endosomes and X-lysosomes.

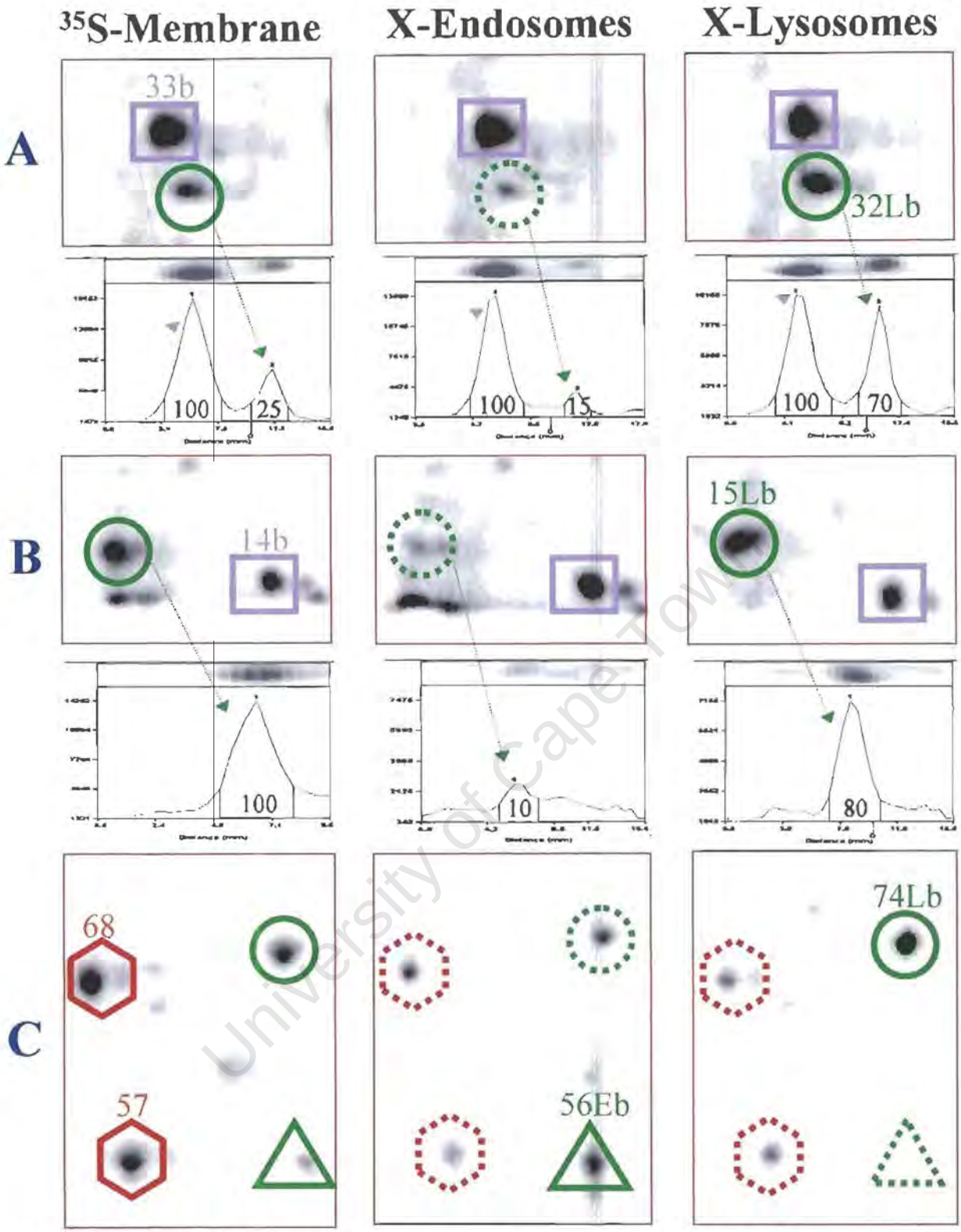

Figure 3.15 : Comparison of 2-Dimensional patterns obtained for X-acceptors from binding assays. The regions (A,B,C) boxed in Figures 3.12-3.14, were enlarged (mainly in a vertical direction) to facilitate direct comparison between what was bound by X-Endosomes (Figure 3.12) and X-Lysosomes (Figure 3.13) from the salt-washed and sonicated ^{35}S-Membrane^{Lf} donor (Figure 3.14). It was evident that X-Lysosomes exhibited enhanced binding of spots 32Lb (region A, circles),15Lb (region B, circles) and 74Lb (region C, circles), while X-Endosomes exhibited enhanced binding of spot 56Eb (region C, triangles). Both acceptors exhibited similar binding capacity for spots 33b (region A, squares) and 14b and (region B, squares). Spots 57 and 68 (region C, hexagons) were examples of the numerous spots not bound by both acceptors. The radioactivity plots of spots 33b, 32Lb and 15Lb were displayed. Their relative intensity ratios were shown within the peak area.

A preparative 2-dimensional gel of unlabelled salt-extracted and sonicated Membrane^{Lf} employed as donor in the binding assays was displayed in Figure 3.16. The spots of interest were excised, digested in-gel with trypsin/Lys-C and then subjected to MALDI-TOF and/or Edman microsequencing [Chapter 6]. Database searching using the peptide masses determined for spot 32Lb (32 kDa/pI 8.5) retrieved Mouse Galectin-3 (27.5 kDa/pI 8.47) as the best matching entry in the databanks. Edman microsequencing [Chapter 6] of a RP-HPLC purified Lys-C peptid from spot 32Ec (32 kDa/pI 8.5) [32**Ec** was found to be especially enriched in the composition of phago-**E**ndosomes, Chapter 5], determined its sequence as (K)EERQSAFPFESGK that matched galectin-3.

MALDI-TOF analysis [Chapter 6] of spots 74Lb (74 kDa/pI 5.1) and 15Lb (15 kDa/pI 9.4) retrieved Mouse BiP (72 kDa/pI 5.11) and Lysozyme C (14.96 kDa/pI 9.47) respectively, as the best matching entries in the databanks. Similarly, the peptide masses of spots 33b (33 kDa/pI 8.6) and 14b (14 kDa/pI 7.5) retrieved Mouse Voltage-Dependent Anion-Selective Channel (30.75 kDa/pI 8.62) and Mouse β2-Microglobulin precursor (13.82 kDa/pI 7.80) respectively.

Thus, it can be stated that the proteins BiP, Galectin-3 and Lysozyme C were bound specifically by X-lysosomes while spot 55Eb(5.2) [still unknown] was bound specifically by X-endosomes.

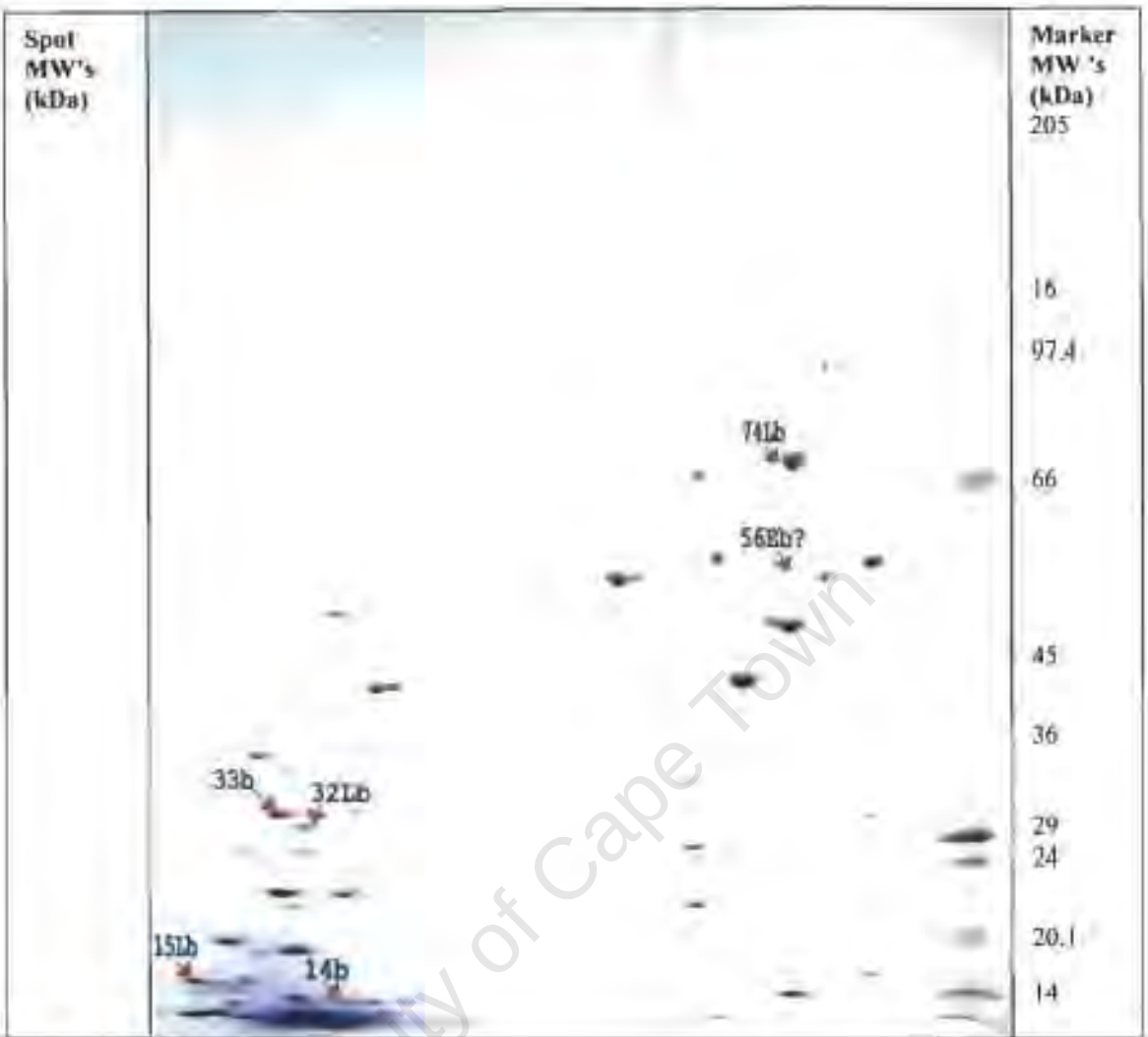

Figure 3.16 : Preparative 2-Dimensional gel of salt-washed and sonicated Membrane^{LT} used for Maldi-MS and Edman sequencing analysis. Proteins (1mg) of salt-washed and sonicated Membrane^{LT} was loaded during reswelling of an IPG strip (pH 3-10 NL, 180mm) in sample buffer (8M urea, 2M Thiourea, 4% CHAPS, 2% pH 3-10 carrier ampholytes, 20mM Tris base, 30mM DTT). Isoelectric focusing was performed at 17°C until equilibrium (65 kVh). The second dimension was performed using a 5-13% gradient SDS-PAGE followed by coomassie staining. The spots of interest were excised and identified by Maldi-MS and Edman microsequencing analysis [Chapter 6].

3.4 DISCUSSION

The proteins bound by the X-acceptors in the binding assays, and identified by mass spectrometry [Chapter 6], might play essential roles along the endocytic pathway. Further investigation is warranted to determine their functional significance. The existing information about these proteins was summarised below.

14b - β_2 microglobulin together with MHC (major histocompatibility complex) class I heavy chain form a complex to present antigenic peptides to T lymphocytes on the cell surface. Class I and II MHC proteins are endocytosed into early endosomes [392-394] facilitating peptide exchange. Intracellular sorting through these compartments is regulated by cytoplasmic phosphorylation of MHC I [395]. Thus the presence of β_2 microglobulin in the endocytic pathway is expected. The binding of Triton X-100 solubilised β_2 microglobulin to X-acceptors in the binding assay might be due to the probable presence of non-complexed MHC heavy chain in endocytic organelles.

33b - The existence of a plasma membrane localised voltage-dependent anion selective channel (PM-Porin) has recently been confirmed [396]. The localisation of PM-Porin isoform to the plasma membrane is driven by a hydrophobic N-terminal leader sequence that is absent in the mitochondrial form of Porin. The functional requirement of a plasma membrane localised Porin is not yet defined. The finding in this study, that X-endosomes bound Porin, might imply a role in the endocytic pathway.

15Lb - Lysozyme C is a glycosyl hydrolase. It hydrolyses 1,4 β-linkages between N-acelyglucosamine and N-acetylmuramic acid of glyco-peptides present in the cell walls of prokaryotes. It is expressed strongly in mature macrophages. Its observed binding to X-lysosomes might be due to intra-luminal glycosyl sites of lysosomes exposed as a result of having removed the membrane lipids by Triton X-100.

32Lb - Galectin-3 [discussed in Chapter 7] is a β-galactose binding lectin. Galectin-3 belongs to the family of mammalian β-Galactoside-binding proteins known as galectins [383,384]. Galectin-3 contains a large N-terminal domain and a carbohydrate-recognition domain (CRD). Galectin-3 is found in the cytoplasm, extracellularly and in the nucleus. Cell-surface galectin-3 is involved in cell adhesion and recognition [386], while nuclear galectin-3 is postulated to play a role in pre-mRNA splicing [387]. However, a function for galectin-3 in the cytoplasm is not proposed. The N-terminal domain of galectin-3 contains nine proline-rich motifs, each containing at least one tyrosine and several glycine residues. These sequences are highly homologous to proline-rich domains present in annexins VII and XI, as implicated to play a role in self-aggregation and intracellular membrane traffic [391]. Thus, it might be that galectin-3 plays a similar role as the annexins in intracellular membrane traffic. To test whether galectin-3 might function in fusion and/or targeting, NH_2-terminal directed (Mac-2) and CRD-directed (CRD) antibodies and thiodigalactoside (a specific ligand) were tested in cell-free fusion assays [Chapter 7].

74Lb - The binding of ER-Bip by X-lysosomes is also novel, if its binding was of a functional nature. Bip belongs to the hsp70 (heat shock protein 70) family of molecular chaperone ATPases that participate in protein folding [403-405], assembly [406], and translocation into organelles [405,407]. They bind hydrophobic regions [408,409] of proteins and prevent their misfolding or aggregation [403,404]. The interaction of hsp70 with protein is regulated by the binding and hydrolysis of ATP [410,411]. Hsp70s localise to cytosol, ER and mitochondria [412]. Hsc70 (hsp70 cognate protein) mediates clathrin and AP release from coated vesicles [413,414]. Recently it has been shown that hsc70 interacts with stathmin, which in-turn interacts with tubulin [415]. Hsc73 is suggested to mediate translocation of cytosolic proteins into lysosomes [416]. Even though the presence of hsc70 in lysosomes is known, it cannot be ruled out that the binding of a non-specific hsp70 to lysosomes may be due to exposed hydrophobic regions of potentially denatured proteins present in the lumen of detergent treated X-linked lysosomes.

CHAPTER 4

THE BEHAVIOUR, PURIFICATION AND INTEGRITY OF LATEX BEAD CONTAINING PHAGOSOMES

4.1 BACKGROUND

To determine whether the banding patterns observed for X-acceptors [Chapter 3] were not dependent on the presence of Triton X-100, a binding assay in the absence of detergent, allowing for intact membrane in both acceptor and membrane donor preparation was required. For this purpose, paramagnetic latex beads [see Section 1.2.5] were sought to purify phago-endosomes and phago-lysosomes as acceptors.

It has been shown that phagosomes that contain hydrophobic beads undergo delayed maturation in that they remain fusogenic towards early endosomes for up to three hours during which time they are unable to fuse with lysosomes [108,109]. In contrast, phagosomes containing hydrophilic latex beads mature normally within less than 15 minutes after which they start fusing with lysosomes [108,109,362,450]. Since the behaviour of non-paramagnetic latex beads has been analysed in bone marrow-derived macrophages (non-transformed cells), the behaviour of paramagnetic latex beads in $P388D_1$ macrophages (a transformed cell line) had to be established. One parameter used in electron microscopy to distinguish between endosomes and lysosomes, is their cytochemical staining patterns after HRP uptake. Endosomal structures are rim stained, whereas the entire lumen of lysosomes is stained with HRP reaction product. This difference was exploited to establish whether the paramagnetic latex bead-containing phagosomes fuse with early endosomes and/or lysosomes, thereby establishing if they were phago-endosomes or phago-lysosomes.

Once their behavour was established, the purification of the phagosomes was attempted. Since the membrane surrounding the beads could be lost during purification, the membrane integrity of the phagosomes was accessed by electron microscopy at each step during the purification process. In addition, to them being used as acceptors in a detergent-free binding assay, the composition of these phagosomes was also analysed [Chapter 5].

4.2 MATERIALS AND METHODS

4.2.1 Phagocytic Uptake

$P388D_1$ macrophages were cultured in 150 mm tissue culture dishes (Greiner, Frickenhausen, Germany). Confluent dishes were incubated for 4 hours with serum-free medium (RPMI-Pen/Strep) before they were fed latex beads (Sigma Chemical Company, St. Louis MO, USA). The paramagnetic latex bead solutions were diluted 1000-fold in serum-free medium. 15 ml of the mixture was added to the dishes, and incubated for 30 min at 37°C. Uningested beads were then washed off with cold medium and replaced with warm medium. The cells were then further incubated at 37°C for 2 hours, with HRP (Seravac, Cape Town, South Africa) added at 1mg/ml during the last 45 min. Cells were then immediately fixed and processed for electron microscopy.

4.2.2 HRP Cytochemistry

Cells were fixed with 2.5 % glutaraldehyde (Sigma Chemical Company, St. Louis MO, USA) in 0.1 M cacodylate buffer pH 7.2 containing 5 mM $CaCl_2$, 5 mM $MgCl_2$ and 0.1 M sucrose. Cells were washed overnight at 4°C with the sucrose-containing cacodylate buffer. The cells were then washed twice with 0.1 M Tris-HCl pH 7.6, then incubated at at room temperature in the dark with DAB (3,3' diaminobenzidine, Sigma Chemical Company, St. Louis MO, USA) at 1 mg/ml in 0.1 M Tris-HCl buffer pH 7.6 for 20 minutes. 20 µl of a 0.3% H_2O_2 (Saarchem, Cape Town, South Africa) solution was added per ml of DAB-Tris-HCl solution, then incubated at at room temperature for 20 minutes in the dark. The cells were washed three times with 0.1 M cacodylate buffer devoid of sucrose, then incubated for 1 hour at room temperature with 1% osmium tetroxide (Sigma Chemical Company, St. Louis MO, USA) in 0.1 M cacodylate buffer devoid of sucrose. The cells were then washed three times with 0.1 M cacodylate buffer devoid of sucrose.

4.2.3 Embedding for Electron Microscopy

Osmium tetroxide fixed cells were scraped off the culture dishes with a rubber policeman and then concentrated in 2% agar prepared in 0.1 M cacodylate buffer devoid of sucrose. The agar blocks were washed with water and then with Veronal buffer (0.03 M Na-Barbital, 0.05 M Na-Acetate, 0.1 M NaCl, 10 mM CaCl, 0.03 N HCl, pH 6), then incubated for 1 hour with 1% uranyl acetate in Veronal buffer. Samples were dehydrated serially with ethanol (25%, 50%, 75%, 90% each for 15 min, and 100% 3X for 30 min). Samples were then washed serially with Epon-ethanol mixtures (1:3, 1:1, 3:1) for 1 hour at room temperature. Samples were then placed in pure Epon at room temperature for 1 hour, then in fresh Epon at 40°C for 1 hour. Samples were then placed with fresh Epon in beams and polymerised for 48 hours at 60°C.

4.2.4 Purification of latex bead-containing Phagosomes [Figure 1.7]

Cells were cultured in 150 mm tissue culture dishes (Greiner, Frickenhausen, Germany). Confluent dishes were incubated for 4 hours with serum-free medium (RPMI-Pen/Strep). The protocol below was then followed:

1. Cells washed with cold medium.
2. Incubated each dish with 15 μℓ Beads in 15 ml medium at 37°C for 30 minutes.
3. Washed with warm medium.
4. Incubated at 37°C for 30 min (hydrophobic beads) or 2 hours (hydrophilic beads).
5. Washed with cold medium.
6. Washed with cold homogenisation buffer.
7. Scraped cells with a rubber policeman in cold homogenisation buffer (2.5 ml / dish).
8. Homogenised by 3 strokes through a pre-chilled stainelss steel ball homogeniser.
9. Mixed homogenate with 5 ml 25 % Percoll in a 50ml tube.
10. Centrifuged at 500g for 5 minutes at 4°C (Beckman TJ-6 centrifuge).

11. Overlaid supernatant onto 5 ml 25 % Percoll.
12. Centrifuged at 500g for 30 minutes at 4°C (Beckman TJ-6 centrifuge).
13. Resuspended pellet gently in 250 μℓ homogenisation buffer in an Eppendorf tube.
14. Centrifuged at 150g for 1 min (Beckman benchtop centrifuge 11).
15. Treated supernatant with 1 M NaCl for 10 minutes at 4°C.
16. Overlaid supernatant onto 0.5 ml 15 % sucrose.
17. Placed tube into a magnetic concentrator for 1 minute.
18. Resuspended pellet in homogenisation buffer.

To analyse the membrane integrity of the phagosomes, samples were taken after steps 7, 8, 13 and 18, then fixed with glutaraldehyde and osmium tetroxide (as discussed above) for electron microscopic analysis.

4.2.5 In-vitro Binding Assays

4.2.5.1 Preparation of Radioactive Donor

The PNS obtained from a homogenate of ^{35}S-methionine metabolically labelled cells [as described in Section 3.2.2.1] was split into 2 fractions. One fraction was centrifuged at 150000g for 30 minutes at 4°C in an airfuge. The resulting high-speed supernatant collected as the ^{35}S-cytosol donor. The second fraction was overlaid onto a 27% percoll gradient and centrifuged at 35000g for $1^1/_2$ hours at 4°C and the low-density fraction collected as the ^{35}S-membrane donor material. The ^{35}S-Membrane was then washed, treated with 1M NaCl, sonicated and washed again with Binding buffer. The washed membrane was then sonicated in the presence of excess (10 times the volume of the labelled donor) liposomes produced from phosphatidylcholine from egg yolk (Sigma), until the opaque solution became transluscent and then incubated at 37°C in a water bath for 10 minutes to allow de-novo coalesensce. The material designated ^{35}S-Membrane^{Lipid} was then placed on ice before use in the Binding assay.

4.2.5.2 Binding Assay

30 µℓ Phagosome acceptor, 30 µℓ Binding buffer (either with an ATP regenerating system or ATP depleting system as required) and 30 µℓ of ^{35}S-Cytosol or ^{35}S-Membrane^{Lipid} donor fraction were mixed and incubated at 37°C in a water bath for 2 hours. The reaction was stopped, by snap cooling on ice. The samples were overlaid onto 0.5 ml of chilled 25% sucrose (prepared with Binding buffer supplemented with or without ATP) and placed in a chilled magnetic concentrator for 5 min at 4°C. After magnetic concentration the supernatant and sucrose were aspirated off and the pellet resuspended in 50µℓ Binding buffer and then added to 50 µℓ 1-D 2x Sample buffer (20% glycerol, 5% SDS, 10% ß-mercaptoethanol, 0,004% bromophenol blue, 0.08 M Tris-HCl, pH 6.8) and boiled for two minutes. Samples were then applied to a 5-13% gradient SDS-polyacrylamide slab gel [described in Section 3.2.4].

4.3 RESULTS AND DISCUSSION

4.3.1 Effect of particle surface properties on phagosome morphology

The fusogenic properties of paramagnetic hydrophobic and hydrophilic latex bead-containing phagosomes in P388D_1 macrophages was analysed to determine if they behaved similar as described for non-paramagnetic latex bead-containing phagosomes in bone-marrow derived macrophages [108,109].

In cells loaded with 0.8 μm hydrophobic paramagnetic latex beads, the phagosome membrane displayed a close apposition with the particle surface [Figure 4.1A]. These hydrophobic paramagnetic latex bead-containing phagosomes were seen fusing with rim HRP stained early endosomes [Figure 4.1C], but were not seen fusing with luminally HRP stained lysosomes [Figure 4.1E] even though they were observed in very close proximity.

In cells loaded with 0.8 μm hydrophilic paramagnetic latex beads, the phagosome membrane displayed a loose association with the particle surface, and regions were observed where the membrane was not aligned with the particle surface [Figure 4.2 B]. These hydrophilic paramagnetic latex bead-containing phagosomes were seen fusing with luminally HRP stained lysosomes [Figure 4.2F], but were not seen fusing with rim HRP stained early endosomes even though fusion between HRP-negative an HRP-positive early endosomes were observed in close proximity [Figure 4.2D].

Though tubular extentions on early endosomes and phagosomes were not clealy visible in this study, they were observed in bone marrow-derived macrophages [109]. This can be expected as the tubular parts of endocytic structures are fragile under fixing conditions and vary in abundance between cell types.

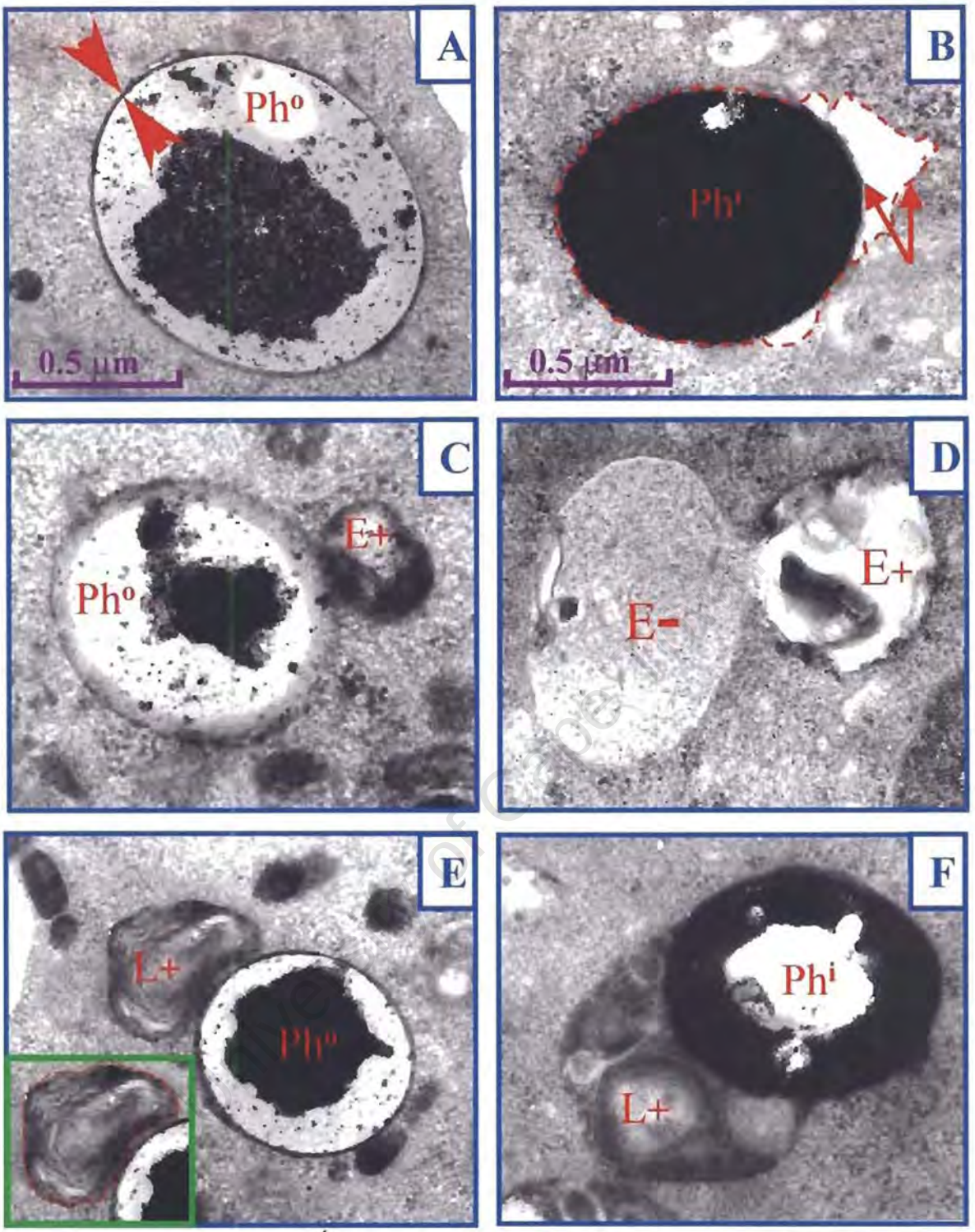

Figure 4.1 : The fusogenic behaviour of paramagnetic hydrophobic and hydrophilic latex bead-containing phagosomes. P388D$_1$ macrophages were fed 0.8 µm paramagnetic latex beads (possessing hydrophobic or hydrophilic surface properties) for 45 min., washed and chased for 2 hours in bead-free RPMI media. HRP was added during the last 45 minutes and then processed for electron microscopy to observe the fusogenic behaviour of the beads [see Section 4.2 for details]. **A)** Hydrophobic bead-containing phagosomes (Ph^o) displayed a close apposition (arrowheads ➤) between bead surface and the membrane. **B)** Hydrophilic bead-containing phagosomes (Ph^i) displayed a loose apposition (arrows ⟶) between bead surface and the membrane (broken line -------). **C)** Ph^o fusing with an HRP-positive endosome (En^+) **D)** HRP-negative endosome (En^-) fusing with an HRP-positive endosome (En^+). **E)** Ph^o resisting fusion (lysosomal membrane outlined in **green box**) with a densely stained HRP-positive lysosome (Ly^+) **F)** Ph^i that has fused with an HRP-positive lysosome (Ly^+). [Representative images]

In this study, the observations thus confirmed what is observed for 0.9 μm non-paramagnetic latex beads, fed to bone marrow-derived macrophages [108,109]. The present results showed that the surface property of the paramagnetic latex beads affected phagosome processing also in $P388D_1$ macrophages. Phagosomes containing paramagnetic latex beads of size 0.8 μm with a hydrophilic surface had already been processed towards phago-lysosomes within 3 hours. In contrast, phagosomes that contained paramagnetic latex beads of size 0.8 μm but with a hydrophobic surface remained fusogenic towards early endosomes for a 3-hour period and remained unable to fuse with lysosomes.

The situation for 0.8 - 1.0 μm hydrophobic latex bead-containing phagosomes however, is not permanent because after a 24 hour chase about 40% eventually resemble phago-lysosomes and are able to fuse with lysosomes. Additionally it is observed that hydrophobic latex beads coated with protein behave like hydrophilic beads to the extent that they are processed normally towards lysosomes [109]. Furthermore, it has been shown that hydrophobic latex beads smaller than 0.5 μm in size are also processed normally into phago-lysosomes [109].

Previously, the surface property of polystyrene beads has not been considered when used as phagocytic particles [106,360-364]. In most cases hydophilic beads [106,360] or protein coated hydrophobic beads [361] are employed which can explain why they are observed as being in phago-lysosomes. However, in studies using blue-dyed 0.8 μm hydrophobic beads it is observed that after a 6 hour chase the relative abundance of endosomal markers (Rab5 and Annexin II) remained constant [362-364].

4.3.2 Membrane integrity of phagosomes during and after purification

After having established that the 0.8 μm paramagnetic hydrophobic beads remained in structures representing phago-endosomes and that the 0.8 μm paramagnetic hydrophilic beads were processed normally to reside in structures representing phago-lysosomes, their purification was attempted.

To ensure that the phagosomal membrane was not lost at any stage during their isolation, samples were taken after steps 8, 13 and 18 during the purification procedure [Section 4.2.4] and fixed for electron microscopic analysis. The existence of a membrane around the particle surface could be observed by electron microscopy, due to glutaraldehyde (which crosslinks proteins) and osmium tetroxide (which crosslinks lipids) fixation.

After scraping the cells off the petri dish with a rubber policeman at 4°C (step 7), a sample was fixed as outlined above. Only 70% of the cells were broken due to scraping (not shown). Post homogenisation to break any unbroken cells (step 8), an aliquot was fixed and analysed by electron microscopy. It was evident that more than 90% of the membrane around the particle surface was still intact [Figure 4.2A]. Other vesicular structures and cell debris was evident.

After centrifugation through Percoll mixtures to remove intact (which pellet at step 10) and broken (which float at step 10 and 13) nuclei, an aliquot after step 13 was also fixed and processed for electron microscopy. About 80% of the phagosomes maintained its membrane allround the particle surface, while approximately 5% of the phagosomes displayed broken regions in their membrane and the rest no membrane at all [Figure 4.2B]. Substantially less of the large structures seen after step 8 was detected. However, around the phagosomes a fenestrated precipitate is visible, which might be contaminating cellular material or an artifact occuring due to fixing conditions. Fortunately, these undefined structures subsequently dissappeared after the final purification steps (see below).

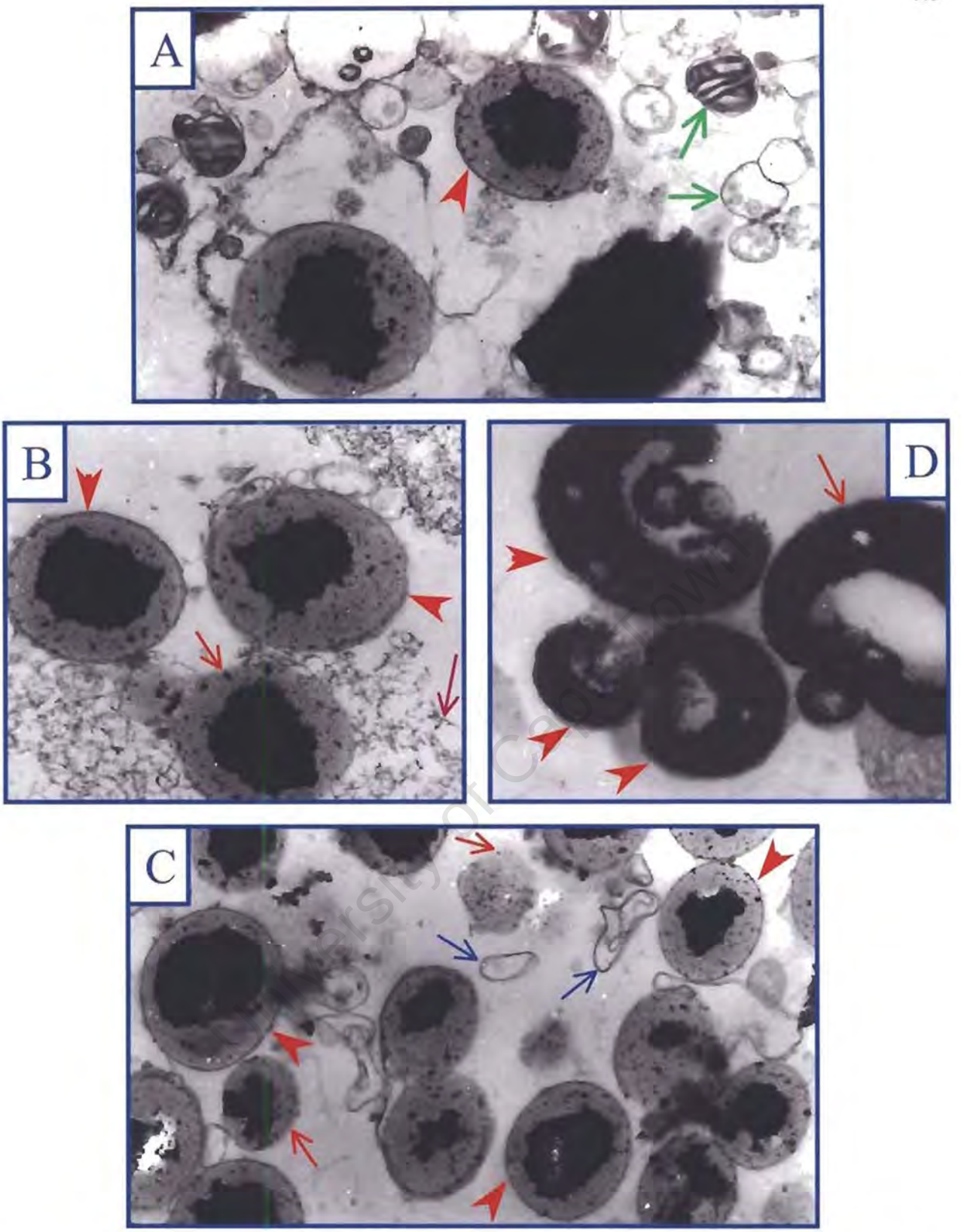

Figure 4.2 : The membrane integrity of latex bead-containing phagosomes during their purification. P388D$_1$ macrophages were fed 0.8 μm paramagnetic latex beads (hydrophobic or hydrophilic) for 45 min., washed and chased for 2 hours in bead-free RPMI media. Phagosomes were then purified [as described in Section 4.2.4], and aliquots processed for electron microscopy after steps 8 (image A), 13 (image B) and 18 (image C for phago-endosomes and image D for phago-lysosomes). **A) red arrowheads** show intact phagosomal membrane and **green arrows** indicate other vesicular structures and cell debri. **B) maroon arrow** point to undefined fenestrated material (possibly DNA fragments). **C and D) red arrows** point to beads lacking a membrane (or broken) and **blue arrows** indicate membrane probably derived from beads which have lost their membrane. [Representative images]

After completing the purification by salt treatment (step 15) followed by magnetic concentration (step 17) and resuspension (step 18), an aliquot of the purified phagosomes was fixed and processed for electron microscopic analysis. Analysis of multiple sections, showed that at least 70% of the phagosomes maintained their membrane all around the particle surface, while approximately 10% of the phagosomes displayed broken regions in their membrane and the rest no membrane at all [Figure 4.2C]. Noticeably the undefined material seen after step 13 [Figure 4.2B], was not present after step 18. The same membrane integrity was observed for purified hydrophilic latex bead-containing phagosomes [Figure 4.2D] as observed for the purified hydrophobic latex bead-containing phagosomes.

In conclusion, it was possible to ultra purify the phagosomes with the majority of them having maintained their membrane intact, in order to analyse their composition. Before this was attempted however, the purified phagosomes were used as acceptors in cytosol and membrane binding assays, to compare their binding activity to that observed for the X-linked acceptors.

4.3.3 Binding Assays using Purified Phagosomes as Acceptors

A binding assay in the absence of detergent, allowing for intact membrane in both acceptor and membrane donor preparation, was required to determine whether the banding patterns observed for X-acceptors [Chapter 3] were not dependent on the presence of detergent. Paramagnetic latex beads were used to purify phago-endosomes and phago-lysosomes as acceptors [Section 4.2.4]. No problems were forseen for them being used in binding assays using cytosol as donor. These results were shown by Figures 4.3 and 4.4. However, a problem was posed for binding assays using detergent solubilised membrane as donor, since Triton X-100 or any other detergent would solubilise the phagosome membrane as well. Instead, membrane donor (designated ^{35}S-Membrane^{lipid}) was prepared by sonicating metabolically labelled membrane in the presence of excess phospholipid in order to separate donor proteins into individual vesicles [Section 4.2.5.1]. The binding assay results using this type of membrane donor was shown by Figure 4.5. Comparison of membrane banding patterns of phagosomes and X-acceptors observed for ATP-depleting conditions was displayed in Figure 4.6.

4.3.3.1 Cytosol binding assays

The radioactive scan displayed in Figure 4.3, showed that the banding pattern for the various nucleotide conditions using phagosomes as acceptors, is similar to what was observed for X-linked acceptors [see Figure 3.5].

As noted before for X-linked acceptors, more bands (though discrete when compared with the input cytosol) were pelleted in an ATP_D system probably due to protein-complex formation. This complex might form non-specifically, but was certainly potentiated by the presence of phagosomes/X-linked acceptors in the binding assay. This complex included 190, 45, 35, 31, 19, 18 and 16 kDa bands, and was discussed previously, are similar in molecular weight to cytoskeletal elements viz. myosin HC (190), tubulin (45), actin (35),

myosin LC1 (19) and myosin LC2 (18) isolated previously [351], also under ATP_D conditions. Even though these polymers form de-novo, specific binding sites have been found on endocytic organelles [354].

There were other bands though, which depended on the presence of ATP or GTP. A myriad of bands were bound in an ATP_D / GTP system [Figure 4.3, lanes 3 & 7], with a 90 kDa band specifically dependent on the presence of GTP alone [Figure 4.3, lanes 3 & 7]. It would appear that the 190 kDa, 31 kDa and 19 kDa bands required an ATP_D system in the absense of GTP [Figure 4.3, lanes 2 & 6], since addition of GTP abolished their binding [Figure 4.2, lanes 3 & 7].

The banding patterns were the same whether phago-endosomes (lanes 1-4) or phago-lysosomes (lanes 5-8) were employed, except that a 55 kDa appeared to be enhanced for phago-endosomes under GTP/ATPγS conditions [Figure 4.4, compare lanes 4 & 8].

In Figure 4.4, the binding differences due to the presence of ATPγS alone or with GTP added, was displayed. For phago-endosomes (lanes 1-4), if lane 1 (ATPγS) and lane 4 (ATPγS/GTP) was compared, it was observed that most of the bands remained basically the same, except bands 90 and 35 kDa. The increased intensity of the 90 and 35 kDa bands was due to the additional presence of GTP. A similar observation could be made for phagos-lysosomes when lane 5 (ATPγS) and lane 8 (ATPγS/GTP) was compared.

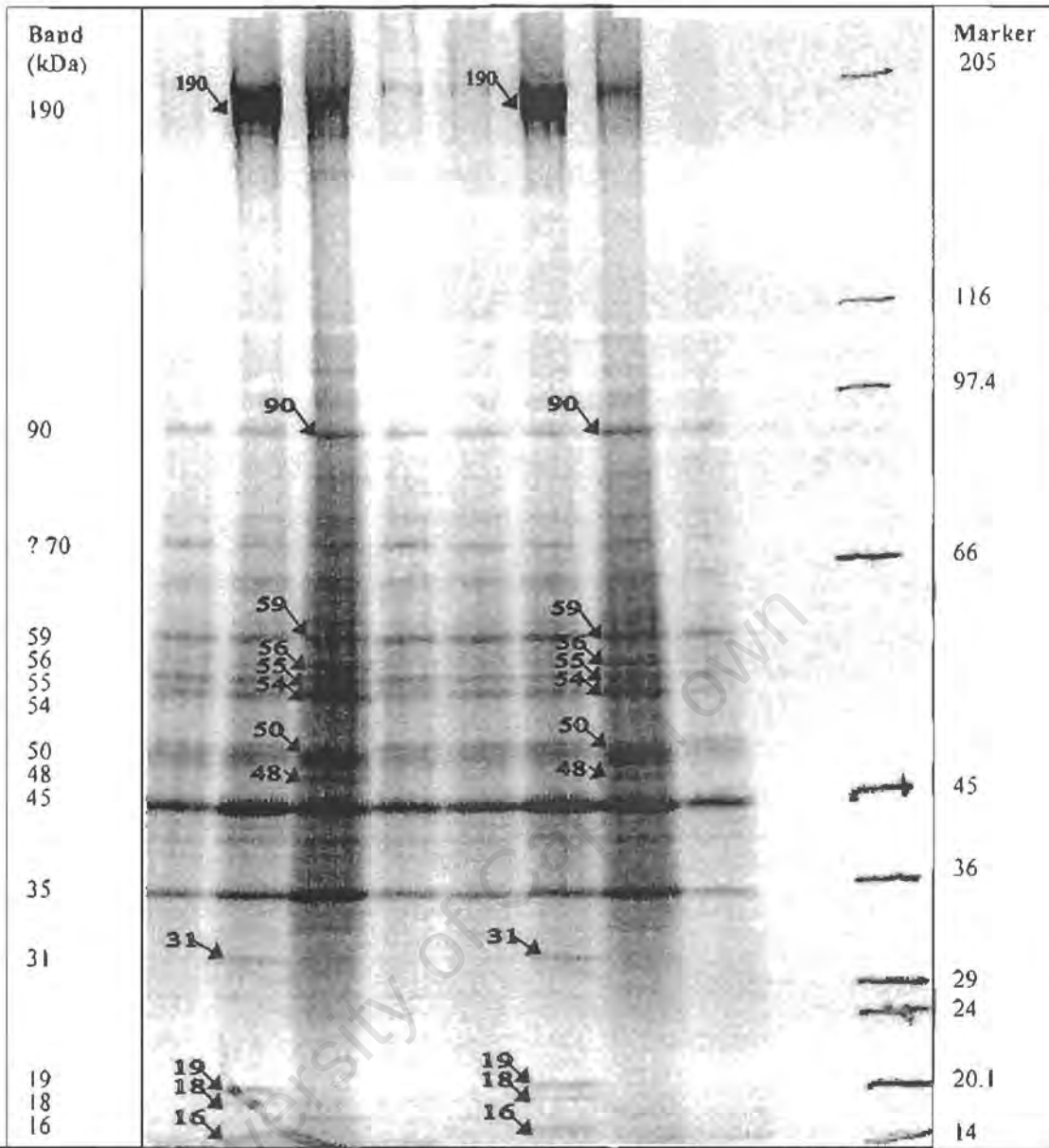

Figure 4.3 : Cytosol binding assay pellets (using Phagosome acceptors) run on a SDS-PAGE gradient gel followed by radioactive scanning. Purified phago-endosomes and phago-lysosomes were resuspended in Binding buffer. The phago-endosomes (lanes 1-4) or phago-lysosomes (lanes 5-8) were incubated at 37°C for 2 hours with fully soluble ^{35}S-Cytosol (lanes 1-8), either in an ATP-regenerating system (lanes 1, 5), or ATP-depleting system (lanes 2, 3, 6 & 7 with 3 & 7 additionally in the presence of GTP), or in the presence of ATPγS (lanes 4 & 8). Samples were overlaid onto 25% sucrose and acceptors with bound radioactive material collected by a magnetic concentrator. The pellets were resuspended and run on a 5-13% SDS-PAGE gradient gel. A control incubation with ^{35}S-Cytosol in the presence of Latex in an ATP-regenerating system was run in lane 9. The Mw Marker was run in lane 10. Bands were labelled according to their molecular weight. [Representative of 3 separate experiments]

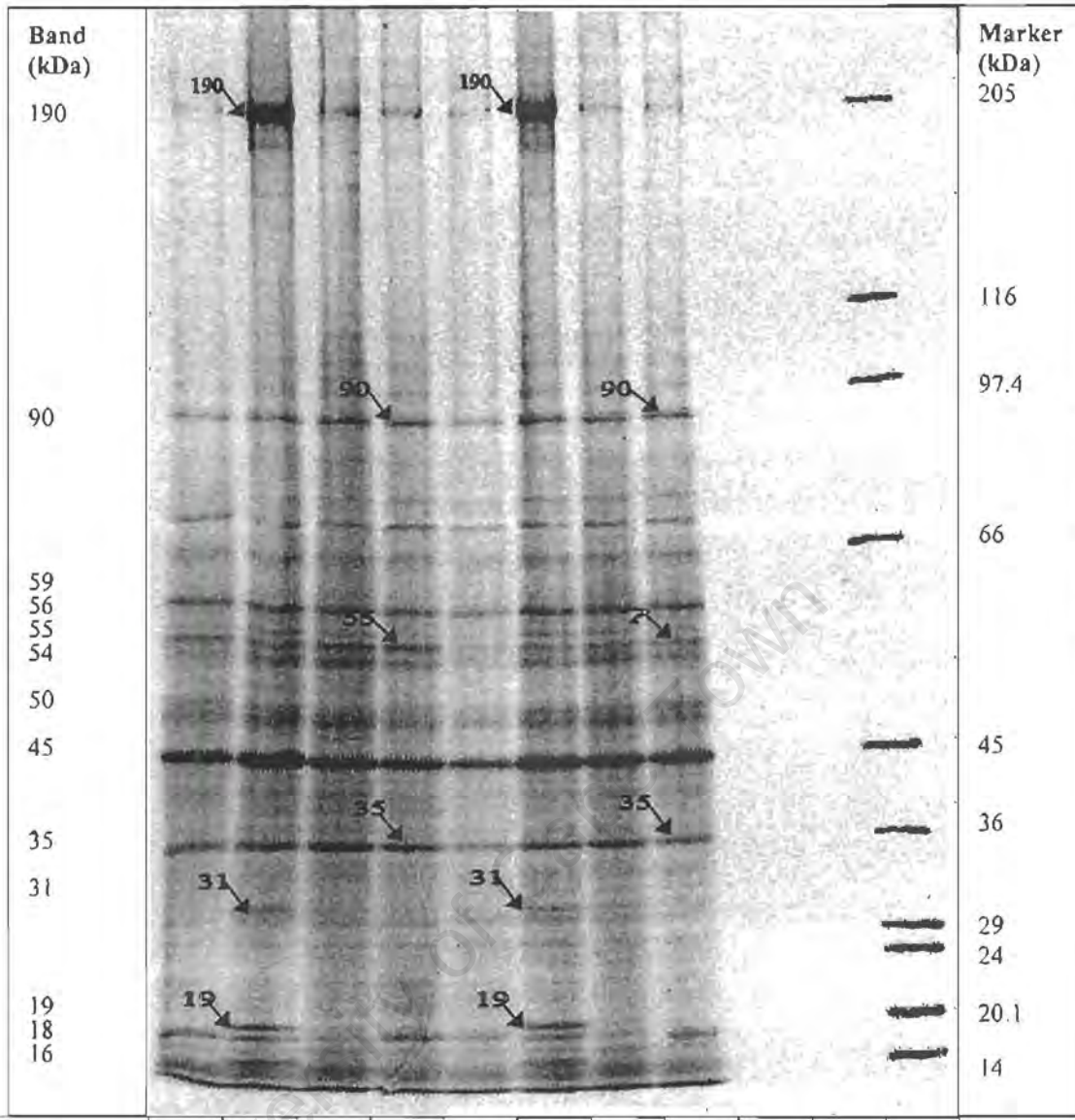

Lane Number	1	2	3	4	5	6	7	8	9	10	11
Acceptor Type	Phago-endosomes				Phago-lysosomes				No Acceptor		Marker
Nucleotide	ATPγS	ATP_D ATPγS	ATP_D ATPγS GTP	ATPγS GTP	ATPγS	ATP_D ATPγS	ATP_D ATPγS GTP	ATPγS GTP	ATP_R	ATP_D	
^{35}S-Donor	^{35}S-Cytosol										

Figure 4.4 : Cytosol binding assay pellets (using Phagosome acceptors) run on a SDS-PAGE gradient gel followed by radioactive scanning. Purified phago-endosomes and phago-lysosomes were resuspended in Binding buffer. The phago-endosomes (lanes 1-4) or phago-lysosomes (lanes 5-8) were incubated at 37°C for 2 hours with fully soluble ^{35}S-Cytosol (lanes 1-8), either in an the presence ATPγS alone (lanes 1 & 5) or ATPγS/ATP_D (lanes 2 & 6) or ATPγS/ATP_D/GTP (lanes 3 & 7) or ATPγS/GTP (lanes 4 & 8). Samples were processed further as described in Figure 4.3. Control incubations with ^{35}S-Cytosol in the absence of acceptors in an ATP-regenerating system (lane 9) or ATP-depleting system (lane 10) was performed. The Mw Marker was run in lane 11. Bands were labelled according to their molecular weight. [Representative of 3 separate experiments]

4.3.3.2 Membrane binding assays

The similarity in the cytosol banding patterns observed for both acceptors was not surprising, since endocytic structures and phagosomes are functionally comparable and do interact by way of fusion in vivo. The next step was to determine whether they behaved similar if membrane was used as donor material in the binding assay. Membrane donor was prepared by sonicating labelled membrane in the presence of excess phospholipid in order to separate donor proteins into individual vesicles [Section 4.2.5.1]. ATP-depleting conditions was employed under which the enhanced binding of the 32 kDa band by X-acceptors was observed, to assess whether the phagosomes could reproduce this result.

Phago-endosomes [Figure 4.5, lanes 1 & 2] and phago-lysosomes [Figure 4.5, lanes 3 & 4] exhibited basically the same banding pattern, except that the 32 kDa was enriched for phago-lysosomes. When phagosomes were washed [Figure 4.5, lanes 2 & 4] after the binding assay, a decrease in all bands was observed in relation to the intensity of the 32 kDa band. To facilitate a direct comparison between the membrane banding patterns of phagosomes [lanes 2 & 4 from Figure 4.5] and X-acceptors [lanes 2 & 3 from Figure 3.10] observed under ATP-depleting conditions, were reproduced [Figure 4.6]. It was obvious that the banding patterns of both phagosomes and X-acceptors were comparable. Moreover, it was evident that the 32 kDa band was enriched for phago-lysosomes [Figure 4.6, lane 3] and X-lysosomes [Figure 4.6, lane 4], as compared to phago-endosomes [Figure 4.6, lane 1] and X-endosomes [Figure 4.6,lane 2].

Thus an acceptor with its lipid coat intact could essentially reproduce the observation witnessed for X-acceptors potentially devoid of a lipid coat. The latter suggests that lysosomal structures have binding sites for the 32 kDa band on their cytoplasmic side, however it cannot be ruled out that luminal sites are also present. The binding assay results confirmed the integrity of the phagosomes and their similarity to endocytic structures. The composition of these phagosomes were then analysed [Chapter 5].

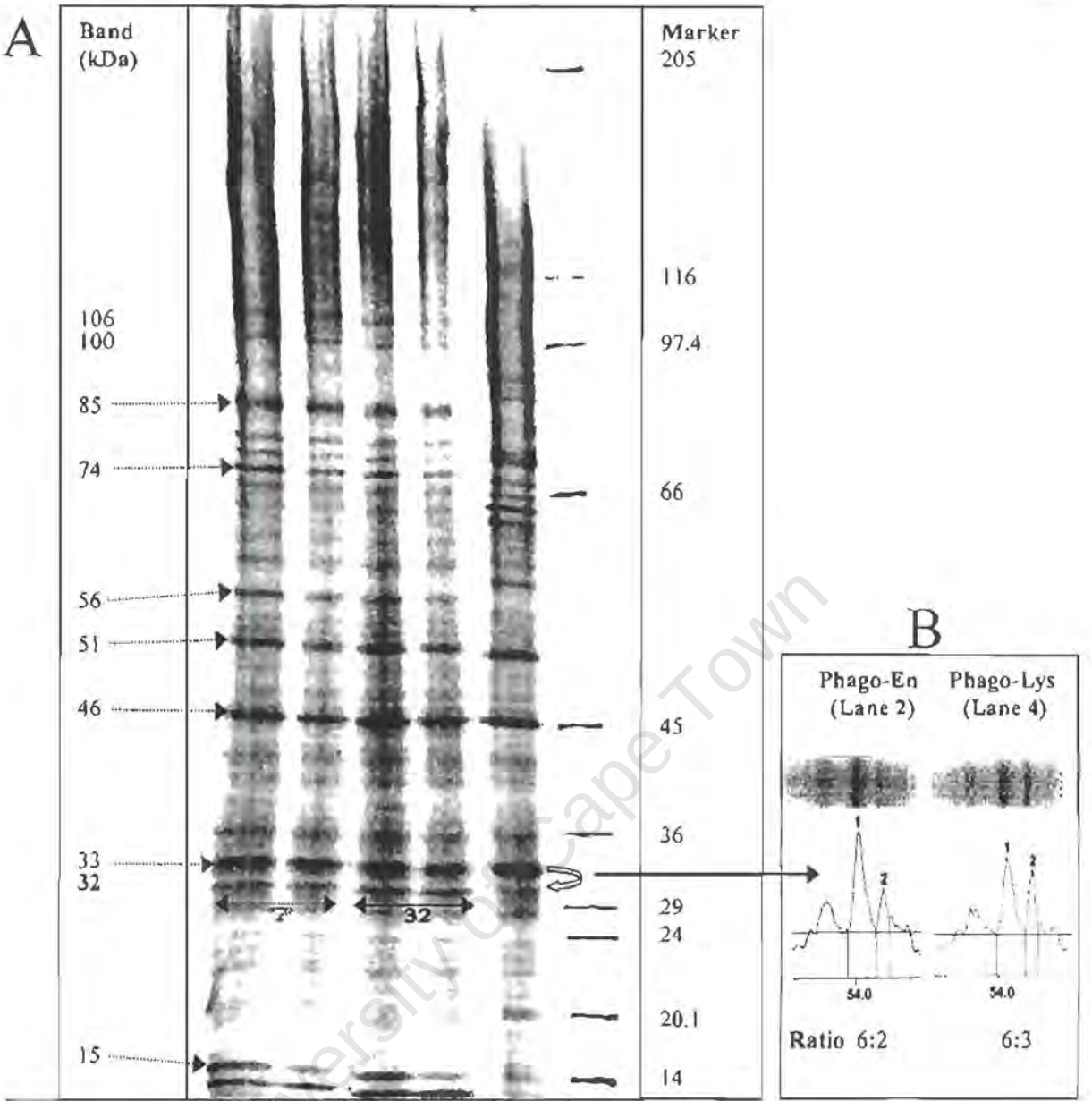

Lane Number	1	2	3	4	5	6
Wash (Buffer)	-	+	-	+	Mem^{LF}	Marker
Acceptor Type	Phago-En		Phago-Ly			
Nucleotide	ATP_D					
^{35}S-Donor	^{35}S-$Membrane^{Lipid}$ + Cytosol					

Figure 4.5 : Membrane binding assay pellets (using Phagosome acceptors) run on an SDS-PAGE gradient gel followed by radioactive scanning. A) Purified phago-endosomes and phago-lysosomes were resuspended in Binding buffer. The phago-En (lanes 1-2) or phago-Ly (lanes 3-4) were then incubated at 37°C for 2 hours with fully soluble ^{35}S-$Membrane^{Lipid}$ (lanes 1-4), in the presence ATP-depleting system. Samples were processed further as described in Figure 4.3. The pellets of lanes 2 & 4 were washed with Binding buffer. A sample of ^{35}S-$Membrane^{Lipid}$ was run in lane 5. B) A radioactivity plot of the 32-35 kDa region for lanes 2 & 4. The relative intensity ratios for bands 33 and 32 kDa are shown. [Representative of 3 separate experiments]

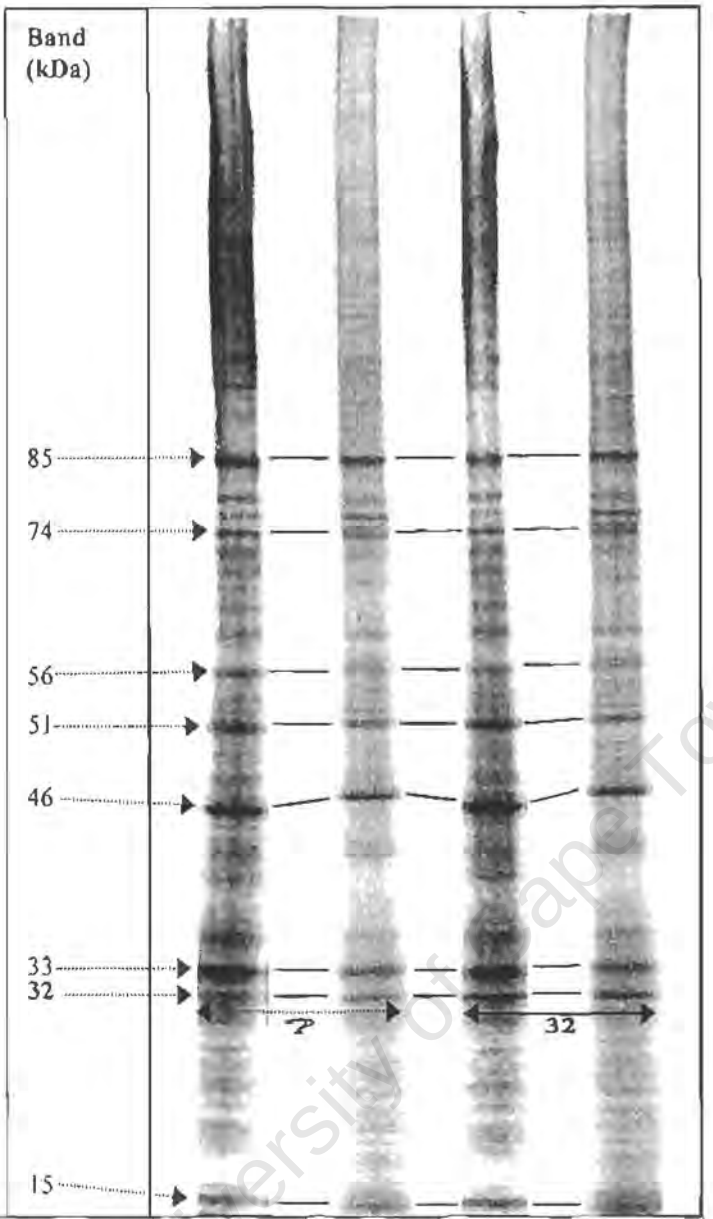

Lane Number	1	2	3	4
Acceptor Type	Phago-En	X-En	Phago-Ly	X-Ly
^{35}S-Donor	^{35}S-Mem^{Lipid}	^{35}S-Mem^{LF}	^{35}S-Mem^{Lipid}	^{35}S-Mem^{LF}
Nucleotide	ATP_D			

Figure 4.6 : Comparison of membrane banding patterns of phagosomes and X-acceptors observed for ATP-depleting conditions. The results obtained for phago-endosomes (lane 1), phago-lysosomes (lane 3), X-endosomes (lane 2) and X-lysosomes (lane 4) under ATP-depleting conditions were reproduced [from Figure 4.5 (lanes 2 & 4) and Figure 3.10 (lanes 2 & 3)] here to facilitate direct comparisons. The horizontal arrow (↔) showed that the 32 kDa band was enriched for phago-lysosomes and X-lysosomes, as compared to both endosome acceptors.

CHAPTER 5

MEMBRANE COMPOSITION OF PHAGOSOMES

5.1 BACKGROUND

Early and late endosomes are morphologically and functionally distinct [40,41,50,53,57,61-63], as well as differing in lumenal pH and protein composition [60,64,65]. The protein composition of early endosomes is significantly different from that of ECVs or late endosomes [281]. Annexin II and the small GTPase Rab5, both colocalize to early endosomes specifically [365], while Lgp-like proteins are abundant in late endosomes, but not detectable in early endosomes [281]. Early and late endosomes appear to have a more complex protein composition than ECVs. In particular, most proteins present in ECVs are also present in late endosomes [69].

Similarly, the polypeptide and lipid composition [363] of phagosomes changes due to interactions [104-105,362,364,360] with endocytic structures. The biochemical transformation of phagosomes is brought about by recycling, fusion with early endocytic and TGN-derived structures. This modulation of composition correlates with the phagosomes' subsequent ability to fuse with lysosomes. It would appear that phosphorylation and dephosphorylation events also play a role in phago-lysosome biogenesis [366].

In this study the composition of purified [Section 4.3.2] paramagnetic latex bead-containing phagosomes were analysed, to identify potential targeting molecules involved in the endocytic pathway. In contrast to previous studies, instead of isolating hydrophilic bead-containing phagosomes at early stages, hydrophobic beads were employed to purify phago-endosomes, confirmed morphologically by electron microscopy [Section 4.3.1]. The composition was analysed initially by 1-dimensional and subsequently by 2-dimensional electrophoresis.

5.2 MATERIALS AND METHODS

5.2.1 SDS Polyacrylamide gel electrophoresis

Protein separation was performed as described in Section 3.2.4. Protein bands were then visualised by silver staining or coomassie blue staining.

5.2.2 2-Dimensional Electrophoresis

5.2.2.1 In-gel sample reswelling procedure for Isoelectric focussing

In-gel sample reswelling procedure was followed as previously described [Section 3.2.5.1]. Purified phagosomes (50 µg for analytical gels, 0.5 mg for preparative gels) was resuspended in 350 µℓ 2-D sample buffer (8M urea, 2M Thiourea, 4% CHAPS, 2% pH 3-10 carrier ampholytes, 20mM Tris base, 30mM DTT).

5.2.2.2 Equilibration of IEF Strips and SDS-PAGE

The procedure for equilibration of IEF Strips and the second dimension SDS-PAGE was followed as described in Section 3.2.5.2. Analytical gels were silver stained [Section 5.2.3.1] and preparative gels were coomassie blue stained [Section 5.2.3.2]. Spots on preparative gels were cut out for subsequent mass spectrometry [Section 6.2.3] or Edman microsequencing [Section 6.2.2] analysis.

5.2.3 Visualisation of protein bands or spots on polyacrylamide gels

5.2.3.1 Silver staining of polyacrylamide gels

Silver staining was performed as previously described [358]. Protein bands on the gels were fixed for 2-3 hours in a 12% trichloroacetic acid, 2% $Cu(II)Cl_2$ and 50% methanol solution. Polyacrylamide gels were then sequentially soaked in the following solutions with continuous agitation. Each solution was aspirated off.

1) 10% ethanol, 5% acetic acid for 20 minutes
2) 0,01% $KMnO_4$ for 10 minutes
3) Solution (1) above for 20 minutes
4) 10% ethanol for 40 minutes
5) De-ionised water for 30 minutes
6) 0,1% $AgNO_3$ for 20 minutes
7) De-ionised water for 1 minute
8) 10% K_2CO_3 for 1½ minutes
9) 2% K_2CO_3, 0.01% formaldehyde for 3-4 minutes
10) De-ionised water for 30 seconds
11) 3% acetic acid for 2-3 hours
12) 5% glycerol overnight.

The gels were then dried in a slab gel drier (Model SE 1150, Hoefer Scientific Instruments, San Francisco) at 60°C for 3 hours under vacuum. The gels were calibrated using the molecular weight markers as reference.

5.2.3.2 Coomassie Blue Staining

Coomassie blue staining was carried out as previously described [359]. Polyacrylamide gels were sequentially soaked in the following solutions while continually being agitated. Each solution was aspirated off.

1) The polyacrylamide gel was placed in a plastic container and covered with Fixing Solution (50 % methanol, 10 % acetic acid) for 2 hours.
2) The Fixing Solution was then replaced with Staining Solution (0.025 % Coomassie blue R-250, 46 % methanol, 8 % acetic acid) for 4 hours.
3) The Staining solution was replaced with Fixing Solution (50 % methanol, 10 % acetic acid) for 2 minutes.
4) The Fixing Solution was then replaced with Destain Solution (10 % methanol, 10 % acetic acid) for 2 hours, and then overnight with cut sponges added.
5) The gels were stored in 3 % acetic acid.

5.3 RESULTS

5.3.1 1-D Electrophoresis

Phagosomes purified from cells incubated with beads in serum-medium [Figure 5.1]

The membrane composition of phago-endosomes (lanes 1-4) and phago-lysosomes (lanes 5-8), as analysed by SDS-PAGE and silver-staining, revealed a few banding pattern differences. The most prominent difference was that phago-lysosomes were enhanced with a 32 kDa band (lane 8). The phago-lysosome specific 32 kDa band was efficiently solubilised by Triton X-100 (lane 6) from the hydrophilic bead (lane 7). The 32 kDa band might have come from the fetal calf serum (FCS) that could have been adsorbed onto the naked beads, just prior to internalisation of the beads by the cells. This was tested by incubating the hydrophobic beads (lane 9) and the hydrophilic beads (lane 10) with FCS-medium at 37°C for 1hour. Upon analysis of the 32 kDa region for both beads (lanes 9 & 10), no band was detectable, which suggested that the 32 kDa phago-lysosome specific band was not derived directly from the FCS-medium. However, the 32 kDa band might be a degradation product of a protein present in the FCS. To investigate the latter, beads were internalised in different media (Figure 5.2).

Phagosomes purified from cells incubated with beads in different media [Figure 5.2]

To further investigate whether the 32 kDa band was not a degradation product of a protein derived from the FCS-medium, the beads were internalised in different media. These were (a) plain medium, (b) medium with BSA or (c) medium with FCS. Both the hydrophobic bead phago-endosomes (lanes 1-3) and the hydrophilic bead phago-lysosomes (lanes 5-7) exhibited no detectable banding pattern differences for the different media used. This proved that the 32 kDa band was not derived from the FCS-medium.

In this gel, a few additional phago-endosome specific bands (viz. 100, 89 and 55 kDa) and phago-lysosome specific bands (viz. 50, 34 and 19 kDa) were observed. If both phago-endosomes (lane 4) and phago-lysosomes (lane 8) were not treated with high salt, a common 33 kDa band was associated with the phagosomes, in amounts comparable to the concentration of the 32 kDa band. This might indicate a cytosolic or peripheral membrane factor associated with the 32 kDa band.

Isolation of phago-endosomes using hydrophilic beads [Figure 5.3]

To investigate whether the 32 kDa band was not perhaps specific because of a tendency to associate preferentially to hydrophilic and not hydrophobic beads, hydrophilic beads (instead of hydrophobic beads) were employed to isolate 10 min phago-endosomes. These hydrophilic bead phago-endosomes (lanes 1 and 2) exhibited the same banding pattern as observed for hydrophobic bead phago-endosomes, specifically in that they contained very little or no 32 kDa band. The Triton X-100 supernatant of phago-lysosomes (lane 3) still exhibited the 32 kDa band. These results would allow for a preliminary proposal that the 32 kDa did not come from the plasma membrane, but had to have been added to the endocytic pathway organelles at the late endosomal/prelysosomal stage. It was evident that the molecular-weight region where highly glycosylated membrane proteins (such as LAMPs) resolved upon SDS-PAGE, was enhanced in intensity for phago-lysosomes (lane 3) compared to phago-endosomes (lane1).

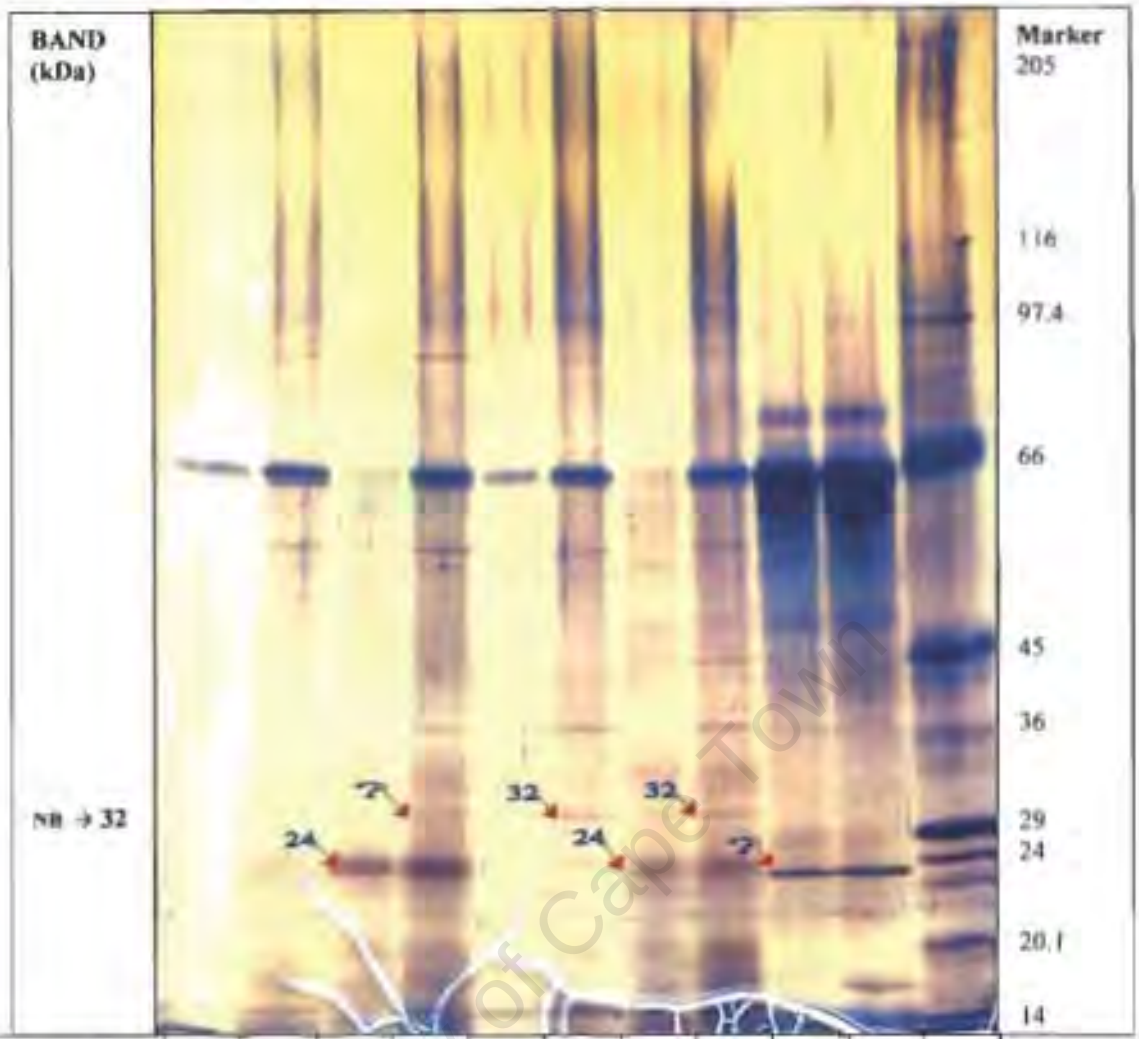

Lane Number	1	2	3	4	5	6	7	8	9	10	11
Bead Type	Hydrophobic				Hydrophilic				Hydro-phobic	Hydro-philic	Marker
Incubation Time	10min Uptake, 2hr Chase								Beads Incubated with FCS-Medium at 37°C, 1 hr Supernatant discarded, and Pellet washed		
Phagosome type	Phago-Endosomes				Phago-Lysosomes						
Phagosome treat	NaCl, TX-100				NaCl, TX-100						
TX-100 Fraction	Sonic Sup of TX-100 Pel (L3)	Sup	Pel	Total	Sonic Sup of TX-100 Pel (L7)	Sup	Pel	Total			

Figure 5.1 : SDS-PAGE of Phagosomal Membrane purified from cells incubated with RPMI-FCS media. P388D1 mouse macrophages incubated with RPMI-FCS media were fed with hydrophobic or hydrophilic paramagnetic latex beads for 10 min, washed and chased for 2 hours. Purified salt-washed and Triton X-100 solubilised phago-endosomes [total material run in lane 4, supernatant run in lane 2, the pellet run in lane 3 and a sonicated supernatant of the Triton X-100 pellet run in lane 1] and phago-lysosomes [total material run in lane 8, supernatant run in lane 6, the pellet run in lane 7 and a sonicated supernatant of the Triton X-100 pellet run in lane5] were run on a 5-13% gradient SDS-PAGE gel. Hydrophobic beads (lane 9) and hydrophilic beads (lane 10) were incubated with RPMI-FCS medium at 37°C for 1hour. The Mw marker was run in lane 11. [Representative of 2 separate experiments]

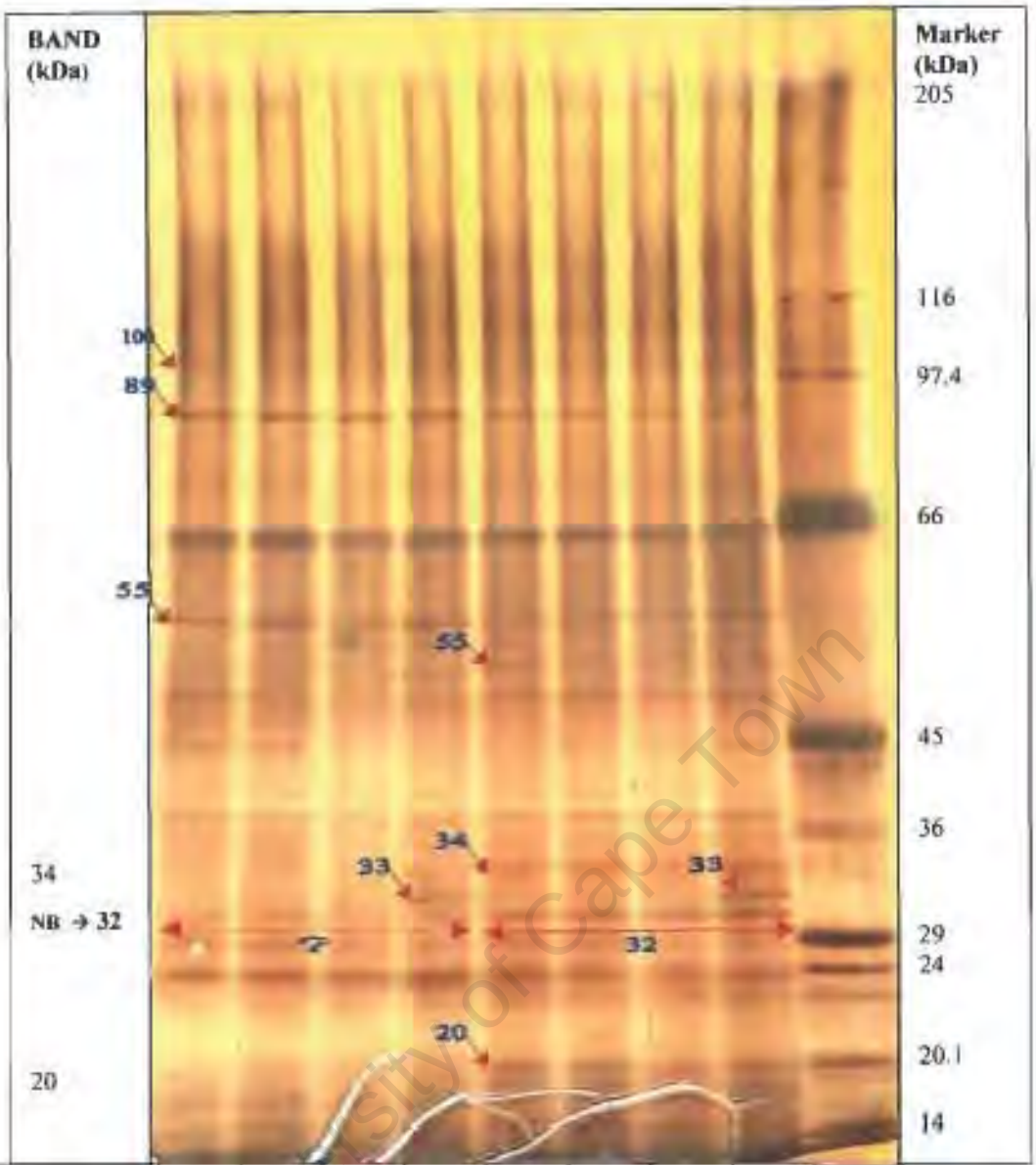

Lane Number	1	2	3	4	5	6	7	8	9
Phagosome type	Phago-Endosomes				Phago-Lysosomes				Marker
Phagosome treat	NaCl			None	NaCl			None	
Bead Type	Hydrophobic				Hydrophilic				
Incubation Time	10min Uptake, 2hr Chase								
Medium Additive	None	BSA	FCS	FCS	None	BSA	FCS	FCS	

Figure 5.2 : SDS-PAGE of Phagosomal Membrane purified from cells incubated with different media. P388D$_1$ mouse macrophages incubated (4 hrs) with different media additives were fed with hydrophobic or hydrophilic paramagnetic latex beads for 10 min, washed with the respective media and chased for 2 hours. The phago-endosomes [NaCl-treated (lanes 1-3) or untreated (lane 4)] and phago-lysosomes [NaCl-treated (lanes 5-7) or untreated (lane 8)] were purified from cells incubated in plain RPMI-1640 medium (lanes 1 & 5) or with BSA added (lanes 2 & 8) or with FCS added (lanes 3, 4, 7 & 8) and run on a 5-13% gradient SDS-PAGE gel. The Mw marker was run in lane 9. [Representative of 2 separate experiments]

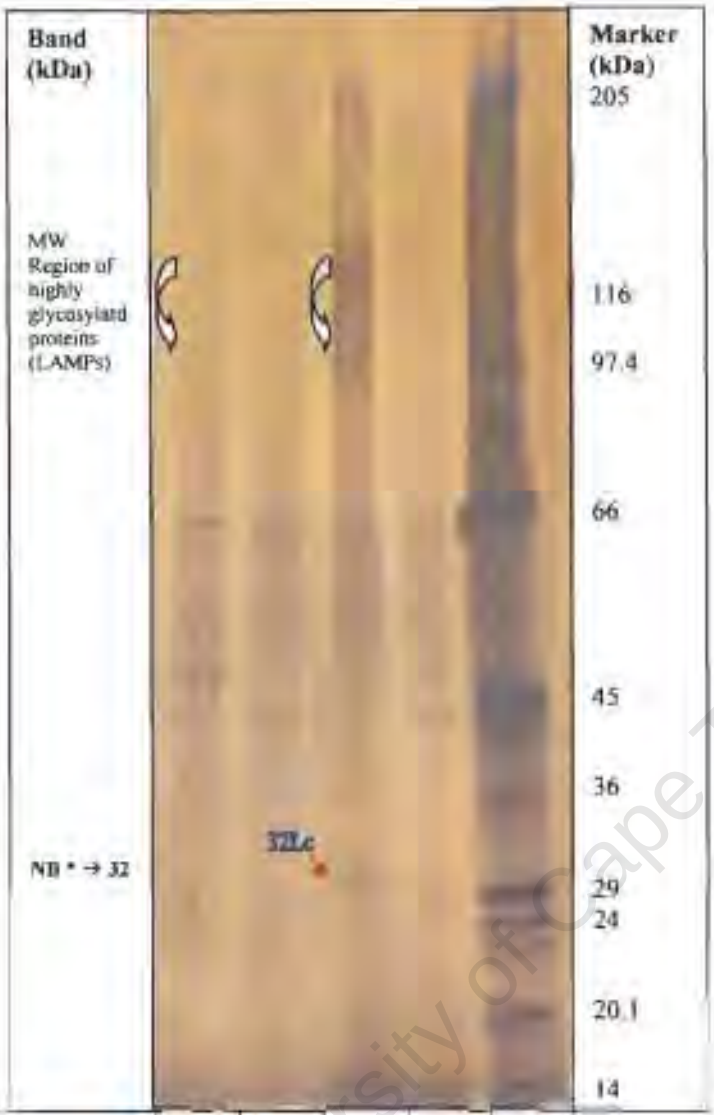

Lane Number	1	2	3	4	5
Phagosome type	Phago-En		Phago-Lys		Marker
Phagosome treat	NaCl				
Bead Type	Hydrophilic				
Incubation Time	10min Uptake 10min Chase		10min Uptake 2hr Chase		
TX-100 Fraction	Sup	Pel	Sup	Pel	

Figure 5.3 : SDS-PAGE of Phagosomal Membrane purified from cells incubated with plain RPMI medium. P388D1 mouse macrophages incubated with RPMI-FCS media were fed with hydrophilic paramagnetic latex beads for 10 min, washed and chased for 10 min (lanes 1 & 2) or 2 hours (lanes 3 & 4). Salt-washed phago-endosomes [Triton X-100 solubilised supernatant (lane 1) and pellet (lane 2)] and phago-lysosomes [Triton X-100 solubilised supernatant (lane 3) and pellet (lane 4)] were run on a 5-13% gradient SDS-PAGE gel. The Mw marker was run in lane 5. [Representative of 2 separate experiments]

5.3.2 2-D Electrophoresis

A comparison [Figure 5.6] of the analytical 2-dimensional gels of purified salt-extracted phago-endosomes [Figure 5.4] and phago-lysosomes [Figure 5.5], revealed that phago-endosomes were compositionally enriched for spots 57Ec(8.0), 55Ec(6.4), 50Ec(5.4), 45Ec(5.4) 34Ec(8.5), **32Ec(8.4)**, 22Ec(8.6) and 18Ec(8.5) while phago-lysosomes were enriched for spots 34Lc(4.9-5.1), **32Lc(4.6)**, 31Lc1(6.5), 31Lc2(6.1), 24Lc1(6.0), 24Lc2(5.6), 22Lc(7.6), 18Lc(8.2), 17Lc(6.6) and 16Lc(7.9). Preparative 2-dimensional gels of purified phago-endosomes [Figure 5.7(A)] and phago-lysosomes [Figure 5.7(B)] were performed for subsequent MALDI-MS and Edman microsequencing [Chapter 6]. Spots 34Ec(8.5), 32Ec(8.4), 22Ec(8.6), 18Ec(8.5), 32Lc(4.5), 22Lc(7.6), and 18Lc(8.2), were scaled up successfully.

MALDI-TOF analysis [Chapter 6] of the phago-endosome composition specific spots, 18Ec (8.5), 22Ec (8.6) and 34Ec (8.5) indicated that they were Mouse Cofilin (pI 8.5), Thioredoxin Peroxidase 2 (22.17 kDa/pI 8.26) and Tyrosine Kinase/Cathepsin K respectively. Edman microsequencing and MALDI-TOF analysis [Chapter 6] of the phago-endosome composition specific spot 32Ec(8.4) [cut out from a preparative 2-dimensional gel of purified salt-extracted phago-endosomes exhibited by Figure 5.7(A)] identified it as Mouse Galectin-3 (a galactose specific lectin). The 2-D position (Mw and pI) of the phago-endosome composition specific spot 32Ec(8.4) coincide with radioactive spot 32Lb(8.4) (bound specifically by X-lysosomes in the membrane binding assay), which was also determined to be galectin-3 by MALDI-TOF analysis.

MALDI-TOF analysis [Chapter 6] of phago-lysosome composition specific spots, 18Lc (8.2), 22Lc(7.6) and 32Lc(4.6) were determined to be Vacuolar ATP Synthase E fragment (26.58 kDa/pI 8.2), Superoxide Dismutase (22.22 kDa/pI 7.3), Annexin IV (35.87 kDa/5.32) respectively.

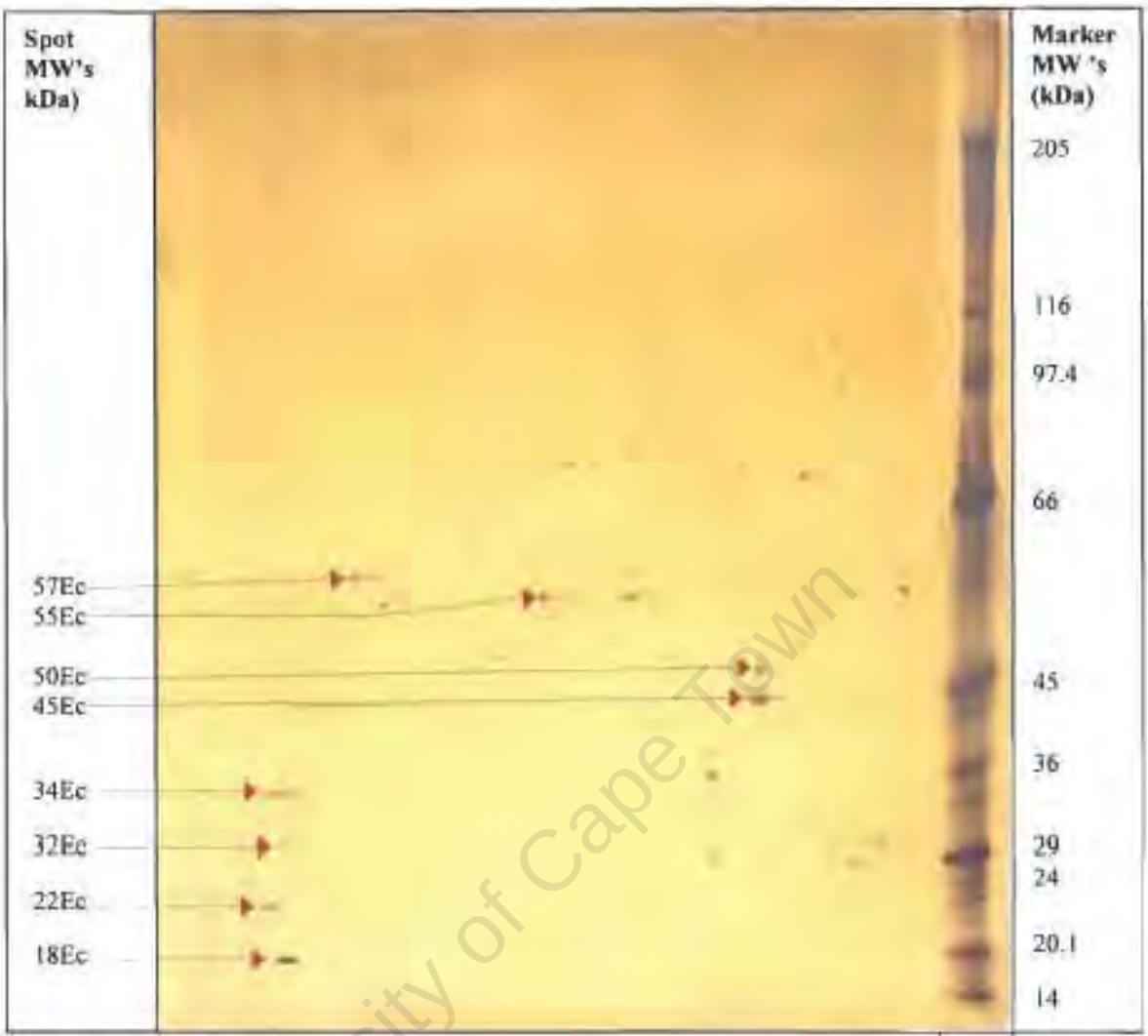

pH-Scale	9.5							4 Marker
Spot No.	57Ec	55Ec	50Ec	45Ec	34Ec	32Ec	22Ec	18Ec
pI-value	8.0	6.4	5.4	5.4	8.5	8.4	8.6	8.5

Figure 5.4 : Analytical 2-Dimensional gel of purified salt washed Phago-Endosomes used as acceptors in the binding assays. A sample of purified salt washed phago-endosomes was loaded during reswelling of an IPG strip (pH 3-10 NL, 180mm) in sample buffer (8M urea, 2M Thiourea, 4% CHAPS, 2% pH 3-10 carrier ampholytes, 20mM Tris base, 30mM DTT). Isoelectric focusing was performed at 17°C until equilibrium (65 kVh). The second dimension was performed using a 5-13% gradient SDS-PAGE followed by silver staining. [Representative of 2 separate experiments]

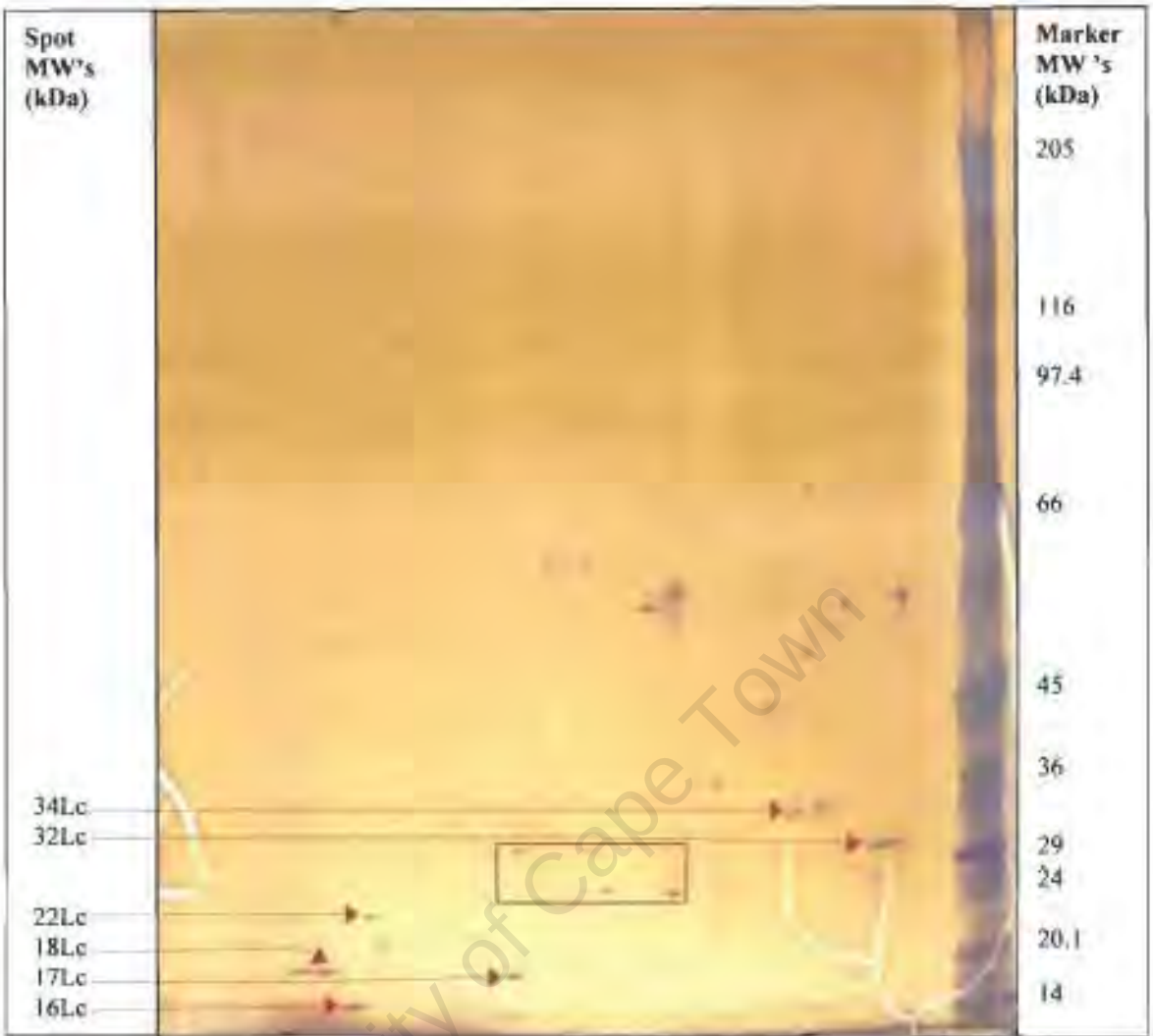

Figure 5.5 : Analytical 2-Dimensional gel of purified salt washed Phago-Lysosomes used as acceptors in the binding assays. A sample of purified salt washed phago-lysosomes was loaded during reswelling of an IPG strip (pH 3-10 NL, 180mm) in sample buffer (8M urea, 2M Thiourea, 4% CHAPS, 2% pH 3-10 carrier ampholytes, 20mM Tris base, 30mM DTT). Isoelectric focusing was performed at 17°C until equilibrium (65 kVh). The second dimension was performed using a 5-13% gradient SDS-PAGE followed by silver staining. [Representative of 2 separate experiments]

(A) 2-Dimensional gel of salt-washed Phago-Endosomes

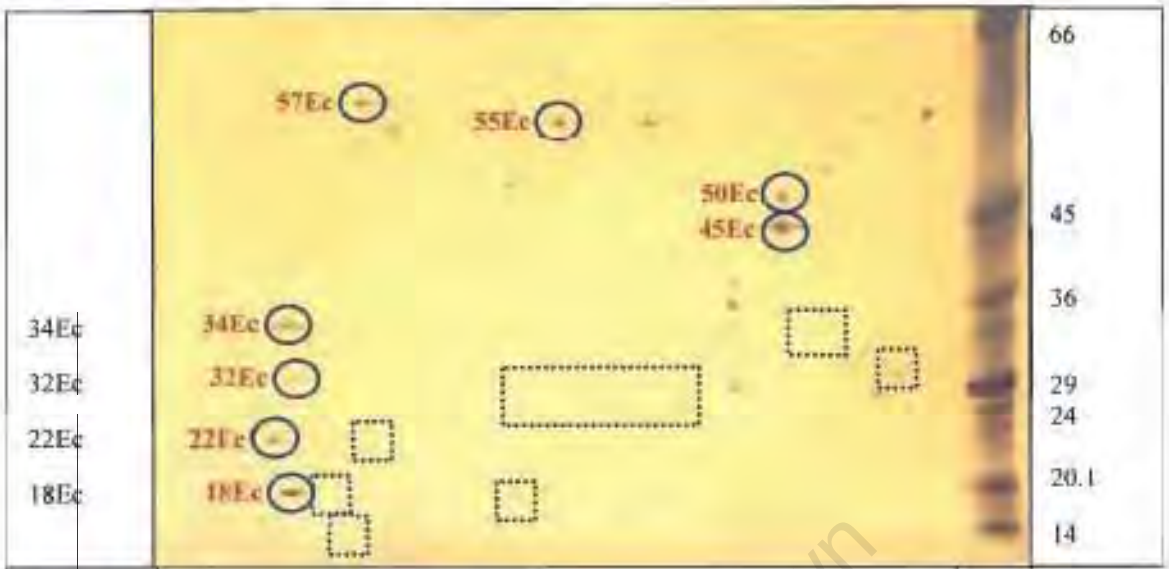

pH-Scale	9.5				4	Marker
Spot No	34Ec	32Ec	22Ec	18Ec		
pI-value	8.5	8.4	8.6	8.5		

(B) 2-Dimensional gel of salt-washed Phago-Lysosomes

pH-Scale	9.5			4	Marker
Spot No.	32Lc	22Lc	18Lc		
pI-value	4.6	7.6	8.2		

Figure 5.6 : A comparative compositional analysis between the silver stained 2-Dimensional gels of Phago-Endosomes (A) and Phago-Lysosomes (B). Spots enhanced in Phago-Endosomes (A) are circled and spots enhanced in Phago-Lysosomes (B) are boxed. Spots 34Ec, 32Ec, 22Ec, 18Ec, 32Lc, 22Lc and 18Lc were successfully scaled up for mass spectrometry [Figure 5.7]

(A) 2-Dimensional gel of salt-washed Phago-Endosomes

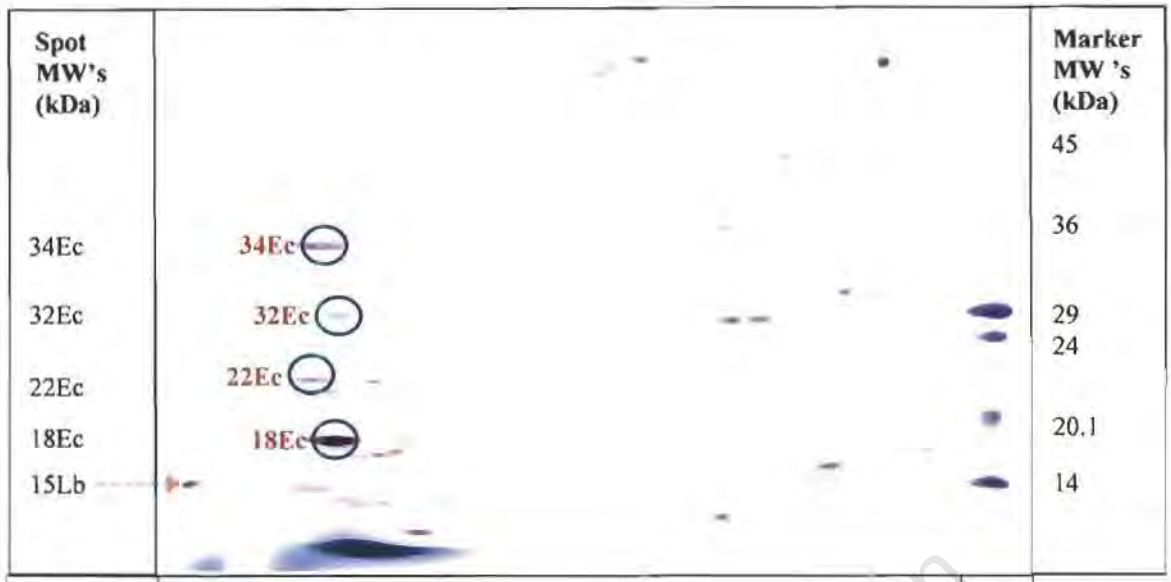

pH-Scale	9.5					4 Marker
Spot No.	34Ec	32Ec	22Ec	18Ec	15Lb	
pI-value	8.5	8.4	8.6	8.5	9.4	

(B) 2-Dimensional gel of salt-washed Phago-Lysosomes

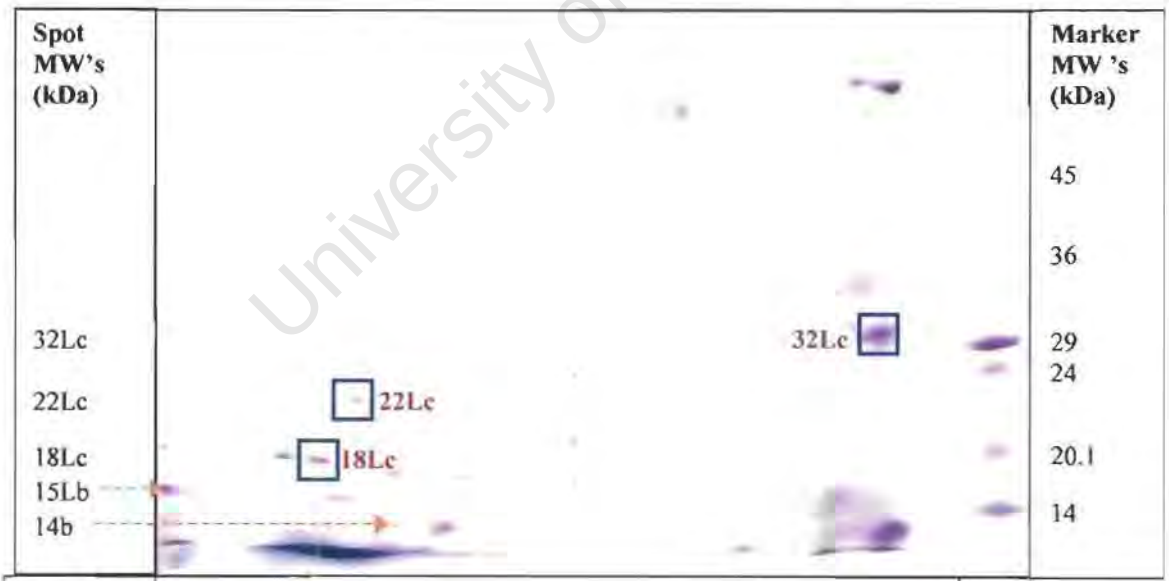

pH-Scale	9.5					4 Marker
Spot No.	32Lc	22Lc	18Lc	15Lb	14b	
pI-value	4.6	7.6	8.2	9.4	7.3	

Figure 5.9 : Preparative 2-Dimensional gels of Phago-Endosomes (A) and Phago-Lysosomes (B). Spots enhanced in Phago-Endosomes (A) are circled and spots enhanced in Phago-Lysosomes (B) are boxed. Spots 34Ec, 32Ec, 22Ec, 18Ec, 32Lc, 22Lc and 18Lc were thus successfully scaled up for mass spectrometry.

5.4 DISCUSSION

The existing information about the proteins differentially enriched in phago-endosomes and phago-lysosomes, identified by mass spectrometry [Chapter 6] was summarised below.

Phago-Endosome composition

18Ec - Cofilin. Cofilin is present in both phago-endosomes and phago-lysosomes but is enriched in phago-endosomes. Cofilin belongs to the ADF/Cofilin (actin depolymerising factor/cofilamentous protein) family. It binds both F-actin and actin monomers [417,418] and is essential for depolymerisation of actin filaments [419]. It has a higher affinity for ADP-actin than for ATP-actin and enhances the off rate of actin at the pointed ends of filaments [420]. Cofilin activity is regulated by phosphorylation carried out by LIM-Kinase [421,422]. The presence of cofilin on phagosomes is consistent since it is known that phagosomes bind F-actin [355,402].

22Ec - Thioredoxin Peroxidase II. Thioredoxin Peroxidase II regulates H_2O_2 concentration inside the cell, protecting cells from apoptosis [423]. TPx I is a cytosolic protein. Its specific association with phago-endosomes is a mystery. However, recently a PM-membrane associated hydroperoxide reductase (hTSA1) has been defined [424]. Thus a membrane associated TPx is not inconceivable.

32Ec - Galectin-3. Why would Galectin-3 be enriched in phago-endosomes? It is now known that galectin-3 is secreted by a process known as ectocytosis. Factors required for secretion must therefore exist in the PM. If these same factors are present in the PM-derived vesicles following endocytosis, then galectin-3 may also become associated with early endosomes / phago-endomes by default. Another possible explanation may be that extracellular cell surface associated galectin-3 enters via endocytosis. In the latter case galectin-3 would be located inside the lumen of endosomes / phago-endosomes. The

interaction here would probably be based on galectin-3 binding to the exposed β-galactose residues of glycoproteins. In this scenario, galectin–3 would cover these exposed galactose sites. Upon exposure to lysosomal proteases the degradation of galectin-3 would perhaps allow exposure of these or new galactose binding sites. This would also explain why X-lysosomes were able to bind galectin-3 in the binding assay. The above may indicate that galectin-3 may function (continuing perhaps its role from the extracellular surface) to target proteins to the lysosomes for degradation. Interestingly in support of the above hypothesis, in many cell types it has been shown that Lamps (lysosome-associated membrane glycoproteins) bind galectin-3 [425-428]. This hypothesis can be extended further, in that galectin-3 may be involved in binding damaged cell-surface receptors (exposing internal galactose moeities) which are normally blocked by capping residues (such as fucose, sialic acid, NAG etc). The binding of galectin-3 in this way may prevent recycling of damaged receptors. This hypothesis will be studied further, but is beyond the scope of this thesis. However, a cytoplasmic role for galectin-3 in endocytosis cannot be excluded and was thus studied further in this regard [Chapter 7]. Interestingly, galectin-3 possesses some homology to annexins VII and XI, implicated to play a role in self-aggregation and intracellular membrane traffic [391].

Phago-lysosome composition

18Lc - Vacuolar (H^+) ATPase. Vacuolar (H^+) ATPases (V-ATPases) are structurally related to the F_1F_0 ATP synthases of mitochondria, chloroplasts and bacteria. They are composed of a peripheral (V_1) and an integral (V_0) domain. The V-ATPases peripheral V_1 domain contains eight subunits (A,B,C,D,E,F,G,H) and the integral V_0 domain contains five subunits (a,d,c,c',c''). Functional studies indicate that the V_1 domain is responsible for ATP hydrolysis, while the V_0 domain is required for proton transport [429-433]. The V-ATPases are a family of ATP-dependent proton pumps. They transport protons across intracellular membranes [429-433]. Acidification of intracellular compartments is important for receptor-mediated endocytosis, intracellular protein targeting and

degradation [429-433]. Recent studies indicate that the V_0 domains of the V-ATPase from opposing membranes form trans-complexes creating a continuous proteolipid-lined channel that may promote subsequent membrane fusion [434]. Mutations of the E-subunit (Vacuolar ATPase E) in yeast grossly affects the actin cytoskeleton organisation, probably indirectly due to unstable V-ATPase complex assembly thereby affecting pH homeostasis [435]. The presence of a truncated form of V-ATPase E subunit in lysosomes is probably due to protease degradation, but a functional role for a truncated form cannot be ruled out.

22Lc - Superoxide dismutase 2 (Mn-SOD). Reactive oxygen radicals such as superoxide ($O_2\cdot$), hydrogen peroxide (H_2O_2) and hydroxyl ($OH\cdot$) are important in host defense, however it may have detrimental effects on the cells. Antioxidant enzymes such as superoxide dismutase, catalase and glutathione peroxidase protect the cell against oxidant injury. Superoxide dismutases catalyse the dismutation of two superoxide radicals into hydrogen peroxide and oxygen. Three isozymes exist in mammals namely Mn-SOD in mitochondria, Cu/Zn-SOD mainly in cytosol but accumulates in lysosomes via autophagy and EC-SOD in the extracellular space. The detection of mitochondrial Mn-SOD in lysosomes in this study may also be due to autophagy but a normal residence cannot be excluded. Since all peptide masses were not matched [Chapter 6, Figure 6.7] perhaps a novel SOD related to Mn-SOD is normally present in lysosomes. Mitochondrial contamination during phagosome purification is also a possibility.

32Lc - Annexin IV. Annexins are a family of about 13 structurally related Ca^{2+}-dependent phospholipid binding proteins. They possess four or eight conserved putative calcium and phospholipid binding repeats and a variable N-terminal domain postulated to confer functional diversity [436,437]. Additionally annexins IV, V and VI possess novel carbohydrate recognition domains, specific for glycosaminoglycans [438,439]. Evidence has accumulated for the role of annexins in membrane traffic [280-287]. The localisation of certain annexins to endocytic structures is known [281,440]. Similar to this study it has previously been shown for J774 macrophages that the level of associated annexin IV was

significantly higher on matured phagosomes [441]. In human neutrophils it has been found that during phagocytosis annexins III, IV and VI translocate from the cytoplasm to the phagosomes, wheras the localisation of annexins I and V remain unchanged [442].

The biochemical transformation of phagosomes, what is known?

Phagocytosis requires an intact actin cytoskeleton [443] and microtubules for transport [444-446,360,362]. Microtubules facilitate interactions between phagosomes and endocytic organelles. Phagosomes with pathogenic mycobacteria retain fusion and intermingling characteristics of early endosomes indefinitely, with concomitant disruption of the actin filament network [356]. The polypeptide and lipid composition of phagosomes changes due to interactions with endocytic structures [104-105,360-364]. The maturing phagosome accumulates proteins like lamp1, lamp2, vacuolar proton-ATPases and Cathepsin D [447,448] as well as annexin II, annexin VI, trimeric G-proteins, heat shock protein 70 family members (including ER-Bip), α-actinin and moesin [363]. Also Rab5, Rab7 and Rap1 sequentially associate with maturing phagosomes [362,449]. In contrast, fusion proteins, synaptobrevins 1 and 2, various syntaxins and NSF remains constantly associated [450-452]. The continued presence of these fusion molecules during all stages of phagosome maturation contradicts their proposed role in targeting phagosomes to specific endocytic organelles. In present study, it was found that phago-endosomes were enriched for galectin-3, thioredoxin peroxidase II and cofilin, while phago-lysosomes were enriched for annexin IV, superoxide dismutase and vacuolar ATP synthase E subunit. Very recently, a major proteomic study [455] report the identity of a host of proteins associated with phagosomes including galectin-3, supporting this studies findings.

Due to the complex nature of the biochemical transformation of phagosomes, it is difficult to place all proteins identified thus far into a simple conceptual framework. In depth functional and interactive analysis of the proteins identified in the present and previous studies is required, to bring about a better understanding of how they work in concert or tandem during phagocytic processing.

CHAPTER 6

MALDI-MS AND EDMAN SEQUENCING ANALYSIS

6.1 BACKGROUND

The living state of a cell at any given time is defined by its protein composition, that is, its proteome. Gel electrophoresis, mass spectrometric peptide mapping and peptide microsequencing combined with sequence database searching and bioinformatics are important tools for protein identification and proteome analysis.

Two-dimensional polyacrylamide gel electrophoresis (2D-PAGE) [367] is the only technique presently available for separating the majority of the proteins from a given cell type. Identification of the proteins present in a spot on a 2D-gel has traditionally been performed by Edman microsequencing [368]. Due to the cost and limited sensitivity of this technique, peptide mapping by matrix-assisted laser desorption/ionization mass spectrometry (MALDI MS) and peptide sequencing by electrospray ionization tandem mass spectrometry (ESI MS/MS) was developed and applied to protein identification [369-372].

For the present analysis, the spots of interest from preparative 2-D gels were excised, washed, cut up into small pieces, rinsed and then digested in-gel with either trypsin or Lys-C. The main 2D spot of interest (i.e. spot **32Ec**) was analysed by Edman microsequencing, while the rest of the spots of interest (i.e. 14b, 15Lb, 18Ec, 18Lc, 22Ec, 22Lc, 32Lc, **32Lb**, 33b, 34Ec and 74Lb) were analysed by MALDI-TOF (matrix-assisted laser desorption/ionization mass spectrometry time-of-flight).

6.2 MATERIALS AND METHODS

6.2.1 Protein Preparation and Protein Separation by Gel Electrophoresis

The proteins from purified phagosomes [phago-endosomes (Figure 5.7A) or phago-lysosomes (Figure 5.7B), Chapter 5] and the binding assay Membrane donor [low-density fraction of a 27% Percoll gradient, Chapter 3 (Figure 3.16)] were separated by 2D-electrophoresis.

6.2.2 Edman Microsequencing Analysis

Digestion of protein in excised gel plugs (in-gel) was performed as described [Section 6.2.3.2]. The peptide mixture was separated by RP-HPLC (reverse phase high performance liquid chromotography, Vydac C18 column) and the fractions were collected. Individual fractions were subjected to automated N-terminal Edman sequencing using a Procise 492 proteinsequencer (PE Biosystems).

6.2.3 MALDI-TOF Analysis

6.2.3.1 In-Gel Digestion of proteins and Extraction of peptides

Digestion of protein in excised gel plugs (in-gel) was performed as described. The excised gel plugs were cut into pieces and transfered into an Eppendorf tube. The following digestion buffers with enzyme were prepared: (A) 0.5µg Trypsin in 15µℓ 50 mM NH_4CO_3 or (B) 2µg Lys-C in 15µℓ 5mM Tris-HC1 pH 8.5. The following Protocol was used:

1) Washed with 200µℓ 50 mM NH_4CO_3 in 30 % (v/v) acetonitrile for 15 min/37°C (3x)
2) Treated with 100% Acetonitrile / dried in speedy vac for 15 minutes
3) Resuspended gel pieces with Enzyme in 15µℓ Digestion buffer (A or B)

4) Covered gel pieces with 20μℓ Digestion buffer
5) Incubated at 37°C / 18 hours in a Hybaid oven (U.K.)
6) Stored supernatant at -20°C.
7) Extracted peptides in 20μℓ 0.1% TFA in 60% Acetonitrile at 35°C / 12 hours (3x)
8) Pooled supernatants of steps 6 and 7, then dried in speedy vac for 1 hour.

6.2.3.2 MALDI-MS analysis of peptides

The dried peptide sample was resuspended in 10μℓ 0.1 % triflouroacetate in 30% acetonitrile. Peptide solution (1μℓ) was mixed with 1μℓ sinapinic acid as a matrix, crystallisation (detected by light microscopy) was allowed to take place at 25°C for 30 minutes. The crystals were subjected to MALDI-MS analysis using a PerSeptive Biosystems Voyager MALDI time-of-flight mass spectrometer (PE Biosystems, Cambridge, MA) in delayed extraction, reflector mode and the ion acceleration voltage set at 20 kV. A calibration mixture comprising bovine carbonic anhydrase *(m/t* 28982.7) or Lysozyme *(m/z* 14955.9) was used.

6.2.3.3 Database Searching

Protein identification using MS data was accomplished using MS-fit Peptide Search software to query sequence databases (SwissProt and NCBI). The MS-fit Peptide Search software is available at Protein Prospector via the Internet at http//www. prospector.ucsf.edu. Other Internet resources for protein research and biological MS are listed below.

Host	World Wide Web site
Odense University Protein Research Group	protein.ou.dk
EMBL Protein and Peptide Group	mann.embl-heidelberg.de
PROWL	proteometrics.com
MOWSE	seqnet.dl.ac.uk/mowse.html

6.3 RESULTS AND DISCUSSION

6.3.1 Edman Microsequencing analysis of spot 32Ec

Spot 32Ec (32 kDa/pI 8.4) was digested in-gel with Lys-C and the peptide mixture was then subjected to reverse phase high performance liquid chromotography (RP-HPLC).

Querying a comprehensive protein sequence database with the sequence [Figure 6.1 (B)] obtained from Edman analysis of HPLC fraction 1 [HPLC plot in Figure 6.1 (A)], retrieved the 5 top ranking sequence entries listed in Figure 6.1 (C). The pI of the top ranking entry Mouse galectin-3 (27.38 kDa/pI 8.5) corresponded well with observed pI (8.4) of spot 32Ec. MS peptide masses (1298.6 & 1908.9) of two more HPLC fractions (2 & 3 respectively) shown in Figure 6.1 (A), also matched the calculated masses of residues 213-223 (1298.7109) and 224-239 (1908.9800) of Mouse Galectin-3 respectively. Furthermore, the origin of species was correct (mouse) and the calculated protein mass (27 kDa) was consistent with the apparent molecular mass of 32 kDa observed on the 2D-gel within an experimental error of 10-20%. In conclusion, these data unambiguously identified the protein.

6.3.2 Protein Identification from 2-D PAGE Gels by MALDI Peptide Mass Mapping

A high performance liquid chromatographic (HPLC) run for separation of peptides is expensive and time-consuming. It is therefore advantageous to first utilise a rapid analysis method, such as high accuracy MALDI peptide mass mapping, for protein identification. Initial screening thereby limits the number of samples for more time-consuming analysis of proteins by chromatography, Edman and MS/MS peptide sequencing.

A

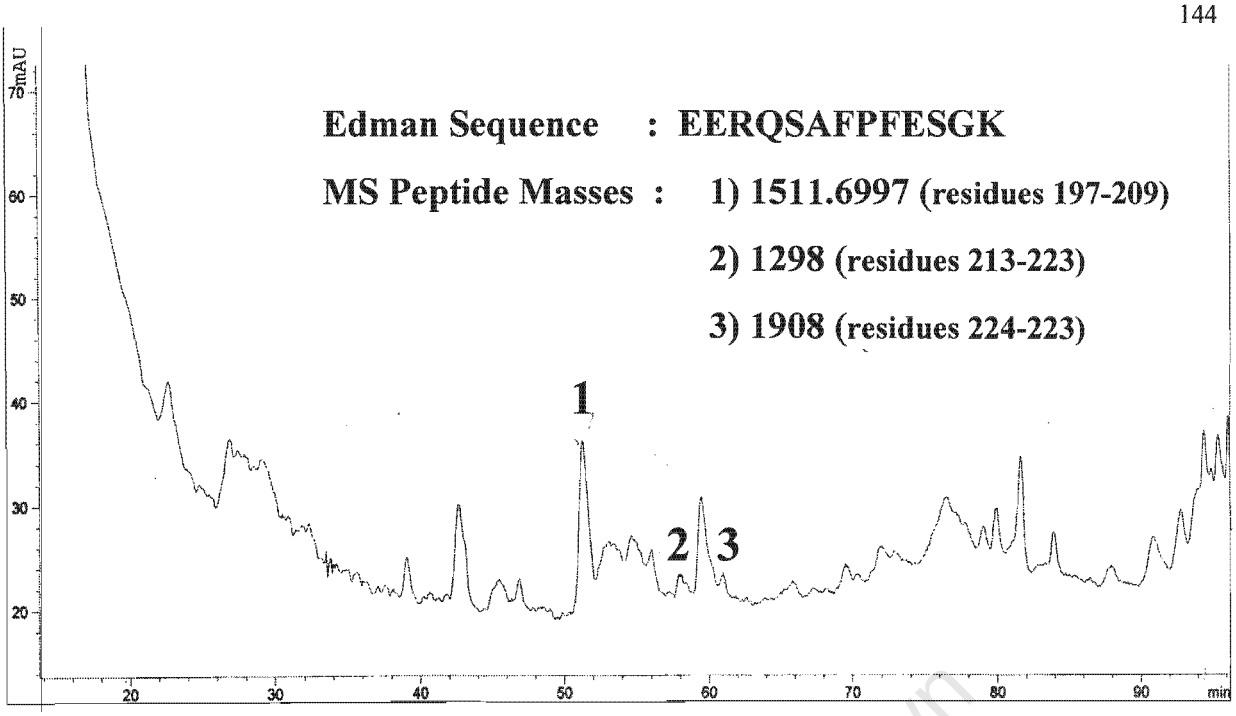

B

Rank	Matching Sequence	Peptide M+H	Protein Mw (Da)/pI	Species	SwissPrt. Access No.	Protein Name
Max Number of Amino Acid Substitutions (3)						
1	(K)EERQSAFPFESGK(P)	1511.7130	27515 / 8.47	Mouse	P16110	Galectin-3 (galactose-specific Lectin 3)
2	(R)EERQSAFPFESGK(P)	1511.7130	27202 / 8.59	Rat	P08699	Galectin-3 (galactose-specific Lectin 3)
3	(K)EERQ**A**AFPFESGK(P)	1495.7181	30330 / 7.78	Canfa	P38486	Galectin-3 (galactose-specific Lectin 3)
4	(R)EERQS**V**FPFESGK(P)	1539.7443	26189 / 8.58	Human	P17931	Galectin-3 (galactose-specific Lectin 3)
5	R)EERQ**TT**FPFE**I**GK(P)	1581.7913	25502 / 8.94	Rabit	P47845	Galectin-3 (galactose-specific Lectin 3)

C **The matched sequence (EERQSAFPFESGK) of 2D spot 32Lb/32Ec (32 kDa/pI 8.4) covered residues 197-209 of Mouse Galectin-3 (27.52 kDa/pI 8.47).**

```
  1 ADSFSLNDALAGSGNPNPQGYPGAWGNQPGAGGYPGAAYPGAYPGQAPPG
 51 AYPGQAPPGAYPGQAPPSAYPGPTAPGAYPGPTAPGAYPGQPAPGAFPGQ
101 PGAPGAYPQCSGGYPAAGPYGVPAGPLTVPYDLPLPGGVMPRMLITIMGT
151 VKPNANRIVLDFRRGNDVAFHFNPRFNENNRRVIVCNTKQDNNWGKEERQ
201 SAFPFESGKPFKIQVLVEADHFKVAVNDAHLLQYNHRMKNLREISQLGIS
251 GDITLTSANHAMI
```

Figure 6.1 : HPLC-plot and MS-Edman search results for 2D spot 32Ec. A) HPLC-RP chromatogram of Lys-C digested 2D spot 32Ec (32 kDa/pI 8.4). **B)** Database searches using the sequence of fraction 1 shown in A, was performed with the maximum number of amino acid substitutions set at 3, and the top 5 matching entries are shown. **C)** The best matching entry was Mouse Galectin-3 (27.52 kDa/pI 8.47). The matched sequence was underlined. MS masses of two more fractions (2 & 3) shown in A, also matched Mouse Galectin-3.

MALDI MS protein identification depends on the detection of a representative set of peptide masses derived from a protein band or spot excised from a gel, rinsed, optionally reduced (e.g. DTT) and S-alkylated (e.g. Iodoacetamide), and then digested in situ in the gel with a sequence-specific protease (e.g. trypsin or Lys-C) [373]. The generated peptide mixture is extracted from the gel and analysed by MS. The method requires that the protein in question exists as an entry in a protein sequence database. Thus, the peptide mass mapping method has its limitations. A complementary method is therefore necessary to obtain amino acid sequence information from proteins which do not exist as an entry in a protein sequence database . Since only 5-10% of a sample is consumed by MALDI MS, a large portion of the sample remains for further analysis.

6.3.2.1 Database Search Parameters for Successful MALDI Peptide Mass Identification

The number of measured peptide masses and the accuracy of peptide mass determination are the two most important parameters for unambiguous identification of proteins by peptide mass maps and database searches. The number of peptides detected decreases as the amount of protein starting material is reduced. Therefore, the sensitivity of the MS methods is limited by the amount of protein starting material and the extraction and detection efficiency of the generated peptides. Accurate peptide mass determination can be facilitated by delayed extraction MALDI-TOF in the reflector mode [374-376] and improves the specificity and selectivity of sequence database searches by MALDI peptide mass maps. Presently it is possible to identify proteins by querying the database with sets of only 4 or 5 peptide masses. In general, 5 or more peptides determined with a mass accuracy of 0.01% or better, usually suffice for unambiguous identification of a protein.

Database search parameters must include common amino acid modifications to possibly assign peptide masses, which may have arisen due to such modifications. N-terminus acetylation (N-Acet) increases a peptide's mass by 45 Da. Oxidation of methionine (Met-ox) to methionine sulfoxide in a peptide often generates an ion signal 16 Da above the non-oxidised peptide species. Observation of a pair of ion signals separated by a mass difference of 16 Da is therefore indicative of a Met containing peptide. This is subsequently confirmed by inspection of the retrieved protein sequences. Unreacted acrylamide from gel casting may react with free cysteine residues to generate S-acrylamidocysteine, which introduces a mass increment of 71 Da per cysteine. To minimise the occurrence of the latter, gels were cast 1 day prior to protein separation. Another modification to be considered is pyroglutamation (pyroGlu) of glutamate at the N-terminus of generated peptides, which decrease their mass by 17 Da. Lastly, if proteins were reduced and S-alkylated, mass increments of 57 Da (carbamidomethylation) or 58 Da (carboxymethylation) per cystein residue must be taken into account.

Missed cleavage sites must also be taken into consideration when performing the database searches. Tandem tryptic cleavage sites such as Lys-Lys or Lys-Arg, commonly occur in proteins. Cleavage at either of these adjacent sites generates a mixed population of peptides differing by an Arg or a Lys residue. If these related peptides are both detected by the mass spectrometer they give rise to peptide signals separated by 128. 1 Da (Lys) or 156.1 Da (Arg). Such peptide pairs differ by a Lys or Arg residue in either the N- or C-termini. Surveying a peptide mass map for the presence of these mass differences is advantageous if protein identification is problematic.

Comigration of two or more proteins in a band (SDS-PAGE) or sometimes in a spot (2-D PAGE) on a gel generates protein mixtures. Previously, such mixtures could only be resolved by chromatographic methods for peptide separation and subsequent peptide sequencing by either Edman degradation or MS/MS. However, the improved mass resolution and mass accuracy of delayed extraction MALDI peptide mass maps also allows

identification of the components of simple protein mixtures [377]. After identification of the first component of the mixture by high accuracy peptide mass mapping and database searching, the unassigned set of peptide masses is then used in a new database search to retrieve the next component of the protein mixture.

6.3.2.2 MALDI Peptide Mass Mapping Identification of 2D-spots

The protein spots of interest (14b, 15Lb, 18Ec, 18Lc, 22Ec, 22Lc, 32Lb, 32Lc, 33b, 34Ec and 74Lb) were excised from the gel, rinsed, and incubated overnight with trypsin or Lys-C. The extracted peptide mixtures were analysed by MALDI-TOF, which generated the mass spectrums shown in Figures 6.2-6.13. Each ion signal (not assigned as trypsin or Lys-C peaks) in the spectrum corresponds to a protonated peptide molecular ion of the sample.

Querying comprehensive protein sequence databases (SwissProt and NCBI) with these sets of measured peptide masses retrieved the sequence entries listed in Figure 6.14. Search parameters were set as follows:

Databases	: SwissProt and NCBI
Species	: Mammals
MW-range	: 1000 Da → 40000 Da or 100 kDa
pI-range	: 3 → 10
No. of missed cleavages	: 3
Peptide mass error	: 0.1% or 0.05%
Min. peptide matches	: ≈ $^1/_2$ peptide masses (0.1% error), 4-5 (0.05% error)
Cysteins modified by	: Carbamidomethylation
Modifications	: N-Acetylation, Met oxidation, Pyroglutamation

Spot 14b

The peptide mass spectrum obtained for trypsin digested spot 14b was displayed in Fig. 6.2(A). A total of 6 peptide masses specific for spot 14b, were determined in the MALDI-TOF experiment.

Searching the protein databases (SwissProt and NCBI) requiring a peptide mass error of less than 0.1 % retrieved the 5 top sequence entries listed in Fig. 6.2(B). All the sequences retrieved matched 4 of the 6 peptide masses submitted, but only 2 sequence entries namely Mouse β-2 Microglobulin precursor and Mouse Transcription Elongation factor S-II, matched all 4 peptide masses with a peptide mass error under 0.05%. Since there was no difference in matched peptide masses from the highest ranking candidate to the next, unambiguous identification was not possible. To decide between these 2 candidates, the observed MW (14 kDa) and pI (7.5) of spot 14b was considered, which made Mouse β-2 Microglobulin precursor (13.82 kDa/pI 7.8) the best matching sequence entry.

The matched peptides displayed in Fig. 6.2(C) covered 24% (29/119 AA's) of the sequence of Mouse β-2 Microglobulin precursor. If the signal sequence (residues 1 to 20) was subtracted from the mass, then the matched peptides actually covered 30% (29/99 AA's) of the matured sequence of Mouse β-2 Microglobulin (11.69 kDa/pI 7.35). The calculated protein mass (11.69 kDa) was consistent with the apparent molecular mass of 14 kDa observed on the 2D-gel within an accepted experimental error of 10-20%.

A

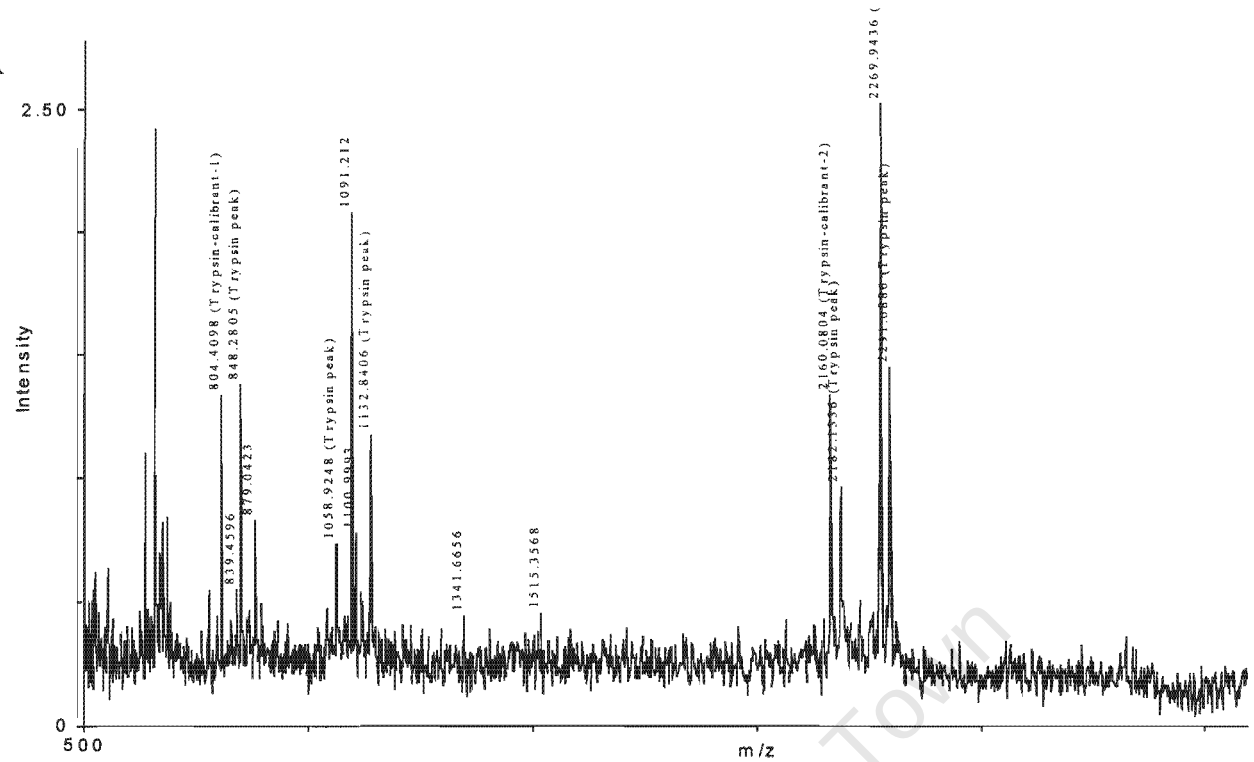

B

Rank	No. of Peptides Matched	Sequence Coverage (%)	Protein MW (Da)/pI	Species	SwissProt. Accession No.	Protein Name
(a) Peptide Mass Tolerance (+/-) 0.1 %, Min. No. of Peptides to Match (4)						
1	4/6	24%	13823 / 7.80	Mouse	P01887	Beta-2-Microglobulin Precursor
2	4/6	22%	17258 / 10.56	Human	Q02877	60S Ribosomal Protein L26
3	4/6	22%	17277 / 10.63	Rat	P12749	60S Ribosomal Protein L26
4	4/6	17%	33880 / 8.64	Mouse	P10712	Transcription Elongation Factor S-II
5	4/6	13%	32688 / 11.27	Human	Q13595	Transformer-2 Protein Homolog (Tra-2 Alpha)
(b) Peptide Mass Tolerance (+/-) 0.05 %, Min. No. of Peptides to Match (3)						
1	4/6	24%	13823 / 7.80	Mouse	P01887	Beta-2-Microglobulin Precursor
2	4/6	17%	33880 / 8.64	Mouse	P10712	Transcription Elongation Factor S-II
3	3/6	13%	29945 / 9.75	Rat	P49242	40S Ribosomal Protein S3a (V-Fos)
4	3/6	9%	32688 / 11.27	Human	Q13595	Transformer-2 Protein Homolog (Tra-2 Alpha)
5	3/6	10%	39837 / 8.72	Bovin	P21793	Bone Proteoglycan II Precursor (Decorin)

C **The matched peptides (4/6) of 2D spot 14b (14 kDa/pI 7.5) covered 24% (29/119 AA's) of Mouse β-2-Microglobulin Precursor (13.82 kDa/pI 7.80).**

m/z submitted	MH^+ matched	Delta %	start	end	Peptide Sequence	Modifications
839.4596	839.4052	0.0065	112	117	(K)TVYWDR(D)	
1091.2120	1091.5849	-0.0342	24	32	(K)TPQIQVYSR(H)	
1100.9993	1101.4675	-0.0425	112	119	(K)TVYWDRDM(-)	1Met-ox
1515.3568	1514.7235	0.0418	66	78	(K)IPKVEMSDMSFSK(D)	1Met-ox

2 unmatched masses: 879.0423 1341.6656

Figure 6.2 : MS data and MS-fit search results for 2D spot 14b. **A)** MALDI peptide mass spectrum of trypsin digested 2D spot 14b (14 kDa/pI 7.5). **B)** Database searches using the peptide masses shown in A, was performed with peptide mass error specified at (a) 0.1 % or (b) 0.05 % and the 5 best matching entries has been shown. **C)** The best matching entry was Mouse β-2-Microglobulin Precursor (13.82 kDa/pI 7.80).

Spot 15Lb

The peptide mass spectrum obtained for trypsin digested spot 15Lb was displayed in Fig. 6.3(A). A total of 8 peptide masses specific for spot 15Lb, were determined in the MALDI-TOF experiment.

Searching the protein databases (SwissProt and NCBI) requiring a peptide mass error of less than 0.1 % retrieved the 5 top sequence entries listed in Fig. 6.3(B). The highest ranking sequence entry was Mouse Lysozyme C precursor (16.69 kDa/pI 9.11) which matched 7 of the 8 peptide masses submitted, with 5 of them under a peptide mass error of 0.05%. The matched peptides displayed in Fig. 6.3(C), covered 33% (49/148 AA's) of the sequence of Mouse Lysozyme C precursor (16.69 kDa/pI 9.11). If the signal sequence (residues 1 to 18) was subtracted from the mass, then the matched peptides actually covered 38% (49/130 AA's) of the matured sequence of Mouse Lysozyme C (14.96 kDa/pI 9.47). The calculated Mw and pI of matured Mouse Lysozyme C (14.96 kDa/pI 9.47) was consistent with the observed MW (15 kDa) and pI (9.4) of spot 15Lb, and served to confirm the identification unambiguously.

Spot 18Ec

The peptide mass spectrum obtained for trypsin digested spot 18Ec was displayed in Fig. 6.4(A). A total of 10 peptide masses specific for spot 18Ec, were determined in the MALDI-TOF experiment.

Searching the protein databases (SwissProt and NCBI) requiring a peptide mass error of less than 0.1 % retrieved the 5 top sequence entries listed in Fig. 6.4(B). The top ranking sequence entry was Mouse Cofilin (18.56 kDa/pI 8.22) which matched 8 of the 10 peptide masses submitted. The matched peptides displayed in Fig. 6.4(C) covered 42% (71/166 AA's) of the sequence of Mouse Cofilin. The MW and pI of Mouse Cofilin (18.56 kDa/pI 8.22) corresponded well with the observed MW (18 kDa) and pI (8.5) of spot 18Ec. The 2 unmatched peptide masses (975.2566 and 1363.1679) might be trypsin peaks. In conclusion the identification is unambiguous.

A

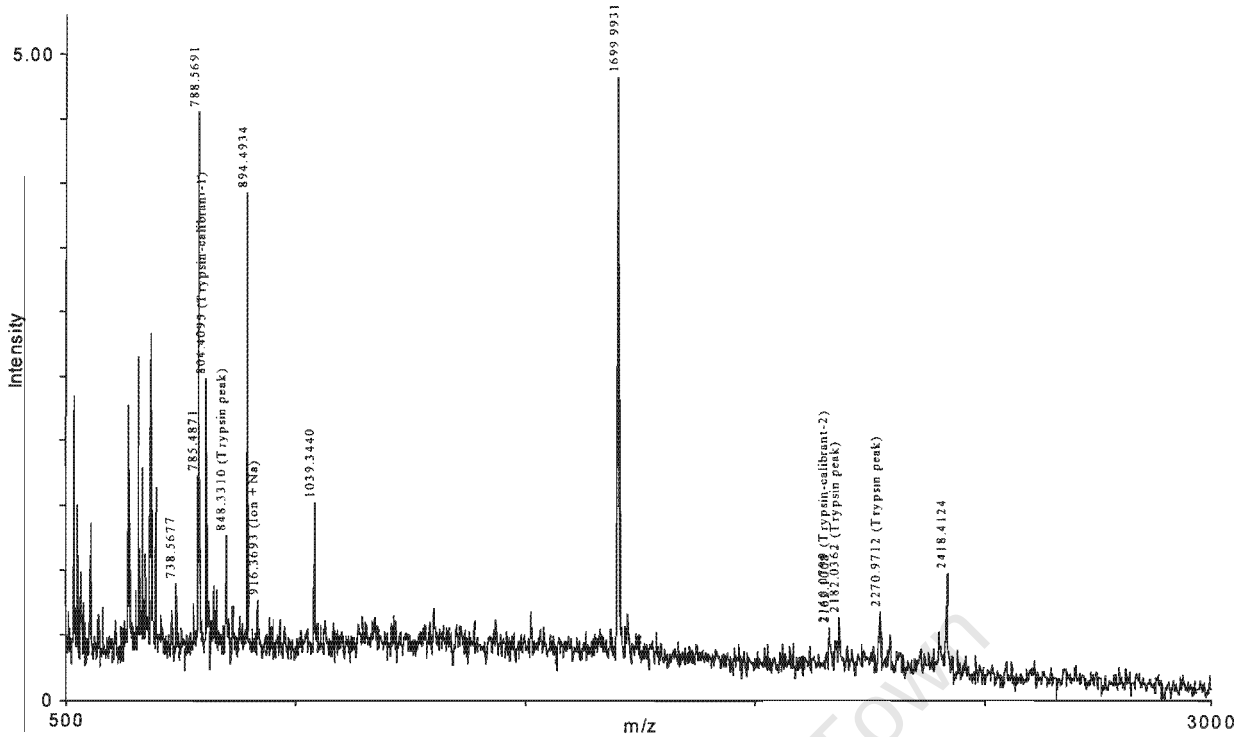

B

Rank	No. of Peptides Matched	Sequence Coverage (%)	Protein MW (Da)/pI	Species	SwissProt. Accession No.	Protein Name
(a) Peptide Mass Tolerance (+/-) 0.1 %, Min. No. of Peptides to Match (5)						
1	7/8	33%	16689 / 9.11	Mouse	P08905	Lysozyme C precursor (β-N-Acetylmuramidase C)
2	5/8	17%	33344 / 8.57	Mouse	P14231	Sodium/Potassium-Transporting ATPase β2 Chain
3	5/8	22%	35026 / 8.71	Rat	P70498	Phospholipase D2
4	5/8	13%	39867 / 8.64	Human	P00326	Alcohol Dehydrogenase γ-Chain
5	6/8	15%	38152 / 8.39	Bovin	O18739	Connective Tissue Growth Factor Precursor
(b) Peptide Mass Tolerance (+/-) 0.05 %, Min. No. of Peptides to Match (4)						
1	5/8	30%	14956 / 9.47	Mouse	P08905	Lysozyme C precursor (β-N-Acetylmuramidase C)
2	4/8	12%	39867 / 8.64	Human	P00326	Alcohol Dehydrogenase γ-Chain
3	4/8	10%	33344 / 8.57	Mouse	P14231	Sodium/Potassium-Transporting ATPase β2 Chain
4	4/8	14%	34014 / 9.63	Rat	P56499	Mitochondrial Uncoupling Protein 3
5	5/8	11%	38152 / 8.39	Bovin	O18739	Connective Tissue Growth Factor Precursor

C **The matched peptides (7/8) of 2D spot 15b (14 kDa/pI 9.4) covered 38% (49/130 AA's) of Matured Mouse Lysozyme C (14.96 kDa/pI 9.47).**

m/z submitted	MH^+ matched	Delta %	start	end	Peptide Sequence	Modification
738.5677	738.3535	0.0290	60	65	(R)ATNYNR(G)	
788.5691	788.4208	0.0188	126	131	(R)AWVAWR(A)	
894.4934	894.4685	0.0028	138	144	(R)DLSQYIR(N)	
1039.3440	1039.6013	-0.0247	117	125	(R)VVRDPQGIR(A)	
1699.9931	1700.7880	-0.0467	66	80	(R)GDQSTDYGIFQINSR(Y)	
2162.1008	2164.0735	-0.0912	120	137	(R)DPQGIRAWVAWRAHCQNR(D)	
2418.4124	2420.1231	-0.0707	60	80	(R)ATNYNRGDQSTDYGIFQINSR(Y)	

1 unmatched mass: 785.4871

Figure 6.3 : MS data and MS-fit search results for 2D spot 15Lb. **A)** MALDI peptide mass spectrum of trypsin digested 2D spot 15Lb (15 kDa/pI 9.4). **B)** Database searches using the peptide masses shown in A, was performed with peptide mass error specified at (a) 0.1 % or (b) 0.05 % and the 5 best matching entries has been shown. **C)** The best matching entry was Mouse Lysozyme C (14.96 kDa/pI 9.47).

A

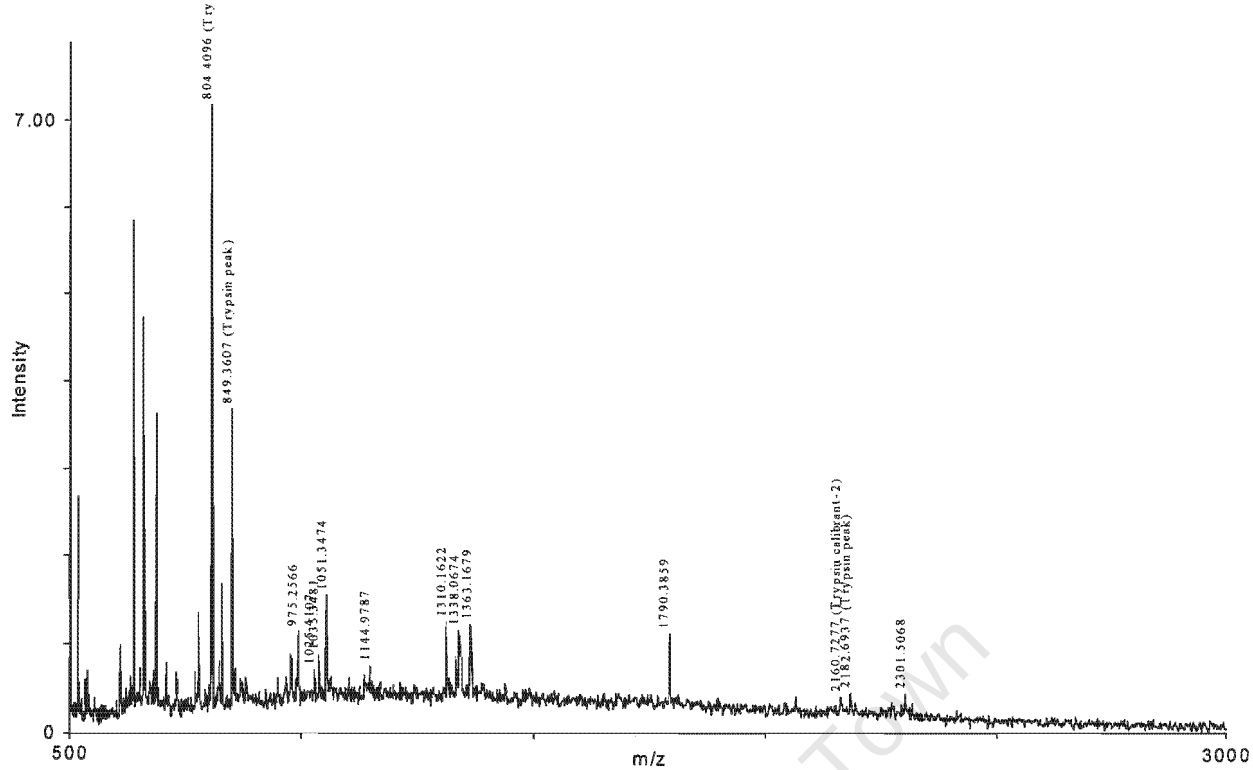

B

Rank	No. of Peptides Matched	Sequence Coverage (%)	Protein MW (Da)/pI	Species	SwissProt. Accession No.	Protein Name
(a) Peptide Mass Tolerance (+/-) 0.1 %, Min. No. of Peptides to Match (5)						
1	8/10	42%	18560 / 8.22	Mouse	P18760	Cofilin (Non-Muscle Isoform)
2	8/10	42%	18533 / 8.22	Rat	P45592	Cofilin (Non-Muscle Isoform)
3	6/10	30%	21493 / 11.35	Human	P02686	Myelin Basic Protein (MBP)
4	6/10	22%	33245 / 5.25	Mouse	P32853	Syntaxin 1B
5	6/10	22%	33275 / 5.25	Bovin	P41414	Syntaxin 1B
(b) Peptide Mass Tolerance (+/-) 0.05 %, Min. No. of Peptides to Match (4)						
1	4/10	30%	18560 / 8.22	Mouse	P18760	Cofilin (Non-Muscle Isoform)
2	4/10	30%	18533 / 8.22	Rat	P45592	Cofilin (Non-Muscle Isoform)
3	4/10	29%	21493 / 11.35	Human	P02686	Myelin Basic Protein (MBP)
4	4/10	19%	33245 / 5.25	Mouse	P32853	Syntaxin 1B
5	4/10	19%	33275 / 5.25	Bovin	P41414	Syntaxin 1B

C **The matched peptides (8/10) of 2D spot 18E (18 kDa/pI 8.5) covered 42% (71/166 AA's) of Mouse Cofilin Non-Muscle Isoform (18.56 kDa/pI 8.22).**

m/z submitted	MH^+ matched	Delta %	start	end	Peptide Sequence	Modification
1025.4107	1024.5250	0.0864	14	21	(K)VFNDMKVR(K)	1Met-ox
1035.3481	1034.4763	0.0845	74	81	(K)MLPDKDCR(Y)	
1051.3474	1050.4712	0.0837	74	81	(K)MLPDKDCR(Y)	1Met-ox
1144.9787	1144.6214	0.0313	1	13	(-)ASGVAVSDGVIK(V)	Acet N
1310.1622	1309.6826	0.0365	34	44	(K)KAVLFCLSEDK(K)	
1310.1622	1309.6826	0.0365	35	45	(K)AVLFCLSEDKK(N)	
1338.0674	1337.6265	0.0332	82	92	(R)YALYDATYETK(E)	
1790.3859	1790.8132	-0.0236	133	146	(K)HELQANCYEEVKDR(C)	
2301.5068	2303.1454	-0.0710	128	146	(K)LTGIKHELQANCYEEVKDR(C)	

2 unmatched masses: 975.2566, 1363.1679

Figure 6.4 : MS data and MS-fit search results for 2D spot 18Ec. A) MALDI peptide mass spectrum of trypsin digested 2D spot 18Ec (18 kDa/pI 8.5). **B)** Database searches using the peptide masses shown in A, was performed with peptide mass error specified at (a) 0.1 % or (b) 0.05 % and the 5 best matching entries has been shown. **C)** The best matching entry was Mouse Cofilin Non-Muscle Isoform (18.56 kDa/pI 8.22).

Spot 18Lc

The peptide mass spectrum obtained for trypsin digested spot 18Lc was displayed in Fig. 6.5(A). A total of 6 peptide masses specific for spot 18Lc, were determined in the MALDI-TOF experiment.

Searching the protein databases (SwissProt and NCBI) requiring a peptide mass error of less than 0.1 % retrieved the 5 top sequence entries listed in Fig. 6.5(B). All the sequences retrieved matched 5 of the 6 peptide masses submitted, but only Mouse Vacuolar ATP Synthase Subunit matched all 5 peptide masses with a peptide mass error under 0.05%. The sequence coverage (< 20%) was low for all entries, but only because their MW was far above the expected MW. Since there was only a small difference in matched peptide masses from the highest ranking candidate to the next, unambiguous identification was not possible. The MW and pI of all the sequence entries did not correspond well with the observed MW (18 kDa) and pI (8.2) of spot 18Lc, and are possibly fragments or perhaps a novel related protein not yet available as an entry in the databases.

Nonetheless, the 5 matched peptide masses of only 1 entry namely Mouse Vacuolar ATP Synthase Subunit E (26.59/pI 9.28) displayed in Fig. 6.5(C) covered a consecutive stretch of sequence (i.e. the N-terminal region from residue 46 to 109). Additionally 4 of the 5 matched peptide masses were under a peptide mass error of 0.03%, which was an excellent match. Considering the above and that the subcellular location of Mouse Vacuolar ATP Synthase Subunit E (26.59/pI 9.28) was correct, made it the best matching entry available in the protein databases.

In conclusion, Mouse Vacuolar ATP Synthase Subunit E (26.59/pI 9.28) was a preliminary identification of spot 18Lc and requires further analysis to confirm the assignment.

A

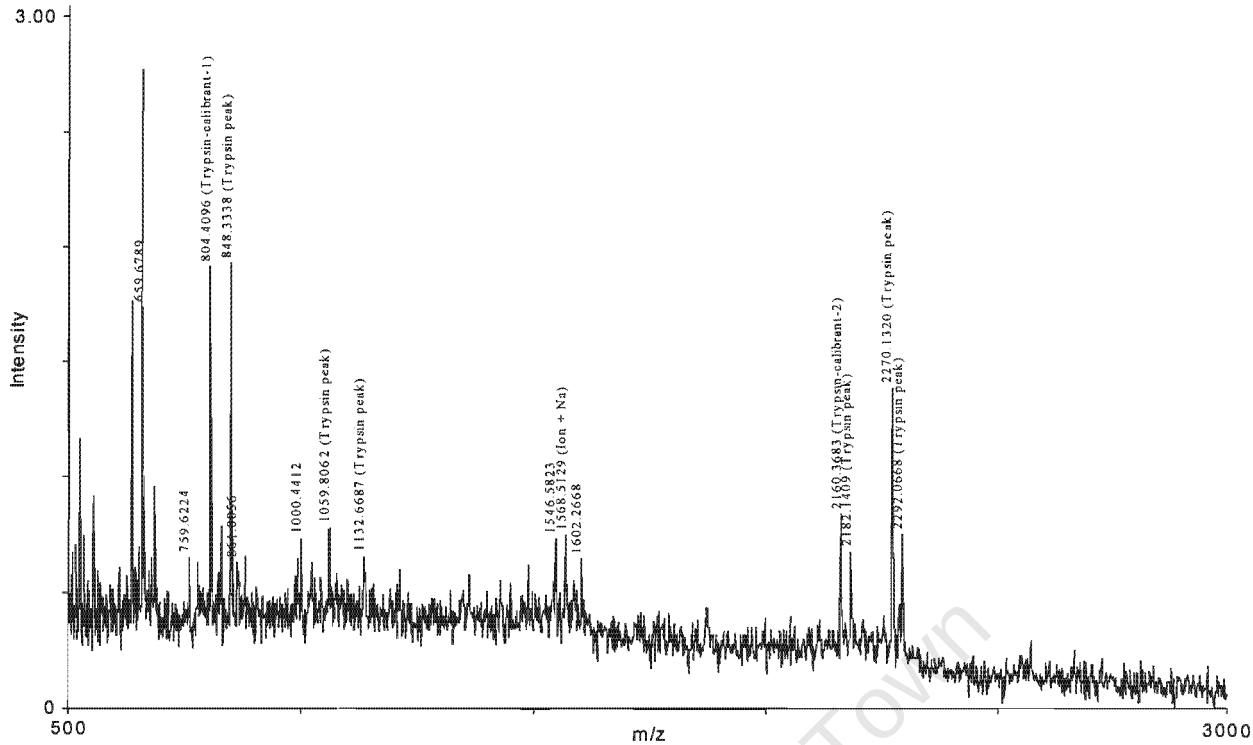

B

Rank	No. of Peptides Matched	Sequence Coverage (%)	Protein MW (Da)/pI	Species	SwissProt. Accession No.	Protein Name
(a) Peptide Mass Tolerance (+/-) 0.1 %, Min. No. of Peptides to Match (5)						
1	5/6	19%	26588 / 9.28	Mouse	P50518	Vacuolar ATP Synthase Subunit E
2	5/6	18%	25678 / 8.51	Human	P09210	Glutathione S-Transferase A2
3	5/6	16%	30444 / 5.68	Rabbit	225913	Apolipoprotein AI
4	5/6	16%	37156 / 9.63	Mouse	2388720	Carnitine Palmitoyltransferase I
5	5/6	15%	34458 / 9.75	Rat	P09895	60S Ribosomal Protein L5
(b) Peptide Mass Tolerance (+/-) 0.05 %, Min. No. of Peptides to Match (4)						
1	5/6	19%	26588 / 9.28	Mouse	P50518	Vacuolar ATP Synthase Subunit E
2	4/6	14%	30444 / 5.68	Rabbit	225913	Apolipoprotein AI
3	4/6	13%	35045 / 8.86	Human	Q00526	Cell Division Protein Kinase 3
4	4/6	9%	37777 / 12.18	Human	860970	HP8 peptide
5	4/6	9%	38849 / 9.45	Mouse	3288547	Transcription Elongation Factor

C **The matched peptides (5/6) of 2D spot 18L (18 kDa/pI 8.2) covered 19% (44/228 AA's) of Mouse Vacuolar ATP Synthase Subunit E (26.59 kDa/pI 9.28).**

m/z submitted	MH^+ matched	Delta %	start	end	Peptide Sequence	Modifications
659.6789	659.3840	0.0447	67	71	(R)QQQKK(I)	
759.6224	759.4365	0.0245	46	51	(R)LLETQR(L)	
1000.4412	1000.6155	-0.0174	46	53	(R)LLETQRLK(I)	
1000.4412	1000.5977	-0.0156	102	109	(K)QRLMKVVK(D)	pyroGlu, Met-ox
1546.5823	1546.8198	-0.0154	72	84	(K)IQMSNLMNQARLK(V)	
1602.2668	1601.8613	0.0253	52	63	(R)LKIMEYYEKKEK(Q)	

1 unmatched mass: 861.0056

Figure 6.5 : MS data and MS-fit search results for 2D spot 18Lc. **A)** MALDI peptide mass spectrum of trypsin digested 2D spot 18L (18 kDa/pI 8.2). **B)** Database searches using the peptide masses shown in A, was performed with peptide mass error specified at (a) 0.1 % or (b) 0.05 % and the 5 best matching entries has been shown. **C)** The best matching entry was Mouse Vacuolar ATP Synthase Subunit E (26.59 kDa/pI 9.28).

Spot 22Ec

The peptide mass spectrum obtained for trypsin digested spot 22Ec was displayed in Fig. 6.6(A). A total of 10 peptide masses specific for spot 22Ec, were determined in the MALDI-TOF experiment.

Searching the protein databases (SwissProt and NCBI) requiring a peptide mass error of less than 0.1 % retrieved the 5 top sequence entries listed in Fig. 6.6(B). The highest ranking sequence entry was Mouse Thioredoxin Peroxidase 2 (22.17 kDa/pI 8.26) which matched 8 of the 10 peptide masses submitted, with 7 of them under a peptide mass error of 0.05%. The matched peptides displayed in Fig. 6.6(C), covered 38% (67/199 AA's) of the sequence of Mouse Thioredoxin Peroxidase 2 (22.17 kDa/pI 8.26). In addition the calculated Mw and pI of Mouse Thioredoxin Peroxidase 2 (22.17 kDa/pI 8.26) was consistent with the observed MW (22 kDa) and pI (8.6) of spot 22Ec, and served to confirm the identification unambiguously. Mouse Thioredoxin Peroxidase 2 was first identified as a Macrophage Stress Factor of 23 kDa.

Spot 22Lc

The peptide mass spectrum obtained for trypsin digested spot 22Lc was displayed in Fig. 6.7(A). A total of 17 peptide masses specific for spot 22Lc, were determined in the MALDI-TOF experiment.

Searching the protein databases (SwissProt and NCBI) requiring a peptide mass error of less than 0.1 % retrieved the 5 top sequence entries listed in Fig. 6.7(B). The highest ranking sequence entry was Mouse Superoxide Dismutase Precursor (24.60 kDa/pI 8.80) which matched 10 of the 17 peptide masses submitted, with 6 of them under a peptide mass error of 0.05%.

A

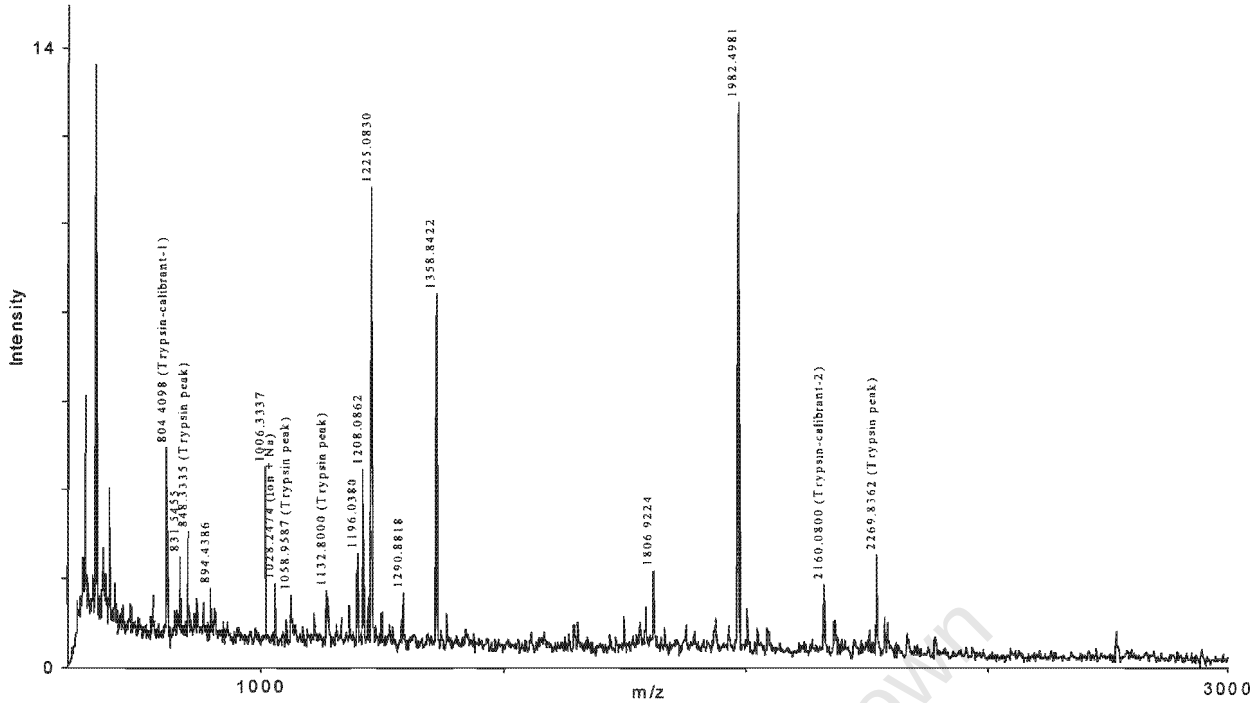

B

Rank	No. of Peptides Matched	Sequence Coverage (%)	Protein MW (Da)/pI	Species	SwissProt. Accession No.	Protein Name
(a) Peptide Mass Tolerance (+/-) 0.1 %, Min. No. of Peptides to Match (5)						
1	8/10	38%	22176 / 8.26	Mouse	P35700	Thioredoxin Peroxidase 2
2	7/10	29%	22109 / 8.27	Rat	Q63716	Thioredoxin Peroxidase 2
3	5/10	28%	17661 / 6.73	Sheep	P19114	Interleukin-2 Precursor
4	5/10	22%	23336 / 4.74	Human	2135800	Synaptosomal Associated Protein 25A (SNAP-25)
5	5/10	18%	23315 / 4.65	Human	P13795	Synaptosomal Associated Protein 25 (SNAP-25)
(b) Peptide Mass Tolerance (+/-) 0.05 %, Min. No. of Peptides to Match (4)						
1	7/10	27%	22176 / 8.26	Mouse	P35700	Thioredoxin Peroxidase 2
2	6/10	23%	22109 / 8.27	Rat	Q63716	Thioredoxin Peroxidase 2
3	4/10	29%	15030 / 4.94	Human	O14810	Complexin 1 (Synaphin 2)
4	4/10	11%	23336 / 4.74	Human	2135800	Synaptosomal Associated Protein 25A (SNAP-25)
5	4/10	11%	23315 / 4.65	Human	P13795	Synaptosomal Associated Protein 25 (SNAP-25)

C **The matched peptides (8/10) of 2D spot 22E (22 kDa/pI 8.6) covered 38% (67/199 AA's) of Mouse Thioredoxin Peroxidase 2 (22.17 kDa/pI 8.26).**

m/z submitted	MH^+ matched	Delta %	start	end	Peptide Sequence	Modifications
831.5455	831.4576	0.0106	152	158	(R)SVDEIIR(L)	
894.4386	894.4321	0.0007	121	128	(K)ADEGISFR(G)	
1006.3337	1006.5362	-0.0201	8	16	(K)IGYPAPNFK(A)	
1196.0380	1196.6315	-0.0496	159	168	(R)LVQAFQFTDK(H)	
1208.0862	1208.6639	-0.0478	141	151	(R)QITINDLPVGR(S)	pyroGlu
1225.0830	1225.6905	-0.0496	141	151	(R)QITINDLPVGR(S)	
1358.8422	1359.8000	-0.0704	129	140	(R)GLFIIDDKGILR(Q)	
1982.4981	1983.0187	-0.0263	111	128	(R)TIAQDYGVLKADEGISFR(G)	

2 unmatched masses: 1290.8818, 1806.9224

Figure 6.6 : MS data and MS-fit search results for 2D spot 22Ec. **A)** MALDI peptide mass spectrum of trypsin digested 2D spot 22E (22 kDa/pI 8.5). **B)** Database searches using the peptide masses shown in A, was performed with peptide mass error specified at (a) 0.1 % or (b) 0.05 % and the 5 best matching entries has been shown. **C)** The best matching entry was Mouse Thioredoxin Peroxidase 2 (22.17 kDa/pI 8.26).

The next matching sequence was Mouse Rab-10 (22.54 kDa/pI 8.58) which matched 6 of the 17 peptide masses submitted, with 4 of them under a peptide mass error of 0.05%. When the remaining 7 peptide masses unassigned to Mouse Superoxide Dismutase Precursor were reused in a new database search (data not shown), 4 of them matched Mouse Rab-10, thus only 2 of the peptide masses overlaped in matching both Superoxide Dismutase and Rab-10. The former suggested that possible comigration of these 2 sequences had occurred on the 2D gel. The matched peptides covered only 33% (67/200 AA's) of the sequence of Mouse Rab-10 (22.54 kDa/pI 8.58). Also the pI of Mouse Rab-10 (pI 8.58) was not consistent with the observed pI (7.6) of spot 22Lc.

The matched peptides displayed in Fig. 6.7(C), covered 55% (127/222 AA's) of the sequence of Mouse Superoxide Dismutase Precursor (24.60 kDa/pI 8.80). If the signal sequence (residues 1 to 24) was subtracted from the mass, then the matched peptides actually covered 65% (127/198 AA's) of the matured sequence of Mouse Superoxide Dismutase (22.22 kDa/pI 7.30). The calculated Mw and pI of matured Superoxide Dismutase (22.22 kDa/pI 7.30) was consistent with the observed MW (22 kDa) and pI (7.6) of spot 22Lc, which served to confirm the identification as unambiguous.

A

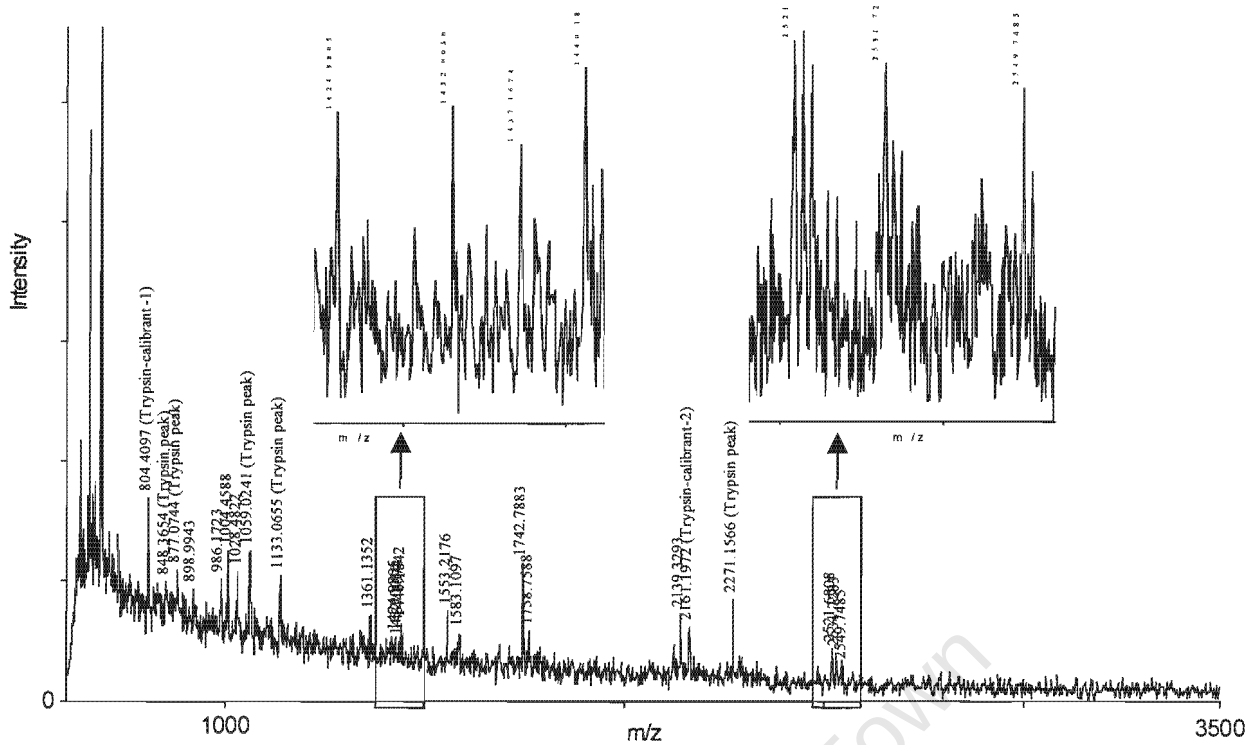

B

Rank	No. of Peptides Matched	Sequence Coverage (%)	Protein MW (Da)/pI	Species	SwissProt. Accession No.	Protein Name
(a) Peptide Mass Tolerance (+/-) 0.1 %, Min. No. of Peptides to Match (8)						
1	10/17	55%	24603 / 8.80	Mouse	P09671	Superoxide Dismutase precursor (Mitochondrial)
2	6/17	33%	22541 / 8.58	Mouse	O88386	Rab-10 (Ras-Related Protein)
3	6/17	33%	22569 / 8.58	Canfa	P24409	Rab-10 (Ras-Related Protein)
4	6/17	30%	22291 / 7.94	Rat	P07895	Superoxide Dismutase (Mitochondrial)
5	6/17	26%	33196 / 6.11	Human	O75558	Syntaxin 11
(b) Peptide Mass Tolerance (+/-) 0.05 %, Min. No. of Peptides to Match (5)						
1	6/17	35%	22222 / 7.30	Mouse	P09671	Superoxide Dismutase precursor (Mitochondrial)
2	4/17	26%	22541 / 8.58	Mouse	O88386	Rab-10 (Ras-Related Protein)
3	4/17	26%	22569 / 8.58	Canfa	P24409	Rab-10 (Ras-Related Protein)
4	4/17	24%	22291 / 7.94	Rat	P07895	Superoxide Dismutase (Mitochondrial)
5	4/17	21%	39031 / 6.40	Human	Q15080	Neutrophil Cytosol Factor 4

C **The matched peptides (10/17) of 2D spot 22L (22 kDa/pI 7.6) covered 65% (127/198 AA's) of Matured Mouse Superoxide Dismutase (22.22 kDa/pI 7.30).**

m/z submitted	MH^+ matched	Delta %	start	end	Peptide Sequence	Modification
986.1723	985.4743	0.0708	123	130	(K)RDFGSFEK(F)	
1004.4588	1004.5529	-0.0094	195	202	(K)NVRPDYLK(A)	
1028.4822	1028.6104	-0.0125	115	123	(K)GELLEAIKR(D)	
1361.1352	1361.6741	-0.0396	124	134	(R)DFGSFEKFKEK(L)	
1440.1842	1440.8062	-0.0432	76	89	(K)GDVTTQVALQPALK(F)	
1553.2176	1553.8651	-0.0417	109	123	(K)GGGEPKGELLEAIKR(D)	
1742.7883	1743.8818	-0.0627	203	216	(K)AIWNVINWENVTER(Y)	
2139.3293	2140.0728	-0.0347	90	108	(K)FNGGGHINHTIFWTNLSPK(G)	
2521.7844	2523.2381	-0.0576	54	75	(K)HHAAYVNNLNATEEKYHEALAK(G)	
2531.7283	2533.2952	-0.0619	135	158	(K)LTAVSVGVQGSGWGWLGFNKEQGR(L)	

7 unmatched masses: 898.6943, 1424.9805, 1432.0050, 1437.1674, 1583.1097, 1758.7588, 2549.7485

Figure 6.7 : MS data and MS-fit search results for 2D spot 22Lc. **A)** MALDI peptide mass spectrum of trypsin digested 2D spot 22L (22 kDa/pI 7.6). **B)** Database searches using the peptide masses shown in A, was performed with peptide mass error specified at (a) 0.1 % or (b) 0.05 % and the 5 best matching entries has been shown. **C)** The best matching entry was Mouse Superoxide Dismutase (22.22 kDa/pI 7.30).

Spot 32Lc

The peptide mass spectrum obtained for trypsin digested spot 32Lc was displayed in Fig. 6.8(A). A total of 11 peptide masses specific for spot 32Lc, were determined in the MALDI-TOF experiment.

Searching the protein databases (SwissProt and NCBI) requiring a peptide mass error of less than 0.1 % retrieved the 5 top sequence entries listed in Fig. 6.8(B). The highest ranking sequence entry was Rat Annexin IV (35.87 kDa/pI 5.32) which matched 8 of the 11 peptide masses submitted, with 5 of them under a peptide mass error of 0.05%. The next matching sequence was Bovin Annexin IV (35.89 kDa/pI 5.54) which matched 6 of the 12 peptide masses submitted, with 5 of them under a peptide mass error of 0.05%.

The matched peptides displayed in Fig. 6.8(C), covered 37% (121/319 AA's) of the sequence of Rat Annexin IV (35.87 kDa/pI 5.32). The calculated Mw and pI Rat Annexin IV (35.87 kDa/pI 5.32) was consistent with the observed MW (32 kDa) and pI (4.6) of spot 32Lc within an experimental error of 10%. Coincidentally, it has been observed that Annexin IV migrates at a MW of 32-33 kDa upon SDS-PAGE [438a,b].

The matched peptides (data not shown), covered 31% (102/319 AA's) of the sequence of Bovin Annexin IV (35.89 kDa/pI 5.54). Similarly, the calculated Mw and pI of Bovin Annexin IV (35.89 kDa/pI 5.54) was consistent with the observed MW (32 kDa) and pI (4.6) of spot 32Lc within an experimental error of 10%. One of the peptide masses (1428.2061) not assigned to Rat Annexin IV, was matched by Bovin Annexin IV and Human Annexin VIII.

Since Mouse Annexin IV (which does exist as an entry in the databases) was not retrieved as a match for the top 5 ranking entries instead of Rat and Bovin Annexin IV, was suggestive of a variant/related Annexin not available as an entry in the protein databases.

A

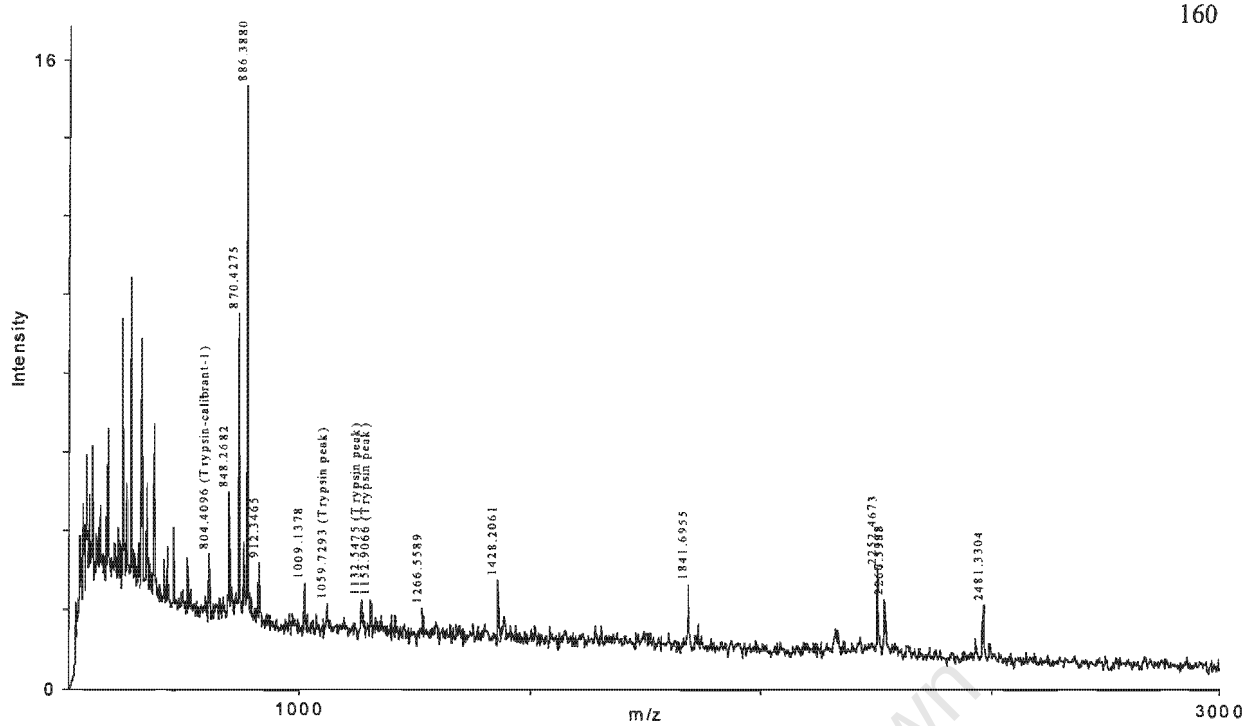

B

Rank	No. of Peptides Matched	Sequence Coverage (%)	Protein MW (Da)/pI	Species	SwissProt. Accession No.	Protein Name
(a) Peptide Mass Tolerance (+/-) 0.1 %, Min. No. of Peptides to Match (6)						
1	8/11	37%	35874 / 5.32	Rat	P55260	Annexin IV (Endonexin I)
2	6/11	31%	35889 / 5.54	Bovin	P13214	Annexin IV (Endonexin I)
3	7/11	29%	36879 / 5.56	Human	P13928	Annexin VIII (Vascular Anticoagulant-Beta)
4	6/11	22%	39361 / 6.21	Rat	P19356	Porphobilinogen Deaminase
5	6/11	20%	33409 / 6.63	Human	P55212	Caspase-6 Precursor (Apoptotic Protease MCH-2)
(b) Peptide Mass Tolerance (+/-) 0.05 %, Min. No. of Peptides to Match (4)						
1	5/11	28%	35874 / 5.32	Rat	P55260	Annexin IV (Endonexin I)
2	5/11	28%	35882 / 5.84	Human	P09525	Annexin IV (Endonexin I)
3	5/11	20%	35889 / 5.54	Bovin	P13214	Annexin IV (Endonexin I)
4	5/11	17%	39361 / 6.21	Rat	P19356	Porphobilinogen Deaminase
5	5/11	15%	31268 / 8.72	Mouse	Q60653	Killer Cell Lectin-Like Cell Surface Receptor 6

C **The matched peptides (8/11) of 2D spot 32Lc (32 kDa/pI 4.6) covered 37% (121/319 AA's) of Rat Annexin IV (Endonexin I) (35.87 kDa/pI 5.32).**

m/z submitted	MH^+ matched	Delta %	start	end	Peptide Sequence	Modification
870.4275	870.3593	0.0078	301	308	(K)GDTSGDYR(K)	
912.3465	913.4856	-0.0947	117	123	(R)NPEEIRR(I)	
1009.1378	1008.5478	0.0585	50	57	(R)QEIRTAYK(S)	
1841.6955	1840.9571	0.0401	201	214	(R)NRNHLLHVFDEYKR(I)	
2252.4673	2252.1142	0.0157	242	259	(K)CMRNKPAYFAERLYKSMK(G)	1Met-ox
2266.3995	2268.1092	-0.0754	242	259	(K)CMRNKPAYFAERLYKSMK(G)	2Met-ox
2267.5388	2268.1092	-0.0251	242	259	(K)CMRNKPAYFAERLYKSMK(G)	2Met-ox
2481.3304	2481.2408	0.0036	1	24	METKGGTVKAASGFNATEDAQVLR(K)	
2481.3304	2480.2772	0.0425	219	241	(K)DIEQSIKSETSGSFEDALLAIVK(C)	

3 unmatched masses: 886.3880, 1266.5589, 1428.2061

Figure 6.8 : MS data and MS-fit search results for 2D spot 32Lc. **A)** MALDI peptide mass spectrum of trypsin digested 2D spot 32Lc1 (32 kDa/pI 4.6). **B)** Database searches using the peptide masses shown in A, was performed with the peptide mass error specified at (a) 0.1 % or (b) 0.05 % and the 5 top matching entries has been shown. **C)** The best matching entry was Rat Annexin IV (Endonexin I) (35.87 kDa/pI 5.32).

Spot 32Lb

The peptide mass spectrum obtained for Lys-C digested spot 32Lb was displayed in Fig. 6.9(A). A total of 8 peptide masses specific for spot 32Lb, were determined in the MALDI-TOF experiment.

Searching the protein databases (SwissProt and NCBI) requiring a peptide mass error of less than 0.1 % or 0.05% retrieved the 5 top sequence entries listed in Fig. 6.9(B). The highest ranking sequence entry was Mouse galectin-3 (27.52 kDa/pI 8.47) which matched 5 of the 8 peptide masses submitted, with all 5 under a peptide mass error of 0.05%. In fact, 4 were under a peptide mass error of 0.01%. Which was an extremely close match.

The matched peptides displayed in Fig. 6.9(C), covered 25% (66/264 AA's) of the sequence of Mouse galectin-3 (27.52 kDa/pI 8.47). The calculated Mw of Mouse galectin-3 (27.52 kDa) was consistent with the observed MW (32 kDa) of spot 32Lb within an experimental error of 15% and the pI was spot on. Coincidentally, it has been observed that Mouse Galectin-3 migrates at a MW of 30-31 kDa upon SDS-PAGE.

One of the peptide masses (883.4320) not assigned might be the Ion-Na species of the calculated peptide mass of 861.3800. Thus leaving only 2 peptide masses (935.1664 and 1863.7467) unassigned to Mouse galectin-3. Further analysis by MS/MS is required to determine whether these peptides perhaps represent variant changes in the amino acid sequence of galectin-3.

Edman microsequencing [Figure 6.1] of the peptide of mass 1511.6997 (HPLC-RP fraction 1) of spot 32 Ec was determined as the sequence EERQSAFPFESGK which matched Mouse galectin-3, which served to unambiguously confirm that the identity of both spots 32Lb and 32Ec was Mouse galectin-3.

A

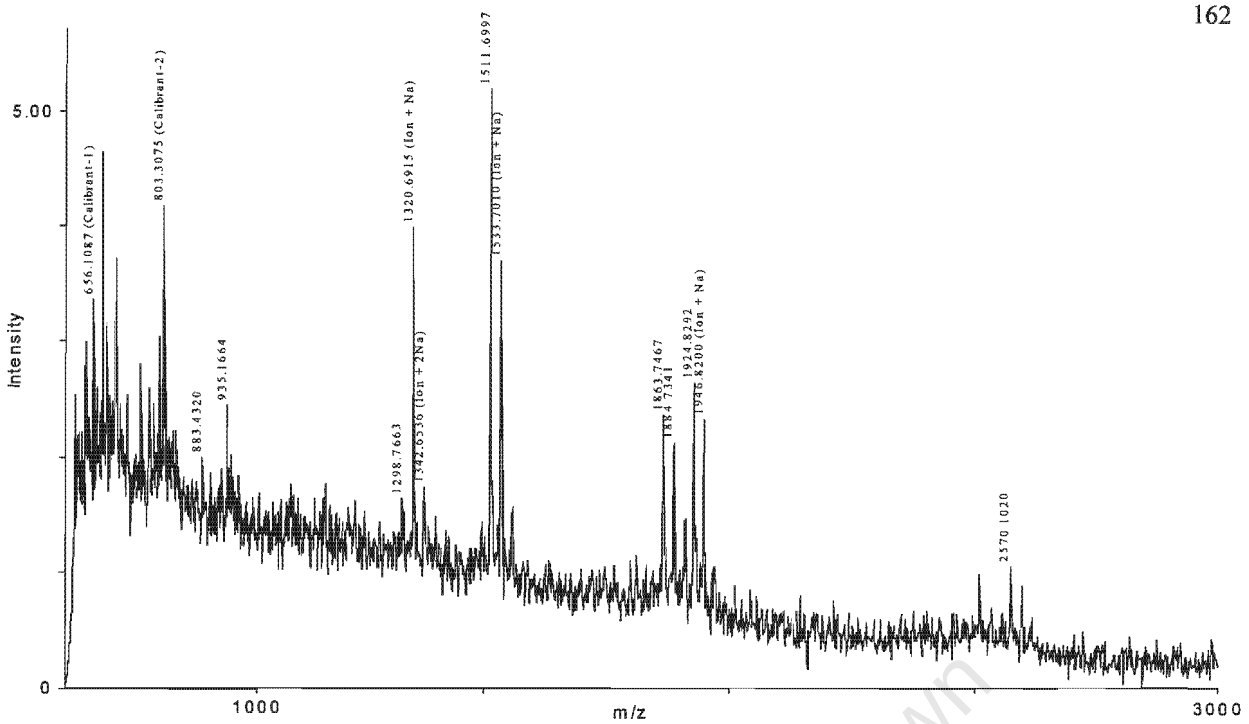

B

Rank	No. of Peptides Matched	Sequence Coverage (%)	Protein MW (Da)/pI	Species	SwissProt. Accession No.	Protein Name
(a) Peptide Mass Tolerance (+/-) 0.1 %, Min. No. of Peptides to Match (4)						
1	5/8	25%	27515 / 8.47	Mouse	P16110	Galectin-3 (galactose-specific Lectin 3)
2	5/8	25%	27429 / 8.58	Mouse	52851	L-34 protein
3	4/8	23%	25059 / 5.09	Human	6716764	Neuroendocrine Differentiation Factor
4	4/8	21%	26395 / 4.85	Human	7688967	Uncharacterized Bone Marrow protein BM036
5	4/8	18%	30174 / 9.82	Human	539695	T cell factor 1 (splice form B)
(b) Peptide Mass Tolerance (+/-) 0.05 %, Min. No. of Peptides to Match (3)						
1	5/8	25%	27515 / 8.47	Mouse	P16110	Galectin-3 (galactose-specific Lectin 3)
2	5/8	25%	27429 / 8.58	Mouse	52851	L-34 protein
3	3/8	18%	30174 / 9.82	Human	539695	T cell factor 1 (splice form B)
4	3/8	12%	34880 / 7.12	Human	4507305	Sulfotransferase 1
5	3/8	10%	36752 / 9.43	Human	5051993	G protein pathway suppressor 2

C **The matched peptides (5/8) of 2D spot 32Lb (32 kDa/pI 8.4) covered 25% (66/263 AA's) of Mouse Galectin-3 (27.52 kDa/pI 8.47).**

m/z submitted	MH^+ matched	Delta %	start	end	Peptide Sequence	Modification
1298.7663	1298.7109	0.0043	213	223	(K)IQVLVEADHFK(V)	
1511.6997	1511.7200	0.0014	197	209	(K)EERQSAFPFESGK(P)	
1884.7341	1883.9292	0.0427	197	212	(K)EERQSAFPFESGKPFK(I)	
1924.8292	1924.9816	-0.0079	224	239	(K)VAVNDAHLLQYNHRMK(N)	1Met-ox
2570.1020	2570.3248	-0.0087	240	263	(K)NLREISQLGISGDITLTSANHAMI(-	1Met-ox

3 unmatched masses : 883.4320, 935.1664, 1863.7467

Figure 6.9 : MS data and MS-fit search results for 2D spot 32Lb. **A)** MALDI peptide mass spectrum of Lys-C digested 2D spot 32Lb (32 kDa/pI 8.4). **B)** Database searches using the peptide masses shown in A, was performed with the peptide mass error specified at (a) 0.1 % or (b) 0.05 % and the 5 top matching entries has been shown. **C)** The best matching entry was Mouse Galectin-3 (27.52 kDa/pI 8.47). The matched peptides and sequence coverage has been shown.

Spot 33b

The peptide mass spectrum obtained for trypsin digested spot 33b was displayed in Fig. 6.10 (A). A total of 22 peptide masses specific for spot 33b, were determined in the MALDI-TOF experiment.

Searching the protein databases (SwissProt and NCBI) requiring a peptide mass error of less than 0.1 % retrieved the 5 top sequence entries listed in Fig. 6.10(B). The top ranking sequence entry was Mouse Voltage-Dependent Anion-Selective Channel (30.75 kDa/pI 8.62), which matched 16 of the 22 peptide masses submitted.

The matched peptides displayed in Fig. 6.10(C), covered 70% (199/283 AA's) of the sequence of Mouse Voltage-Dependent Anion-Selective Channel (30.75 kDa/pI 8.62). The calculated Mw and pI of Mouse Voltage-Dependent Anion-Selective Channel (30.75 kDa/pI 8.62) was consistent with the observed MW (33 kDa) and pI (8.6) of spot 33b.

When the remaining 6 peptide masses unassigned [Fig. 6.11(A)] to Mouse Voltage-Dependent Anion-Selective Channel were reused in a new database search shown in Fig. 6.11(B), 5 of them were matched by Mouse Max Interacting Protein and Human Cytokeratin 8 [dispayed in Fig. 6.13(C)]. Since the bulk of the peptide masses (16/22) were matched already, comigration of a second protein is ruled out. Thus the remaining peptide masses in all probability were derived from contaminating human keratin (i.e. Cytokeratin 8).

A

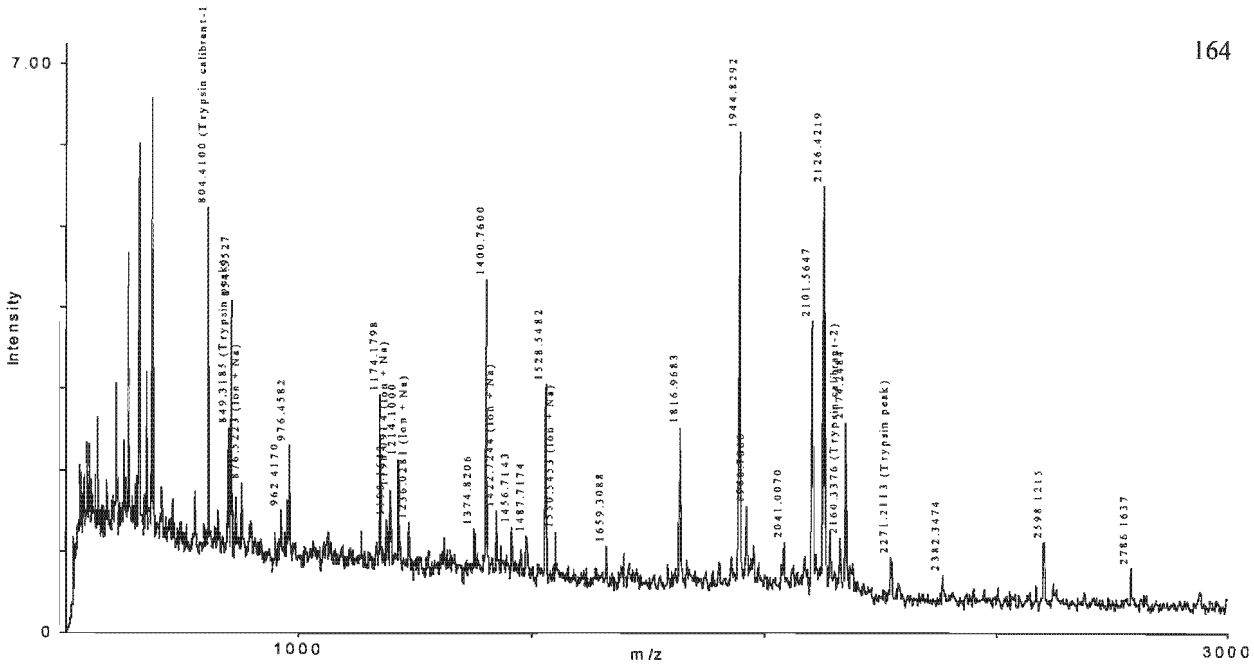

B

Rank	No. of Peptides Matched	Sequence Coverage (%)	Protein MW (Da)/pI	Species	SwissProt. Accession No.	Protein Name
(a) Peptide Mass Tolerance (+/-) 0.1 %, Min. No. of Peptides to Match (7)						
1	16/22	70%	30755 / 8.62	Mouse	Q60932	Voltage-Dependent Anion-Selective Channel
2	14/22	63%	30772 / 8.62	Human	P21796	Voltage-Dependent Anion-Selective Channel
3	8/22	51%	29493 / 5.88	Rat	5070662	Kinesin heavy chain
4	8/22	46%	26093 / 5.89	Human	7019877	Unnamed protein product
5	8/22	38%	38284 / 7.80	Mouse	387403	Annexin I
(b) Peptide Mass Tolerance (+/-) 0.05 %, Min. No. of Peptides to Match (5)						
1	9/22	32%	30772 / 8.62	Human	P21796	Voltage-Dependent Anion-Selective Channel
2	9/22	28%	30755 / 8.62	Mouse	Q60932	Voltage-Dependent Anion-Selective Channel
3	6/22	42%	23256 / 8.69	Human	P49798	G-Protein Signaling Regulator
4	6/22	27%	30375 / 5.53	Rabit	71790	Apolipoprotein A-I
5	5/22	21%	34165 / 5.84	Mouse	P70452	Syntaxin 4

C **The matched peptides (16/22) of 2D spot 33b (33 kDa/pI 8.6) covered 70% (199/283 AA's) of Mouse Voltage-Dependent Anion-Selective Channel (30.75 kDa/pI 8.62).**

m/z submitted	MH^+ matched	Delta %	start	end	Peptide Sequence	Modifications
854.5527	854.4776	0.0088	21	28	(K)GYGFGLIK(L)	
1174.1798	1173.6156	0.0481	1	12	(-)AVPPTYADLGK(S)	Acet N
1214.1000	1213.6217	0.0394	164	174	(R)VTQSNFAVGYK(T)	
1374.8206	1374.6582	0.0118	64	74	(R)WTEYGLTFTEK(W)	
1400.7600	1400.6156	0.0103	225	236	(K)YQVDPDACFSAK(V)	
1456.7143	1456.7549	-0.0028	162	174	(K)SRVTQSNFAVGYK(T)	
1487.7174	1487.7858	-0.0046	1	15	(-)AVPPTYADLGKSAR(D)	Acet N
1528.5482	1528.7647	-0.0142	97	110	(K)LTFDSSFSPNTGKK(N)	
1816.9683	1817.9146	-0.0521	202	218	(K)LETAVNLAWTAGNSNTR(F)	
1944.8292	1946.0096	-0.0607	201	218	(K)KLETAVNLAWTAGNSNTR(F)	
1960.7860	1959.8783	0.0463	35	53	(K)SENGLEFTSSGSANTETTK(V)	
2101.5647	2103.1814	-0.0769	237	256	(K)VNNSSLIGLGYTQTLKPGIK(L)	
2126.4219	2128.0133	-0.0748	121	139	(R)EHINLGCDVDFDIAGPSIR(G)	
2174.2484	2176.0522	-0.0829	75	93	(K)WNTDNTLGTEITVEDQLAR(G)	
2598.1215	2600.1905	-0.0796	175	197	(K)TDEFQLHTNVNDGTEFGGSIYQK(V)	
2786.1637	2788.3125	-0.0771	35	61	(K)SENGLEFTSSGSANTETTKVNGSLETK(Y)	

6 unmatched masses: 962.4170, 976.4582, 1190.1642, 1659.3088, 2041.0070, 2382.3474

Figure 6.10 : MS data and MS-fit search results for 2D spot 33b. **A)** MALDI peptide mass spectrum of trypsin digested 2D spot 33b (33 kDa/pI 8.6). **B)** Database searches using the peptide masses shown in A, was performed with peptide mass error specified at (a) 0.1 % or (b) 0.05 % and the 5 best matching entries has been shown. **C)** The best matching entry was Mouse Voltage-Dependent Anion-Selective Channel (30.75 kDa/pI 8.62).

A

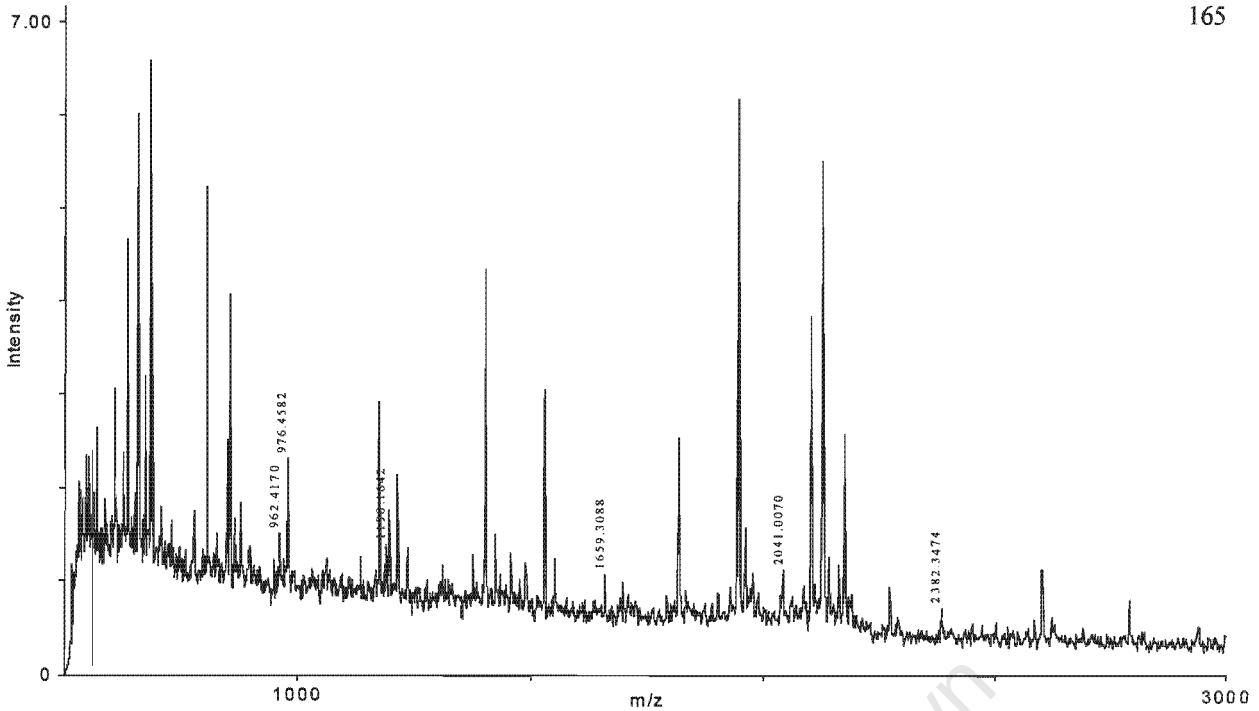

B

Rank	No. of Peptides Matched	Sequence Coverage (%)	Protein MW (Da)/pI	Species	SwissProt. Accession No.	Protein Name
(a) Peptide Mass Tolerance (+/-) 0.1 %, Min. No. of Peptides to Match (4)						
1	5/6	26%	25978 / 6.81	Mouse	P50540	Max Interacting Protein 1
2	5/6	21%	30859 / 4.91	Human	30313	Cytokeratin 8
3	4/6	18%	39079 / 9.74	Human	Q14093	Cylicin II
4	4/6	18%	24297 / 9.72	Human	7106840	HSPC225
5	4/6	17%	25500 / 9.81	Human	7020793	Unnamed protein product

C **The matched peptides (5/6) of 2D spot 33b (33 kDa/pI 8.6) covered 26% (60/228 AA's) of Mouse Max Interacting Protein (25.98 kDa/pI 6.81).**

m/z submitted	MH^+ matched	Delta %	start	end	Peptide Sequence	Modifications
962.4170	962.5536	-0.0142	42	49	(R)LQHSKPPR(R)	
976.4582	976.5692	-0.0114	136	142	(R)EQRFLKR(R)	
1190.1642	1190.6421	-0.0401	12	21	(R)LLEAAEFLER(R)	
2041.0070	2039.0933	0.0939	142	157	(K)RRLEQLQGPQEMERIR(M)	
2382.3474	2380.0563	0.0963	22	41	(R)RERECEHGYASSFPSMPSPR(L)	

1 unmatched mass: 1659.3088

The matched peptides (5/6) of 2D spot 33b (33 kDa/pI 8.6) cover 21% (61/279 AA's) of Human Cytokeratin 8 (30.86 kDa/pI 4.91).

m/z submitted	MH^+ matched	Delta %	start	end	Peptide Sequence	Modifications
962.4170	961.4954	0.0958	101	108	(K)TEISEINR(N)	
1190.1642	1190.6381	-0.0398	99	108	(R)TKTEISEINR(N)	
1659.3088	1660.8982	-0.0957	99	112	(R)TKTEISEINRNISR(L)	
2041.0070	2040.0586	0.0465	92	108	(K)HGDDLRRTKTEISEINR(N)	
2382.3474	2381.1659	0.0496	49	69	(R)SLDMDSIIAEVKAQYEDIANR(S)	
2382.3474	2383.1862	-0.0352	159	177	(R)AKQDMARQLREYQELMNVK(L)	2Met-ox

1 unmatched mass: 975.3977

Figure 6.11 : MS data and MS-fit search results for 2D spot 33b. A) The remaining peptide masses of MALDI peptide mass spectrum of trypsin digested 2D spot 33b (33 kDa/pI 8.6) unassigned to Mouse Voltage-Dependent Anion-Selective Channel. **B)** Database searches using the peptide masses shown in A, was performed with peptide mass error specified at (a) 0.1 % or and the 5 best matching entries has been shown. **C)** The best matching entries were Mouse Max Interacting Protein (25.98 kDa/pI 6.81) and Human Cytokeratin 8 (30.86 kDa/pI 4.91).

Spot 34Ec

The peptide mass spectrum obtained for trypsin digested spot 34Ec was displayed in Fig. 6.12(A). A total of 6 peptide masses specific for spot 34Ec, were determined in the MALDI-TOF experiment.

Searching the protein databases (SwissProt and NCBI) requiring a peptide mass error of less than 0.1 % and 0.05% retrieved the 5 top sequence entries listed in Fig. 6.12(B). At 0.1% mass error the 2 top ranking sequence entries were Human Tyrosine Kinase (39.87 kDa/pI 8.10) and Mouse Cathepsin K precursor (36.75 kDa/pI 8.62) which matched 4 of the 6 peptide masses submitted. The matched peptides displayed in Fig. 6.12(C), covered only 18% of Human Tyrosine Kinase (39.87 kDa/pI 8.10) and 15% (46/314 AA's) of the sequence of Matured Mouse Cathepsin K (35.01 kDa/pI 8.5). Of these only the matured form of Mouse Cathepsin K (35.01 kDa/pI 8.5) corresponded well with the observed MW (34 kDa) and pI (8.5) of spot 34Ec.

In conclusion the identification was ambiguous and thus requires further analysis by either MS/MS or Edman microsequencing to determine the identity of spot 34Ec.

A

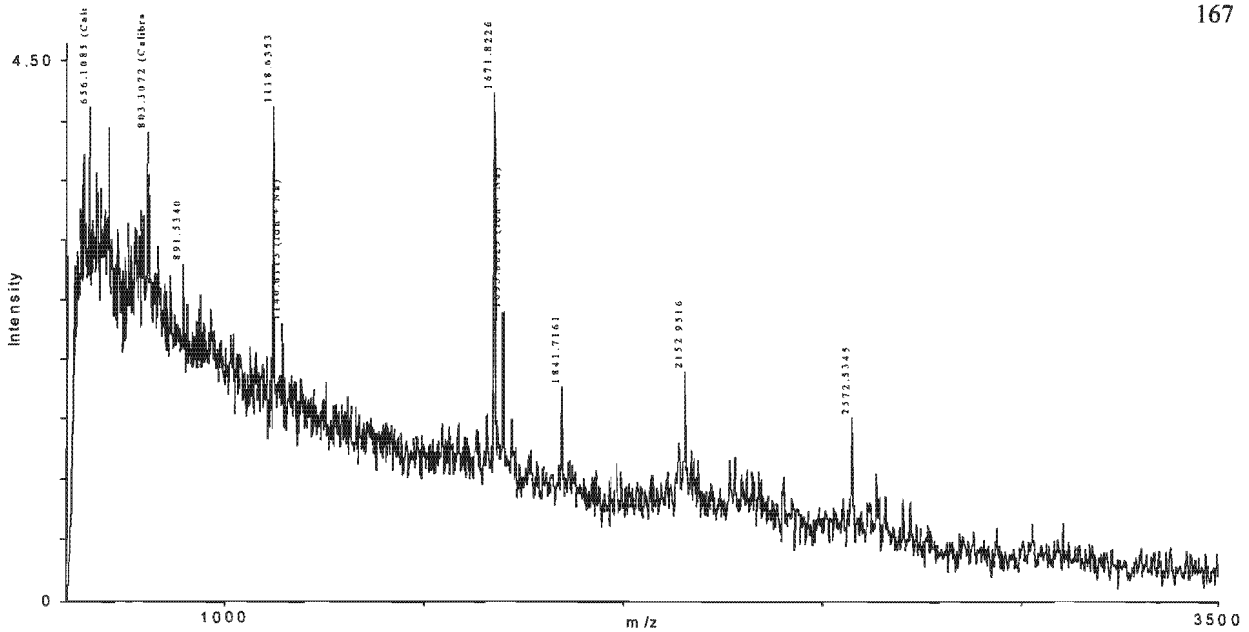

B

Rank	No. of Peptides Matched	Sequence Coverage (%)	Protein MW (Da)/pI	Species	SwissProt. Accession No.	Protein Name
(a) Peptide Mass Tolerance (+/-) 0.1 %, Min. No. of Peptides to Match (4)						
1	4/6	18%	39868 / 8.10	Human	5804911	Tyrosine Kinase
2	4/6	13%	36749 / 8.62	Mouse	P55097	Cathepsin K precursor
3	3/6	17%	31438 / 8.83	Rat	P20974	T-cell Ecto-ADP-Ribosyltransferase 2 precursor
4	3/6	15%	33684 / 9.64	Human	P51815	Zinc Finger protein 75
5	3/6	14%	39467 / 6.19	Human	4249644	Homer-2A protein
(b) Peptide Mass Tolerance (+/-) 0.05 %, Min. No. of Peptides to Match (3)						
1	3/6	15%	39868 / 8.10	Human	5804911	Tyrosine Kinase
2	3/6	16%	32003 / 5.18	Rat	56649	Myosin Heavy chain fragment
3	3/6	14%	31438 / 8.83	Rat	P20974	T-cell Ecto-ADP-Ribosyltransferase 2 precursor
4	3/6	11%	36749 / 8.62	Mouse	P55097	Cathepsin K precursor
5	3/6	8%	35132 / 5.96	Human	7022306	Unnamed protein product

C

The matched peptides (4/6) of 2D spot 32Lb (34 kDa/pI 8.5) covered 18% (46/314 AA's) of Human Tyrosine Kinase (39.87 kDa/pI 8.10).

m/z submitted	MH^+ matched	Delta %	start	end	Peptide Sequence	Modification
891.5340	891.3994	0.0151	51	58	(K)GNDGLCQK(L)	
1841.7161	1842.0125	-0.0161	75	89	(K)DAWEIPRESLKLEKK(L)	
2152.9516	2154.0442	-0.0500	90	108	(K)LGAGQFGEVWMATYNKHTK(V)	1Met-ox
2572.5345	2570.3032	0.0868	109	132	(K)VAVKTMKPGSMSVEAFLAEANVMK(T)	2Met-ox

2 unmatched masses : 1118.6353, 1671.8226

The matched peptides (4/6) of 2D spot 32Lb (34 kDa/pI 8.6) covered 15% (46/314 AA's) of Matured Mouse Cathepsin K (35.06 kDa/pI 8.50).

m/z submitted	MH^+ matched	Delta %	start	end	Peptide Sequence	Modification
891.5340	891.5304	0.0004	124	131	(K)KGYVTPVK(N)	
1671.8226	1671.7293	0.0056	315	329	(K)NNACGITNMASFPKM(-)	1Met-ox
1841.7161	1841.9087	-0.0105	291	305	(K)HWIIKNSWGESWGNK(G)	
2152.9516	2151.0736	0.0873	296	314	(K)NSWGESWGNKGYALLARNK(N)	

2 unmatched masses : 1118.6353, 2572.5345

Figure 6.12 : MS data and MS-fit search results for 2D spot 34Ec. A) MALDI peptide mass spectrum of Lys-C digested 2D spot 34Ec (34 kDa/pI 8.5). **B)** Database searches using the peptide masses shown in A, was performed with the peptide mass error specified at (a) 0.1 % or (b) 0.05 % and the 5 top matching entries has been shown. **C)** The best matching entries were Human Tyrosine Kinase (39.87 kDa/pI 8.10) and Matured Mouse Cathepsin K (35.06 kDa/pI 8.50). The matched peptides and sequence coverage has been shown.

Spot 74Lb

The peptide mass spectrum obtained for trypsin digested spot 74Lb was displayed in Fig. 6.13(A). A total of 14 peptide masses specific for spot 74Lb, were determined in the MALDI-TOF experiment.

Searching the protein databases (SwissProt and NCBI) requiring a peptide mass error of less than 0.1 % and 0.05% retrieved the 5 top sequence entries listed in Fig. 6.13(B). The highest ranking sequence entry was Mouse BiP precursor (72.42 kDa/pI 5.07) that matched 10 of the 14 peptide masses submitted under a peptide mass error of 0.013%, which was an extremely good match.

The matched peptides displayed in Fig. 6.13(C), covered 19% (126/655 AA's) of the sequence of Mouse BiP Precursor (72.42 kDa/pI 5.07). If the signal sequence (residues 1 to 19) was subtracted from the mass, then the matched peptides actually covered 20% (126/636 AA's) of the sequence of Matured Mouse BiP (70.47 kDa/pI 5.01). In addition the calculated Mw and pI of Mouse BiP (70.47 kDa/pI 5.01) was consistent with the observed Mw (74 kDa) and pI (5.1) of spot 74Lb, and served to confirm the identification unambiguously.

A

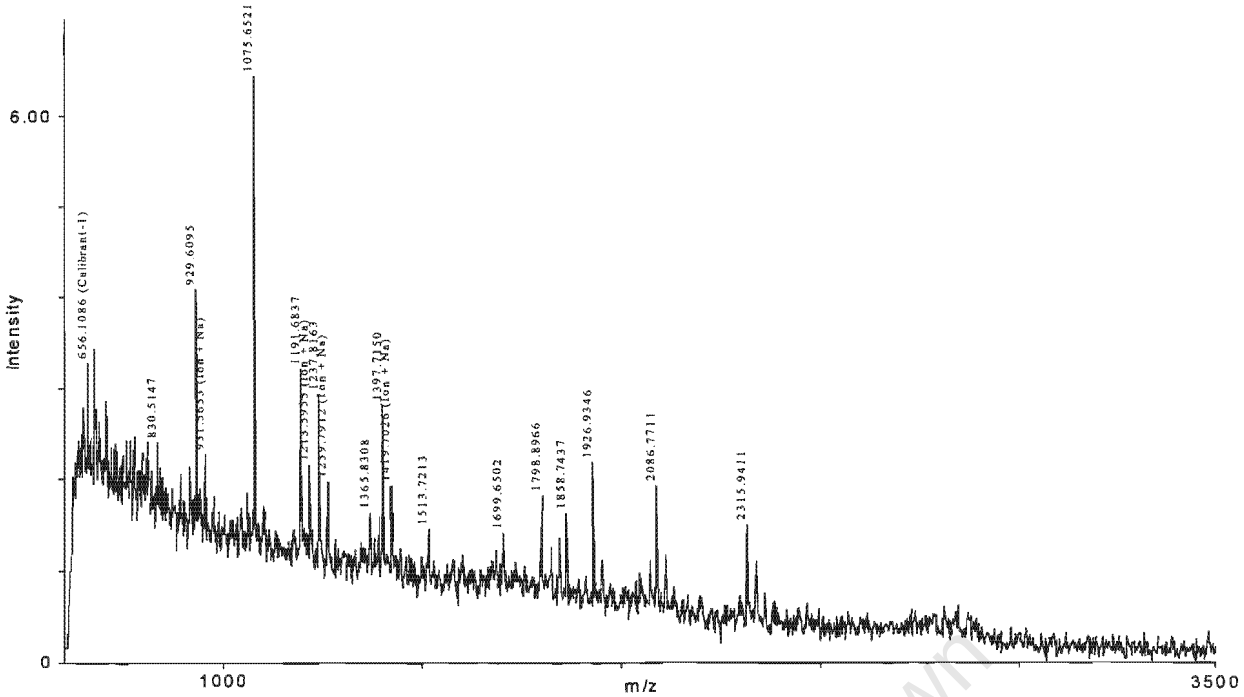

B

Rank	No. of Peptides Matched	Sequence Coverage (%)	Protein MW (Da)/pI	Species	SwissProt. Accession No.	Protein Name
(a) Peptide Mass Tolerance (+/-) 0.1 %, Min. No. of Peptides to Match (7)						
1	10/14	19%	72422 / 5.07	Mouse	P20029	BiP Glucose-regulated protein precursor (Grp 78)
2	10/14	19%	70931 / 5.22	Human	6470150	BiP protein
3	10/14	19%	72116 / 5.03	Human	P11021	BiP Glucose-regulated protein precursor (Grp 78)
4	7/14	18%	56574 / 8.60	Mouse	P35562	G-Protein activated potassium channel
5	8/14	12%	84032 / 5.64	Human	O75330	Hyaluronan mediated motility receptor (intracell)
(b) Peptide Mass Tolerance (+/-) 0.05 %, Min. No. of Peptides to Match (4)						
1	10/14	19%	72422 / 5.07	Mouse	P20029	BiP Glucose-regulated protein precursor (Grp 78)
2	10/14	19%	70931 / 5.22	Human	6470150	BiP protein
3	8/14	17%	72116 / 5.03	Human	P11021	BiP Glucose-regulated protein precursor (Grp 78)
4	4/14	10%	58778 / 8.39	Human	P49643	DNA Primase (large subunit)
5	4/14	5%	96583 / 8.18	Mouse	P35329	B-Cell Receptor

C **The matched peptides (10/14) of 2D spot 74Lb (74 kDa/pI 5.1) covered 20% (126/636 AA's) of Matured Mouse BiP (70.47 kDa/pI 5.01).**

m/z submitted	MH^+ matched	Delta %	start	end	Peptide Sequence	Modification
830.5147	830.4484	0.0080	282	288	(K)DNRAVQK(L)	
929.6095	929.5532	0.0061	289	295	(K)LRREVEK(A)	
1191.6837	1191.6374	0.0039	466	475	(K)VYEGERPLTK(D)	
1237.8163	1237.7632	0.0043	437	447	(K)LIPRNTVVPTK(K)	
1365.8308	1365.8582	-0.0020	437	448	(K)LIPRNTVVPTKK(S)	
1397.7150	1397.7892	-0.0053	623	634	(K)ELEEIVQPIISK(L)	
1798.8966	1798.9915	-0.0053	355	371	(K)SDIDEIVLVGGSTRIPK(I)	
1926.9346	1927.0864	-0.0079	354	371	(K)KSDIDEIVLVGGSTRIPK(I)	
2086.7711	2087.0409	-0.0129	558	574	(K)ERIDTRNELESYAYSLK(N)	
2315.9411	2316.1433	-0.0087	26	47	(K)EDVGTVVGIDLGTTYSCVGVFK(N)	
2315.9411	2316.2101	-0.0116	166	186	(K)VTHAVVTVPAYFNDAQRQATK(D)	

4 unmatched masses : 1075.6521, 1513.7213, 1699.6502, 1858.7437

Figure 6.13 : MS data and MS-fit search results for 2D spot 74Lb. **A)** MALDI peptide mass spectrum of trypsin digested 2D spot 74Lb (74 kDa/pI 5.1). **B)** Database searches using the peptide masses shown in A, was performed with the peptide mass error specified at (a) 0.1 % or (b) 0.05 % and the 5 top matching entries has been shown. **C)** The best matching entry was Mouse BiP (70.47 kDa/pI 5.01). The matched peptides and sequence coverage has been shown.

Observed 2-D Spots			Database Peptide Mass Identification		
Spot No.	MW (kDa)	pI (units)	Identified Proteins	MW (kDa)	pI (units)
Phago-Endosomes					
34Ec	34	8.5	Tyrosine Kinase	39.87	8.10
			Cathepsin-K	35.06	8.50
32Ec	32	8.4	Galectin-3 (MALDI-MS and Sequencing)	27.38	8.50
22Ec	22	8.5	Thioredixin Peroxidase 2	22.17	8.26
18Ec	18	8.5	Cofilin (Non-Muscle Isoform)	18.56	8.22
[illegible]					
32Lc	32	4.6	Annexin IV	35.87	5.32
22Lc	22	7.6	Superoxide Dismutase	22.22	7.30
18Lc	18	8.2	Vacuolar ATP Synthase E (fragment)	26.58	9.28
[illegible]					
74Lb	74	5.10	BiP (Hsp70 family member)	72	5.11
32Lb	32	8.4	Galectin-3 (MALDI-TOF only)	27.38	8.50
15Lb	15	9.4	Lysozyme C	14.96	9.47
55Eb	55	5.2	Dynamin - related	?	?
33b	33	8.6	Voltage-depend. Anion-selective Channel	30.75	8.62
14b	14	7.5	β-2 Microglobulin Precursor	13.82	7.80

Figure 6.14 : Tabulated list of the best matching sequences retrieved querying SwissProt and NCBI protein databases with the peptide mass maps obtained by the Maldi-TOF experiment. The identity of 56Eb is still being determined. Preliminary data suggest that it may be related to the GTPase Dynamin.

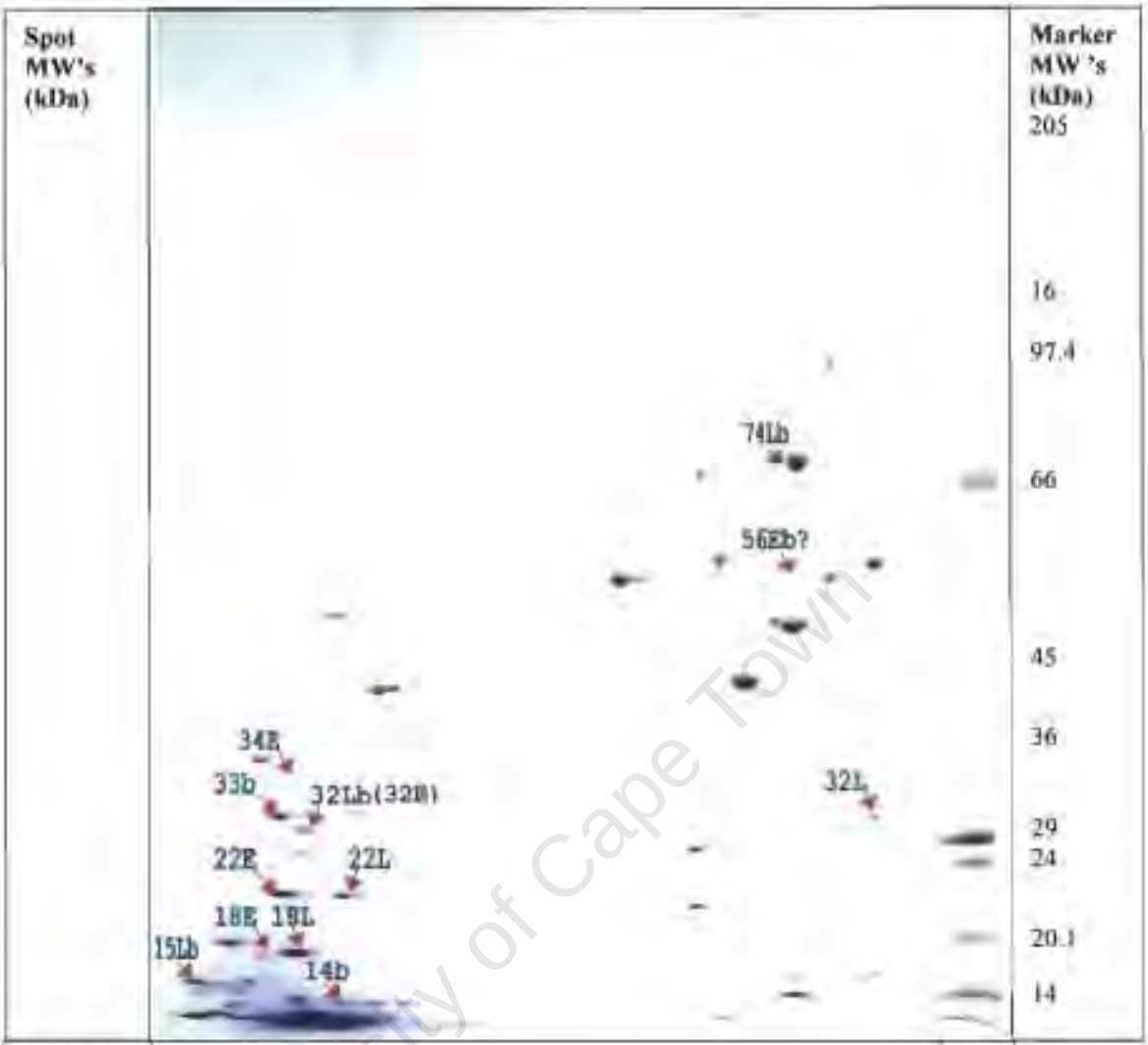

pH-Scale	9.5									4	Marker
Spot No.	74Lb	33b	32E	32L	22E	22L	34E	18E	18L	15Lb	14b
pI-value	5.1	8.5	8.4	4.6	8.6	7.6	8.6	8.5	8.2	9.4	7.3
Identity	BiP	PM-Porin	(fol-)	AnxIV	TrP2	SD	CatK	Cofilin	ATPe	LyzC	β2Mic

Figure 6.15 : Preparative 2-Dimensional gel of salt-washed/sonicated Membrane^{LF} used for Maldi-MS and Edman sequencing analysis. Proteins (1mg) of NaCl/Sonicated/NaCl treated Membrane^{LF} was loaded during reswelling of an IPG strip (pH 3-10 NL, 180mm) in sample buffer (8M urea, 2M Thiourea, 4% CHAPS, 2% pH 3-10 carrier ampholytes, 20mM Tris base, 30mM DTT). Isoelectric focusing was performed at 17°C until equilibrium (65 kVh). The second dimension was performed using a 5-13% gradient SDS-PAGE followed by coomassie staining.

6.4 CONCLUSION

MALDI-TOF peptide mass mapping and database searching has proved to be a rapid and sensitive method for screening of proteins separated by 2D-PAGE. However, tandem mass spectrometry (MS/MS) or Edman microsequencing is still required when an unambiguous identification is not possible.

Efficient electrophoretic protein separation methods, high performance mass spectrometers and bioinformatics can thus afford analysis of multiprotein complexes, regulatory pathways, and whole cell protein profiles, to understand cellular organisation.

The only protein spot that was analysed by both MALDI-MS and Edman microsequencing was 32Ec/32Lb, which was identified as galectin-3. The observation that galectin-3 was found compositionally enriched in phago-endosomes (32Ec, Chapter 5) and was bound specifically by X-linked lysosomes (32Lb, Chapter 3) in the binding assay, suggested a possible role in endocytosis. To test whether galectin-3 might function in fusion and/or targeting, anti-galectin-3 antibodies and thiodigalactoside (a specific substrate) were tested in cell-free fusion assays [Chapter 7].

CHAPTER 7
A POSSIBLE ROLE FOR GALECTIN-3 IN ENDOCYTOSIS

7.1 BACKGROUND

Lectins (bacterial, plant and animal) are a class of carbohydrate-binding proteins [378]. Animal lectins are involved in diverse functions such as protein folding and transport and cell-cell/matrix interactions [379]. The specific recognition of exposed or internally placed monosaccharides (e.g. galactose, mannose, sialic acid, and acetylated/ phosphorylated/sulphated derivatives) and multivalency are crucial for lectin function [380,381]. Lectins have been grouped according to similarities in their carbohydrate-recognition domains (CRDs) [382]. P-type CRDs selectively bind mannose 6-phosphate, S-type CRDs bind β-Galactosides, I-type CRDs bind sialic acid, and C-type CRDs bind a variety of sugars in a Ca^{2+}-dependent fashion. Galectin-3 is a β-galactose binding lectin. Galectin-3 belongs to the family of mammalian β-Galactoside-binding proteins known as galectins [383,384]. Each galectin contains a conserved carbohydrate-recognition domain (CRD) spanning about 130 amino acids [385].

Galectin-3 is unique in that it contains a large N-terminal domain, made up of sequence repeats rich in proline, glycine, tyrosine and glutamine and lacking charged or large hydrophobic residues. Galectin-3 is found in the cytoplasm, extracellularly and in the nucleus. Cell-surface galectin-3 is involved in cell adhesion and recognition [386], while nuclear galectin-3 is postulated to play a role in pre-mRNA splicing [387]. Although galectins are found in the cytoplasm and extracellularly, they do not exhibit a signal sequence for secretion and are in fact secreted by an unorthodox pathway which involves accumulation in aggregates underlying the plasma membrane followed by outward blebbing (known as ectocytosis) and release of extracellular vesicles [388]. The secretion of galectin-3 is dependent on determinants in the N-terminal domain, particularly residues 89-96 [389]. The leader sequence (residues 1-12) appears to direct translocation of

galectin-3 to the plasma membrane and the nucleus [390]. The N-terminal domain of galectin-3 contains nine proline-rich motifs, each containing at least one tyrosine and several glycine residues. These sequences are highly homologous to proline-rich domains present in annexins VII and XI, as implicated to play a role in self-aggregation and intracellular membrane traffic [391].

In this study, galectin-3 was found compositionally enriched in phago-endosomes (corroborated by a recent proteomic study [455] on phagosomes) and to bind specifically to X-linked lysosomes in the binding assay, suggestive of a possible role in endocytosis. To test whether galectin-3 may function in fusion and/or targeting, NH_2-terminal directed (Mac-2) and CRD-directed (CRD) antibodies and thiodigalactoside (a specific subsrate) were tested in cell-free fusion assays.

A novel biochemical assay was set up to investigate the fusion of highly purified paramagnetic latex bead-containing phagosomes with a mixed endosome/lysosome population of organelles. The assay was based on monitoring the transfer of HRP from endocytic organelles to phagosomes as a measure of fusion.

7.2 MATERIALS AND METHODS

7.2.1 Preparation of Acceptor Phagosomes

Hydrophilic bead phagosomes (45 min uptake, 15 min chase) were prepared as described [Section 4.2.4] up to step 13, except that the phagosomes were resuspended in Fusion/ Binding buffer (250 mM sucrose, 50 mM KCl, 0.5 mM EGTA, 20 mM Hepes-KOH, pH 7.4, 1 mM dithiothreitol, 1.5 mM $MgCl_2$, 1 mM PMSF, 0.1 mM Leupeptin, 1 μM Pepstatin) [44,104,327].

7.2.2 Preparation of Donor

Cells were washed twice in cold RPMI-BSA (RPMI 1640 medium, 0.1% BSA) before resuspension at 10 x 10^6 cells/ml in this buffer in a 100 ml Elenmeyer flask. The cell suspension was then warmed to 37°C for 15 minutes. At time zero, horse-radish peroxidase (HRP) was added at 1 mg/ml and the cells allowed to internalise the marker for 15 minutes. This filled early endosomes and lysosomes with HRP. After the incubation period, the cell suspension was made up to 50 ml with cold Hepes-Saline-BSA and the cells pelleted by centrifugation at 200g for 5 minutes at 4°C. The cells were then washed once with cold low pH buffer (150 mM NaCl, 20 mM Na-Acetate, pH 4.5), then twice with cold Hepes-Saline-BSA and lastly once with homogenisation buffer prior to homogenisation [Section 2.2.4]. The post-nuclear supernatant (PNS) was centrifuged at 15000g for 90 minutes at 4°C in a benchtop centrifuge (Beckman Instruments). The pellet was resuspended in Fusion buffer (5μℓ / 10^6 cells).

7.2.3 Preparation of Cytosol

Cytosol was prepared as described in Section 3.2.1.2.

7.2.4 *In vitro* Fusion Assay

30 µℓ Phagosome acceptor, 30 µℓ Fusion buffer (either with an ATP regenerating system or ATPγS) and 30 µℓ of cytosol and 5µℓ donor were mixed and incubated at 37°C in a water bath for the times indicated. The reaction was stopped by snap cooling on ice and then treated with 1M NaCl for 5 minutes on ice. The samples were overlaid onto 0.5 ml of chilled 25% sucrose and placed in a chilled magnetic concentrator for 2 min at 4°C. After magnetic concentration, the supernatant and sucrose were aspirated off and the pellet resuspended in 40µl 1% Triton X-100 in deionised water. The HRP content of the phagosomes was measured as described [Section 2.2.6.2].

To test the role of galectin-3, the fusion assays were performed with the following additions.

1) Thiodigalactoside (Sigma) - a specific substrate for galectin-3.

2) Mac-2 antibodies (kindly provided by Dr. Colin Hughes) - Rabbit monoclonal antibodies directed towards the N-terminus of galectin-3.

3) CRD antibodies (kindly provided by Dr. Colin Hughes) - polyclonal antibodies directed towards the C-terminal carbohydrate-recognition domain (CRD) of galectin-3.

7.2.5 Electron Microscopy of in-vitro Fusion Assays.

Samples (taken prior to phagosome isolation) of all fusion assays (performed as described in Section 7.2.4) were processed for electron microscopy (as described in Sections 4.2.2 and 4.2.3).

7.3 RESULTS

7.3.1 Preparation of phagosomes and endosomes/lysosomes

To study the fusion of organelles consisting of a mixture of endosomes/lysosomes with phagosomes, a cell-free in vitro fusion assay was established. The assay was based on monitoring the transfer of HRP from endocytic organelles to phagosomes as a measure of fusion. Cells were loaded with 0.8μm paramagnetic hydrophilic beads for 45 min. and chased for 15 min. The phagosomes were purified as described [Section 7.2.1]. The endocytic counterpart was produced by loading the cells with HRP for 15 min.

7.3.2 In vitro Fusion Assay

The fusion assay was performed by mixing on ice the phagosomes (45min uptake, 15min chase) with the mixed endosome/lysosome (15min pulse of HRP) population in an ATP-regenerating system and cytosol (3 mg/ml). After mixing, the reaction was warmed to 37°C for the indicated times. The maximal fusion signal corresponded to a transfer to phago-lysosomes of 5-10% of total HRP present in the reaction mixture. Such low *in-vitro* fusion efficiencies, ranging from 5-20%, are typical for *in vitro* fusion assays [460]. Fusion was expressed as a percentage of maximal fusion, to gauge the effects of drugs. Fusion was dependent on ATP, since addition of ATPγS inhibited fusion by about 90% [Figure 7.1B].

7.3.3 Effects of Thiodigalatoside (TDG) and anti Galectin-3 Antibodies

Addition of TDG (50 mM) to the full assay (ATP-regenerating, 60 min.) inhibited fusion by about 40% [Figure 7.1B]. Addition of Mac-2 (monoclonal antibody directed towards the N-terminus) or CRD (polyclonal antibody directed towards the carbohydrate recognition domain) galectin-3 antibodies inhibited fusion by approximately 80% and 50% respectively. The above results were suggestive of a role for galectin-3 in targeting/fusion.

7.3.4 Electron Micrographs of in-vitro Fusion Assays

Electron microscopic analysis of the fusion assays (aliquots taken before addition of 1M NaCl and phagosome isolation) performed under different conditons were displayed in Figure 7.2. From the electron micrographs the following observations were made. HRP-positive phago-lysosomes (i.e. fusion product, Ph^+) were observed for the full assay [Figure 7.2(B)]. For incubations performed at 4°C, phago-lysosomes (Ph^-) and HRP-positive lysosomes (Ly^+) were seen in close contact, but no fusion product was evident [Figure 7.2 (A)]. Similarly, no fusion product was seen for assays at 37°C in the presence of ATPγS or Mac-2 antibodies. Mass precipitation of organelles (including phagosomes and HRP-positive lysosomes) were observed due to the presence of anti-galectin-3 CRD antibody in the fusion assay (prior salt-extraction to break up the aggregates) [Figure 7.2(C)]. This might explain the high HRP measurement (50%) [Figure 7.1(B)], even though no HRP-positive fusion product was evident upon electon microscopic analysis.

A) Fusion as a Function of Time

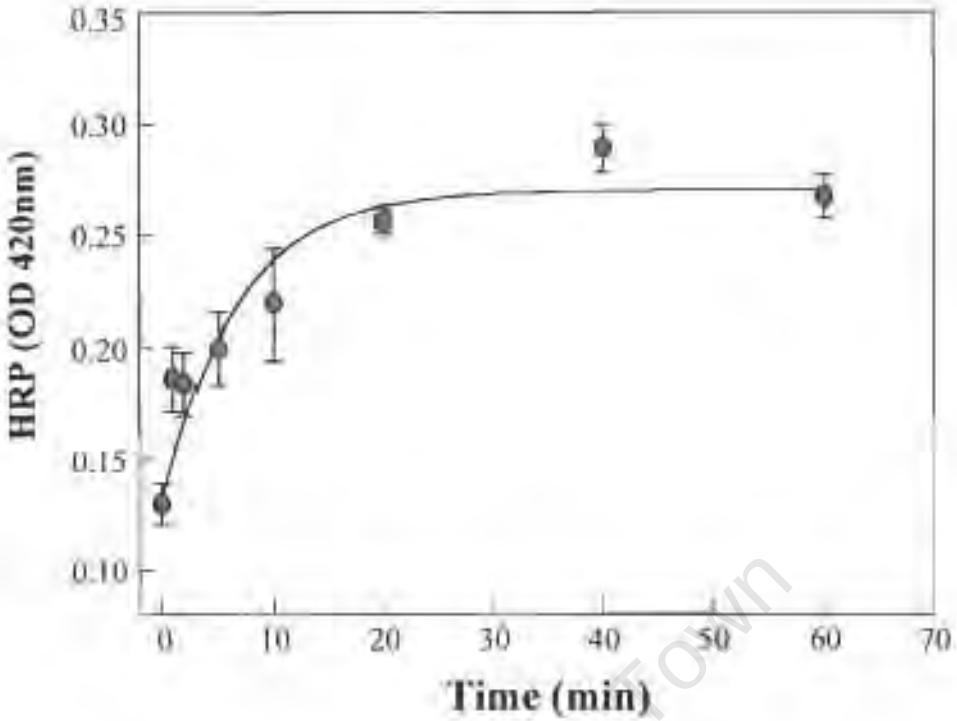

B) Effects of Drugs and anti-Galectin-3 Antibodies on Fusion

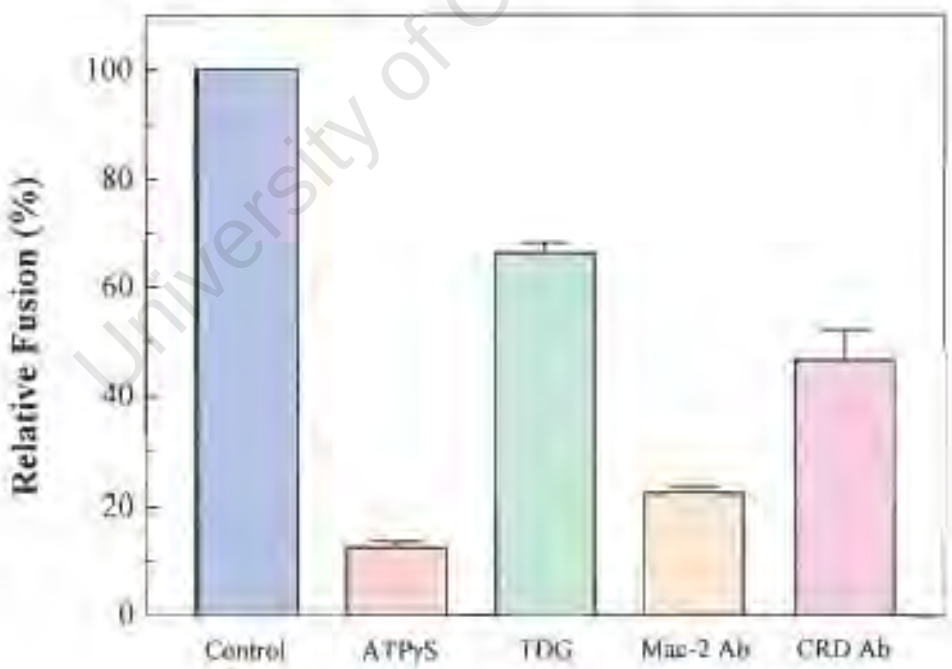

Figure 7.1 : In vitro Fusion Assay. **A)** The fusion assay was performed by mixing on ice the phagosomes (45min uptake, 15min chase) with the mixed endosome/lysosome (15min pulse of HRP) population in an ATP-regenerating system and cytosol (4 mg/ml). After mixing the reaction was warmed to 37°C for the indicated times. **B)** The fusion assay was performed (as in A) for 60 minutes as a control, or with ATPγS (2mM), thiodigalactoside (50mM), or anti-galectin-3 antibodies (Mac-2 or CRD) added before incubation. (Data from independent experiments)

7.4 DISCUSSION

Several fusion assays have been developed over the past decade [42-45,99,100b,401] to reconstitute endocytic and phagocytic fusion events *in vitro*. Fusion has been shown to be dependent on ATP, cytosol and temperature [44]. The requirement of individual components such as NSF [326,339], Rab 5 [239], Rab 7 [251], Syntaxin 8 [225], VAMP 8 [221], Syntaxin 7 [223,224a,b], Vamp 7 [218,220,224b], EEA [262], and various annexins [280-287,440-441] have been demonstrated.

In this study, a novel biochemical assay was set up to investigate the fusion of purified paramagnetic latex bead-containing phagosomes with a mixed endosome/lysosome population of organelles. ATPγS completely inhibited fusion and no detectable fusion occurred at 4 °C, as expected [44]. Previously, it has been demonstrated that aggregation of endosomes precedes fusion, and is dependent on ATP hydrolysis and cytosol [327].

Addition of TDG to the full assay inhibited fusion by about 40%. Addition of Mac-2 (monoclonal antibody directed towards the N-terminus) or CRD (polyclonal antibody directed towards the carbohydrate recognition domain) galectin-3 antibodies inhibited fusion by approximately 80% and 50% respectively. The mass precipitation of organelles observed due to the presence of anti-galectin-3 CRD antibody in the fusion assay (prior salt-extraction) might explain the high HRP measurement (50%), even though no HRP-positive fusion product was evident upon electon microscopic analysis. The above results were suggestive of a role for galectin-3 in targeting or fusion.

Galectin-3 contains nine proline-rich motifs homologous to proline-rich domains present in annexins VII and XI implicated to play a role in self-aggregation and intracellular membrane traffic [391]. The accumulation of galectin-3 aggregates underlying the plasma membrane followed by outward blebbing appears to be dependent on determinants in the N-terminal domain, particularly residues 89-96 [389]. The leader sequence (residues 1-12)

appears to direct translocation of galectin-3 to the plasma membrane and the nucleus [390]. Thus it is not inconceivable that galectin-3 aggregates are associated with the cytosolic face of endosomes as these organelles are derived from the plasma membrane.

Galectin-3 is structurally related to the annexins. Evidence has accumulated which indicates a role for the annexins in vesicle aggregation and fusion. Annexin VII promotes liposome fusion [287] and chromaffin granule aggregation in vitro [268], while annexin II is involved in aggregation and fusion of chromaffin granules with phospholipid vesicles and the PM and has also been suggested to play a role in homotypic early endosome fusion [281-283]. Different annexins are localised to particular organelles, for example annexins I, II, III and V are detected on early endosomes, annexin V is present on late endosomes, annexins I and II are distributed along the plasma membrane non-uniformly and annexin IV is enriched on matured phagosomes [441-442].

Considering the above, it is not inconceivable that galectin-3 also plays a similar role as the annexins in intracellular membrane traffic. A model was proposed [Figure 7.3] that postulates that galectin-3 may either target matured endosomes to lysosomes or possibly be directly involved in the fusion process after docking. The precise role of the lectin domain and the phospholipid binding domain of the annexins have not been clearly defined. It may be that other lectin families play similar roles, perhaps localised to particular organelles rich in specific lipids/glycolipids, to confer an extra level of fusion fidelity beyond the targeting specificity co-ordinated by the Velcro factors, Rabs and SNAREs.

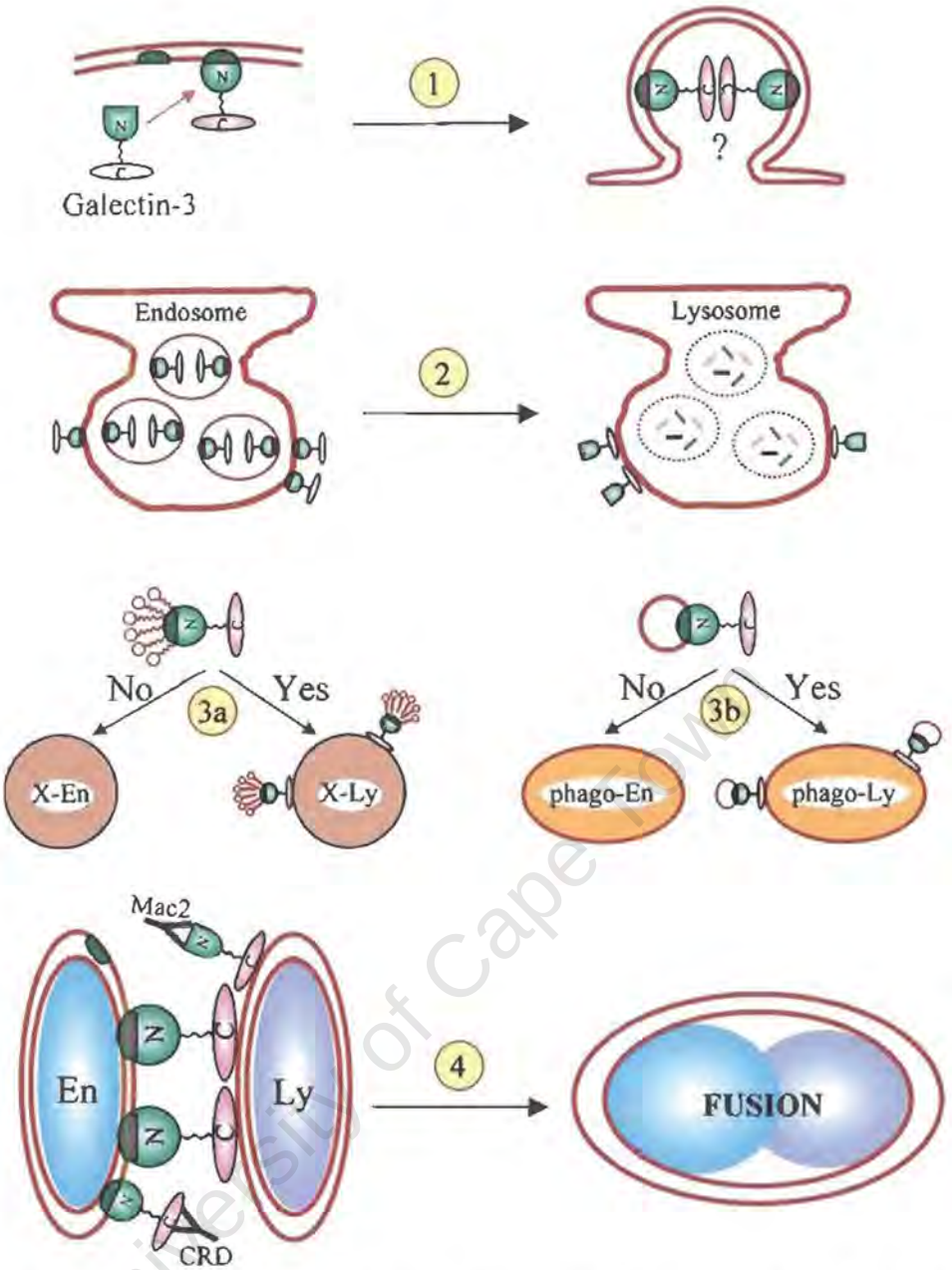

Figure 7.3 : Proposed model for explaining the present observations and for the possible role of Galectin-3 along the endocytic pathway. 1) Galectin-3 can undergo self-aggregation and appears to cause blebbing of the plasma membrane resulting in its release within extracellular vesicles [388]. **2)** By inference, galectin-3 could therefore also be involved in the formation of luminal vesicles of multivesicular bodies. The luminal galectin-3 might become degraded upon transfer to lysosomes. Thus, at steady state, endosomes would exhibit a higher abundance of galectin-3 as observed in this study. **3)** Since the N-terminal domain is required for translocation of galectin-3 to the plasma membrane [389,390], it possibly associates (either directly with lipid or via the interaction with a membrane protein ▬) with the plasma membrane and early endosomes via its N-terminal domain. Furthermore, since galectin-3 was found to specifically bind to X-lysosomes but not to X-endosomes, it is proposed that the C-terminal domain instead is involved in the association of galectin-3 with lysosomes. According to the diagram, solubilisation of galectin-3 by detergent (**3a**) or sonication in the presence of excess liposomes (**3b**), will free the C-terminal domain but, not the N-terminal domain. **4)** Galectin-3, specifically associated with matured endosomes, could target these to lysosomes and/or be directly involved in the fusion process after docking. Also shown are the interactions of Mac2 and CRD antibodies that may interfere with the binding of galectin-3, thereby preventing fusion as observed in this study.

CONCLUDING REMARKS

The observations of the present study could be divided into two aspects. First, it distinguished between factors that bound specifically to either early endosomes or to late endosomes/lysosomes. Second, it analysed differences in protein composition between these two compartments, in particular to determine the source of factors for which specific binding was observed.

Lysosomes especially bound galectin-3, ER-BiP and lysozyme C from fully soluble membrane donor, whereas both endosomes and lysosomes bound voltage-dependent anion-selective channel and β_2 microglobulin. Phago-endosomes were enriched for galectin-3, thioredoxin peroxidase II and cofilin, while phago-lysosomes were enriched for annexin IV, superoxide dismutase and vacuolar ATP synthase E subunit. With the exception of cofilin, these proteins form part of a list of proteins identified as associated with phagosomes in a major proteomic study [455].

This study concentrated only on the analysis of specific differences in binding and composition of endosomes and lysosomes. Since molecules that are known to be involved in targeting and fusion between organelles, such as synaptobrevins 1 and 2, various syntaxins and NSF, remain associated during all stages of organellar processing [450-452], were not expected to appear in the present binding assays as specifically binding factors. Other prominent fusion factors such as SNAREs (≈ 15-35 kDa, pI 4.5-9.5) and Rabs (≈ 24 kDa, pI 5-9) were probably present in the majority of visible proteins in the molecular weight range of 15-35 kDa, but were not analysed because their roles are well established. Additionally, it must be considered that salt-extraction probably removed factors peripherally associated with the cytosolic surface of the isolated organelles.

Due to the complex nature of the biochemical transformation of phagosomes, it is not possible to place all proteins identified in the context of phagosome processing into a simple conceptual framework. In depth functional and interactive analysis of the proteins would be required to bring about a better understanding of how they work in concert or tandem during phagocytic processing. However, based on the main observation of the this research, that galectin-3 bound preferentially to lysosomes while it displayed a higher steady-state abundance on early endosomes, a model could be proposed for the role of galectin-3 during interaction between these organelles [Figure 7.3].

REFERENCES

1. Palade G.E. (1975) *Intracellular aspects of the process of protein synthesis.* Science 189, 347-358.
2. Jamieson J.D., and Palade G.E. (1967) *Intracellular transport of secretory proteins in the pancreatic exocrine cell.* J. Cell Biol. 34, 577-615.
3. Dingwall C., and Laskey R. (1992) *The nuclear membrane.* Science 258, 942-947.
4. Pfaller R., Smythe C., and Newport J. (1991) *Assembly/disassembly of the nuclear envelope membrane: cell cycle-dependent binding of nuclear membrane vesicles to chromatin in vitro.* Cell 65, 209-217.
5. Wilson K., and Newport J. (1988) *A trypsin-sensitive receptor on membrane vesicles required for nuclear envelope formation in vitro.* J. Cell Biol. 107, 57-68.
6. Vigers G.P.A., and Lohka M.J. (1991) *A distinct vesicle population targets membranes and pore complexes to the nuclear envelope in Xenopus eggs.* J. Cell Biol. 112, 545-556.
7. Newport J., and Dunphy W. (1992) *Characterization of the membrane binding and fusion events during nuclear envelope assembly using purified components.* J. Cell Biol. 116, 295-306.
8. **{a}** Blobel G., and Dobberstein B (1975) *Transfer of proteins across membranes.* J. Cell Biol. 67, 835-862.
   {b} Ellgaard L., Molinari M., and Helenius A. (1999) *Setting the standards: quality control in the secretory pathway.* Science 286, 1882-1888.
9. Tisdale E.J., Plutner H., Matteson J., and Balch W.E. (1997) *p53/58 binds COPI and is required for selective transport through the early secretory pathway* J. Cell Biol. 137, 581-593.
10. Cosson P., and Letourneur F. (1994) *Coatomer interaction with di-lysine endoplasmic reticulum retention motifs.* Science 263, 1629-1631.
11. Jackson M.R., Nilsson T., and Peterson P.A. (1993) *Retrieval of transmembrane proteins to the endoplasmic reticulum.* J. Cell Biol. 121, 317-333.
12. Lewis M.J., and Pelham H.R (1990) *A human homologue of the yeast HDEL receptor.* Nature 348, 162-163.
13. Rothman J.E., and Orci L. (1992) *Molecular dissection of the secretory pathway.* Nature 355, 409-415.
14. **{a}** Martinez-Menarguez J.A., Geuze H.J., Slot J.W., and Klumperman J. (1999) *Vesicular tubular clusters between the ER and Golgi mediate concentration of soluble secretory proteins by exclusion from COPI-coated vesicles.*Cell 98, 81-90.

{b} Gonzales L.Jr., and Scheller R.H. (1999) *Regulation of membrane trafficking: structural insights from a Rab/effector complex.* Cell 96, 755-758.

15. Presley J.F., Cole N.B., Schroer T.A., Hirschberg K., Zaal K.J.M., and Lippincott-Schwartz J. (1997) *ER-to-Golgi transport visualized in living cells.* Nature 389, 81-85.

16. Weisz O.A., Swift A.M., and Machamer C.E. (1993) *Oligomerization of a membrane protein correlates with its retention in the Golgi complex.* J. Cell Biol. 122, 1185-1196.

17. Munro S. (1991) *Sequences within and adjacent to the transmembrane segment of alpha-2,6-sialyltransferase specify Golgi retention.* EMBO J. 10, 3577-3588.

18. **{a}** Orci L., Stamnes M., Ravazzola M., Amherdt M., Perrelet A., Sollner T.H., and Rothman J.E. (1997) *Bidirectional transport by distinct populations of COPI-coated vesicles.* Cell 90, 335-349.

{b} Allan B.B., and Balch W.E. (1999) *Protein sorting by directed maturation of Golgi compartments.* Science 285, 6-9

19. Griffiths G., and Simons K. (1986) *The trans Golgi network: sorting at the exit site of the Golgi complex.* Science 234, 438-444.

20. Herman B., and Albertini D.F. (1984) *A time-lapse video image intensification analysis of cytoplasmic organelle movements during endosome translocation.* J. Cell Biol. 98, 565-576.

21. Griffiths G., Back R., and Marsh M. (1989) *A quantitative analysis of the endocytic pathway in baby hamster kidney cells.* J. Cell Biol. 109, 2703-2720.

22. Pearse B.M, and Bretscher M.S. (1981) *Membrane recycling by coated vesicles.* Ann. Rev. Biochem. 50, 85-101.

23. Anderson R.G.W., and Kaplan J. (1983) *Receptor-mediated endocytosis.* Modern Cell Biol. 1, 1-52

24. Goldstein J.L., Anderson R.G.W., and Brown M.S. (1979) *Coated pits, coated vesicles, and receptor-mediated endocytosis.* Nature 279, 679-685.

25. van Renswoude J., Bridges K.R., Harford J.B., and Klausner R.D. (1982) *Receptor-mediated endocytosis of transferrin and the uptake of fe in K562 cells: identification of a nonlysosomal acidic compartment.* Proc. Natl. Acad. Sci. USA 79, 6186-6190.

26. Carpenter G., and Cohen S. (1976) *^{125}I-labeled epidermal growth factor. Binding, internalization, and degradation in human fibroblasts.* J. Cell Biol. 71, 159-171.

27. Steinman R.M., Mellman I.S., Muller W.A., and Cohn Z.A. (1983) *Endocytosis and the recycling of plasma membrane.* J. Cell Biol. 96, 1-27.

28. Gonnella P.A., and Neutra M.R. (1984) *Membrane-bound and fluid-phase macromolecules enter separate prelysosomal compartments in absorptive cells of suckling rat ileum.* J. Cell Biol. 99, 909-917.

29. Obar R.A., Collins C.A., Hammarback J.A., Shpetner H.S., and Vallee R.B. (1990) *Molecular cloning of the microtubule-associated mechanochemical enzyme dynamin reveals homology with a new family of GTP-binding proteins.* Nature 347, 256-261.

30. van der Bliek A.M., and Meyerowitz E.M. (1991) *Dynamin-like protein encoded by Drosophila shibire gene associated with vesicular traffic.* Nature 351, 411-414.

31. Chen M.S., Obar R.A., Schroeder C.C., Austin T.W., Poodry C.A., Wadsworth S.C., and Vallee R.B. (1991) *Multiple forms of dynamin are encoded by shibire, a Drosophila gene involved in endocytosis.* Nature 351, 583-586.

32. Kosaka T., and Ikeda K. (1983) *Possible temperature-dependent blockage of synaptic vesicle recycling induced by a single gene mutation in Drosophila.* Neurobiol. 14, 207-225.

33. Tsuruhara T., Koenig J.H., and Ikeda K. (1990) *Synchronized endocytosis studied in the oocyte of a temperature-sensitive mutant of Drosophila melanogaster.* Cell Tissue Res. 259, 199-207.

34. Damke H., Baba T., Warnock D.E., and Schmid S.L. (1994) *Induction of mutant dynamin specifically blocks endocytic coated vesicle formation.* J. Cell Biol. 127, 915-934.

35. Hinshaw J.E., and Schmid S.L. (1995) *Dynamin self-assembles into rings suggesting a mechanism for coated vesicle budding.* Nature 374, 190-192.

36. Takei K., McPherson P.S. Schmid S.L., and De Camilli P. (1995) *Tubular membrane invaginations coated by dynamin rings are induced by GTP-γS in nerve terminals.* Nature 374, 186-190.

37. Sever S., Muhlberg A.B., and Schmid S.L. (1999) *Impairment of dynamin's GAP domain stimulates receptor-mediated endocytosis.* Nature 398, 481-486.

38. Schlossman D.M., Schmid S.L., Braell W.A., and Rothman J.E. (1984) *An enzyme that removes clathrin coats: purification of an uncoating ATPase.* J. Cell Biol. 99, 723-734.

39. Tycko B., and Maxfield F.R. (1982) *Rapid acidification of endocytic vesicles containing alpha 2-macroglobulin.* Cell 28, 643-651.

40. Wall D.A., Wilson G., and Hubbard A.L. (1980) *The galactose-specific recognition system of mammalian liver: the route of ligand internalization in rat hepatocytes.* Cell 21, 79-93.

41. Geuze H.J., Slot J.W., Strous G..J., Lodish H.F., and Schwartz A.L. (1983) *Intracellular site of asialoglycoprotein receptor-ligand uncoupling: double-label immunoelectron microscopy during receptor-mediated endocytosis.* Cell 32, 277-287.

42. Gruenberg J.E., and Howell K.E. (1986) *Reconstitution of vesicle fusions occurring in endocytosis with a cell-free system.* EMBO J. 5, 3091-3101.

43. Braell W.A. (1987) *Fusion between endocytic vesicles in a cell-free system.* Proc. Natl. Acad. Sci. USA 84, 1137-1141.

44. Diaz R., Mayorga L., and Stahl P. (1988) *In vitro fusion of endosomes following receptor-mediated endocytosis.* J. Biol. Chem. 263, 6093-6100.

45. Woodman P.G., and Warren G. (1988) *Fusion between vesicles from the pathway of receptor-mediated endocytosis in a cell-free system.* Eur. J. Biochem. 173, 101-108.

46. Mellman I., Fuchs R., and Helenius A. (1986) *Acidification of the endocytic and exocytic pathways.* Annu. Rev. Biochem. 55, 663-700.

47. Tycko B., Keith C.H., and Maxfield F.R. (1983) *Rapid acidification of endocytic vesicles containing asialoglycoprotein in cells of a human hepatoma line.* J. Cell Biol. 97, 1762-1776.

48. Davis C.G., Goldstein J.L., Südhof T.C., Anderson R.G., Russell D.W., and Brown M.S. (1987) *Acid-dependent ligand dissociation and recycling of LDL receptor mediated by growth factor homology region.* Nature 326, 760-765.

49. Linderman J.J., and Lauffenburger D.A. (1988) *Analysis of intracellular receptor/ligand sorting in endosomes.* J. Theor. Biol. 132, 203-245.

50. Marsh M., Griffiths G., Dean G.E., Mellman I., and Helenius A., (1986) *Three-dimensional structure of endosomes in BHK-21 cells.* Proc. Natl. Acad. Sci. USA 83, 2899-2904.

51. Mueller S.C., and Hubbard A.L. (1986) *Receptor-mediated endocytosis of asialoglycoproteins by rat hepatocytes: receptor-positive and receptor-negative endosomes.* J. Cell Biol. 102, 932-942.

52. Gonatas N.K., Stieber A., Hickey W.F., Herbert S.H., and Gonatas J.O. (1984) *Endosomes and Golgi vesicles in adsorptive and fluid phase endocytosis.* J. Cell Biol. 99, 1379-1390.

53. Gruenberg J., Griffiths G., and Howell K.E. (1989) *Characterization of the early endosome and putative endocytic carrier vesicles in vivo and with an assay of vesicle fusion in vitro.* J. Cell Biol. 108, 1301-1316.

54. Stoscheck C.M., and Carpenter G. (1984) *Down regulation of epidermal growth factor receptors: direct demonstration of receptor degradation in human fibroblasts.* J. Cell Biol. 98, 1048-1053.

55. Ciechanover A., Schwartz A.L., and Lodish H.F. (1983) *The asialoglycoprotein receptor internalizes and recycles independently of the transferrin and insulin receptors.* Cell 32, 267-275.

56. Harding C., Heuser J., and Stahl P. (1983) *Receptor-mediated endocytosis of transferrin and recycling of the transferrin receptor in rat reticulocytes.* J. Cell Biol. 87, 329-339.

57. Hopkins C.R., and Trowbridge I.S. (1983) *Internalization and processing of transferrin and the transferrin receptor in human carcinoma A431 cells.* J. Cell Biol. 97, 508-521.

58. Mellman I., Plutner H., and Ukkonen P.(1984) *Internalization and rapid recycling of macrophage Fc receptors tagged with monovalent antireceptor antibody: possible role of a prelysosomal compartment.* J. Cell Biol. 98, 1163-1169.

59. Oka J.A., Weigel P.H. (1983) *Recycling of the asialoglycoprotein receptor in isolated rat hepatocytes. Dissociation of internalized ligand from receptor occurs in two kinetically and thermally distinguishable compartments.* J. Biol. Chem. 258, 10253-10262.

60. Schmid S.L., Fuchs R., Male P., and Mellman I. (1988) *Two distinct subpopulations of endosomes involved in membrane recycling and transport to lysosomes.* Cell 52, 73-83.

61. Wall D.A., and Hubbard A.L. (1985) *Receptor-mediated endocytosis of asialoglycoproteins by rat liver hepatocytes: biochemical characterization of the endosomal compartments.* J. Cell Biol. 101, 2104-2112.

62. Griffiths G., Hoflack B., Simons K., Mellman I., and Kornfeld S. (1988) *The mannose 6-phosphate receptor and the biogenesis of lysosomes.* Cell 52, 329-341.

63. Woods J.W., Goodhouse J., and Farquhar M.G. (1989) *Transferrin receptors and cation-independent mannose-6-phosphate receptors deliver their ligands to two distinct subpopulations of multivesicular endosomes.* Eur. J.Cell Biol. 50,132-143.

64. Baenziger J., and Fiete D. (1986) *Separation of two populations of endocytic vesicles involved in receptor-ligand sorting in rat hepatocytes.* J. Biol. Chem. 261, 7445-7454.

65. Yamashiro D., and Maxfield F.R. (1987) *Acidification of morphologically distinct endosomes in mutant and wild-type Chinese hamster ovary cells.* J. Cell Biol. 105, 2723-2733.

66. Murphy R.F. (1991) *Maturation models for endosome and lysosome biogenesis.* Trends Cell Biol. 1, 77-82.

67. Stoorvogel W., Strous G.J., Geuze H.J., Oorschot V., and Schwartz A.L. (1991) *Late endosomes derive from early endosomes by maturation.* Cell 65, 417-427.

68. Dunn K.W., and Maxfield F.R. (1992) *Delivery of ligands from sorting endosomes to late endosomes occurs by maturation of sorting endosomes.* J. Cell Biol. 117, 301-310.

69. Aniento F., Emans N., and Gruenberg J. (1993) *Cytoplasmic dynein-dependent vesicular transport from early to late endosomes.* J. Cell Biol. 123, 1373-1387.

70. Griffiths G., and Gruenberg J. (1991) *The arguments for pre-existing early and late endosomes.* Trends Cell Biol. 1, 5-9.

71. Racoosin E.L., and Swanson J.A. (1993) *Macropinosome maturation and fusion with tubular lysosomes in macrophages.* J. Cell Biol. 121, 1011-1020.

72. Thilo L., Stroud E., and Haylett T. (1995) *Maturation of early endosomes and vesicular traffic to lysosomes in relation to membrane recycling.* J. Cell Sci. 108, 1791-1803.

73. Hirsch J.G. (1962) *Cinemicrophotographic observations on granule lysis in Polymorphonuclear Leucocytes.* J. Exp. Med. 116, 827-833.

74. Pastan I., and Willingham W.C. (1981) *Journey to the center of the cell: role of the receptosome.* Science 214, 504-509.

75. Herman B., and Albertini D.F. (1984) *A time-lapse video image intensification analysis of cytoplasmic organelle movements during endosome translocation.* J. Cell Biol. 98, 565-576.

76. Parton R.G., Simons K., and Dotti C.G. (1992) *Axonal and dendritic endocytic pathways in cultured neurons.* J. Cell Biol. 119, 123-137.

77. DeBrabander M., Nuydens R., Geerts H., and Hopkins C. (1988) *Dynamic behaviour of the transferrin receptor followed in living epidermoid carcinoma (A431) cells with nanovid microscopy.* Cell Motil. Cytoskeleton 9, 30-47.

78. Bomsel M., Parton R., Kuznetsov S.A., Schroer T.A., and Gruenberg J. (1990) *Microtubule- and motor-dependent fusion in vitro between apical and basolateral endocytic vesicles from MDCK cells.* Cell 62, 719-731.

79. Kuznetsov S.A., Langford G.M., and Weiss D.G. (1992) *Actin-dependent organelle movement in squid axoplasm.* Nature 356, 722-725.

80. Matteoni R., and Kreis T.E. (1987) *Translocation and clustering of endosomes and lysosomes depends on microtubules.* J. Cell Biol. 105, 1253-1265.

81. Swanson J., Bushnell A., and Silverstein S.C. (1987) *Tubular lysosome morphology and distribution within macrophages depend on the integrity of cytoplasmic microtubules.* Proc. Nat. Acad. Sci. USA 84, 1921-1925.

82. Scheel J., Matteoni R., Ludwig T., Hoflack B., and Kreis T.E. (1990) *Microtubule depolymerization inhibits transport of cathepsin D from the Golgi apparatus to lysosomes.* J. Cell Sci. 96, 711-720.

83. Mithieux G., and Rousset B. (1989) *Identification of a lysosome membrane protein which could mediate ATP-dependent stable association of lysosomes to microtubules.* J. Biol. Chem. 264, 4664-4668.

84. Schroer T.A., Schnapp B.J., Reese T.S., and Sheetz M.P. (1988) *The role of kinesin and other soluble factors in organelle movement along microtubules.* J. Cell Biol. 107, 1785-1792.

85. Schroer T.A., Steuer E.R., and Sheetz M.P. (1989) *Cytoplasmic dynein is a minus end-directed motor for membranous organelles.* Cell 56, 937-946.

86. Wolkoff A.W., Klausner R.D., Ashwell G., and Harford J. (1984) *Intracellular segregation of asialoglycoproteins and their receptor: a prelysosomal event subsequent to dissociation of the ligand-receptor complex.* J.Cell Biol.98,375-381.

87. Kolset S.O., Tolleshaug H., and Berg T. (1979) *The effects of colchicine and cytochalasin B on uptake and degradation of asialo-glycoproteins in isolated rat hepatocytes.* Exp. Cell Res. 122, 159-167.

88. Clarke B.L., and Weigel P.H. (1989) *Differential effects of leupeptin, monensin and colchicine on ligand degradation mediated by the two asialoglycoprotein receptor pathways in isolated rat hepatocytes.* Biochem. J. 262, 277-284.

89. Kaufman S.S., Blain P.L., Park J.H.Y., and Tuma D.J. (1990) *Altered role of microtubules in asialoglycoprotein trafficking in developing liver.* Am. J. Physiol. 258, G129-137.

90. Goltz J.S., Wolkoff A.W., Novikoff P.M., Stockert R.J., and Satir P. (1992) *A role for microtubules in sorting endocytic vesicles in rat hepatocytes.* Proc. Natl. Acad. Sci. USA 89, 7026-7030.

91. Oda H., Stockert R.J., Collins C., Wang H., Novikoff P.M., Satir P., and Wolkoff A.W. (1995) *Interaction of the microtubule cytoskeleton with endocytic vesicles and cytoplasmic dynein in cultured rat hepatocytes.* J. Biol. Chem. 270, 15242-15249.

92. Gill S.R., Schroer T.A., Szilak I., Steuer E.R., Sheetz M.P., and Cleveland D.W. (1991) *Dynactin, a conserved, ubiquitously expressed component of an activator of vesicle motility mediated by cytoplasmic dynein.* J. Cell Biol. 115, 1639-1650.

93. Paschal B.M., Holzbaur E.L.F., Pfister K.K., Clark S., Meyer D.I., and Vallee R.B. (1993) *Characterization of a 50-kDa polypeptide in cytoplasmic dynein preparations reveals a complex with p150GLUED and a novel actin.* J. Biol. Chem. 268, 15318-15323.

94. **{a}** Schroer T.A. (2000) *Motors, clutches, and brakes for membrane traffic: A commemorative review in honor of Thomas Kreis.* Traffic 1, 3-10.
{b} Tuxworth R.I., and Titus M.A. (2000) *Unconventional myosins: Anchors in the membrane traffic relay.* Traffic 1, 11-18.

95. Parton R.G., Schrotz P., Bucci C., and Gruenberg J. (1992) *Plasticity of early endosomes.* J. Cell Sci. 103, 335-348.

96. Scheel J., and Kreis T.E. (1991) *Motor protein independent binding of endocytic carrier vesicles to microtubules in vitro.* J. Biol. Chem. 266, 18141-18148.

97. Roederer M., Barry J.R., Wilson R.B., and Murphy R.F. (1990) *Endosomes can undergo an ATP-dependent density increase in the absence of dense lysosomes.* Eur. J. Cell Biol. 51, 229-234.

98. Mullock B.M., Branch W.J., van Schaik M., Gilbert L.K., and Luzio J.P. (1989) *Reconstitution of an endosome-lysosome interaction in a cell-free system.* J. Cell Biol. 108, 2093-2099.

99. Mullock B.M., Perez J.H., Kuwana T., Gray S.R., and Luzio J.P. (1994) *Lysosomes can fuse with a late endosomal compartment in a cell-free system from rat liver.* J. Cell Biol. 126, 1173-1182.

100. **{a}** Ferris A.L., Brown J.C., Park R.D., and Storrie B. (1987) *Chinese hamster ovary cell lysosomes rapidly exchange contents.* J. Cell Biol. 105, 2703-2712.
{b} Ward D.M., Leslie J.D., and Kaplan J. (1997) *Homotypic lysosome fusion in macrophages: analysis using an in vitro assay.* J. Cell Biol. 139, 665-673.

101. Greenberg S., and Silverstein S.C. (1993) Phagocytosis. In: W.E. Paul (ed.): Fundamental Immunology, 941-964. Raven Press. New York.

102. Lang T., de Chastellier C., Ryter A., and Thilo L. (1988) *Endocytic membrane traffic with respect to phagosomes in macrophages infected with non-pathogenic bacteria: phagosomal membrane acquires the same composition as lysosomal membrane.* Eur. Cell Biol. 46, 39-50.

103. Hart P.D., and Young M.R. (1991) *Ammonium chloride, an inhibitor of phagosome-lysosome fusion in macrophages, concurrently induces phagosome-endosome fusion, and opens a novel pathway: studies of a pathogenic mycobacterium and a nonpathogenic yeast.* J. Exp. Med. 174, 881-889.

104. Mayorga L.S., Bertini F., and Stahl P.D. (1991) *Fusion of newly formed phagosomes with endosomes in intact cells and in a cell-free system.* J. Biol. Chem. 266, 6511-6517.

105. Pitt A., Mayorga L.S., Schwartz A.L., and Stahl P.D. (1992) *Transport of phagosomal components to an endosomal compartment.* J. Biol. Chem. 267, 126-132.

106. Russell D.G., Dant J., and Sturgill-Koszycki S. (1996) *Mycobacterium avium- and Mycobacterium tuberculosis-containing vacuoles are dynamic, fusion-competent vesicles that are accessible to glycosphingolipids from the host cell plasmalemma.* J. Immunol. 156, 4764-4773.

107. Clemens D.L., and Horwitz M.A. (1996) *The Mycobacterium tuberculosis phagosome interacts with early endosomes and is accessible to exogenously administered transferrin.* J. Exp. Med. 184, 1349-1355.

108. de Chastellier C., Lang T., and Thilo L. (1995) *Phagocytic processing of the macrophage endoparasite, Mycobacterium avium, in comparison to phagosomes which contain Bacillus subtilis or latex beads.* Eur. J. Cell Biol. 68, 167-182.

109. de Chastellier C., Thilo L. (1997) *Phagosome maturation and fusion with lysosomes in relation to surface property and size of the phagocytic particle.* Eur. J. Cell Biol. 74, 49-62.

110. Rothman J.E. (1992) *Purification of Golgi cisternae-derived non-clathrin-coated vesicles, NSF, SNAPs, coat protomers.* Methods Enzym. 219, 286-337.

111. Novick P., Field C., Schekman R. (1980) *Identification of 23 complementation groups required for post-translational events in the yeast secretory pathway.* Cell 21, 205-215.

112. Schekman R. (1992) *Genetic and biochemical analysis of vesicular traffic in yeast.* Curr. Opin. Cell Biol. 4, 587-592.

113. Novick P., Ferro S., Schekman R. (1981) *Order of events in the yeast secretory pathway.* Cell 25, 461-469.

114. Balch W.E., Dunphy W.G., Braell A.W., and Rothman J.E. (1984) *Reconstitution of the transport of protein between successive compartments of the Golgi measured by the coupled incorporation of N-acetylglucosamine.* Cell 39, 405-416.

115. Fries E., and Rothman J.E. (1980) *Transport of vesicular stomatitis virus glycoprotein in a cell-free extract.* Proc. Natl. Acad. Sci. USA 77, 3870-3874.

116. Dunphy W.G., Fries E., Urbani L.J., and Rothman J.E. (1981) *Early and late functions associated with the Golgi apparatus reside in distinct compartments.* Proc. Natn. Acad. Sci. USA 78, 7453-7457.

117. Rothman J.E., Urbani L.J., and Brands R. (1984) *Transport of protein between cytoplasmic membranes of fused cells: correspondence to processes reconstituted in a cell-free system.* J. Cell Biol. 99, 248-271.

118. Braell W.A., Balch W.E., Dobbertin D.C., and Rothman J.E. (1984) *The glycoprotein that is transported between successive compartments of the Golgi in a cell-free system resides in stacks of cisternae.* Cell 39, 511-524.

119. Balch W.E., Glick B.S., and Rothman J.E. (1984) *Sequential intermediates in the pathway of intercompartmental transport in a cell-free system.* Cell 39, 525-536.

120. Orci L., Glick B.S., and Rothman J.E. (1986) *A new type of coated vesicular carrier that appears not to contain clathrin: its possible role in protein transport within the Golgi stack.* Cell 46, 171-184.

121. Pearse B.M.F., and Robinson M.S.A. (1990) *Clathrin, adaptors, and sorting.* Rev. Cell Biol. 6, 151-171.

122. Melancon P., Glick B.S., Malhotra V., Weidman P.J., Serafini T., Gleason M.L., Orci L., and Rothman J.E. (1987) *Involvement of GTP-binding "G" proteins in transport through the Golgi stack.* Cell 51, 1053-1062.

123. Malhotra V., Orci L., Glick B.S., Block M.R., and Rothman J.E. (1988) *Role of an N-ethylmaleimide-sensitive transport component in promoting fusion of transport vesicles with cisternae of the Golgi stack.* Cell 54, 221-227.

124. Orci L., Malhotra V., Amherdt M., Serafini T., and Rothman J.E. (1989) *Dissection of a single round of vesicular transport: sequential intermediates for intercisternal movement in the Golgi stack.* Cell 56, 357-368.

125. Aridor M., Bannykh S.I., Rowe T., and Balch W.E. (1999) *Cargo can modulate COPII vesicle formation from the endoplasmic reticulum.* J. Biol. Chem 274, 4389-4399.

126. Springer S., and Schekman R. (1998) *Nucleation of COPII vesicular coat complex by endoplasmic reticulum to Golgi vesicle SNAREs.* Science 281, 698-700.

127. Peng R., Grabowski R., De Antoni A., and Gallwitz D. (1999) *Specific interaction of the yeast cis-Golgi syntaxin Sed5p and the coat protein complex II component Sec24p of ER-derived transport vesicles.* Proc. Natl. Acad. Sci. 96, 3751-3756.

128. Seaman M.N., McCaffery J.M., and Emr S.D. (1998) *A membrane coat complex essential for endosome-to-Golgi retrograde transport in yeast.* J. Cell Biol. 142, 665-681.

129. Malhotra V., Serafini T., Orci L. Shepherd J.C., and Rothman J.E. (1989) *Purification of a novel class of coated vesicles mediating biosynthetic protein transport through the Golgi stack.* Cell 58, 329-336.

130. Serafini T., Orci L., Amherdt M., Brunner M., Kahn R.A., and Rothman J.E. (1991) *ADP-ribosylation factor is a subunit of the coat of Golgi-derived COP-coated vesicles: a novel role for a GTP-binding protein.* Cell 67, 239-253.

131. Gaynor E.C., Graham T. R., and Emr S.D. (1998) *COPI in ER/Golgi and intra-Golgi transport: do yeast COPI mutants point the way?* Biochim. Biophys. Acta 1404, 33-51.

132. Waters M.G., Serafini T., and Rothman J.E. (1991) *'Coatomer': a cytosolic protein complex containing subunits of non-clathrin-coated Golgi transport vesicles.* Nature 349, 248-251.

133. **{a}** Whitney J.A., Gomez M., Sheff D., Kreis T.E., and Mellman I. (1995) *Cytoplasmic coat proteins involved in endosome function.* Cell 83, 703-713.
{b} Gu F., Aniento F., Parton R.G., and Gruenberg J. (1997) *Functional dissection of COP-I subunits in the biogenesis of multivesicular endosomes.* J. Cell Biol. 139, 1183-1195.

134. Donaldson J.G., Finazzi D., and Klausner R.D. (1992) *Brefeldin A inhibits Golgi membrane-catalysed exchange of guanine nucleotide onto ARF protein.* Nature 360, 350-352.

135. Helms J.B., and Rothman J.E. (1992) *Inhibition by brefeldin A of a Golgi membrane enzyme that catalyses exchange of guanine nucleotide bound to ARF.* Nature 360, 352-354.

136. Helms J.B., Palmer D.J., and Rothman J.E. (1993) *Two distinct populations of ARF bound to Golgi membranes.* J. Cell Biol. 121, 751-760.

137. Donaldson J.G., Cassel D., Kahn R.A., and Klausner R.D. (1992) *ADP-ribosylation factor, a small GTP-binding protein, is required for binding of β-COP to Golgi membranes.* Proc. Natl. Acad. Sci. USA 89, 6408-6412.

138. Orci L., Palmer D.J., Amherdt M., and Rothman J.E. (1993) *Coated vesicle assembly in the Golgi requires only coatomer and ARF proteins from the cytosol.* Nature 364, 732-734.

139. Orci L., Palmer D.J., Ravazzola M., Perrelet A., Amherdt M., and Rothman J.E. (1993) *Budding from Golgi membranes requires the coatomer complex of non-clathrin coat proteins.* Nature 362, 648-652.

140. Palmer D.J., Helms J.B., Beckers C.J.M., Orci L., and Rothman J.E. (1993) *Binding of coatomer to Golgi membranes requires ADP-ribosylation factor.* J. Biol. Chem. 26, 12083-12089.

141. Rothman J.E., and Warren G. (1994) *Implications of the SNARE hypothesis for intracellular membrane topology and dynamics.* Curr. Biol. 4(3), 220-233.

142. Ostermann J., Orci L., Tani K., Amherdt M., Ravazzola M., and Rothman J.E. (1993) *Stepwise assembly of functionally active transport vesicles.* Cell 75, 1015-1025.

143. Tanigawa G., Orci L., Amherdt M., Helms J.B., and Rothman J.E. (1993) *Hydrolysis of bound GTP by ARF protein triggers uncoating of Golgi-derived COP-coated vesicles.* J. Cell Biol. 123, 1365-1371.

144. Barr F.A., and Huttner W.B. (1996) *A role for ARF, but not COP I, in secretory vesicle biogenesis from the trans-Golgi network.* FEBS Lett. 384, 65-70.

145. Springer S., Spang A., and Schekman R. (1999) *A primer on vesicle budding.* Cell 97, 145-148.

146. Pearse B.M.F. (1976) *Clathrin: a unique protein associated with intracellular transfer of membrane by coated vesicles.* Proc. Natl. Acad. Sci USA 73,1255-1259.

147. Barlowe C., Orci L., Yeung T., Hosobuchi M., Hamamoto S., Salama N., Rexach M.F., Ravazzola M., Amherdt M., and Schekman R. (1994) *COPII: a membrane coat formed by Sec proteins that drive vesicle budding from the endoplasmic reticulum.* Cell 77, 895-907.

148. Barlowe C. (1998) *COPII and selective export from the endoplasmic reticulum.* Biochim Biophys. Acta 1404, 67-76.

149. Nakano A., and Muramatsu M. (1989) *A novel GTP-binding protein, Sar1p, is involved in transport from the endoplasmic reticulum to the Golgi apparatus.* J. Cell Biol. 109, 2677-2691.

150. Ahle S., Mann A., Eichelsbacher U., and Ungewickell E. (1988) *Structural relationships between clathrin assembly proteins from the Golgi and the plasma membrane.* EMBO J. 7, 919-929.

151. Duden R., Griffiths G., Frank R., Argos P., and Kreis T.E. (1991) *β-COP, a 110 kd protein associated with non-clathrin-coated vesicles and the Golgi complex, shows homology to β-adaptin.* Cell 64, 649-665.

152. Glick B.S., and Rothman J.E. (1987) *Possible role for fatty acyl-coenzyme A in intracellular protein transport.* Nature 326, 309-312.

153. Block M.R., Glick B.S., Wilcox C.A., Wieland F.T., and Rothman J.E. (1988) *Purification of an N-ethylmaleimide-sensitive protein catalyzing vesicular transport.* Proc. Natl. Acad. Sci. USA 85, 7852-7856.

154. Tagaya M., Wilson D.W., Brunner M., Arango N., and Rothman J.E. (1993) *Domain structure of an N-ethylmaleimide-sensitive fusion protein involved in vesicular transport.* J. Biol. Chem. 268, 2662-2666.

155. Whiteheart S.W., Rossnagel K., Buhrow S., Jaenicke R., and Rothman J.E. (1994) *N-ethylmaleimide-sensitive fusion protein: a trimeric ATPase whose hydrolysis of ATP is required for membrane fusion.* J. Cell Biol. 126, 945-954.

156. Wilson D.W., Wilcox C.A., Flynn G.C., Chen E., Kuang W.J., Hengel W.J., Block M.R., Ullrich A., and Rothman J.E. (1989) *A fusion protein required for vesicle-mediated transport in both mammalian cells and yeast.* Nature 339, 355-359.

157. Paquet M.R., Pfeffer S.R., Burczak J.D., Glick B.S., and Rothman J.E. (1986) *Components responsible for transport between successive Golgi cisternae are highly conserved in evolution.* J. Biol. Chem. 261, 4367-4370.

158. Diaz R., Mayorga L.S., Weidman P.J., Rothman J.E., and Stahl P.D. (1989) *Vesicle fusion following receptor-mediated endocytosis requires a protein active in Golgi transport.* Nature 339, 398-400.

159. Beckers C.J.M., Block M.R., Glick B.S., Rothman J.E., and Balch W.E. (1989) *Vesicular transport between the endoplasmic reticulum and the Golgi stack requires the NEM-sensitive fusion protein.* Nature 339, 397-398.

160. Graham T.R., and Emr S.D. (1991) *Compartmental organization of Golgi-specific protein modification and vacuolar protein sorting events defined in a yeast sec18 (NSF) mutant.* J. Cell Biol. 114, 207-218.

161. Clary D.O., and Rothman J.E. (1990) *Purification of three related peripheral membrane proteins needed for vesicular transport.* J. Biol. Chem. 265, 10109-10117.

162. Clary D.O., Griff I.C., and Rothman J.E. (1990) *SNAPs, a family of NSF attachment proteins involved in intracellular membrane fusion in animals and yeast.* Cell 61, 709-721.

163. Whiteheart S.W., Griff I.C., Brunner M., Clary D.O., Mayer T., Buhrow S.A., and Rothman J.E. (1993) *SNAP family of NSF attachment proteins includes a brain-specific isoform.* Nature 362, 353-355.

164. Kaiser C.A., and Schekman R. (1990) *Distinct sets of SEC genes govern transport vesicle formation and fusion early in the secretory pathway.* Cell 61, 723-733.

165. Griff I.C., Schekman R., Rothman J.E., and Kaiser C.A. (1992) *The yeast SEC17 gene product is functionally equivalent to mammalian alpha-SNAP protein.* J. Biol. Chem. 267, 12106-12115.

166. Segev N., Mulholland J., and Botstein D. (1988) *The yeast GTP-binding YPT1 protein and a mammalian counterpart are associated with the secretion machinery.* Cell 52, 915-924.

167. Weidman P.J., Melancon P. Block M.R., and Rothman J.E. (1989) *Binding of an N-ethylmaleimide-sensitive fusion protein to Golgi membranes requires both a soluble protein(s) and an integral membrane receptor.* J. Cell Biol. 108, 1589-1596.

168. Whiteheart S.W., Brunner M., Wilson D.W., Wiedmann M., and Rothman J.E. (1992) *Soluble N-ethylmaleimide-sensitive fusion attachment proteins (SNAPs) bind to a multi-SNAP receptor complex in Golgi membranes.* J. Biol. Chem. 267, 12239-12243.

169. DeBello W.M., O'Connor V., Dresbach T., Whiteheart S.W., Wang S.S-H., Schweizer F.E., Betz H., Rothman J.E., and Augustine G.J. (1995) *SNAP-mediated protein-protein interactions essential for neurotransmitter release.* Nature 373, 626-630.

170. Oyler G.A., Higgins G.A., Hart R.A., Battenberg E., Billingsley M., Bloom F.E., and Wilson M.C. (1989) *The identification of a novel synaptosomal-associated protein, SNAP-25, differentially expressed by neuronal subpopulations.* J. Cell Biol. 109, 3039-3052.

171. Trimble W.S., Cowan D.M., and Scheller R.H. (1988) *VAMP-1: a synaptic vesicle-associated integral membrane protein.* Proc. Natl. Acad. Sci. USA 85, 4538-4542.

172. Hanson P.I., Roth R., Morisaki H., Jahn R., and Heuser J.E. (1997) *Structure and conformational changes in NSF and its membrane receptor complexes visualized by quick-freeze/deep-etch electron microscopy.* Cell 90, 523-535.

173. Sutton R.B., Fasshauer D., Jahn R., and Brunger A.T. (1998) *Crystal structure of a SNARE complex involved in synaptic exocytosis at 2.4 A resolution.* Nature 395, 347-353.

174. Wilson D.W., Whiteheart S.W., Wiedmann M., Brunner M., and Rothman J.E. (1992) *A multisubunit particle implicated in membrane fusion.* J. Cell Biol 117, 531-538.

175. Söllner T., Bennett M.K., Whiteheart S.W., Scheller R.H., and Rothman J.E. (1993) *A protein assembly-disassembly pathway in vitro that may correspond to sequential steps of synaptic vesicle docking, activation, and fusion.* Cell 75, 409-418.

176. White J.M. (1992) *Membrane fusion.* Science 258, 917-924.

177. Skehel J.J., and Wiley D.C. (1998) *Coiled coils in both intracellular vesicle and viral membrane fusion.* Cell 95, 871-874.

178. Mayer A., Wickner W, and Haas A.(1996) *Sec18p (NSF)-driven release of Sec17p (α-SNAP) can precede docking and fusion of yeast vacuoles.* Cell 85, 83-94.

179. Söllner T., Whiteheart S.W., Brunner M. Erdjument-Bromage H., Geromanos S., Tempst P., and Rothman J.E. (1993) *SNAP receptors implicated in vesicle targeting and fusion.* Nature 362, 318-324.

180. Weber T., Zemelman B.V., McNew J.A., Westermann B., Gmachl M., Parlati F., Söllner T.H., and Rothman J.E. (1998) *SNAREpins: minimal machinery for membrane fusion.* Cell 92, 759-772.

181. Spring J., Kato M., and Bernfield M. (1993) *Epimorphin is related to a new class of neuronal and yeast vesicle targeting proteins.* Trends Biochem. Sci.18,124-125.

182. Kutay U., Hartmann E., and Rapoport T.A. (1993) *A class of membrane proteins with a C-terminal anchor.* Trends Cell Biol 3, 72-75.

183. Hess D.T., Slater T.M., Wilson M.C., Skene J.H.P. (1992) *The 25 kDa synaptosomal-associated protein SNAP-25 is the major methionine-rich polypeptide in rapid axonal transport and a major substrate for palmitoylation in adult CNS.* J. Neurosci. 12, 4634-4641.

184. Schiavo G., Benfenati F., Poulain B., Rossetto O., Polverino De Laureto P., DasGupta B.R., and Montecucco C. (1992) *Tetanus and botulinum-B neurotoxins block neurotransmitter release by proteolytic cleavage of synaptobrevin.* Nature 359, 832-835.

185. Blasi J., Chapman E.R., Yamasake S., Binz T., Niemann H., and Jahn R. (1993) *Botulinum neurotoxin C1 blocks neurotransmitter release by means of cleaving HPC-1/syntaxin.* EMBO J. 12, 4821-4828.

186. Blasi J., Chapman E.R., Link E., Binz T., Yamasaki S., De Camilli P., Südhof T.C., Niemann H., and Jahn R. (1993) *Botulinum neurotoxin A selectively cleaves the synaptic protein SNAP-25.* Nature 365, 160-163.

187. Bennett M.K., Calakos N., and Scheller R.H. (1992) *Syntaxin: a synaptic protein implicated in docking of synaptic vesicles at presynaptic active zones.* Science 257, 255-259.

188. Inoue A., Obata K., and Akagawa K. (1992) *Cloning and sequence analysis of cDNA for a neuronal cell membrane antigen, HPC-1.* J. Biol. Chem. 267, 10613-10619.

189. Schiavo G., Rossetto O., Catsicas S., Polverino de Laureto P., DasGupta B.R., Benfenati F., and Montecucco C. (1993) *Identification of the nerve terminal targets of botulinum neurotoxin serotypes A, D, and E.* J. Biol. Chem. 268, 23784-23787.

190. Baumert M., Maycox P.R., Navone F., De Camilli P., and Jahn R. (1989) *Synaptobrevin: an integral membrane protein of 18,000 daltons present in small synaptic vesicles of rat brain.* EMBO J. 8, 379-384.

191. Bennett M.K., and Scheller R.H. (1994) *A molecular description of synaptic vesicle membrane trafficking.* Annu. Rev. Biochem. 63, 63-100.

192. Poirier M.A., Xiao W., Macosko J.C., Chan C., Shin Y.-K., and Bennet M.K. (1998) *The synaptic SNARE complex is a parallel four-stranded helical bundle.* Nat. Struct. Biol. 5, 765-769.

193. Yang B., Gonzalez L., Prekeris R., Steegmaier M., Advani R.J., and Scheller R.H. (1999) *SNARE interactions are not selective. Implications for membrane fusion specificity.* J. Biol. Chem. 274, 5649-5653.

194. McMahon H.T., Ushkaryov Y.A., Edelmann L., Link E., Binz T., Niemann H., Jahn R., and Südhof T.C. (1993) *Cellubrevin is a ubiquitous tetanus-toxin substrate homologous to a putative synaptic vesicle fusion protein.* Nature 364, 346-349.

195. Bennett M.K., Garcia-Arrarás J.E., Elferink L.A., Peterson K., Fleming A.M., Hazuka C.D., and Scheller R.H. (1993) *The syntaxin family of vesicular transport receptors.* Cell 74, 863-873.

196. **{a}**Link E., McMahon H., Fischer von Mollard G., Yamasaki S., Niemann H., Südhof T.C., and Jahn R. (1993) *Cleavage of cellubrevin by tetanus toxin does not affect fusion of early endosomes.* J. Biol. Chem. 2687, 18423-18426.
{b} Galli T., Chilcote T., Mundigl O., Binz T., Niemann H., and De Camilli P. (1994) *Tetanus toxin-mediated cleavage of cellubrevin impairs exocytosis of transferrin receptor-containing vesicles in CHO cells.* J.Cell Biol. 125,1015-1024.

197. Dascher C., Ossig R., Gallwitz D., and Schmitt H.D. (1991) *Identification and structure of four yeast genes (SLY) that are able to suppress the functional loss of YPT1, a member of the RAS superfamily.* Molec. Cell Biol. 11, 872-885.

198. Shim J., Newman A., and Ferro-Novick S. (1991) *The BOS1 gene encodes an essential 27-kD putative membrane protein that is required for vesicular transport from the ER to the Golgi complex in yeast.* J. Cell Biol. 113, 55-64.

199. Protopopov, V., Govindan B., Novick P., and Gerst J.E. (1993) *Homologs of the synaptobrevin/VAMP family of synaptic vesicle proteins function on the late secretory pathway in S. cerevisiae.* Cell 74, 855-861.

200. Aalto M.K., Ronne H., and Keranen S. (1993) *Yeast syntaxins Sso1p and Sso2p belong to a family of related membrane proteins that function in vesicular transport.* EMBO J. 12, 4095-4104.

201. Lian J.P., and Ferro-Novick S. (1993) *Bos1p, an integral membrane protein of the endoplasmic reticulum to Golgi transport vesicles, is required for their fusion competence.* Cell 73, 735-745.

202. Brennwald P., Kearns B., Champion K., Keranen S., Bankaitis V., and Novick P. (1994) *Sec9 is a SNAP-25-like component of a yeast SNARE complex that may be the effector of Sec4 function in exocytosis.* Cell 79, 245-258.

203. Sato T.K., Darsow T., and Emr S.D. (1998) *Vam7p, a SNAP-25-like molecule, and Vam3p, a syntaxin homolog, function together in yeast vacuolar protein trafficking.* Mol. Cell Biol. 18, 5308-5319.

204. Gerst J.E., Rodgers L., Riggs M., and Wigler M. (1992) *SNC1, a yeast homolog of the synaptic vesicle-associated membrane protein/synaptobrevin gene family: genetic interactions with the RAS and CAP genes.* Proc. Natl. Acad. Sci. USA 89, 4338-4342.

205. Newman A.P., Shim J., and Ferro-Novkck S. (1990) *BET1, BOS1, and SEC22 are members of a group of interacting yeast genes required for transport from the endoplasmic reticulum to the Golgi complex.* Molec. Cell Biol. 10, 3405-3414.

206. Newman A.P., Groesch M., and Ferro-Novick S. (1992) *Bos1p, a membrane protein required for ER to Golgi transport in yeast, co-purifies with the carrier vesicles and with Bet1p and the ER membrane.* EMBO J. 12, 3609-3617.

207. Sogaart M., Tani K., Ye R.R., Geromanos S., Tempst P., Kirchhausen T., Rothman J.E., and Söllner T. (1994) *A rab protein is required for the assembly of SNARE complexes in the docking of transport vesicles.* Cell 78, 937-948.

208. Ungermann C., Nichols B.J., Pelham H.R.B., and Wickner W. (1998) *A vacuolar v-t-SNARE complex, the predominant form in vivo and on isolated vacuoles, is disassembled and activated for docking and fusion.* J. Cell Biol. 140, 61-69.

209. **{a}** Fischer von Mollard G., Nothwehr S.F., and Stevens T.H. (1997) *The yeast v-SNARE Vti1p mediates two vesicle transport pathways through interactions with the t-SNAREs Sed5p and Pep12p.* J. Cell Biol 137, 1511-1524.

{b} Fischer von Mollard G., and Stevens T.H. (1999) *The Saccharomyces cerevisiae v-SNARE Vti1p is required for multiple membrane transport pathways to the vacuole.* Mol. Biol. Cell 10, 1719-1732.

210. Seron K., Tieaho V., Prescianotto-Baschong C., Aust T., Blondel M.O., Guillaud P., Devilliers G., Rossanese O.W., Glick B.S., Riezman H., Keranen S., and Haguenauer-Tsapis R. (1998) *A yeast t-SNARE involved in endocytosis.* Mol. Biol. Cell. 10,2873-2889.

211. Patel S.K., Ingig F.E., Olivieri N., Levine N.D., and Latterich M. (1998)

Organelle membrane fusion: a novel function for the syntaxin homolog Ufe1p in ER membrane fusion. Cell 92, 611-620.

212. Banfield D.K., Lewis M.J., Rabouille C., Warren G., and Pelham H.R.B. (1994) *Localization of Sed5, a putative vesicle targeting molecule, to the cis-Golgi network involves both its transmembrane and cytoplasmic domains.* J. Cell Biol. 127, 357-371.

213. Hardwick K.G., and Pelham H.R.B. (1992) *SED5 encodes a 39-kD integral membrane protein required for vesicular transport between the ER and the Golgi complex.* J. Cell Biol. 119, 513-521.

214. Becherer K.A., Rieder S.E., Emr S.D., and Jones E.W. (1996) *Novel syntaxin homologue, Pep12p, required for the sorting of lumenal hydrolases to the lysosome-like vacuole in yeast.* Mol. Biol. Cell 7, 579-594.

215. **{a}** Wada Y., Nakamura N., Ohsumi Y., and Hirata A. (1997) *Vam3p, a new member of syntaxin related protein, is required for vacuolar assembly in the yeast Saccharomyces cerevisiae.* J. Cell Sci. 110, 1299-1306.

{b} Darsow T., Rieder S.E., and Emr S.D. (1997) *A multispecificity syntaxin homologue, Vam3p, essential for autophagic and biosynthetic protein transport to the vacuole.* J. Cell Biol. 138, 517-529.

216. Elferink L.A., Trimble W.S., and Scheller R.H. (1989) *Two vesicle-associated membrane protein genes are differentially expressed in the rat central nervous system.* J. Biol. Chem. 264, 11061-11064.

217. Archer B.T. III, Oezcelik T., Jahn R., Francke U., and Sudhof T.C. (1990) *Structures and chromosomal localizations of two human genes encoding synaptobrevins 1 and 2.* J. Biol. Chem. 265, 17267-17273.

218. Advani R.J., Bae H.R., Bock J.B., Chao D.S., Doung Y.C., Prekeris R., Yoo J.S., and Scheller R.H. (1998) *Seven novel mammalian SNARE proteins localize to distinct membrane compartments.* J. Biol. Chem. 273, 10317-10324.

219. Zeng Q., Subramaniam V.N., Wong S.H., Tang B.L., Parton R.G., Rea S., James D.E., and Hong W. (1998) *A novel synaptobrevin/VAMP homologous protein (VAMP5) is increased during in vitro myogenesis and present in the plasma membrane.* Mol. Biol. Cell 9, 2423-2437.

220. Advani R.J., Yang B., Prekeris R., Lee K.C., Klumperman J., and Scheller R.H. (1999) *VAMP-7 mediates vesicular transport from endosomes to lysosomes.* J. Cell Biol. 146, 765-775.

221. Wong S.H., Zhang T., Xu Y., Subramaniam V.N., Griffiths G., and Hong W. (1998) *Endobrevin, a novel synaptobrevin/VAMP-like protein preferentially*

associated with the early endosome. Mol. Biol. Cell 9, 1549-1563.

222. Bock J.B., Klumperman J., Davanger S., and Scheller R.H. (1997) *Syntaxin 6 functions in trans-Golgi network vesicle trafficking.* Mol. Biol. Cell 8, 1261-1271.

223. Wang H., Frelin L., and Pevsner J. (1997) *Human syntaxin 7: a Pep12p/Vps6p homologue implicated in vesicle trafficking to lysosomes.* Gene 199, 39-48.

224. **{a}** Nakamura N., Yamamoto A., and Futai M. (2000) *Syntaxin 7 mediates endocytic trafficking to late endosomes.* J. Biol Chem. 275, 6523-6529.

{b} Ward D.M., Pevsner J., Scullion M.A., Vaughn M., and Kaplan J. (2000) *Syntaxin 7 and VAMP-7 are soluble N-ethylmaleimide-sensitive factor attachment protein receptors required for late endosome-lysosome and homotypic lysosome fusion in alveolar macrophages.* J. Mol. Biol. Cell 11, 2327-2333.

225. Steegmaier M., Yang B., Yoo J.S., Huang B., Shen M., Yu S., Luo Y., and Scheller R.H. (1998) *Three novel proteins of the syntaxin/SNAP-25 family.* J. Biol. Chem. 273, 34171-34179.

226. Tang B.L., Low D.Y., Tan A.E., and Hong W. (1998) *Syntaxin 10: a member of the syntaxin family localized to the trans-Golgi network.* Biochem. Biophys. Res. Commun. 242, 345-350.

227. Valdez A.C., Cabaniols J.-P., Brown M.J., and Roche P.A. (1999) *Syntaxin 11 is associated with SNAP-23 on late endosomes and the trans-Golgi network.* J. Cell Sci. 112, 845-854.

228. Tang B.L., Tan A.E., Lim L.K., Lee S.S., Low D.Y., and Hong W (1998) *Syntaxin 12, a member of the syntaxin family localized to the endosome.* J. Biol. Chem. 273, 6944-6950.

229. Prekeris R., Klumperman J., Chen Y.A., and Scheller R.H. (1998) *Syntaxin 13 mediates cycling of plasma membrane proteins via tubulovesicular recycling endosomes.* J. Cell Biol. 143, 957-971.

230. Tang B.L., Low D.Y., Lee S.S., Tan A.E., and Hong W. (1998) *Molecular cloning and localization of human syntaxin 16, a member of the syntaxin family of SNARE proteins.* Biochem. Biophys. Res. Commun. 242, 673-679.

231. Ravichandran V., Chawla A., and Roche P.A. (1996) *Identification of a novel syntaxin- and synaptobrevin/VAMP-binding protein, SNAP-23, expressed in non-neuronal tissues.* J. Biol. Chem. 271:13300-13303.

232. McNew J.A., Sogaard M., Lampen N.M., Machida S., Ye R.R., Lacomis L., Tempst P., Rothman J.E., and Sollner T.H. (1997) *Ykt6p, a prenylated SNARE essential for endoplasmic reticulum-Golgi transport.* J. Biol. Chem. 272, 17776-17783.

233. Hay J.C., Chao D.S., Kuo C.S., and Scheller R.H. (1997) *Protein interactions regulating vesicle transport between the endoplasmic reticulum and Golgi apparatus in mammalian cells.* Cell 89, 149-158.

234. Lowe S.L., Peter F., Subramaniam V.N., Wong S.H., and Hong W. (1997) *A SNARE involved in protein transport through the Golgi apparatus.* Nature 389, 881-884.

235. Skehel P.A., Martin K.C., Kandel E.R., and Bartsch D. (1995) *A VAMP-binding protein from Aplysia required for neurotransmitter release.* Science 269, 1580-1583.

236. Weir M.L., Klip A., and Trimble W.S. (1998) *Identification of a human homologue of VAMP-associated protein of 33 kDa (VAP-33): a broadly expressed protein that binds to VAMP.* Biochem. J. 333, 247-251.

237. Nishimura Y., Hayashi M., Inada H., and Tanaka T. (1999) *Molecular cloning and characterization of mammalian homologues of vesicle-associated membrane protein-associated (VAMP-associated) proteins.* Biochem. Biophys. Res. Commun. 254, 21-26.

238. **{a}** Brennwald P., and Novick P. (1993) *Interactions of three domains distinguishing the Rab proteins Ypt1 and Sec4.* Nature 362, 560-563.
{b} Dunn B., Stearns T., and Botstein D. (1993) *Specificity domains distinguish the Ras-related GTPases Ypt1 and Sec4.* Nature 362, 563-565.

239. Bucci C., Parton R.G., Mather I.H., Stunnenberg H., Simons K., Hoflack B., and Zerial M. (1992) *The small GTPase rab5 functions as a regulatory factor in the early endocytic pathway.* Cell 70, 715-728.

240. Davidson H.W., and Balch W.E. (1993) *Differential inhibition of multiple vesicular transport steps between the endoplasmic reticulum and trans Golgi network.* J. Biol. Chem. 268, 4216-4226.

241. Fernandez J.M., Neher E., and Gomperts B.D. (1984) *Capacitance measurements reveal stepwise fusion events in degranulating mast cells.* Nature 312, 453-455.

242. Novick P., and Zerial M. (1997) *The diversity of Rab proteins in vesicle transport.* Curr. Opin. Cell Biol. 9, 496-504.

243. Huber L., Pimplikar S., Parton R., Virta H., Zerial M., and Simons K. (1993) *Rab8, a small GTPase involved in vesicular traffic between the TGN and the basolateral plasma membrane.* J. Cell Biol. 123, 35-45.

244. Lledo P.M., Vernier P., Vincent J.D., Mason W.T., and Zorec R. (1993) *Inhibition of Rab3B expression attenuates Ca(2+)-dependent exocytosis in rat anterior pituitary cells.* Nature 364, 540-544.

245. Lombardi D., Soldarti T., Riederer M.A., Goda Y., Zerial M., and Pfeffer S.R. (1993) *Rab9 functions in transport between late endosomes and the trans Golgi network.* EMBO J. 12, 677-682.

246. Salminen A., and Novick P.J. (1987) *A ras-like protein is required for a post-Golgi event in yeast secretion.* Cell 49, 527-538.

247. Tisdale E.J., Bourne J.R., Khosravi-Far R., Der C.J., and Balch W.E. (1992) *GTP-binding mutants of rab1 and rab2 are potent inhibitors of vesicular transport from the endoplasmic reticulum to the Golgi complex.* J. Cell Biol. 119, 749-761.

248. van der Sluijs P., Hull M., Webster P., Male P., Goud B., and Mellman I. (1992) *The small GTP-binding protein rab4 controls an early sorting event on the endocytic pathway.* Cell 780, 729-740.

249. Wichmann H., Hengst L., and Gallwitz D. (1992) *Endocytosis in yeast: evidence for the involvement of a small GTP-binding protein (Ypt7p).* Cell 71, 1131-1142.

250. Goud B., Zahraoui A., Tavitian A., and Saraste J. (1990) *Small GTP-binding protein associated with Golgi cisternae.* Nature 345, 553-556.

251. **{a}** Feng Y., Press B., and Wandinger-Ness A. (1995) *Rab 7: an important regulator of late endocytic membrane traffic.* J. Cell Biol. 131, 1435-1452.
{b} Meresse S., Gorvel J.P., and Chavrier. (1995) *The rab7 GTPase resides on a vesicular compartment connected to lysosomes.* J. Cell Sci. 108, 3349-3358

252. Horazdovsky B.F., Busch G.R., and Emr S.D. (1994) *VPS21 encodes a rab5-like GTP binding protein that is required for the sorting of yeast vacuolar proteins.* EMBO J. 13, 1297-1309.

253. Ullrich O., Reinsch S., Urbe S., Zerial M., and Parton R. (1996) *Rab11 regulates recycling through the pericentriolar recycling endosome.* J. Cell Biol. 135, 913-924.

254. Burstein E.S., and Macara I.G. (1992) *Characterization of a guanine nucleotide-releasing factor and a GTPase-activating protein that are specific for the ras-related protein p25rab3A.* Proc. Natl. Acad. Sci. USA 89, 1154-1158.

255. Moya M., Roberts D., and Novick P. (1993) *DSS4-1 is a dominant suppressor of sec4-8 that encodes a nucleotide exchange protein that aids Sec4p function.* Nature 361, 460-463.

256. Strom M., Vollmer P., Tan T.J., and Gallwitz D. (1993) *A yeast GTPase-activating protein that interacts specifically with a member of the Ypt/Rab family* Nature 361, 736-739.

257. Takai Y., Kaibuchi A., and Kawata N. (1992) *Small GTP-binding proteins.* Int. Rev. Cytol. 133, 187-230.

258. Wang Y., Okamoto M., Schmitz F., Hofmann K., and Sudhof T.C. (1997) *Rim is a putative Rab3 effector in regulating synaptic-vesicle fusion.* Nature 388, 593-598.

259. Kato M., Sasaki T., Ohya T., Nakanishi H., Nishioka H., Imamura M., and Takai Y. (1996) *) Physical and functional interaction of rabphilin-3A with alpha-actinin.* J. Biol. Chem. 271, 31775-31778.

260. Kotake K., Ozaki N., Mizuta M., Sekiya S., Inagaki N., and Seino S. (1997) *Noc2, a putative zinc finger protein involved in exocytosis in endocrine cells.* J. Biol. Chem. 272, 29407-29410.

261. Vitale G., Rybin V., Christoforidis S., Thornqvist P., McCaffrey M., Stenmark H., and Zerial M. (1998) *Distinct Rab-binding domains mediate the interaction of Rabaptin-5 with GTP-bound Rab4 and Rab5.* EMBO J. 17, 1941-1951.

262. Christoforidis S., McBride H.M., Burgoyne R.D., and Zerial M. (1999) *The Rab5 effector EEA1 is a core component of endosome docking.* Nature 397, 621-625.

263. Echard A., Jollivet F., Martinez O., Lacapere J.J., Rousselet A., Janoueix-Lerosey I., Goud B. (1998) *Interaction of a Golgi-associated kinesin-like protein with Rab6.* Science 279, 580-585.

264. Diaz E., Schimmoller F., and Pfeffer S.R. (1997) *A novel Rab9 effector required for endosome-to-TGN transport.* J. Cell Biol. 138, 283-290.

265. Bean A.J, Seifert R., Chen Y.A., Sacks R., and Scheller R.H. (1997) *Hrs-2 is an ATPase implicated in calcium-regulated secretion.* Nature 385, 826-829.

266. Diaz E., and Pfeffer S.R. (1998) *TIP47: a cargo selection device for mannose 6-phosphate receptor trafficking.* Cell 93, 433-443.

267. **{a}** TerBush D.R., Marice T., Roth D., and Novick P. (1996) *The Exocyst is a multiprotein complex required for exocytosis in Saccharomyces cerevisiae.* EMBO J. 15, 6483-6494.

{b} Guo W., Roth D., Walch-Solimena C., and Novick P. (1999) *The exocyst is an effector for Sec4p, targeting secretory vesicles to sites of exocytosis.* EMBO J. 18, 1071-1080.

268. Peterson M.R., Burd C.G., and Emr S.D. (1999) *Vac1p coordinates Rab and phosphatidylinositol 3-kinase signaling in Vps45p-dependent vesicle docking/fusion at the endosome.* Curr. Biol. 9, 159-162.

269. Aalto M.K., Keränen S., and Ronne H. (1992) *A family of proteins involved in intracellular transport.* Cell 68, 181-182.

270. Wada Y., Kitamoto K., Kanbe T., Tanaka K., and Anraku Y. (1990) *The SLP1 gene of Saccharomyces cerevisiae is essential for vacuolar morphogenesis and function.* Mol. Cell. Biol. 10, 2214-2223.

271. Pevsner J., Hsu S.C., and Scheller R.H. (1994) *n-Sec1: a neural-specific syntaxin-binding protein.* Proc. Natl. Acad. Sci USA 91, 1445-1449.

272. Pevsner J., Hsu S.C., Braun J.E.A., Calakos N., Ting A.E., Bennett M.K., and Scheller R.H. (1994) *Specificity and regulation of a synaptic vesicle docking complex.* Neuron 13, 353-361.

273. Waters M.G., Clary D.O., and Rothman J.E. (1992) *A novel 115-kD peripheral membrane protein is required for intercisternal transport in the Golgi stack.* J. Cell Biol. 118, 1015-1026.

274. Barroso M., Nelson D.S., and Sztul E. (1995) *Transcytosis-associated protein (TAP)/p115 is a general fusion factor required for binding of vesicles to acceptor membranes.* Proc. Natl. Acad. Sci. USA. 92, 527-531.

275. Nakajima H., Hirata A., Ogawa Y., Yonehara T., Yoda K., and Yamasaki M. (1991) *A cytoskeleton-related gene, uso1, is required for intracellular protein transport in Saccharomyces cerevisiae.* J. Cell Biol. 113, 245-60.

276. **{a}** Cao X., Ballew N., Barlowe C. (1998) *Initial docking of ER-derived vesicles requires Uso1p & Ypt1p, but independent of SNAREs.* EMBO J. 17, 2156-2165.
{b} Sacher M., Jiang Y., Barrowman J., Scarpa A., Burston J., Zhang L., Schieltz D., Yates J.R. III, Abeliovich H., and Ferro-Novick S. (1998) *TRAPP, a highly conserved novel complex on the cis-Golgi that mediates vesicle docking and fusion.* EMBO J. 17, 2494-2503.

277. Sonnichsen B., Lowe M., Levine T., Jamsa E., Dirac-Svejstrup B., and Warren G. (1998) *A role for giantin in docking COPI vesicles to Golgi membranes.* J. Cell Biol. 140, 1013-1021.

278. Linstedt A.D, and Hauri H.P. (1993) *Giantin, a novel conserved Golgi membrane protein containing a cytoplasmic domain of at least 350 kDa.* Mol. Biol. Cell 4, 679-693.

279. **{a}** Nakamura N., Rabouille C., Watson R., Nilsson T., Hui N., Slusarewicz P., Kreis T.E., and Warren G. (1995) *Characterisation of a cis-Golgi matrix protein, GM130.* J Cell Biol. 131, 1715-1726.
{b} Nakamura N., Lowe M., Levine T.P., Rabouille C., and Warren G. (1997) *The vesicle docking protein p115 binds GM130, a cis-Golgi matrix protein, in a mitotically regulated manner.* Cell 89, 445-455.

280. Creutz C.E. (1992) *The annexins and exocytosis.* Science 258, 924-931.

281. Emans N., Gorvel J.P., Walter C., Gerke V., Griffiths G., and Gruenberg J. (1993) *Annexin II is a major component of fusogenic endosomal vesicles.* J. Cell Biol. 120, 1357-1370.

282. Ali S.M., Geisow M.J., and Burgoyne R.D. (1989) *A role for calpactin in calcium-dependent exocytosis in adrenal chromaffin cells.* Nature 340, 313-315.

283. Blackwood R.A., and Ernst J.D. (1990) *Characterization of Ca^{2+}-dependent phospholipid binding, vesicle aggregation and membrane fusion by annexins.* Biochem. J. 266, 195-200.

284. Creutz C.E., Pazoles C.J., and Pollard H.B. (1978) *Identification and purification of an adrenal medullary protein (synexin) that causes calcium-dependent aggregation of isolated chromaffin granules.* J. Biol. Chem. 253, 2858-2866.

285. Lin H.C., Südhof T.C., and Anderson R.G.W. (1992) *Annexin VI is required for budding of clathrin-coated pits.* Cell 70, 283-291.

286. Oshry L., Meers P., Mealy T., and Tauber A.I. (1991) *Annexin-mediated membrane fusion of human neutrophil plasma membranes and phospholipid vesicles.* Biochim. Biophys. Acta 1066, 239-244.

287. Pollard H.B., Burns A.L., and Rojas E. (1990) *Synexin (annexin VII): a cytosolic calcium-binding protein which promotes membrane fusion and forms calcium channels in artificial bilayer and natural membranes.* J. Mem. Biol. 117, 101-112.

288. Zaks W.J., and Creutz C.E. (1990) *Annexin-chromaffin granule membrane interactions: a comparative study of synexin, p32 and p67.* Biochim. Biophys. Acta 1029, 149-160.

289. Balch W. (1992) *From G-minor to G-major.* Curr. Biol. 2, 157-160.

290. Bomsel M., and Mostov K. (1992) *Role of heterotrimeric G proteins in membrane traffic.* Molecular Biol. Cell 3, 1317-1328.

291. Kaziro Y., Itoh H., Kozasa T., Nakafuku M., and Satoh T. (1991) *Structure and function of signal-transducing GTP-binding proteins.* Annu. Rev. Biochem. 60, 349-400.

292. Ali N., Milligan G., and Evans W.H. (1989) *Distribution of G-proteins in rat liver plasma-membrane domains and endocytic pathways.* Biochem. J. 261, 905-912.

293. Ransnás L.A., Svoboda P., Jasper J.R., and Insel P.A. (1989) *Stimulation of beta-adrenergic receptors of S49 lymphoma cells redistributes the alpha subunit of the stimulatory G protein between cytosol and membranes.* Proc. Natl. Acad. Sci. USA 86, 7900-7903.

294. Negishi M., Hashimoto H., Ichikawa A. (1992) *Translocation of alpha subunits of stimulatory guanine nucleotide-binding proteins through stimulation of the prostacyclin receptor in mouse mastocytoma cells.* J. Biol. Chem. 267, 2364-2369.

295. Chabre M. (1990) *Aluminofluoride and beryllofluoride complexes: new phosphate analogs in enzymology.* Trends Biochem. Sci. 15, 6-10.

296. Khan R.A. (1991) *Flouride is Not an activator of the smaller (20-25) GTP-binding proteins.* J. Biol. Chem. 266, 15595-15597.

297. Mayorga L.S., Diaz R., and Stahl P.D. (1989) *Regulatory role for GTP-binding proteins in endocytosis.* Science 244, 1475-1478.

298. Ercolani L., Stow J.L., Boyle J.F., Holtzman E.J., Lin H., Grove R., and Ausiello D.A. (1990) *Membrane localization of the pertussis toxin-sensitive G-protein subunits alpha i-2 and alpha i-3 and expression of a metallothionein-alpha i-2 fusion gene in LLC-PK1 cells.* Proc. Natl. Acad. Sci USA 87, 4635-4639.

299. Stow J.L., de Almeida J.B., Narula N., Holtzman E.J., Ercolani L., and Ausiello D.A. (1991) *A heterotrimeric G protein, G alpha i-3, on Golgi membranes regulates the secretion of a heparan sulfate proteoglycan in LLC-PK1 epithelial cells.* J. Cell Biol. 114, 1113-1124.

300. Barr F.A., Leyte A., Mollner S., Pfeuffer T., Tooze S.A., and Huttner W.B. (1991) *Trimeric G-proteins of the trans-Golgi network are involved in the formation of constitutive secretory vesicles and immature secretory granules.* FEBS Lett. 294, 239-243.

301. Schwaninger R., Plutner H., Bokoch G.M., and Balch W.E. (1992) *Multiple GTP-binding proteins regulate vesicular transport from the ER to Golgi membranes.* J. Cell Biol. 5, 1077-1096.

302. Pimplikar S.W., and Simons K. (1993) *Regulation of apical transport in epithelial cells by a G_s class of heterotrimeric G protein.* Nature 362, 456-458.

303. Haraguchi K., and Rodbell M. (1991) *Carbachol-activated muscarinic (M1 and M3) receptors transfected into Chinese hamster ovary cells inhibit trafficking of endosomes.* Proc. Natl. Acad. Sci. USA 88, 5964-5968.

304. Colombo M.I., Mayorga L.S., Nishimoto I., Ross E. M., and Stahl P.D. (1994) *G_s regulation of endosome fusion suggests a role for signal transduction pathways in endocytosis.* J. Biol. Chem. 269, 14919-14923.

305. Ikonen E., Tagaya M., Ullrich O., Montecucco C., and Simons K. (1995) *Different requirements for NSF, SNAP, and Rab proteins in apical and basolateral transport in MDCK cells.* Cell 81, 571-580.

306. Latterich M., and Schekman R. (1994) *The karyogamy gene KAR2 and novel proteins are required for ER-membrane fusion.* Cell 78, 87-98.

307. Latterich M., Fröhlich K.U., and Scheckman R. (1995) *Membrane fusion and the cell cycle: Cdc48p participates in the fusion of ER membranes.* Cell 82, 885-893.

308. Fröhlich K.U., Fries H.W., Rudiger M., Erdmann R., Botstein D., and Mecke D. (1991) *Yeast cell cycle protein CDC48p shows full-length homology to the*

mammalian protein VCP and is a member of a protein family involved in secretion, peroxisome formation, and gene expression. J. Cell Biol. 114, 443-453.

309. Egerton M., Ashe O.R., Chen D., Druker B.J., Burgess W.H., and Samelson L.E. (1992) *VCP, the mammalian homolog of cdc48, is tyrosine phosphorylated in response to T cell antigen receptor activation.* EMBO J. 11, 3533-3540.

310. Koller K.J., and Brownstein M.J. (1987) *Use of a cDNA clone to identify a supposed precursor protein containing valosin.* Nature 325, 542-545.

311. Peters J.M., Walsh M.J., and Franke W.W. (1990) *An abundant and ubiquitous homo-oligomeric ring-shaped ATPase particle related to the putative vesicle fusion proteins Sec18p and NSF.* EMBO J. 9, 1757-1767.

312. Pleasure I.T., Black M.M., and Keen J.H. (1993) *Valosin-containing protein, VCP, is a ubiquitous clathrin-binding protein.* Nature 365, 459-462.

313. Zhang L., Ashendel C.L., Becker G.W., and Morre D.J. (1994) *Isolation and characterization of the principal ATPase associated with transitional endoplasmic reticulum of rat liver.* J. Cell Biol. 127, 1871-1883.

314. Erdmann R., Wiebel, F.F., Flessau A., Rytka J., Beyer A., Fröhlich K.U., and Kunau W.H. (1991) *PAS1, a yeast gene required for peroxisome biogenesis, encodes a member of a novel family of putative ATPases.* Cell 64, 499-510.

315. Thorsness P.E., White K.H., and Ong W.C. (1993) *AFG2, an essential gene in yeast, encodes a new member of the Sec18p, Pas1p, Cdc48p, TBP-1 family of putative ATPases.* Yeast 9, 1267-1271.

316. Warren G. (1993) *Membrane partitioning during cell division.* Annu. Rev. Biochem. 62, 323-348.

317. Lucocq J.M., Berger E.G., and Warren G. (1989) *Mitotic Golgi fragments in HeLa cells and their role in the reassembly pathway.* J. Cell Biol. 109, 463-474.

318. Lupashin V.V., and Waters M.G. (1997) *t-SNARE activation through transient interaction with a rab-like guanosine triphosphatase.* Science 276, 1255-1258.

319. Rabouille C., Levine T.P., Peters J.M., and Warren G. (1995) *An NSF-like ATPase, p97, and NSF mediate cisternal regrowth from mitotic Golgi fragments.* Cell 82, 905-914.

320. Goda Y., and Pfeffer S.R. (1991) *Identification of a novel, N-ethylmaleimide-sensitive cytosolic factor required for vesicular transport from endosomes to the trans-Golgi network in vitro.* J. Cell Biol. 112, 823-831.

321. Acharya U., Jacobs R., Peters J.M., Watson N., Farquhar M.G., and Malhotra V. (1995) *The formation of Golgi stacks from vesiculated Golgi membranes requires two distinct fusion events.* Cell 82, 895-904.

322. Dirac-Svejstrup A.B., Soldati T., Shapiro A.D., and Pfeffer S.R. (1994) *Rab-GDI presents functional Rab9 to the intracellular transport machinery and contributes selectivity to Rab9 membrane recruitment.* J. Biol. Chem. 269, 15427-15430.

323. Elazar Z., Mayer T., and Rothman J.E. (1994) *Removal of Rab GTP-binding proteins from Golgi membranes by GDP dissociation inhibitor inhibits inter-cisternal transport in the Golgi stacks.* J. Biol. Chem. 269, 794-797.

324. Peter F., Nuoffer C., Pind S.N., and Balch W.E. (1994) *Guanine nucleotide dissociation inhibitor is essential for Rab1 function in budding from the endoplasmic reticulum and transport through the Golgi stack.* J. Cell Biol. 126, 1393-1406.

325. Gorvel J.P., Chavrier P., Zerial M., and Gruenberg J. (1991) *rab5 controls early endosome fusion in vitro.* Cell 64, 915-925.

326. Rodriguez L., Stirling C.J., and Woodman P.G. (1994) *Multiple N-ethylmaleimide-sensitive components are required for endosomal vesicle fusion.* Mol. Biol. Cell 5, 773-783.

327. Diaz R., Mayorga L.S., Mayorga L.E., and Stahl P. (1989) *In vitro clustering and multiple fusion among macrophage endosomes.* J. Biol. Chem. 264, 13171-13180.

328. Wessling-Resnick M., and Braell W.A. (1990) *Characterization of the mechanism of endocytic vesicle fusion in vitro.* J. Biol. Chem. 265, 690-699.

329. Tooze J., and Hollinshead M. (1991) *Tubular early endosomal networks in AtT20 and other cells.* J. Cell Biol. 115, 635-653.

330. Waldo G.L., Northup J.K., Perkins J.P., and Harden T.K. (1983) *Characterization of an altered membrane form of the beta-adrenergic receptor produced during agonist-induced desensitization.* J. Biol. Chem. 258, 13900-13908.

331. Fleischer S., and Kervina M. (1974) *Subcellular fractionation of rat liver.* Methods Enzymol. 31, 6-39.

332. Bretz R., and Staubli W. (1977) *Detergent influence on rat-liver galactosyltransferase activities towards different acceptors.* Eur. J. Biochem. 77, 181-192.

333. Bergeron J.J.M. (1979) *Golgi fractions from livers of control and ethanol-intoxicated rats. Enzymic and morphologic properties following rapid isolation.* Biochim. Biophys. Acta 555, 493-503.

334. Haylett T., and Thilo L. (1986) *Limited and selective transfer of plasma membrane glycoproteins to membrane of secondary lysosomes.* J. Cell Biol. 103, 1249-1256.

335. Hall C.W., Liebaers I., Di Natale P., and Neufeld E.F. (1978) *Enzymic diagnosis of genetic mucopolysaccharide storage disorders.* Methods Enzymol. 50, 439-456.

336. Haylett T., and Thilo L. (1991) *Endosome-lysosome fusion at low temperature.* J. Biol. Chem. 266, 8322-8327.

337. Thilo L. (1983) *Labelling of plasma membrane glycoconjugates by terminal glycosylation (galactosyltransferase and glycosidase).* Methods Enzymol. 98, 415-421.

338. Colombo M.I., Gonzalo S., Weidman P., and Stahl P. (1991) *Characterization of trypsin-sensitive factor(s) required for endosome-endosome fusion.* J. Biol. Chem. 266, 23438-23445.

339. Mullock B.M., Bright N.A., Fearon C.W., Gray S.R., and Luzio J.P. (1998) *Fusion of lysosomes with late endosomes produces a hybrid organelle of intermediate density and is NSF dependent.* J. Cell Biol. 140, 591-601.

340. Courtoy P.J., Quintart J., and Baudhuin P. (1984) *Shift of equilibrium density induced by 3,3'-diaminobenzidine cytochemistry: a new procedure for the analysis and purification of peroxidase-containing organelles.* J. Cell Biol. 98, 870-876.

341. Quintart J., Courtoy P.J., and Baudhuin P. (1984) *Receptor-mediated endocytosis in rat liver: purification and enzymic characterization of low density organelles involved in uptake of galactose-exposing proteins.* J. Cell Biol. 98. 877-884.

342. Ajioka R.S., and Kaplan J. (1987) *Characterization of endocytic compartments using the horseradish peroxidase-diaminobenzidine density shift technique.* J. Cell Biol. 104, 77-85.

343. Thilo L., and Burgert H-G. (1983) *Monensin does not prevent recycling of plasma membrane glycoconjugates.* Exp. Cell Res. 147, 297-302.

344. Burgert H-G., and Thilo L. (1983) *Internalization and recycling of plasma membrane glycoconjugates during pinocytosis in the macrophage cell line, P388D1. Kinetic evidence for compartmentation of internalized membranes.* Exp. Cell Res. 144, 127-142.

345. Gorodinsky A., and Harris D.A. (1995) *Glycolipid-anchored proteins in neuroblastoma cells form detergent-resistant complexes without caveolin.* J. Cell Biol. 129, 619-627.

346. Letarte-Muirhead M., Acton R.T., and Williams A.F. (1974) *Preliminary characterization of Thy-1.1 and Ag-B antigens from rat tissues solubilized in detergents.* Biochem. J. 143, 51-61.

347. Low M.G. (1989) *The glycosyl-phosphatidylinositol anchor of membrane proteins.* Biochim. Biophys. Acta 988, 427-454.

348. Vitetta E.S., Boyse E.A., and Uhf J.W. (1973) *Isolation and characterization of a molecular complex containing Thy-1 antigen from the surface of murine thymocytes and T cells.* Eur. J. Immuno. 3, 446-453.

349. Chang W.-J., Ying Y., Rothberg K.G., Hooper, N.M., Turner, A.J., Gambliel H.A., De Gunzburg J., Mumby S.M., Gilman A.G., and Anderson R.G.W. (1994) *Purification and characterization of smooth muscle cell caveolae.* J. Cell Biol. 126, 127-138.

350. Lisanti M.P., Scherer P.E., Vidugiriene J., Tang Z.-L., Hermanowski-Vosatka A., Tu Y.-H., Cook R.F., and Sargiacomo M. (1994) *Characterization of caveolin-rich membrane domains isolated from an endothelial-rich source: implications for human disease.* J. Cell Biol. 126, 111-126.

351. Kurzchalia T.V., Gorvel J-P., Dupree P., Parton R., Kellner R., Houthaeve T., Gruenberg J., and Simons K. (1992) *Interactions of rab5 with cytosolic proteins.* J. Biol. Chem. 267, 18319-18323.

352. **{a}** Sanchez J.C., Rouge V., Pisteur M., Ravier F., Tonella L., Moosmayer M., Wilkins M.R., and Hochstrasser D.F. (1997) *Improved and simplified in-gel sample application using reswelling of dry immobilized pH gradients.* Electrophoresis 18, 324-327.

{b} Pasquali C., Fialka I., and Huber L.A. (1997) *Preparative two-dimensional gel electrophoresis of membrane proteins.* Electrophoresis 18, 2573-2581.

{c} Rabilloud T., Adessi C., Giraudel A., and Lunardi J. (1997) *Improvement of the solubilization of proteins in two-dimensional electrophoresis with immobilized pH gradients.* Electrophoresis 18, 307-316.

353. Robinson M.S., Watts C., and Zerial M. (1996) *Membrane dynamics in endocytosis.* Cell 84, 13-21.

354. Pierre P., Scheel J., Rickard J.E., and Kreis T.E. (1992) *CLIP-170 links endocytic vesicles to microtubules.* Cell 70, 887-900..

355. Defacque H., Egeberg M., Antzberger A., Ansorge W., Way M., and Griffiths G. (2000) *Actin assembly induced by polylysine beads or purified phagosomes: quantitation by a new flow cytometry assay.* Cytometry 41, 46-54.

356. Guerin I., and de Chastellier C. (2000) *Pathogenic mycobacteria disrupt the macrophage actin filament network.* Infect. Immun. 68, 2655-2662.

357. Laemmli U.K. (1970) *Cleavage of structural proteins during the assembly of the head of bacteriophage T4.* Nature 227, 680-685

358. Merril C.R., Goldman D., and Van Keuren M.L. (1984) *Gel protein stains: silver stain.* Methods Enzymol. 104, 441-447.

359. Wilson C.M. (1983) *Staining of proteins on gels: comparisons of dyes and procedures.* Methods Enzymol. 91, 236-247.

360. Jahraus A., Storrie B., Griffiths G., and Desjardins M. (1994) *Evidence for retrograde traffic between terminal lysosomes and the prelysosomal/late endosome compartment.* J. Cell Sci. 107, 145-157.

361. Oh Y-K., and Swanson J.A. (1996) *Different fates of phagocytosed particles after delivery into macrophage lysosomes.* J. Cell Biol. 132, 585-593.

362. Desjardins M., Huber L.A., Parton R.G., and Griffiths G. (1994) *Biogenesis of phagolysosomes proceeds through a sequential series of interactions with the endocytic apparatus.* J. Cell Biol. 124, 677-688.

363. Desjardins M., Celis J.E., van Meer G., Dieplinger H., Jahraus A., Griffiths G., and Huber L.A. (1994) *Molecular characterization of phagosomes.* J. Biol. Chem. 269, 32194-32200.

364. Rabinowitz S., Horstmann H., Gordon S., and Griffiths G. (1992) *Immunocytochemical characterization of the endocytic and phagolysosomal compartments in peritoneal macrophages.* J. Cell Biol. 116, 95-112.

365. Chavrier P., Parton R.G., Hauri H.P., Simons K., and Zerial M. (1990) *Localization of low molecular weight GTP binding proteins to exocytic and endocytic compartments.* Cell 62, 317-329.

366. Emans N., Nzala N.N., and Desjardins M. (1996) *Protein phosphorylation during phagosome maturation.* FEBS Letters 398, 37-42.

367. **{a}** O'Farrel P.H. (1975) *High-resolution two-dimensional electrophoresis of proteins.* J. Biol. Chem. 250, 4007-4021.

{b} Gorg A., Postel W., and Gunther S. (1988) *Current state of two-dimensional electrophoresis with immobilized pH gradients.* Electrophoresis 9, 531-546.

{c} Bjellquist B., Pasquali C., Ravier F., Sanchez J.C., and Hochstrasser D.F. (1993) *A nonlinear wide-range immobilized pH gradient for two-dimensional electrophoresis and its definition in a relevant pH scale.* Electrophoresis 14, 1357-1365.

368. Celis J.E., Ratz G.P., Madsen P. et.al. (1989) *Comprehensive, human cellular protein databases and their implication for the study of genome organization and function.* FEBS Letters 244, 247-254.

369. Hentzel W.J., Billeci T.M., Stults J.T., Wong S.C., Grimley C., and Watanabe C. (1993) *Identifying proteins from two-dimensional gels by molecular mass searching of peptide fragments in protein sequence databases.* Proc. Natl. Acad. Sci. USA 90, 5011-5015.

370. Pappin D.J.C., Hojrup O., and Bleasby A.J. (1993) *Rapid identification of proteins by peptide mass fingerprints.* Curr. Biol. 3, 327-332.

371. James P., Quadroni M., Carafoli E., Gonnet G. (1993) *Protein identification by mass profile fingerprinting.* Biochem. Biophys. Res. Commun. 195, 58-64.

372. Yates J.R. III, Speicher S., Griffin P.R., and Hunkapiller T. (1993) *Peptide mass maps: a highly informative approach to protein identification.* Anal. Biochem. 214, 397-408.

373. Shevchenco A., Wilm M., Vorm O., and Mann M. (1996) *Mass spectrometric sequencing of proteins silver-stained polyacrylamide gels.* Anal. Chem. 68, 850-858.

374. Brown R.S., and Lennon J.J. (1995) *Mass resolution improvement by incorporation of pulsed ion extraction in a matrix-assisted laser desorption/ionization linear time-of-flight mass spectrometer.* Anal. Chem. 67, 1998-2003.

375. Whittal R., and Li L. (1995) *High-resolution matrix-assisted laser desorption/ionization in a linear time-of-flight mass spectrometer.* Anal. Chem. 67, 1950-1954.

376. Vestal M.L., Juhasz P., and Martin S.A. (1995) *Delayed extraction matrix-assisted laser-desorption ionization time-of-flight mass spectrometry.* Rapid Commun. Mass. Spectrom. 9, 1044-1050.

377. Jensen O.N., Podtelejnikov A., and Mann M. (1997) *Identification of the components of simple protein mixtures by high-accuracy peptide mass mapping and database searching.* Anal. Chem. 69, 4741-4750.

378. Sharon N., and Lis. H (1989) Lectins, Chapman and Hall, London.

379. Gabius H.J. (1997) *Animal lectins.* Eur. J. Biochem. 243, 543-576.

380. Drickamer K., and Taylor M.E. (1998) *Evolving views of protein glycosylation.* Trends Biochem. Sci. 23, 321-324.

381. Weis W.I., and Drickamer K. (1996) *Structural basis of lectin-carbohydrate recognition.* Annu. Rev. Biochem. 65, 441-473.

382. Rini J.M., and Lobsanov Y.D. (1999) *New animal lectin structures.* Curr. Opin. Struc. Biol. 9, 578-584.

383. Barondes S.H., Cooper D.N., Gitt M.A., and Leffler H. (1994) *Galectins. Structure and function of a large family of animal lectins.* J. Biol. Chem. 269, 20807-20810.

384. Hughes R.C. (1997) *The galectin family of mammalian carbohydrate-binding molecules.* Biochem. Soc. Trans. 25, 1194-1198.

385. Cooper D.N., and Barondes S.H. (1997) *God must love galectins; he made so many of them.* Glycobiology 9, 979-984.

386. Inohara H., and Raz A. (1995) *Functional evidence that cell surface galectin-3 mediates homotypic cell adhesion.* Cancer Res. 55, 3267-3271.

387. Dagher S.F., Wang J.L., and Patterson R.J. (1995) *Identification of galectin-3 as a factor in pre-mRNA splicing.* Proc. Natl. Acad. Sci. USA 92, 1213-1217.

388. Mehul B., and Hughes R.C. (1997) *Plasma membrane targetting, vesicular budding and release of galectin 3 from the cytoplasm of mammalian cells during secretion.* J. Cell Sci. 110, 1169-1178.

389. Menon R.P., and Hughes R.C. (1999) *Determinants in the N-terminal domains of galectin-3 for secretion by a novel pathway circumventing the endoplasmic reticulum-Golgi complex.* Eur. J. Biochem. 264, 569-576.

390. Gong H.A., Honjo Y., Naggia-Makker P., Hogan V., Mazurak N., Bresalier R.S., and Raz A. (1999) *The NH2 terminus of galectin-3 governs cellular compartmentalization and functions in cancer cells.* Cancer Res. 59, 6239-6245.

391. Zhang-Keck Z.Y., Burns A.L., and Pollard H.B. (1993) *Mouse synexin (annexin VII) polymorphisms and a phylogenetic comparison with other synexins.* Biochem. J. 289, 735-741.

392. Huet C., Ash J.F., and Singer S.J. (1980) *The antibody-induced clustering and endocytosis of HLA antigens on cultured human fibroblasts.* Cell 21, 429-438.

393. Dasgupta J.D., Watkins S., Slayter H., and Yunis E.J. (1988) *Receptor-like nature of class I HLA: endocytosis via coated pits.* J. Immunol. 141, 2577-2580.

394. Chiu I., Davis D.M., and Strominger J.L. (1999) *Trafficking of spontaneously endocytosed MHC proteins.* Proc. Natl. Acad. Sci. 96, 13944-13949.

395. Capps G.G., and Zuniga M.C. (2000) *Phosphorylation of class I MHC molecules in the absence of phorbol esters is an intracellular event and may be characteristic of trafficking molecules.* Mol. Immunol. 37, 59-71.

396. Buettner R., Papoutsoglou G., Scemes E., Spray D.C., and Dermietzel R. (2000) *Evidence for secretory pathway localization of a voltage-dependent anion channel isoform.* Proc. Natl. Acad. Sci. 97, 3201-3206.

397. Chilcote T.J., Galli T., Mundigl O., Edelmann L., McPherson P.S., Takei K., and De Camilli P. (1995) *Cellubrevin and synaptobrevins: similar subcellular localization and biochemical properties in PC12 cells.* J. Cell Biol. 129, 219-231.

398. Grote E., Hao J.C., Bennett M.K., and Kelly R.B. (1995) *A targeting signal in VAMP regulating transport to synaptic vesicles.* Cell 81, 581-589.

399. Gotte M., and von Mollard G.F. (1998) *A new beat for the SNARE drum.* Trends Cell Biol. 8, 215-218.

400. Grote E., and Novick P. (1999) *Promiscuity in Rab-SNARE interactions.* Mol. Biol. Cell 10, 4149-4161.

401. Jahraus A., Tjelle T.E., Berg T., Habermann A., Storrie B., Ullrich O., and Griffiths G. (1998) *In vitro fusion of phagosomes with different endocytic organelles from J774 macrophages.* J. Biol. Chem. 273, 30379-30390.

402. Shonn M.A., Blocker A., Burkhardt J.K., Griffiths G., Weis D.G., and Kusnetsov S.A. (1995) *The interaction between phagosomes and actin filaments in vitro.* Mol. Biol. Cell (Abstr. suppl.) 6, 272a.

403. Langer T., Lu C., Echols H., Flanagan J., Hayer M. K., and Hartl F. (1992) *Successive action of DnaK, DnaJ and GroEL along the pathway of chaperone-mediated protein folding.* Nature 356, 683-689.

404. Schröder H., Langer T., Hartl F.-U., and Bukau B. (1993) *DnaK, DnaJ and GrpE form a cellular chaperone machinery capable of repairing heat-induced protein damage.* EMBO J. 12, 4137-4144.

405. Lain B., Iriarte A., and Martinez-Carrion M. (1994) *Dependence of the folding and import of the precursor to mitochondrial aspartate aminotransferase on the nature of the cell-free translation system.* J. Biol. Chem. 269, 15588-15596.

406. Hutchison K.A., Dittmar K.D., Czar M.J., and Pratt W. B. (1994) *Proof that hsp70 is required for assembly of the glucocorticoid receptor into a heterocomplex with hsp90.* J. Biol. Chem. 269, 5043-5049.

407. Deshaies R. J., Koch B. D., Werner-Washburne M., Craig E., and Schekman R. (1988) *A subfamily of stress proteins facilitates translocation of secretory and mitochondrial precursor polypeptides.* Nature 332, 800-805.

408. Flynn G.C., Pohl J., Flocco M.T., and Rothman J.E. (1991) *Peptide-binding specificity of the molecular chaperone BiP.* Nature 353, 726-730.

409. Blond-Elguindi S., Cwirla S.E., Dower W.J., Lipshutz R.J., Sprang S.R., Sambrook J.F., and Gething M.J. (1993) *Affinity panning of a library of peptides displayed on bacteriophages reveals the binding specificity of BiP.* Cell 75, 717-728.

410. Flynn G.C., Chappell T.G., and Rothman J.E. (1989) *Peptide binding and release by proteins implicated as catalysts of protein assembly.* Science 245, 385-390.

411. Palleros D.R., Reid K.L., Shi L., Welch W.J., and Fink A.L. (1993) *ATP-induced protein-Hsp70 complex dissociation requires K+ but not ATP hydrolysis.* Nature 365, 664-666.

412. Craig E. A., Baxter B.K., Becker J., Halladay J., and Ziegelhoffer T. (1994) in The Biology of Heat Shock Proteins and Molecular Chaperones (Morimoto, R. I., Tissieres, A., and Georgopoulos, C., eds), pp. 31-52, Cold Spring Harbor Laboratory Press, NY.

413. Schlossman D.M., Schmid S.L., Braell W.A., and Rothman J.E. (1984) *An enzyme that removes clathrin coats: purification of an uncoating ATPase.* J. Cell Biol. 99, 723-733.

414. Manceau V., Gavet O., Curmi P., and Sobel A. (1999) *Stathmin interaction with HSC70 family proteins.* Electrophoresis 20, 409-417.

415. Buxbaum E., and Woodman P.G. (1995) *Selective action of uncoating ATPase towards clathrin-coated vesicles from brain.* J. Cell Sci. 108, 1295-1306.

416. Agarraberes F.A., Terlecky S.R., and Dice J.F. (1997) *An intralysosomal hsp70 is required for a selective pathway of lysosomal protein degradation.* J. Cell Biol. 137, 825-834.

417. Yonezawa N., Nishida E., Ohba M., Seki M., Kumagai H., and Sakai, H. (1989) *An actin-interacting heptapeptide in the cofilin sequence.* Eur. J. Biochem. 183, 235-238.

418. Hayden S.M., Miller P.S., Brauweiler A., and Bamburg J.R. (1993) *Analysis of the interactions of actin depolymerizing factor with G- and F-actin.* Biochemistry 32, 9994-10004.

419. Theriot J.A. (1997) *Accelerating on a treadmill: ADF/cofilin promotes rapid actin filament turnover in the dynamic cytoskeleton.* J. Cell Biol. 136, 1165-1168.

420. Carlier M.F., Laurent V., Santolini J., Melki R., Didry D., Xia G.X., Hong Y., Chua N.H., and Pantaloni D. (1997) *Actin depolymerizing factor (ADF/cofilin) enhances the rate of filament turnover: implication in actin-based motility.* J. Cell Biol. 136, 1307-1322.

421. Arber S., Barbayannis F., Hanser H., Schneider C., Stanyon C., Bernard O., and Caroni P. (1998) *Regulation of actin dynamics through phosphorylation of cofilin by LIM-kinase.* Nature 393, 805-809.

422. Yang N., Higuchi O., Ohashi K., Nagata K., Wada A., Kangawa K., Nishida E., and Mizuno K. (1998) *Cofilin phosphorylation by LIM-kinase 1 and its role in Rac-mediated actin reorganization.* Nature 393, 809-812.

423. Zhang P., Liu B., Kang S.W., Seo M.S., Rhee S.G., and Obeid L.M. (1997) *Thioredoxin peroxidase is a novel inhibitor of apoptosis with a mechanism distinct from that of Bcl-2.* J. Biol. Chem. 272, 30615-30618.

424. Cha M.K., Yun C.H., and Kim I.H. (2000) *Interaction of human thiol-specific antioxidant protein 1 with erythrocyte plasma membrane.* Biochemistry 39, 6944-6950.

425. Ohannesian D.W., Lotan D., Thomas P., Jessup J.M., Fukuda M., Gabius H.J., and Lotan R. (1995) *Carcinoembryonic antigen and other glycoconjugates act as ligands for galectin-3 in human colon carcinoma cells.* Cancer Res. 55, 2191-2199.

426. Dong S., and Hughes R.C. (1997) *Macrophage surface glycoproteins binding to galectin-3 (Mac-2-antigen).* Glycoconj. J. 14, 267-274.

427. Sarafian V., Jadot M., Foidart J.M., Letersson J.J., Van den Brule F., Castronovo V., Wattiaux R., and Coninck S.W. (1998) *Expression of Lamp-1 and Lamp-2 and their interactions with galectin-3 in human tumor cells.* Int. J. Cancer 75, 105-111.

428. Feuk-Lagerstedt E., Jordan E.T., Leffler H., Dahlgren C., and Karlsson A. (1999) *Identification of CD66a and CD66b as the major galectin-3 receptor candidates in human neutrophils.* J. Immunol. 163, 5592-5598.

429. Stevens T.H., and Forgac M. (1997) *Structure, function and regulation of the vacuolar (H+)-ATPase.* Annu. Rev. Cell Dev. Biol. 13, 779-808.

430. Margolles-Clark E., Tenney K., Bowman E.J., and Bowman B.J. (1999) *The structure of the vacuolar ATPase in Neurospora crassa.* J. Bioenerg. Biomembr. 31, 29-38.

431. Kane P.M. (1999) *Biosynthesis and regulation of the yeast vacuolar H+-ATPase.* J. Bioenerg. Biomembr. 31, 49-56.

432. Anraku Y., Umemoto N., Hirata R., and Ohya Y. (1992) *Genetic and cell biological aspects of the yeast vacuolar H(+)-ATPase.* J. Bioenerg. Biomembr. 24, 395-406.

433. Nelson N. (1992) *Structural conservation and functional diversity of V-ATPases.* J. Bioenerg. Biomembr. 24, 407-414.

434. Peters C., Bayer M.J., Buhler S., Andersen J.S., Mann M., and Mayer A. (2001) *Trans-complex formation by proteolipid channels in the terminal phase of membrane fusion.* Nature 409, 567-568.

435. Zhang J.W., Parra K.J., Liu J., and Kane P.M. (1998) *Characterization of a temperature-sensitive yeast vacuolar ATPase mutant with defects in actin distribution and bud morphology.* J. Biol. Chem. 18470-18480.

436. Raynal P., and Pollard H.B. (1994) *Annexins: the problem of assessing the biological role for a gene family of multifunctional calcium- and phospholipid-binding proteins.* Biochim. Biophys. Acta. 1197, 63-93.

437. Swairjo M.A., and Seaton B.A. (1994) *Annexin structure and membrane interactions: a molecular perspective.* Annu. Rev. Biophys. Biomol. Struct. 23, 193-213.

438. **{a}** Kojima K., Ogawa H.K., Seno N., Yamamoto K., Irimura T., Osawa T., and Matsumoto I. (1992) *Carbohydrate-binding proteins in bovine kidney have consensus amino acid sequences of annexin family proteins.* J Biol. Chem. 267, 20536-20539.

{b} Kojima K., Yamamoto K., Irimura T., Osawa T., Ogawa H., and Matsumoto, I. (1996) *Characterization of carbohydrate-binding protein p33/41: relation with Annexin IV, molecular basis of doublet forms (p33 & p41), and modulation of the carbohydrate binding activity by phospholipids.* J. Biol. Chem. 271, 7679-7685.

439. Ishitsuka R., Kojima K., Utsumi H., Ogawa H., and Matsumoto I. (1998) *Glycosaminoglycan binding properties of annexin IV, V, and VI.* J. Biol. Chem. 273, 9935-9941.

440. Pol A., Ortega D., and Enrich C. (1997) *Identification of cytoskeleton-associated proteins in isolated rat liver endosomes.* J. Biochem. 327, 741-746.

441. Diakonova M., Gerke V., Ernst J., Liautard J.P., van der Vusse G., and Griffiths G. (1997) *Localization of five annexins in J774 macrophages and on isolated phagosomes.* J. Cell Sci. 110, 1199-1213.

442. Majeed M., Perskvist N., Ernst J.D., Orselius K., and Stendahl O. (1998) *Roles of calcium and annexins in phagocytosis and elimination of an attenuated strain of M. tuberculosis in human neutrophils.* Microb. Patholog. 24, 309-320.

443 Silverstein S.C., Greenberg S., DiVirgilio F., and Steinberg T.H. (1989) pp. 703-720, Fundamental Immunology, Raven Press, New York.

444 Hart P.D., Young M.R., Jordan M.M., Perkins W.J., and Geisow M.J. (1983) *Chemical inhibitors of phagosome-lysosome fusion in cultured macrophages also inhibit saltatory lysosomal movements. A combined microscopic and computer study.* J. Exp. Med. 158, 477-492.

445 Hart P.D, Young M.R., Gordon A.H., and Sullivan K.H. (1987) *Inhibition of phagosome-lysosome fusion in macrophages by certain mycobacteria can be explained by inhibition of lysosomal movements observed after phagocytosis.* J. Exp. Med. 166, 933-946.

446 Toyohara A., and Inaba K. (1989) *Transport of phagosomes in mouse peritoneal macrophages.* J. Cell Sci. 94, 143-153.

447 Pitt A., Mayorga L.S., Stahl P.D., and Schwartz A.L. (1992) *Alterations in the protein composition of maturing phagosomes.* J. Clin. Invest. 90, 1978-1983.

448 Sturgill-Koszycki S., Schaible U.E., and Russel D.G. (1996) *Mycobacterium-containing phagosomes are accessible to early endosomes and reflect a transitional state in normal phagosomes.* EMBO J. 15, 6960-6968.

449 Pizon V., Desjardins M., Bucci C., Parton R.G., and Zerial M. (1994) *Association of Rap1a and Rap1b proteins with late endocytic/phagocytic compartments and Rap2a with the Golgi complex.* J. Cell Sci. 107, 1661-1670.

450 Desjardins M., Nzala N.N., Corsini R., and Rondeau C. (1997) *Maturation of phagosomes is accompanied by changes in their fusion properties and size-selective acquisition of solute from endosomes.* J. Cell Sci. 110, 2303-2314.

451 Hackam D.J., Rotstein O.D., Bennett M.K., Klip A., Grinstein S., and Manolson M.F. (1996) *Characterization and subcellular localization of target membrane soluble NSF attachment protein receptors (t-SNAREs) in macrophages. Syntaxins 2, 3, and 4 are present on phagosomal membranes.* J. Immunol. 156, 4377-4383.

452 Alvarez-Dominguez C., Roberts R., and Stahl P.D. (1997) *Internalized Listeria monocytogenes modulates intracellular trafficking and delays maturation of the phagosome.* J. Cell Sci. 110, 731-743.

453 Gatfield J., and Pieters J. (2000) *Essential role for cholesterol in entry of mycobacteria into macrophages.* Science 288, 1647-1650.

454 Ferrari G., Langen H., Naito M., and Pieters J. (1999) *A coat protein on phagosomes involved in intracellular survival of mycobacteria.* Cell 97,435-447.

455 Garin J., Diez R., Kieffer S., Dermine J.F., Duclos S., Gagnon E., Sadoul R., Rondeau C., and Desjardins M. (2001) *The Phagosome Proteome. Insight into phagosome functions.* J. Cell Biol. 152, 165-180.

456 Fratti R.A., Verge I., Chua J., Skidmore J., and Deretic V. (2000) *Regulators of membrane trafficking and Mycobacteria tuberculosis phagosome maturation block.* Electrophoresis 21, 3378-3385.

457 Smythe E., Smith P.D., Jacob S.M., Theobald J., and Moss S.E. (1994) *Endocytosis occurs independently of annexin VI in human A431 cells.* J. Cell Biol.124, 301-306.

458 van Weert A.W., Dunn K.W., Gueze H.J., Maxfield F.R., and Stoorvogel W. (1995) *Transport from late endosomes to lysosomes, but not sorting of integral membrane proteins in endosomes, depends on the vacuolar proton pump.* J Cell Biol. 130, 821-834.

459 Jahraus A., Tjelle T.E., Berg T., Habermann A., Storrie B., Ullrich O., and Griffiths G. (1998) *In vitro fusion of phagosomes with different endocytic organelles from J774 macrophages.* J. Biol. Chem. 273, 30379-30390.